NEUROPATHOLOGICAL CHANGES ASSOCIATED WITH *Clostridium perfringens* TYPE D EPSILON TOXIN

JOHN WALKER FINNIE

B.Sc., B.V.Sc.

Department of Pathology

University of Adelaide

A thesis presented for the Degree of Master of Science,

February, 1983.

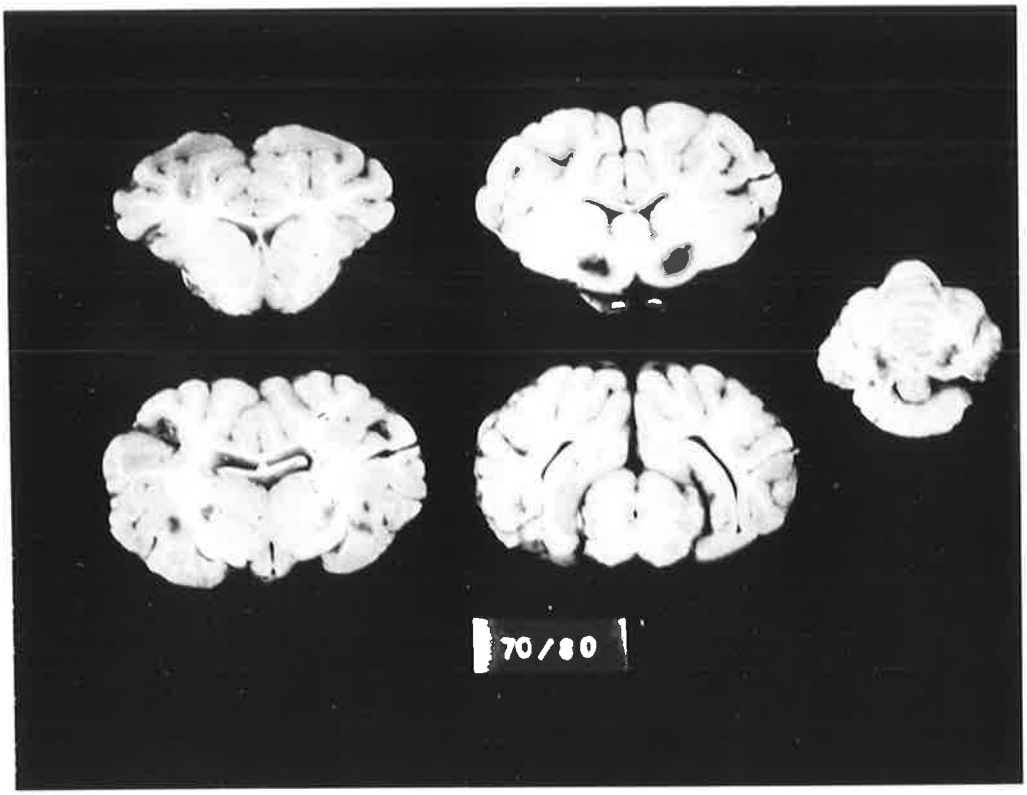
70/80

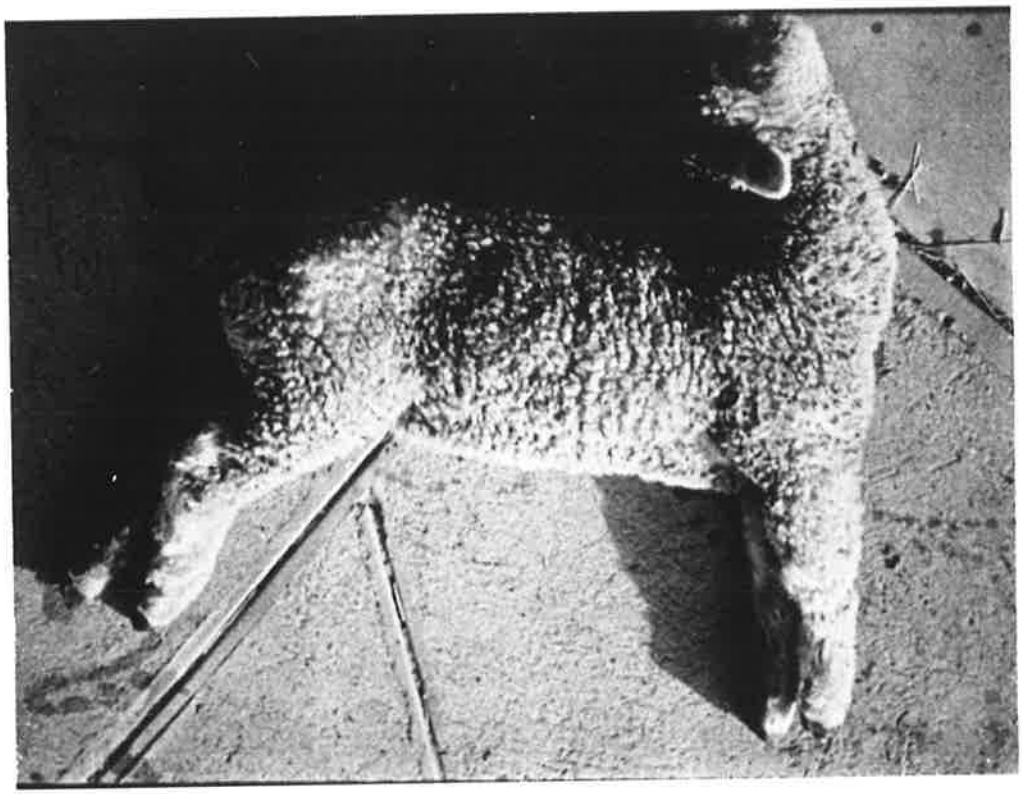

Focal symmetrical encephalomalacia. Bilaterally symmetrical foci of haemorrhage and softening.

Intoxicated lamb showing marked ophistotonos and hyperextension of the forelimbs.

(Courtesy of Dr. W.J. Hartley).

TABLE OF CONTENTS

ACKNOWLEDGEMENTS

Many people within the Department of Pathology and the Institute of Medical and Veterinary Science (I.M.V.S.) were generous with their time and professional skills in the preparation of this thesis. In particular I would like to thank my supervisor, Professor B. Vernon-Roberts, Chairman, Department of Pathology and Head, Division of Tissue Pathology, I.M.V.S., for his interest and guidance during the course of this work and Drs. D.E. Gardner, Director, Veterinary Division, I.M.V.S., T. Mukherjee, Head, Electron Microscope Unit, I.M.V.S. and P. Blumbergs, Neuropathologist, I.M.V.S. for their helpful advice whenever sought. I am also grateful for the technical assistance given by the staff of the Veterinary Division, I.M.V.S., Misses A. Galvin and R. Williams of the Electron Microscope Unit, I.M.V.S. and Miss M.A. Quin of the Pathology Department for the preparation of histological sections. I greatly appreciate the considerable efforts made by the secretarial staff of the I.M.V.S. and Ms. V. Jones in the typing of the manuscript and Messrs. M. Fitzgerald and D. Caville in the preparation of the photographs for this thesis. My thanks also to the Victorian Department of Agriculture and the University of Adelaide whose financial assistance allowed me to undertake this study.

CHAPTER I

INTRODUCTION

All the serotypes of bacteria classified as *Clostridium perfringens (welchii)* are potential causes of enterotoxaemia in sheep but Type D is of greatest economic importance, despite reductions in losses as a result of vaccination, and is catholic in its distribution. The disease classically affects rapidly growing lambs in excellent condition, although adult sheep may become afflicted. The aetiological agent is normally resident in the intestine of most healthy sheep and only assumes pathogenic properties when certain conditions prevail in the intestinal milieu which favour the rapid proliferation of these organisms with the production of toxin. The effects of the toxin are systemic with involvement of the alimentary tract, brain, lungs, heart and kidneys but clinical signs mainly reflect pathological changes in the central nervous system. Two forms of the disease are recognised, an acute intoxication with multisystem pathology and a chronic condition characterised by a focal symmetrical encephalomalacia.

The genesis of the acute lesions appears to be associated with toxin damage to the vascular endothelium but the precise sequence of events from the apparent initial diffuse cerebral oedema to the development of malacic foci in the brain is poorly understood, both in terms of the ultrastructural alterations which lead to necrosis and the apparent selective vulnerability of certain regions in the brain to the action of this toxin at the anatomical level.

Advances in electron microscopy, particularly with respect to the development of electron opaque vascular tracer substances such as horseradish peroxidase and ferritin, afford the opportunity to explore the early cerebral vessel-related changes attendant upon their exposure to this toxin in an attempt to find a cogent explanation for the development of lesions recognised grossly as a focal symmetrical encephalomalacia.

Furthermore, the brain cannot be examined in total isolation as changes in other organs, especially the cardiorespiratory system, influence the final expression of the central nervous system lesions and are therefore pertinent to a consideration of toxin-induced cerebral pathology.

The employment of models for this ovine disease is both useful and expedient, especially since widespread vaccination against this condition and the high percentage of non-vaccinated animals with significant antitoxin titres, mitigates against achieving any consistent response to the toxin in the experimental situation, unless colostrum-deprived lambs are used.

A study of the brain lesions produced by *Clostridium perfringens* Type D is also relevant to the larger themes of cerebral oedema, selective vulnerability and the operation of the so-called "blood-brain barrier". Most types of cerebral oedema produced experimentally in animals, or encountered clinically in man, are incited by focal lesions or insults and Type D intoxication may prove to be a useful model for oedema which appears to be initially diffuse, or at least very rapidly becomes so.

CHAPTER II

HISTORICAL REVIEW

The epsilon toxin of *Clostridium perfringens (welchii)* Type D is associated with two diseases of sheep - an acute enterotoxaemia and a focal symmetrical encephalomalacia (FSE). The former condition represents an acute or peracute intoxication while FSE is almost certainly the result of a more protracted clinical course and may be regarded as the chronic neurological manifestation of enterotoxaemia which develops when the disease is not immediately fatal. Pienaar and Thornton (1964) considered that, under field conditions, FSE may be assocated with very low antitoxin levels, insufficient to protect the animal completely but adequate enough to prevent the acute deaths normally seen in enterotoxaemia. Clinical signs in both conditions are mainly referable to the central nervous system. In general, in animals suffering from FSE, lesions are confined to the brain (Blood *et al*, 1979) although some cases occur showing lesions of acute enterotoxaemia with concurrent central nervous pathology (Hartley, 1956; Gay *et al*., 1975).

All ages of sheep are susceptible to the action of epsilon toxin. The disease is rare in lambs under 7 days old and the predisposition is greatest between the ages of 3 weeks and 18 months (Bullen, 1970). The majority of enterotoxaemia cases occur between 3 and 10 weeks (Blood *et al*, 1979). In lambs, the duration of the illness is very short, often lasting less than 2 hours and never longer than 12 hours, and many animals are found dead without premonitory signs. Adult sheep usually survive for longer periods, up to 24 hours (Blood *et al*, 1979). FSE usually affects an older age of sheep. Gay *et al* (1975) investigated 14 outbreaks of FSE and found that in 5 outbreaks the majority of animals were between 10 and 12 months of age and the remaining 9 outbreaks occurred in mature sheep 3 years or older. In FSE the clinical course is usually from several days to a week.

The morbidity rate of acute enterotoxaemia seldom exceeds 10% but the mortality rate approaches 100%; similarly in FSE the morbidity rate is low (but may attain 15%), however the case fatality rate is high (Blood *et al*, 1979).

In acute enterotoxaemia listlessness and depression are usually observed with violent clonic convulsions heralding sudden death. Animals surviving for a few hours present with a greenish diarrhoea, incoordination, recumbency, ophistotonos, convulsions, coma and death (Bullen, 1970).

Gill (1927) described 3 clinical types of enterotoxaemia : 1) a peracute form with convulsions and rapid death, 2) an acute form with convulsions and a ophistotonos which followed a slightly more protracted course, and 3) a subacute form characterized by lethargy, depression and blindness. However, since toxin was not demonstrable in the intestinal contents of the latter 2 forms, Gill considered that a diagnosis of enterotoxaemia was only appropriate in the peracute syndrome. The subacute form may have corresponded to FSE but no pathological examination of the brain was performed. Bennetts (1932) reported two types of enterotoxaemia: an acute "convulsive" form and a subacute "comatose" form. The first type was characterized by convulsions, lateral recumbency with a galloping motion of the limbs, nystagmus, excessive salivation, grinding of the teeth and marked retraction of the head. The subacute form consisted of a "dummy" syndrome with gait abnormalities, recumbency, hyperaesthesia, blindness and a quiet death following coma. These two syndromes described by Bennetts are similar to those subsequently designated acute enterotoxaemia and FSE, respectively.

At autopsy, lambs with acute enterotoxaemia demonstrate an excessive volume of pericardial fluid rich in fibrin, pulmonary congestion and oedema, and haemorrhage beneath the endocardium of the left ventricle. Haemorrhages are also commonly found beneath the parietal peritoneum and in the epicardium. The kidneys are very soft and congested, and the mucosa of the small intestine is

hyperaemic and the contents creamy (with rapid death) or fluid and greenish in colour if survival is more prolonged (Jubb and Kennedy, 1970).

In order for enterotoxaemia to develop, the following requirements must be met: (1) organisms must gain access to the intestine. This is readily achieved since *Clostridium perfringens* Type D usually establishes itself as part of the normal intestinal flora at an early age; (2) in the intestine, these bacteria must be able to multiply and establish themselves in large numbers; (3) they must be able to produce toxin from the substrate present in the intestinal contents; and (4) the toxin must be absorbed from the gut into the bloodstream.

Bullen *et al* (1953) examined the fate of cultures of Type D introduced into the rumen of normal sheep via fistulae. Cultures were rapidly destroyed in the rumen and there was some evidence that the organisms were also killed in their passage between the rumen and the duodenum. Some bacteria reached the small intestine where they multiplied rapidly for a short period, then declined dramatically. During this phase of multiplication, however, considerable quantities of epsilon toxin were produced, albeit for a short period, indicating that the intestinal contents of normal sheep provide a suitable substrate both for the multiplication of *Clostridium perfringens* Type D and for the production of epsilon toxin.

The resistance of normal sheep to large oral doses of *Clostridium perfringens* Type D was attributed by Bullen *et al* (1953), in part, to rapid destruction of organisms in the rumen and the prevention of toxin accumulation in the duodenum by peristalsis. Other conditions were obviously required for the development of acute enterotoxaemia and experiments by Bullen and Scarisbrick (1957) elucidated some of these factors. They found that normal sheep developed acute enterotoxaemia when cultures were introduced into the intestine after the animals had consumed large amounts of grain or lush, rapidly growing pasture. In the absence of this excessive intake sheep remained clinically normal. This finding is in accord with clinical experience in the

field where susceptible animals are almost invariably those on a high plane of nutrition and in excellent body condition. It appeared that the presence of undigested or partially digested food in the intestine encouraged the rapid proliferation of *Clostridium perfringens* Type D. This prerequisite for the development of the acute disease was confirmed by Bullen (1971) who produced typical enterotoxaemia in normal sheep by infusing cultures of Type D into the intestine with added dextrin. In all cases of successful experimental reproduction of the disease, high concentrations of epsilon toxin needed to be maintained in the duodenum for several hours; low concentrations of toxin in the intestine, even for long periods, were harmless. Conversely, high concentrations of toxin were ineffective if present for only very short periods. Sheep with high epsilon antitoxin levels were refractory, even when the duodenum contained high concentrations of epsilon toxin for extended periods of time. Gardner (1973) also produced acute entertoxaemia in lambs in a similar manner.

Thus it appears that a dietary change combined with excessive intake of an appropriate diet allows large quantities of partially digested, readily fermentable material to pass into the intestine, presumably as a result of the inability of the rumen microflora to adapt rapidly enough to the large amounts of unfamiliar substrate presented to it. This conclusion is supported by the good experimental correlation between the presence of undigested starch in the duodenum and the successful reproduction of acute enterotoxaemia. The toxin rapidly increases the permeability of the intestine, facilitating its own absorption, and large quantities of toxin are presented to the circulation. Death from acute epsilon intoxication may then ensue in a few hours.

FSE was first reported by Hartley (1956) in New Zealand as a neurological disorder of young lambs characterized by bilaterally symmetrical malacic lesions in the internal capsule adjacent to the basal ganglia, lateral to the iter beneath the posterior corpora quadrigemina, in the mid-thalamic region and in the cerebellar peduncles. The macroscopic appearance of the lesions depended

upon the duration of the clinical course and the blood content. Malacic foci in animals affected up to 6 days were focal haemorrhagic or gelatinous softenings with older lesions a yellowish-grey colour.

Many of these lambs were derived from flocks where enterotoxaemia had been diagnosed or suspected. Hartley (1956) examined 36 lambs at necropsy and divided them into 4 groups based on the duration of neurological signs. These animals showed a variety of neurological signs including mental dullness and dejection, incoordination, blindness, head pressing, aimless wandering, ophistotonos, paddling movements of the limbs when prostrate, circling and ataxia. The 4 lambs in Group 1 were found dead and were the only animals to show the characteristic lesions of acute enterotoxaemia. Three of these lambs had macroscopic lesions of FSE and Type D toxin was demonstrated in the intestinal contents of one lamb. Lesions in the 24 lambs comprising Group 2 (affected 1-6 days) and the 8 of Group 3 (affected 7 to 14 days) were confined to the brain and seen in all but 5 animals. Toxin was sought in the intestinal contents of 9 lambs in Group 2, with 3 recording positive results. The single lamb in Group 4 (affected over 2 weeks) showed no significant pathological changes in the brain or other organs. Microscopically, the cerebral lesions consisted of large, focal non-inflammatory areas of necrosis with vascular dilation and capillary haemorrhage. At 48 hours, moderate numbers of neutrophil polymorphs had invaded the lesions and were present for 2-3 days. At the periphery of these foci, retraction bulbs of swollen degenerating axons were found. From the third day, compound granular corpuscles (gitter cells) were seen migrating into the lesion with proliferating capillaries and by the tenth day the necrotic focus was completely filled with gitter cells. At this time macrophages in these foci often contained haemosiderin. Erythrocytes had disappeared from the lesions by about the sixth day.

Innes and Saunders (1962) reported that this condition had also been described by Jubb (1957) in Canada; by Barlow (1958), and Robertson and Wilson (1958) in England; and by Harlow (1956) in Montana, U.S.A.

Jubb and Kennedy (1970) described two patterns of lesions in the brain, both bilaterally symmetrical, which they considered to be a more chronic form of enterotoxaemia. The most frequent pattern of lesions was of haemorrhage and softening in the basal ganglia, internal capsule, dorsolateral thalamus and substantia nigra. The second pattern was of lysis and liquefaction of the frontal gyri, sparing only the association fibres.

Pienaar and Thornton (1964) reported four outbreaks of FSE in 6 to 10 month old lambs in South Africa. In all cases lesions were present in the region of the internal capsule lateral to the basal ganglia, less frequently in the cerebellar peduncles and thalamus and, in one case, in the white matter of the frontal gyri. These yellowish-grey gelatinous foci were bilaterally symmetrical in distribution and some lesions showed cavitation. Lesions contained numerous gitter cells and, in the adjacent parenchyma, capillary proliferation, vacuolation, depletion of myelin and swollen degenerating axis cylinders were evident. Malacic lesions were restricted to the white matter.

Gay *et al.* (1975) described two broad clinical syndromes based upon observations in 14 outbreaks of FSE. Lesions were confined to the brain with an occasional sheep, succumbing after a brief clinical course, showing pulmonary congestion and oedema and early renal autolysis. In the acute syndrome, death occurred within 4 to 24 hours of the observed onset of clinical signs and affected sheep showed incoordination and muscle spasms and, when in lateral recumbency, convulsions and ophisthotonos. In the more chronic form, sheep survived up to 7 days and displayed a "dummy" syndrome with weakness during movement, aimless wandering and gradual collapse to sternal recumbency.

Griner (1961) produced an acute and subacute form of Type D intoxication in lambs by slow intravenous infusion of *Clostridium pefringens* Type D epsilon

toxin. Of fifty experimental lambs studied 42 were classified as acutely, and 8 subacutely, intoxicated. The lambs were conventionally reared with low antibody titres to epsilon toxin. In the acute form, the time of onset of clinical signs of intoxication following toxin administration varied from zero to 4 hours, depending upon the dose received, and death occurred between 30 minutes and 4 hours after signs were first observed. In the more protracted form, lambs exhibited signs of intoxication for up to 11 hours. In the acutely intoxicated group, no gross lesions were found, but multiple malacic foci were present in 3 lambs classified as subacute. These bilaterally symmetrical lesions were seen in the internal capsule, corpus striatum, putamen, thalamus, subcortical white matter, substantia nigra, hippocampus and cerebellar peduncles. Microscopically, the brain from acutely intoxicated lambs showed pronounced perivascular and intercellular oedema, the latter imparting a spongy appearance to the neuropil and was more severe in the white matter tracts of the basal ganglia, thalamus and cerebellar peduncles. Perivascular spaces frequently contained plasma protein. Some arteriolar walls appeared hyalinized. The areas of apparent predilection showed focal degeneration and necrosis. Lesions in the subacutely affected lambs were similar in nature but were more severe with malacic foci in white and grey matter, especially in the white matter tracts of the corpus striatum, internal capsule and thalamus. An occasional neutrophil was present in necrotic foci but, in general, inflammatory cells were absent.

Griner (1961) also produced brain lesions in mice by the administration of epsilon toxin. Although the extent and severity of the lesions was not always of the same degree on both sides of the brain, the anatomical distribution of lesions was reasonably consistent. Malacic lesions commonly were found in the basal ganglia, thalamus, corpus callosum, medial and lateral geniculate bodies, reticular substance, brachium pontis, vestibular nuclei and tracts and granular layer of the cerebellum. Less frequently, lesions were present in the

substantia nigra, red nucleus, medial lemniscus, roof nuclei of the fourth ventricle, corpus medullare cerebelli, and genu of the 7th cranial nerve and cerebral cortex. Neurological signs of intoxication included hyperaesthesia, chorea, ophistotonos, torticollis, incoordination, circling, convulsions and rolling. Microscopically, at 7 hours the neuropil appeared vacuolated in focal areas, perivascular spaces were widened but contained little plasma protein and a few groups of ganglion cells occasionally showed mild degenerative changes. At 18-24 hours, multiple malacic lesions were apparent in the cerebral cortex, basal ganglia, corpus callosum, cerebellar peduncles and white matter of the cerebellar folia but had not progressed to liquefaction necrosis. By 30 to 36 hours many lesions had liquefied, especially in the basal ganglia and thalamus. Extravasated erythrocytes were encountered frequently in these necrotic foci but neutrophils were absent. The granular layer of the cerebellum contained foci of necrotic cells. From the third day onward, astrocytic proliferation commenced in these areas of malacia and capillaries were invading from the periphery. Gitter cells, however, were not present at any stage. It was concluded that the pathogenesis of the brain lesions in intoxicated mice was an initial increase in vascular permeability followed by oedema, softening, liquefaction necrosis and resolution by glial scarring. The changes in neurones and glia were secondary to oedematization of the white matter.

Griner and Carlson (1961) using radioiodinated human serum albumin, demonstrated a dramatic increase (average 61 fold) in the distribution of the isotope in the brains of lambs intoxicated with epsilon toxin, indicating a marked increase in vascular permeability. The increase in brain weight compared to controls varied from 4.7 to 17.6%. Worthington *et al.* (1975) found that epsilon toxin had the effect of allowing the passage of ^{125}I-polyvinyl pyrrolidine and ^{125}I-human serum albumin into the mouse brain. These substances did not enter the brain of normal mice. Albumin passed very rapidly

into the brain and, with large doses of toxin, death ensued in 2-3 minutes by which time 1.5% of injected albumin had already entered the brain.

Worthington *et al.* (1973) had previously demonstrated that mice could be protected from the effects of epsilon toxin by the prior administration of relatively non-toxic formalinized prototoxin (FSP), the precursor of epsilon toxin. Subsequently Buxton (1976) provided some evidence for the existence of specific receptor sites for epsilon toxin on vascular endothelium. Using horseradish peroxidase (HRP) as a measure of vascular integrity, it was found that administration of epsilon toxin alone caused heavy diffuse deposits of reaction product throughout the brain, and it was concluded that most blood vessels were susceptible to the action of this toxin. By contrast, animals which had received FSP prior to the administration of toxin showed no extravasation of HRP. Since FSP is antigenically similar to epsilon toxin, it was hypothesized that FSP was bound to receptor sites, thus competitively blocking the action of epsilon toxin on the vascular endothelium, albeit for a short period. Buxton (1976) therefore considered that a tenable hypothesis for the genesis of the early changes in the brain in enterotoxaemia could be due to binding of epsilon toxin to receptor sites on the vascular endothelium causing deleterious changes in these cells which resulted in the opening of tight junctions and an egress of fluid. Astrocytic end-feet would swell progressively and eventually rupture into the extracellular space resulting in cerebral oedema.

Proposed receptor sites for this toxin were further investigated by Buxton (1978) who gave an intravenous dose of FSP and employed an indirect immunoperoxidase technique to demonstrate the presence of this antigen in various tissues. Reaction product was absent from control preparations but deposits were found in mice exposed to toxin on the luminal surface of vascular endothelium in many vessels in the thalamus, cerebral cortex, cerebellar white matter, cerebellar peduncles, pons and cerebral and cerebellar meninges. Buxton

did not mention whether these deposits were restricted to vessels in areas of apparent selective vulnerability to epsilon toxin, but implied that deposits were widespread in the brain. Ultrastructural observations in the kidney showed that reaction product was closely associated with the luminal surface of epithelial cells in the loop of Henle and distal convoluted tubules while only small amounts were present on capillary luminal surfaces. No reaction product was found in glomeruli, proximal convoluted tubules or collecting ducts. In the liver, reaction product was located on the luminal aspect of sinusoids, many centrilobular veins, a few large vessels, and several bile ducts. Some of the larger veins in the lung showed sparse deposits of reaction product and small deposits were found associated with capillary luminal surfaces in the myocardium. No reaction product was detected in small or large intestine or skeletal muscle. Buxton (1978) postulated that these binding sites represented the receptors for epsilon toxin as Buxton (1976) had shown that FSP and epsilon toxin could compete for the same receptor sites.

Bacterial enterotoxin has been shown to stimulate adenyl cyclase to produce increased amounts of cyclic 3',5'-monophosphate (cAMP), the latter causing enhanced fluid production by the intestine (Buxton, 1978). In view of these findings, Buxton (1978) investigated whether epsilon toxin could act by a similar mechanism. The toxin was found to elevate the plasma concentration of cAMP in mice. It has also been suggested that there is a cAMP-mediated mechanism in the skin for promoting increased vascular permeability which is not dependent upon mast cell histamine (Buxton, 1978). Buxton (1978) showed that epsilon toxin was apparently able to use this mechanism after intradermal injection into guinea-pig skin (in which histamine activity had been suppressed) to increase the permeability of cutaneous vessels to Evans blue dye. Thus epsilon toxin may be able to damage endothelial cells, after binding to receptor sites, by a mechanism mediated by an adenylcyclase-cAMP system.

In any review of the pathogenetic mechanisms involving cerebral vasculature cognizance must be taken of the 'blood - brain' barrier (BBB) phenomenon. This concept was introduced by Ehrlich a century ago based on the observation that dyes injected intravenously in laboratory animals, although escaping into the tissues of other organs, did not enter the brain parenchyma.

The anatomical component of the BBB is probably the endothelial cell of capillaries, and the overlapping edges of these cells with their continuous tight junctions make them unique. Other postulated structural components are the endothelial basement membrane, and the astrocytic end-feet which completely invest the surface of cerebral capillaries. In larger cerebral vessels, the vascular and glial basement membranes are distinctly separate but become fused at the capillary level. These glial foot-processes may have a regulatory transport role in fluid and electrolyte homeostasis (Manz, 1974). Ependymal cells covering the choroid plexus and the meninges have also been implicated. Pericytes are enclosed within leaves of the basement membrane and assist in removing substances from the extracellular space or those leaving the vascular lumen. In addition, the small size of the interstitial space in the brain may also conceivably restrict the movement of plasma solutes (Tschirgi, 1962). Finally, the metabolic activities of the central nervous system determine the rate of accumulation of blood borne solutes, and it has been proposed that metabolically inert compartments (e.g. myelin) exchange with surrounding fluids at a very slow rate.

The term BBB implies an anatomical barrier but may be more accurately looked at from the biochemical viewpoint as a time-dependent metabolic process since the mechanisms which prevent or permit passage through the endothelial cell are numerous and vary with the class of compound under consideration. Thus, to some compounds the endothelial cell represents a physical wall, others are degraded in these cells, and yet other compounds diffuse freely or are transported more rapidly when metabolic demands deem this appropriate. It

appears that solutes travel mainly through, and not between, endothelial cells in their passage from the plasma to extravascular fluids in the brain (Tschirgi, 1962).

In cerebral capillaries, a transendothelial ferrying system via scant pinocytotic vesicles is of minor importance, being apparently responsible only for transport of protein molecules and particles. Interendothelial tight junctions may act as a filter for small ions but unless injured prevent diffusion of large molecules. The basement membrane performs some barrier function for large molecules, and pericytes are phagocytic.

In most parts of the normal brain the three possible routes for penetration of tracer material across the endothelium of other organs (between endothelial cells, via cytoplasmic vesicles or through fenestrae) are not functional. Injected tracer material is halted at the tight junctionsbetween endothelial cells and the few cytoplasmic vesicles present remain free of tracer apart from a few at the luminal surface (Manz, 1974).

In oedema states, tracer permeates nearly all the extracellular space in oedematous areas. Cytoplasmic vesicles become much more numerous and fill with tracer material and many regard this as the major pathway for transport of tracers. Since tracer is also found lining the spaces between endothelial cells during oedema it is possible that tight junctions open under these conditions and permit passage of tracer substance out of vessels. In most regions of the brain, although very attenuated, endothelial cells do not possess fenestrae but in some chronic oedema states, fenestrae have been observed to develop in endothelial cells, allowing egress of large amounts of haematogenous material (Manz, 1974).

Klatzo (1967) proposed that cerebral oedema be classified as either 'vasogenic' or 'cytotoxic' while recognizing, however, that both types depend ultimately on some degree of enhanced vascular permeability, that one type may eventually secondarily assume some of the characteristics of the other, and some

injurious agents may result in the expression of both of these types of oedema

In vasogenic oedema, there is severe damage to endothelial cells which become incompetent and allow all plasma constituents to leave the blood vessels. The oedema accumulates chiefly in the white matter with enlargement of the extracellular space, and swelling of astrocytes and perivascular foot processes occurs in grey matter (the extracellular space in grey matter appears of normal size).

Cytotoxic oedema is manifest fundamentally as intracellular swelling due to a direct effect of the noxious influence on cellular elements of the parenchyma. The endothelial cells remain intact and the exuded fluid is a plasma ultrafiltrate. Depending on the inciting agent, oedema may be localized to grey or white matter with swelling of these cells and their processes and the extracellular space constitutes the immediate source of fluid which enters these cells in abnormal amounts. In its purest form cytotoxic oedema should result in a retraction of this space (provided cell membranes do not rupture). There is evidence to support this assumption (Klatzo, 1967).

It has long been recognized that white matter is much more susceptible to oedema and it is here that oedema can lead to tissue destruction (Manz, 1974). The cerebral cortex, on the other hand, is not particularly oedema prone. This situation is understandable as spaces in white matter may be in excess of 800 A^{o} in diameter whereas in grey matter unit membranes appear to be separated by only 100 to 200 A^{o} (Klatzo, 1967). Under increased fluid pressure in the extracellular space, cells being fluid -filled cannot be compressed but only separated and it is apparent that such separation may occur more easily between regularly arranged, parallel, myelinated nerve fibres in the white matter whereas the tangled connections between cells and lack of direct linear pathways in grey matter make fluid spread more difficult. Hydrodynamic forces induce fluid spread by diffusion, although coordinated movements of astrocytic membranes may assist in the spread of extravasated fluid (Klatzo,

1967). Vascular permeability at the site of injury is increased for a limited number of days and there may be no increase in the permeability of vessels in oedematous areas peripheral to the initial site of fluid exudation (Manz, 1974). Feigin and Popoff (1962) proposed that the relative sparing of the cortex in the presence of great enlargement of the white matter was due to the mechanical barrier posed by the arcuate fibres and their similarly disposed oligodendrocytes which are tangentially arranged to the cortex and thus fluid movement into the cortical grey matter is significantly impeded.

Oedema in the white matter is characterized by increased extracellular space and swelling of astrocytic processes; in grey matter fluid is largely confined to astrocytes, although rupture of cell membranes in severely swollen cells or in necrotic areas may cause dilation of extracellular spaces (Klatzo, 1967). Astrocytic swelling in oedematous conditions is so prominent that it was once considered that, unlike other tissues, oedema in the brain was intracellular with astrocytes being the equivalent of extracellular space in other organs (Hirano, 1980). Ultrastructural observations revealed very compact neuropil in the brain with very little extracellular space and fluid movement was thought to occur through the cytoplasm of astroglial cells (Klatzo, 1967). Markers used to estimate the size of the extracellular compartment, however, indicated that the extracellular space comprised 4-15% of brain volume (compared to 25-45% in other tissues), with very slow equilibration rates leading to the concept of a "blood- brain barrier" (Manz, 1974). Cerebral oedema, therefore, was essentially the same as that encountered in other organs with astrocytes perhaps constituting a "functional" extracellular space.

A number of mechanisms have been proposed for the resolution of oedema in the brain. Most of the fluid is thought to be removed by vessels in the parenchyma or subarachnoid spaces (Manz, 1974), although passage of fluid across the ependyma is a feasible route. Lymph capillaries are not present in the brain. Klatzo *et al*, (1980) considered, however, that oedema fluid was

cleared primarily by astrocytes. Plasma proteins can be phagocytosed by microglia and pericytes (Manz, 1974). Movement of fluid into capillaries in vesicles by retrograde pinocytosis has also been postulated (Cervos-Navarro and Ferszt, 1980).

CHAPTER III

EPSILON TOXIN

Bacteria classified as *Clostridium perfringens* are divided into the five groups, A to E, based on their ability to produce any of the 4 major lethal toxins (Table 2). Without exception, these toxins are proteins which are synthesized and released from intact cells during growth and, therefore, are true exotoxins (Hauschild, 1971). As these toxins are antigenic, typing is achieved by neutralization of lethal toxin with type specific antisera.

The molecular weight of epsilon toxin has been variously estimated as 38,000 (Orlans *et al*, 1960), 40,500 (Thomson, 1962) and 24,000 (Habeeb, 1969). The peculiar property of epsilon toxin, which it shares with iota toxin (not produced by Type D), is that it is produced as a non-toxic precursor (prototoxin) which requires proteolytic digestion for activation (Thomson, 1963). Prototoxin can be activated very rapidly by trypsin (but not by pepsin) which explains why all the epsilon toxin found in the intestinal contents of infected sheep is in the fully activated form and enters the circulation in a highly toxic state (Bullen, 1970). Only epsilon and iota toxins of *Clostridium perfringens* are absorbed from the intestinal tract (Willis, 1977). The disease is a pure toxaemia with no invasion of tissues by the organism.

The contribution of the other major lethal toxin produced by Type D strains, alpha toxin, to the pathogenesis of enterotoxaemia may be discounted. In addition to the presence of alpha toxin in Type D cultures contributing insignificantly to the assay of total lethal toxin, it is rapidly inactivated by trypsin, intestinal absorption does not occur (Hauschild, 1971) and alpha toxin does not pass the blood - brain barrier (Ellner, 1961) (it has, however, been shown to increase capillary permeability by Elder and Miles, 1957).

The conversion of prototoxin to toxin is due to the removal by proteolytic hydrolysis of a peptide, the fragment split off during this reaction being a very small part of the molecule. This fragment, while it is still attached to

the toxin molecule, prevents the molecule from exerting any toxic effect but does not alter its combination with antibody. All the antigenic determinants of the toxin give rise to neutralizing antibody (Orlans *et al*, 1960). Adequate levels of circulating epsilon antitoxin afford complete protection against enterotoxaemia (Hauschild, 1971).

The *Clostridia* have two primary habitats in nature, the soil and the intestinal contents of apparently normal sheep. *Clostridium perfringens* Type D, however, is largely restricted to the intestine and cannot long survive in the soil, and is probably unable to compete with Type A strains present (Smith, 1957). The presence of Type D organisms in the alimentary tract of large numbers of normal sheep is important since these organisms could provide the focus for a potentially fatal intoxication if conditions transpired which were favourable for the rapid multiplication of these strains (Bullen, 1970). Moreover, since bacteria cannot be eliminated from this site, a continuing program of vaccination is necessary to prevent the occurrence of clinical disease. Furthermore, measurable amounts of epsilon toxin have been found in serum of clinically normal, non-vaccinated, sheep indicating that epsilon toxin is produced without necessarily causing disease (Hauschild, 1971). Epsilon antitoxin has been demonstrated in up to 90% of carrier sheep in flocks where no vaccination was practiced (Hauschild, 1971).

Mouse protection test

The lethal effect of the toxin in mice was neutralized by Type D antiserum. A mouse protection test was performed by administering 0.2 ml of Pulpy Kidney Antitoxin (Commonwealth Serum Laboratories), containing not less than 60 units of antitoxin per ml, intravenously to 10 mice and, 5 hours later, 5 mice received 0.5 ml of a $^{1}/_{100}$ dilution and 5 mice a $^{1}/_{1000}$ dilution of activated prototoxin intravenously. All mice remained alive after 24 hours. Unprotected control mice died within this period.

LD_{50} estimations were performed using the method of Reed and Muench (1938). Activated prototoxin was prepared on October 31, 1981. Groups of 5 mice were used at each dilution and animals were injected intraperitoneally with 0.5 ml of toxin at dilutions ranging from 10^{-1} to 10^{-5}. The LD_{50} was defined as that dose of toxin which killed 50% of test mice within 24 hours. The following results were obtained:

Date performed	LD_{50}	Interval from toxin preparation
25/11/81	$10^{-3.72}$	25 days
17/4/82	$10^{-3.62}$	167 days
25/8/82	$10^{-3.33}$	295 days

This persistence of high levels of toxicity is in agreement with Niilo (1980) who reported that Type D filtrate (trypsinized) from sheep with enterotoxaemia maintained full toxicity for 326 days at 4°C. Cooling is an important factor in preserving toxicity of Type D filtrates. Gardner (1972) found toxicity was still detectable after 336 days in samples of ileal contents held at 4°C, but was lost in 84 days in aliquots held at room temperature. Toxicity is also maintained longer when the contents are removed from the intestine and filtered (Kohler and Freimuth 1971; Niilo, 1980).

Immune status of lambs

In order to assess the immune status of lambs used in this study, serum samples were collected from 9, 8-40 day old lambs which were contemporaries of the experimental animals and derived from ewes which had been vaccinated with *Clostridium perfringens* Type D toxoid 2-4 weeks prior to parturition. The assay for epsilon antitoxin was performed by the Bacteriology R and D section, Commonwealth Serum Laboratories, Melbourne and the results are set out in Table 1. It was apparent that high levels of immunity had been conferred by vaccination as levels of 0.1 to 0.2 *u*/ml are considered protective (Middleton, personal communication).

CHAPTER IV

MORPHOLOGICAL STUDIES OF THE BRAIN

Experimental studies by Gardner (1973), using immersion fixation, and Morgan and Kelly (1974) and Buxton and Morgan (1976), who employed the perfusion technique, in mice and lambs produced conflicting results regarding the site of primary morphological damage in brain exposed to epsilon toxin. The earliest pathological changes in such intoxicated brains, therefore, warrant further investigation. Some of the differing changes reported by these authors may have been due to the method of fixation employed and thus it was decided to study alterations in control and intoxicated brains by both immersion and perfusion techniques. Artifacts consequent upon removal of the brain after death and immersion in fixative are absent when the brain is fixed *in vivo* by intravascular perfusion (Blackwood and Corsellis, 1976).

The two cytological artifacts which could interfere with the interpretation of results in this study are the so-called "dark" or hyperchromatic neuron and swelling of astrocytic processes, especially around capillaries and neurones. In paraffin sections, dark neurones appear unevenly shrunken and stain intensely acidophilic with haematoxylin and eosin and ultrastructurally there is increased electron density of the nucleus and cytoplasm. This neuronal artifact, however, decreases as the interval between death and autopsy increases and does not occur in primates if this interval exceeds 10 hours (Brierley, 1973). The delay in human autopsies of this order explains why this artifact is uncommonly seen in such brains.

The evaluation of changes occuring in the later stages of a disease process in the brain is little hindered by immersion fixation but the unequivocal assessment of the earliest changes necessitates that neural tissue be perfusion-fixed (Blackwood and Corsellis, 1976).

MATERIALS AND METHODS

Experimental animals:

Studies were conducted on 8-12 week old, outbred Swiss white mice weighing 20-30 gm from the Waite Research Institute and Koonoona Merino lambs from the Turretfield Research Centre, Lyndoch, S.A. Details of the ages and weights of these lambs are given in Table 3.

Toxin preparation:

The toxin used in experimental studies was a partially purified prototoxin prepared from filtrates of broth cultures of *Clostridium perfringens* Type D and destined for use in the commercial production of a vaccine against ovine enterotoxaemia. One gram of 0.25% trypsin (Difco) was dissolved in 25 ml of phosphate buffered saline and 1 ml of a final dilution of this 1:250 solution added to 1 ml of prototoxin. This mixture was incubated at 37°C for 45 minutes to permit enzyme activation of the toxin, then stored in aliquots at -20°C until required.

Toxin administration:

Trypsin activated, partially purified epsilon toxin was injected intraperitoneally in mice in a single bolus of 0.5 ml. A $^{1}/_{300}$ dilution of toxin constituted a lethal dose and mice were dead 4-6 hours after administration. Mice given a sublethal dose of toxin received a $^{1}/_{3000}$ dilution. Control animals were given 0.5 ml saline intraperitoneally.

In lambs, toxin was administered via the jugular vein. Because the susceptibility of these animals to the toxin had not been determined prior to these experiments and since their immune status was uncertain, they were given 5 ml aliquots of undiluted toxin until nervous signs became apparent. The doses of toxin given to each lamb are recorded in Table 3. Lamb K2-420, however, received ~~a much smaller dose~~ < 5ml aliquot of toxin as it was thought to have been colostrum-deprived.

Fixation techniques:

a) Immersion

Mice were anaesthetized, decapitated, and the brain rapidly removed by a circumferential incision in the calvarium beginning and ending at the foramen magnum. One mm thick serial coronal sections were cut and placed in 10% buffered formalin or 2.5% glutaraldehyde in cacodylate buffer, for 24 hours and 2 hours, respectively, before further processing.

b) Perfusion:

Mice were anaesthetized with chloroform, the thorax opened rapidly, the right auricle incised and 20 ml of heparinized saline (9 g NaCl/1 containing 0.02 % of heparin) was injected into the left ventricle through a needle in the apex of the heart. When this solution had been infused and clear fluid issued from the auricle, the injection of 2.5% glutaraldehyde buffered in 0.1 M cacodylate buffer (pH 7.3) was commenced in a similar manner into the beating left ventricle. Fixation of the brain was heralded by muscle spasms which gradually progressed to rigidity of the carcass and 20 ml of fixative (kept at or close to body temperature) was administered via the ventricle. The calvarium was removed and the fixative applied to the exposed brain surface. The brain was then rapidly removed, immediately immersed in glutaraldehyde and small blocks of tissue were cut for processing for electron microscopy. Coronal slices were also sectioned for light microscope examination.

Tissue processing:

a) For light microscopy, tissues were processed to paraffin wax, 6 μm

sections cut and stained with haematoxylin and eosin (H & E). The embedding schedule is outlined below:

70% alcohol	60 minutes
80% alcohol	60 minutes
95% alcohol	60 minutes
100% alcohol, 2 changes each	60 minutes
100% alcohol (1 volume), methyl benzoate (1 volume)	180 minutes
1% celluloidin in methyl benzoate	overnight
"Peelaway" wax (Peelaway Scientific, California, U.S.A.) (in vacuum impregnator, 3 changes during)	90 minutes

Embedded in "Peelaway" wax.

In addition, selected tissues were stained with periodic acid - Schiff (PAS), luxol fast blue and the peroxidase - anti peroxidase (PAP) technique to detect glial fibrillary acidic protein (GFAP).

b) For electron microscopy, tissues were fixed in 2.5% glutaraldehyde buffered in 0.1 M cacodylate (pH 7.3) for 2 hours and post-fixed in 2% osmium tetroxide buffered in 0.1 M cacodylate (pH 7.3) for 1 hour. The tissue pieces were then dehydrated in increasing concentrations of ethanol, cleared in propylene oxide and embedded in an Epon-Araldite mixture (TAAB Laboratories, Reading, Berks., England).

The dehydrating and embedding schedules for tissue blocks are shown below:

Dehydration

30% ethanol	5 minutes
50% ethanol	5 minutes
75% ethanol	10 minutes
95% ethanol	10 minutes
100% ethanol	30 minutes
100% ethanol	30 minutes

Embedding

1) 100% propylene oxide, 2 changes, 15 minutes each.

2) Epon-araldite mixture (1 volume), propylene oxide (1 volume), 30 minutes.

3) Epon-araldite mixture (3 volumes), propylene oxide (1 volume), 60 minutes.

4) Epon-araldite mixture, 2 changes, 60 minutes each.

5) polymerize resin in moulds at 60^{o} overnight.

TAAB embedding mixture:

MNA (methyl nadic anhydride)	15.78 gm.
DDSA (dodecenyl succinic anhydride)	7.86 gm.
Embedding resin	26.35 gm.
DMP (2,4,6 tri (dimethylaminomethyl)phenol)	0.67 gm.

Sections (1 um) were stained with toluidine blue for screening by light microscopy. Ultrathin sections were cut on a Porter-Blum MT-2 ultramicrotome, mounted on copper grids, stained with uranyl acetate and lead citrate and examined with a JEOL 100C electron microscope.

Experiment 1:

In order to determine the distribution, severity and frequency of occurrence of lesions in different areas of the brain, two groups of mice were given a sublethal dose of toxin and sacrificed 24 hours post-inoculation. The first group contained 60 mice and received 3 such doses of toxin over the 24

hour period while the second group comprising 30 mice, received only a single dose. Brains were fixed by immersion in 10% buffered formalin.

Results are shown in Table 4.

Experiment 2:

This study was designed to examine the sequential changes in brain morphology during intoxication. One group of mice were given a lethal dose of toxin and groups of 5 animals sacrificed from 30 minutes to 6 hours post-injection and the brain fixed *in vivo* by perfusion with 2.5% glutaraldehyde in 0.1 M cacodylate buffer at pH 7.3. Another group were given multiple sublethal doses of toxin, the brain fixed by immersion and mice were killed from 6 hours to 7 days post-injection. Tissues were subjected to both light and electron microscopic examination and ultrastructural observations were based on blocks of tissue removed from the cerebral and cerebellar cortices and the corpus callosum of each animal.

CHAPTER V

MORPHOLOGICAL STUDIES OF THE BRAIN

CLINICAL FEATURES

Mice receiving a lethal dose of toxin showed signs of depression, uneasiness and reluctance to move about 30 minutes after administration. This soon progressed to severe depression, rapid, shallow respiration and hyperaesthesia. Head pressing was sometimes observed and at 4 hours, when mice were moribund, muscle tremors and convulsions commonly occurred. Many mice also demonstrated signs consistent with vestibular impairment such as head tilt, circling and violent rolling movements which could be precipitated by tactile or auditory stimulation. When these mice exhibiting cerebellar involvement were lifted by the tail they were clearly disoriented and often commenced a spinning motion.

Mice injected with a sublethal dose of toxin became moderately depressed with mild dyspnoea about 1 hour later or remained apparently normal. The number of mice showing clinical signs increased when 2-3 sublethal doses of toxin were administered over a 24 hour period and severely affected animals displayed signs described earlier but a proportion of mice always remained clinically normal. A few mice which appeared to be in the terminal stages of intoxication survived with no apparent neurological impairment or had a persistent head tilt.

These studies indicated that there was a considerable range of individual susceptibility to a given dose of toxin.

Intoxicated lambs became depressed, listless and incoordinated with dyspnoea being one of the earliest signs. The rapid, shallow respiration became gradually more pronounced and even sterterous, and marked cyanosis was evident prior to death. Excessive salivation occurred in the later stages of the illness. The gait became unsteady and progressed to sternal and then lateral recumbency. In the latter position, violent paddling movements of the limbs and convulsions were frequent, heralded and succeeded by hyperextension of

the forelimbs, arching of the back, and pronounced dorsiflexion of the head (ophistotonos).

GROSS PATHOLOGY

Mice:

With good perfusion, the carcass was hardened and rigid with slight yellowing of the tissues. The brain was firm, somewhat rubbery and yellowish in colour with no blood in meningeal vessels. Only brains which conformed to these criteria were used for further study.

The lungs were white in colour and the lobes enlarged, protruding out of the opened thoracic cavity when perfusion was completed. This appearance contrasted with the collapsed, pinkish coloured lungs of unperfused pulmonary tissue. The heart was yellowish in colour with coronary vessels devoid of blood. The reddish-tan colour of normal liver and kidney was replaced by a yellowish hue although it was apparent that fixation of abdominal organs was not always as complete as that obtained with brain and thoracic viscera by this method of perfusion. The kidney, in particular, often showed imperfectly perfused reddish coloured parenchyma juxtaposed with well-perfused yellow renal tissue.

Affected mice showed no significant gross alterations apart from the occasional animal in which the cerebellum was partially herniated through the foramen magnum.

Sheep:

In lamb K2-420, the brain was macroscopically normal except for very obvious congestion of meningeal vessels. The lungs were firm, wet, and reddish-grey in colour, and the thoracic cavity contained about 200 ml of straw-coloured fluid. A few petechial haemorrhages were present in the epicardium and endocardium and the pericardial sac contained an excess amount of clear fluid. The kidneys were markedly congested but otherwise of normal appearance and

consistency. The mucosa of the small intestine was intensely hyperaemic and the contents slightly more fluid than normal. The stomach was devoid of colostrum.

The brain from lamb K2-420 was used for further studies as it was considered that this animal had been "mismothered" and colostrum-deprived (no colostrum was found at autopsy) and it demonstrated the classical clinical and post-mortem findings of acute enterotoxaemia and thus probably approximated to the field situation. It was thought that the very large doses of toxin required to induce neurological signs in the other lambs may have rendered the latter situation somewhat atypical of the occurrence of the natural disease.

HISTOPATHOLOGY

Mice

In perfusion fixed control brain stained with H and E, the neuropil was compact with nerve fibres and glial processes imparting a fine, uniform granularity and a fibrillary arrangement was evident in the larger white matter tracts. In some areas of neuropil a very fine vacuolation was apparent, particularly beneath the ependyma and the cortex adjacent to the meninges and, to a lesser degree, in heavily myelinated fibre tracts. In the polymorphic and pyramidal layers of the hippocampus quite large clear vacuoles about 20 μm in diameter with no obvious cellular association and sometimes traversed by delicate strands of tissue were consistently present. The neuropil in this region also was slightly more coarsely vacuolated (about 5-7 μm in diameter) than in other sites.

Blood vessels were preserved in an open state and only a very occasional vessel contained a single erythrocyte. Capillaries were in direct apposition to the contiguous neuropil (Fig. 11, 12) but sometimes around larger vessels a small clear perivascular or Virchow-Robin space was discernible. Astrocytic end-feet were not identifiable by light microscopy.

Astrocytic nuclei were open and a little smaller than those of neurones sometimes possessing a basophilic dot or centrosome. The cytoplasm was not visible. Oligodendrocytes were represented by small, round deeply basophilic nuclei, resembling small lymphocytes, and cytoplasm was not apparent. Microglial cells had moderately basophilic, elongated rod-shaped nuclei, without detectable cytoplasm. Neurones were generally well-preserved with distinct nuclear membranes and uniformly distributed chromatin; cytoplasmic outlines were faint. In the cerebral cortex were scattered a few neurones with small dark-staining nuclei and deeply acidophilic cytoplasm which had a shrunken, angular appearance. Nuclear and cytoplasmic membranes of Purkinje cells were definite and only an occasional cell showed the "dark neuron" artifact. A few Purkinje

cells had small clear spaces around them which probably represented mild swelling of adjacent astrocytic processes and their cell bodies. The internal granular layer was compact with very little extracellular space.

In immersion fixed material, the neuropil was more loosely arranged with a more appreciable and widespread fine vacuolation. The vacuoles in the hippocampus mentioned earlier were somewhat larger. Many blood vessels, especially the smaller ones, were partially or completely collapsed and erythrocytes filled the lumina. In comparison to perfused nervous tissue, more blood vessels possessed a small non-staining perivascular space, sometimes traversed by fine strands, and this change was more obvious as the calibre of the vessel increased. Some astrocytes, particularly the fibrous type, were separated from the adjacent neuropil by a small clear space. Neurones in immersion fixed brain had a better defined, lightly basophilic, cytoplasm and post-mortem pyknomorphic chromophilia was more widespread. In the cerebellum, the majority of Purkinje cells showed shrinkage with more densely staining nuclei and enhanced acidophilia of the cytoplasm. These cells usually were suspended in irregular clear spaces and the granular layer was less compact.

In intoxicated brains subjected to a lethal dose of toxin, lesions were examined sequentially for up to 4 hours and the brain was perfusion fixed. At 1 hour, the most obvious change was the presence of clear spaces around most vessels, sometimes imparting a scalloped appearance around vessels of capillary size (Fig. 14). While blood vessels could still be readily found with lumina fixed in the fully open state and in close opposition to the neuropil, many were collapsed and not uncommonly contained apparently trapped erythrocytes which were not flushed out during perfusion and probably represented vascular stasis. Nearby vessels which were fully patent very rarely contained erythrocytes.

Fine vacuolation of the neuropil was present in many areas, particularly in the larger white matter tracts and areas such as the corpus striatum and thalamus and to a much lesser degree in the cerebral cortex. Many astrocytes

were surrounded by clear spaces and the nuclei of these cells were larger and paler than normal. Some neurones, notably those in the corpus striatum and thalamus, were also surrounded by small clear spaces but the neurones themselves appeared unaltered. In the Purkinje cell layer of the cerebellum many neurones were surrounded by non-staining spaces.

The above changes became progressively more obvious and at 4 hours, the neuropil, especially in white matter of paraventricular areas (Fig. 15), internal capsule, corpus callosum (Fig. 13) and vestibular tracts, had a coarse vacuolar appearance with separation of fibres by clear spaces imparting a coarse fibrillary appearance. Cerebral cortical grey matter was conspicuously much less involved in this process. In some of these areas, discrete vacuoles gave a distinctly bubbly appearance to the neuropil. Occasionally there were large spaces in the white matter with considerable separation and some fragmentation of nerve fibres and many astrocytes in these lesions now possessed a visible amount of eosinophilic cytoplasm.

At 4 hours, vacuolation of the Purkinje cell layer in the cerebellum was now quite conspicuous and the granular layer was less compactly arranged. A few small foci of necrosis were present in the granular layer with pyknotic nuclei of granule cells disposed in a non-staining matrix (Fig. 22).

Since most mice had succumbed to a lethal dose of toxin at 4 hours, the following description is based upon observations made in mice receiving multiple sublethal doses of toxin and fixed by immersion.

At 6 hours, there was readily apparent perivascular and intercellular oedema. Perivascular spaces were distended but contained no plasma exudate and most vessels were markedly hyperaemic. In the white matter, capillary haemorrhage was sometimes observed (Fig. 18) and astrocytes were reactive forming gemistocytes or occasionally degenerating with nuclear pyknosis and karyorrhexis. Vacuolation and rarefaction of the neuropil was most extensive in the corpus callosum and callosal radiations, the area lateral to the lateral

ventricle, corpus medullare cerebelli, vestibular area, corpus striatum and thalamus.

At 12 hours, small amounts of faintly eosinophilic plasma exudate were found adjacent to a few small blood vessels and astrocytic nuclei were swollen, vesicular and hypochromatic. In a few oligodendrocytes, a narrow rim of deeply eosinophilic cytoplasm was now visible and many capillary endothelial cells appeared hypertrophied. Occasionally oval, eosinophilic bodies representing swollen axons (spheroids, torpedoes or retraction bulbs) were visible in areas of white matter damage.

At 18 hours, fragmentation of glia in white matter lesions was more evident and in some of these areas, especially the corpus callosum, there were lakes of deeply eosinophilic plasma exudate (Fig. 17) which had a foamy, vacuolar appearance and stained strongly positive with the PAS technique. In the middle and deeper layers of the cerebral cortex discrete foci of spongy change (Fig. 16, 23) were sometimes found, occasionally contiguous with similar lesions in the subcortical white matter, and neurones in affected areas were shrunken and deeply eosinophilic; neurones in adjacent unaffected areas of cortex, however, appeared normal. In areas of corpus striatum (where grey and white matter are closely admixed) showing severe oedematization, some neurones demonstrated large vesicular nuclei and cytoplasmic vacuolation (Fig. 20) and a few were shrunken and deeply acidophilic. At this time, especially in the vestibular tracts, axons not uncommonly showed irregular, beaded swellings and were surrounded by an expanded, varicose, non-staining myelin sheath (Fig. 19). With fragmentation and retraction of the axon and its sheath, ellipsoids formed and often enclosed an oval, eosinophilic swollen axon (digestion chambers) (Fig. 25, 26). At a later stage, ellipsoids became less well-defined leaving an irregular pale-staining focus containing eosinophilic axonal debris and at the periphery of which compound granular corpuscles (gitter cells) had appeared.

At 24 hours, white matter lesions in some areas had progressed to malacia with the neuropil presenting a lacy appearance with fibres widely separated by clear spaces containing a few small, round deeply basophilic nuclei, most of which represented pyknotic astrocytic nuclei with a few surviving oligodendrocytes (Fig. 21, 24). Extravasated erythrocytes were sometimes numerous in malacic foci and, at the periphery of these lesions, astrocytic nuclei were enlarged and hypochromatic, endothelial cells were swollen and there was a slight increase in the number of rod-shaped microglial cells. When sections were stained with luxol fast blue, they revealed extensive loss of myelin and correlation of malacic foci with control sections of brain stained with luxol fast blue indicated that the majority of lesions were confined to heavily myelinated regions of brain (Fig. 3, 5). No polymorphs or lymphocytes were seen in any malacic foci in the brain at any stage. A few necrotic areas had undergone complete liquefaction necrosis with empty spaces devoid of any tissue and this change was most commonly observed in the corpus callosum, sometimes resulting in separation of the white matter from the overlying cerebral cortical grey matter. In brains examined at 7 days, the malacic foci were almost completely filled with gitter cells (Fig. 27, 29, 30), which had small, round nuclei with clumps of chromatin and a clear, vacuolated or finely granular cytoplasm (Fig. 32). These lesions also contained fibrous astrocytes, whose processes stained dark brown with the PAP technique to detect GFAP, and axonal debris. Capillaries were seen to be invading the organizing focus at the periphery. In a few brains incidentally, lesions in an advanced stage of resolution were found. These cellular foci were composed of proliferating glial cells with oval to elongated nuclei, which probably represented fibrous astrocytes, together with peripheral invasion by capillaries (Fig. 31).

Lesions consistently manifested three features. The malacic foci were often focal; they were commonly, though not always, bilaterally symmetrical; and they were usually confined to the white matter with neuronal changes apparently

secondary to oedematization of the neuropil. Furthermore, mice given the same dose of toxin different in their susceptibility. Some animals showed minimal or no lesions when sacrificed and lesions were often at different stages of development at the same time post-administration of toxin. There was a tendency for lesions to occur consistently in certain regions of apparent selective vulnerability but the extent of these lesions increased with enhanced susceptibility of the host animal to the action of the toxin. Therefore, the above histopathological description represents a picture of the most typical sequential development of lesions.

Lesions were most commonly found in the corpus callosum, radiato corporis callosi, corpus striatum (especially the caudate nucleus, putamen and internal capsule and less commonly the globus pallidus), cerebral cortex, vestibular nuclei and tracts, corpus medullare cerebelli, thalamus, granular layer of the cerebellum, roof nuclei of the IV ventricle and the paraventricular area lateral to the lateral ventricles. Less frequently, malacic lesions were found in the anterior commissures, substantia nigra, the fimbria and alveus hippocampi and the fornix (Fig. 1,2,4,6,7,8,9,10). No malacic foci were found in the spinal cord.

Sheep

In lambs, brains were fixed by immersion and central nervous tissue from control animals was morphologically similar to that of control mice. The neuropil was compact but more coarsely granular than in mice with a fine fibrillary pattern usually discernible and in some areas a fine vacuolation was present. In the heavily myelinated fibre tracts in sheep the larger fibre size imparted a much more coarse fibrillary pattern. Neuronal preservation was generally good with nuclear and cytoplasmic membranes well-defined and the cytoplasm showing a light basophilia. Most neurones were closely apposed to the surrounding neuropil but some possessed a small perineuronal clear space. There were, however, always a few shrunken, deeply amphophilic neurones present with

larger surrounding clear spaces. A small number of astrocytic nuclei were also surrounded by a small clear space. Some blood vessels were surrounded by small non-staining spaces traversed by fine strands giving a somewhat serrated appearance; occasionally these perivascular spaces were quite large. A proportion of vessels were seen to be partially collapsed.

In lamb K2-420, which died 3 hours after administration of toxin, perivascular spaces were considerably enlarged compared to controls and discontinuity was often observed in the fine strands which spanned these spaces. Blood vessels were very congested and the lumen appeared to be considerably narrowed in those with the greatest perivascular swelling. Rarely, a small amount of proteinaceous exudate was found in these spaces. The majority of neurones were also possessed of a surrounding clear space between the cell membrane and adjacent neuropil as were astrocytic and oligodendroglial nuclei. A small amount of eosinophilic cytoplasm was sometimes visible in these glial cells. Neuronal changes were usually not detected, except for a scattering of "dark" neurones also seen in controls, but a few neurones showed more hypochromatic nuclei and a few small cytoplasmic vacuoles. Extravasation of erythrocytes was rarely encountered. In many areas the neuropil was finely vacuolated but in some regions vacuoles were larger (5-8μ in diameter) and were present in greatest concentration in the neuropil adjacent to affected blood vessels. Purkinje cells were well preserved with only a few neurones showing shrinkage and marked eosinophilia and there was no increase in the number of the latter cells compared to controls. The Purkinje cell and granular layers were somewhat less compact in K2-420 compared to cerebellum from control lambs.

ULTRASTRUCTURAL PATHOLOGY

In control mice with good perfusion of the cerebral cortex, the neuropil was compact with close apposition of cell membranes and very little extracellular space. The neuropil (Fig. 41) in cortices was composed largely of the processes of protoplasmic astrocytes (in some of which fibrils were visible in the cytoplasm), non-myelinated axons (differentiated from other elements by the presence of synaptic vesicles in the axoplasm) and dendrites (recognized by their uniformly distributed complement of microtubules and irregular outline in transverse section) ~~(Fig. 41)~~. The occasional myelinated axon was also present.

In sections taken from the corpus callosum, where myelinated axons were in abundance, a proportion of these axons showed separation of myelin lamellae which, however, was restricted to segments of the sheath and caused focal distortion of the shape of the myelin sheath (Fig. 45). This disturbance of myelin lamination has been reported to occur in many careful preparations of nervous tissue.

Neurones were generally well-preserved in perfusion fixed material but in brain fixed by immersion, neurones sometimes appeared shrunken, distorted and very electron dense with multi-vacuolation of the cytoplasm.

In perfusion fixed brain, capillary endothelial cells showed moderately electron dense cytoplasm containing a few mitochondria and sparse endoplasmic reticulum; glycogen granules were usually numerous and a few small micropinocytotic vesicles were present. The lumen was fully patent and the endothelial cell of uniform thickness. Intercellular junctions were closely apposed and tight junctions were commonly seen in sections. The basal lamina appeared as a moderately electron dense, amorphous band of uniform thickness and in some sections divided to enclose a pericyte. Occasionally small "blebs" of endothelial cytoplasm protruded into the lumen.

The astrocytic end-feet directly surrounded the capillary and were closely applied to the endothelial basal lamina (Fig. 41, 42). The cytoplasm contained both mitochondria and endoplasmic reticulum.

In brain tissue fixed by immersion, the capillary lumen was irregular in outline, the endothelium not of uniform thickness and the endothelial cytoplasm slightly more electron lucent than perfused material. The preservation of organelles was poorer with mitochondria, in particular, often being swollen and less electron dense with disruption of cristae. The lumina of vessels often contained erythrocytes and finely granular, moderately electron dense, precipitated serum proteins. Astrocytic end-feet were nearly always swollen to some degree (Fig. 43) resulting in the vessel being surrounded by a scalloped clear space traversed by cell membranes of glial cells and containing improperly preserved organelles. In brain fixed by perfusion the neuropil displayed a uniform, moderate electron density, but in immersion fixed tissue the neuropil was less compact and appeared patchily electron lucent due mainly to swelling of astrocytes and their processes. Axons and dendrites were also less electron opaque and cytoplasmic organelles imperfectly preserved.

Around larger vessels the potential perivascular or Virchow-Robin space contained cell bodies and processes and collagen fibres; this space was not present at the capillary level.

In the cerebellum, the Purkinje cells in perfused brain were generally well-preserved (Fig. 44) but in some cells both nucleus and cytoplasm showed shrinkage and marked electron density. There was occasionally mild swelling of the surrounding processes of the protoplasmic astrocytes. The nuclei of these astrocytes were irregular in shape with relatively homogeneous karyoplasm, although condensations occurred beneath the nuclear envelope and in a few sites in the centre of the nucleus (Fig. 44); the cytoplasm was confined to a thin rim around the nucleus and contained only a few organelles. The granule cells were small neurones and as a result most of the cell body was occupied by the nucleus

which contained several large chromatin aggregates (Fig 44). The plasma membranes of these granule cells were often closely apposed.

The following description of the sequential development of the early lesions in the brain resulting from a lethal dose of toxin is restricted to perfusion fixed material from mice.

At 30 minutes post-administration, the most conspicuous change was marked enlargement of astrocytic end-feet (Fig. 48). These foot processes were large, electron lucent spaces spanned by cell membranes of glial cells, some of which were discontinuous. Present in this clear space were ghost outlines of organelles and swollen mitochondria, with either severely disrupted cristae or lacking entirely any internal structure were prominent. Adjacent to capillaries small pools of finely granular, moderately electron dense proteinaceous material were sometimes observed (Fig. 50). In capillaries, intercellular junctions appeared less closely apposed (especially on the luminal aspect), pinocytotic vesicles were slightly augmented in size and number, and the cytoplasm was less electron dense. Mitochondria were swollen with disorganization of cristae, and the basal lamina appeared slightly more electron dense. The lumina of affected vessels sometimes appeared to be greatly narrowed (Fig. 48). Occasionally, swollen astrocytes with a more electron lucent nucleus and cytoplasm, the former showing less evenly distributed chromatin, were seen lying close to these vessels (Fig. 47). In the neuropil, astrocytic processes were enlarged and of decreased electron density (Fig. 74), and structures immediately adjacent to these expanded processes appeared somewhat compressed. Neurones appeared to be unaffected.

In the cerebellum, the cytoplasm of astrocytes was very swollen with greatly dilated endoplasmic reticulum and mitochondria, many of the latter possessing little discernible internal architecture (Fig. 46, 49). Cytoplasmic boundaries of these cells were often indistinct and appeared to be ruptured in some areas. Many granule cells had expanded, electron lucent cytoplasm with,

little organelle detail apparent (Fig. 53). Granule cell nuclei were less electron dense with reduced chromatin clumping in some. The nuclei and cytoplasm of a few Purkinje cells were very dark, but, as this change was also seen in controls, it is probably not significant. Astrocytic processes around Purkinje cells were also swollen.

At this stage, apart from mitochondrial swelling, degenerative changes were not seen in capillary endothelial cells and the most obvious alteration was the marked enlargement of astrocytes and their processes, especially in the perivascular extension of these cells.

At 1 hour, perivascular end-feet swelling was still marked but, in addition, evidence of severe damage to endothelial cells was present. Finely granular, moderately electron dense pools of plasma exudate were now more common near vessels (Fig. 50) and this finding was much more frequently encountered at the ultrastructural than the light microscope level. Affected endothelium was often so electron dense that the internal structure of the cytoplasm was obscured. Clear cytoplasmic vacuoles (Fig. 64) were often present and the endothelium frequently appeared very attenuated. Some endothelial cell nuclei were pyknotic and very electron dense and the luminal surface was irregular with conspicuous "blebbing" (Fig. 55). The basal lamina was more electron dense than controls and appeared to be split at some sites. Pericytes usually appeared comparatively normal at this time, apart from the mitochondrial changes described earlier in the endothelium. It was noted, however, that some vessels in areas where other pathological changes were well advanced appeared relatively normal (Fig. 69) and this was a consistent finding at all stages of lesion development studied. Moreover, glial end-feet swelling was sometimes mild when endothelial damage in contiguous vessels was severe. A few neurones showed a modest increase in electron lucency of the nucleus and cytoplasm and occasionally the cytoplasm of oligodendrocytes was slightly increased in amount and clarity (Fig. 72).

In the cerebellum, swelling of astrocytes was more severe with fragments of organelles dispersed in an enlarged, clear cytoplasm often lacking definite cell outlines (Fig. 56, 58, 61). Clumping of chromatin in the nuclei of these cells was more pronounced and changes in granule cells were of a similar magnitude to those described at 30 minutes.

At 2 hours, changes similar to those seen at 1 hour were observed in endothelium with "blebbing" more prominent. Some vessels also appeared to be at an intermediate stage of degeneration with the cytoplasm condensed into electron dense bands (Fig. 65, 73).

In the corpus callosum, lamellation of myelin was more severely disturbed with spaces of decreased electron density between the myelin layers. Although this change was also observed in controls, splitting of the sheath was more severe and less segmented in toxin treated mice (Fig. 63). Axon cylinders appeared distended (Fig. 66, 67, 68) and there was enlargement of the extracellular space with increased distance between cellular elements; sometimes axons appeared to be floating in a structureless matrix of low electron density (Fig. 70). Progressive swelling of astrocytes was apparent in the cerebellum (Fig. 57, 60) with rupture of cell membranes creating a "pseudo-extracellular space" in some areas.

At 3 hours, the endothelium of many capillaries was reduced to a thin, electron dense band with multivacuolation of the cytoplasm in which no sub-cellular structure such as organelles could be detected. The pericyte nuclei appeared unaffected, and the cytoplasm, although more electron lucent, appeared to be reasonably well-preserved. The basal lamina was now quite electron dense in some vessels and "blebbing" in many lumina was severe. Sometimes, perivascular swelling had progressed to such a degree that stenosis of the capillary lumen was apparent, and, at a short distance from such a vessel in the neuropil, there was a focal area of degeneration with fragments of cell processes and remnants of organelles scattered in an electron lucent matrix.

Once again, it was not uncommon to find damaged blood vessels in close association with more normal vessels.

Some granule cells in the cerebellum possessed nuclei of much reduced size and slightly enhanced electron density, and there was loss of cytoplasmic detail and appreciable cellular borders.

At 4 hours, changes were similar to those evident 1 hour earlier, but it was not uncommon to find in the cerebellum capillaries showing attenuation and marked electron density of the cytoplasm with, however, little or no swelling of astrocytic end-feet (Fig. 59).

At 5 hours, pericyte nuclei were showing condensation of nuclear chromatin and enhanced electron density; the cytoplasm was much less electron dense with some disintegration of organelles. In a few vessels with "dark" endothelial cells the basal lamina, in addition to its greater electron density, appeared to be thickened over some of its length. A few neurones now showed mild shrinkage with enhanced electron density and mild cytoplasmic vacuolation (Fig. 69).

At 24 hours, in mice given a single sublethal dose of toxin and examined at 24 hours, there was mild to moderate swelling of astrocytic end-feet and processes. In some capillaries, stenosis of the lumen appeared to be present only where end-feet were greatly swollen; where swelling was mild or minimal around the same vessel, the lumen was apparently patent (Fig. 62). Apart from mitochondrial swelling, capillaries appeared morphologically unaffected. Swelling of astrocytes and the cytoplasm of granule cells in the cerebellum was moderately severe.

Rarely, in immersion fixed brain, evidence of stasis and platelet aggregations (Fig. 80) was apparent in the lumina of some vessels. In blood vessels showing stasis, erythrocytes, leucocytes and finely granular serum protein were found in the lumen. In these vessels, endothelial cells were either comparatively normal or showed increased electron density. Present in a few capillaries were aggregates of platelets closely packed together.

In a few sections were present large lakes of homogeneous, moderately electron dense proteinaceous material (Fig. 71, 72) with marked enlargement of extracellular spaces with glial processes and nerve fibres widely separated; the axons and dendrites were often very dilated with increased electron lucency and little internal structure.

In lamb K2-420, which died 3 hours after injection of toxin, ultrastructural findings were similar to those described in mice. Perivascular endfeet were greatly swollen resulting in a large electron lucent space around capillaries with loss of detail of many glial limiting membranes and remnants of organelles adrift in this structureless matrix. The "dark" endothelial cells seen in mice at this stage, however, did not have their counterpart in this lamb. Endothelial cells were attenuated with either slightly increased electron density or enhanced electron lucency of the cytoplasm with some disintegration of organelles evident. In some vessels the basal lamina demonstrated a marked increase in electron density. A small amount of granular, moderately electron dense protein exudate was noted around some blood vessels. In the neuropil, astrocytic processes were very dilated with clear "watery" cytoplasm largely devoid of organelles. Both myelinated and non-myelinated axons were swollen with a few mitochondria in various stages of dissolution being the only reminder of any pre-existing internal structure. Myelin sheaths showed considerable splitting of lamellae often with intramyelinic vacuole formation; sometimes only one or two lamellae remained and the outer layer occasionally appeared to have ruptured into the extracellular space.

Discussion

Experiment 1

Lesions were very variable in their distribution and severity but were consistent with findings in mice by Griner (1961) and Morgan and Kelly (1974) and similar to the distribution of lesions in lambs described by Hartley (1956) and Griner (1961). In mice, however, more regions of the brain appeared to be susceptible to the action of epsilon toxin than sheep.

Areas of the mouse brain most commonly affected in this study were the cerebral cortex, corpus striatum, vestibular area, corpus callosum and corpus medullare cerebelli and the proportion of mice which developed lesions increased when multiple rather than a single dose of toxin was given. This latter finding agrees with observations by Morgan and Kelly (1974). These authors considered that the dorsolateral aspect of the corpus medullare cerebelli and the paraventricular area lateral to the lateral ventricles were the sites where the initial lesions developed since lesions occured in these two areas in all mice where histological changes were detected and were the only areas affected in 8 of 16 mice. In the group of mice given a single dose of toxin, lesions only occured in a few mice but the granular layer of the cerebellum was the region where lesions were seen with the greatest frequency in these animals. Light and ultra structural findings in experiment 2 lend support to the view that this was possibly the area where lesions first developed in the present study.

Experiment 2

The earliest ultrastructural change in mice exposed to epsilon toxin was swelling of astrocytes and their processes, particularly the perivascularly disposed extensions of these cells, at 30 minutes. Also at this time prominent swelling

of astrocytes, and to a lesser degree granule cells, was evident in the cerebellum. At 1 hour, the above changes were more severe but, in addition, damage to capillary endothelial cells was apparent with endothelium attenuated, vacuolated and very electron dense. Cytoplasmic "blebs" projecting into the vessel lumen were prominent and swelling of astrocytic end-feet appeared to be causing stenosis of many capillary lumina. Leakage of plasma protein was observed. It was consistently found that not all capillaries were affected and, even in areas of extensive parenchymal damage, severely damaged vessels could be seen near capillaries showing no apparent abnormality. In white matter tracts, axonal swelling and separation of myelin lamellae were observed relatively early in the disease. Involvement of neurones and pericytes in the degenerative process was a comparatively late phenomenon and generally mild. As lesions developed, evidence of egress of large amounts of plasma protein was occasionally noted.

It appears, therefore, that changes in the neuropil preceded evidence of *morphological* changes in capillary endothelium, albeit by a short time interval, and that lesions developed rapidly after toxin administration. In intoxicated mice, the sequence of pathological events at the ultra structural level appeared initially to be damage to capillary endothelium severe enough to cause fluid transudation from blood vessels but not manifest in this early phase by morphologically detectable changes in capillaries. Concomitant with this escape of fluid was swelling of perivascular end-feet and astrocytes and their processes in the neuropil. Astrocytes in the cerebellum appeared to be especially vulnerable. Distortion of myelin lamellation with electron lucent spaces between the layers of myelin was found by Long *et al* (1966) in human cerebral

oedema and is present in a number of other intoxications. This change is generally attributed to fluid accumulation between myelin lamellae.

The present results were consistent with findings by Morgan and Kelly (1974) to the extent that the earliest morphological changes in mice were in the neuropil. These authors, however, regarded periaxonal and intramyelinic oedema in the white matter and swelling of axon terminals and dendrites in grey matter as the sites of earliest lesion development. They found that, apart from mitochondrial swelling, no morphological changes were present in capillaries in the early lesions and capillary endothelial damage was considered to be feature of more mature lesions in the brain. Morgan and Kelly concluded, however, that the primary lesion was probably in the vascular endothelium, possibly involving mitochondria, rather than a direct effect of the toxin on brain parenchyma. They observed that in malacic lesions, leakage of plasma proteins and erythrocytes always occured in association with platelet thrombi in vessels and may have been a result of microthrombosis, but conceded that platelet adhesion may have been a reflection of pre-existing damage to capillary endothelium. Such thrombi were rarely seen in this study.

Gardner (1973) regarded astrocytic swelling in the cerebellar granular layer as the site of initial pathological events in the brain of mice. Gardner concluded that the basic lesion was vascular endothelial damage and other changes, swelling of astrocytes and their processes around blood vessels and in the neuropil, were the result of this vascular injury. Endothelial changes reported by Gardner (1973) and Morgan and Kelly (1974) were of the type found in this study. Gardner (1973) described discontinuities in the endothelial lining, with platelet adhesion in some cases, but the basal lamina was unaffected;

neurones appeared normal. Gardner used immersion fixation whereas Morgan and Kelly (1974) employed perfusion. Morgan *et al* (1975) found that the earliest change detected by light or electron microscopy in mice, in the absence of a tracer, was 6 hours after administration of toxin. Morgan *et al* (1975), using horseradish peroxidase, proved that vascular leakage occured several hours before morphological changes were evident as escape of tracer material was noted 20 minutes after injection in intoxicated mice. Gardner (1974) also found extravasation of HRP in the brains of mice 1 hour after administration of toxin and the mean water content of the brains of intoxicated mice was significantly greater than controls. Morphological changes were detected much earlier in this study.

The findings in lamb K2-420 were similar to changes seen in mice at 3 hours but evidence of severe endothelial damage in this lamb was lacking. Morgan and Kelly (1976), however, using colostrum-deprived lambs, reported that the principle ultrastructural change was "dark" endothelial cells showing increased electron density, nuclear pyknosis and loss of cytoplasmic organelles, surrounded by swollen astrocytic end-feet. Astrocytes in the Purkinje layer of the cerebellum were consistently found to be swollen in this lamb.

The clear perivascular spaces seen in haematoxylin and eosin sections corresponded to swelling of astrocytic end-feet. The light microscope counterpart of the ultrastructural changes in the neuropil was a status spongiosus with the vacuoles in the parenchyma being a reflection of swollen astrocytes and their processes, hydropic axonal swelling, intramyelinic fluid accumulation and enlarged extracellular spaces. The perineuronal clear spaces sometimes observed corresponded to swelling of surrounding astrocytic processes. Swelling of astrocytes and granule cells accounted for the vacuolation

observed in the Purkinje and granular layers of the cerebellum. Vacuolated neurones and swelling of oligodendrocytes may also contribute to this vacuolar appearance in central nervous tissue but changes in these cells were minimal in intoxicated mice.

Swelling of astrocytic cytoplasm is the most common and least specific finding in the early glial reaction to injury in the brain, especially in oedematous states. This accounts for swelling of astrocytes and their processes, particularly in perivascular locations, in control brains fixed by immersion or improperly perfused as some degree of post-mortem autolysis had occured under these conditions.

Lesions in intoxicated brains were essentially confined to the white matter which is recognized as being much more susceptible than grey matter to oedema and the changes attributable to oedema consist essentially of degeneration of white matter.

In general, oedema in white matter is characterized by widening of extracellular spaces and swelling of astrocytic processes; in grey matter fluid accumulation is confined to cells, especially astrocytes (Adornato and Lampert, 1971). At the light microscope level, astrocytic swelling is suspected when vacuoles are seen in regions known to be occupied by astrocytic processes i.e. around blood vessels and nerve cells. In contrast, status spongiosus confined principally to grey matter is related mainly to swelling or vacuolation of nerve cells or neuronal processes and has a distinctive light microscopic appearance with vacuoles located within the neuropil but rarely around blood vessels.

The early changes in epsilon intoxicated brain correspond to Klatzo's (1967) vasogenic oedema in which the mechanism of fluid accumulation is via severe endothelial damage and oedema fluid is chiefly localized to white matter and composed of plasma filtrate, including plasma proteins. Perivascular astrocytic foot processes are swollen and the extracellular space increases in size.

The histological findings in older lesions in the present study resembled those described in mice by Griner (1961). Griner found lesions of non-inflammatory necrosis and haemorrhage at 18-24 hours which progressed to liquefaction necrosis by 30-36 hours. No neutrophils or other inflammatory cells were found in this study either. Also in Griner's experiments, at no stage of the development of neurological lesions in mice were gitter cells found which is surprising as these cells are to be anticipated in any malacic lesion undergoing resolution, particularly where extensive destruction of myelin has occured. In the present study gitter cells were numerous in malacic foci undergoing resolution. From day 4, lesions were characterized by capillary invasion and astrocytic infiltration into these malacic foci.

Three prominent histological changes found in the present study, namely perivascular oedema, haemorrhages and focal malacia in certain regions of the brain, although not diagnostic in themselves, were considered by Buxton *et al* (1978) to be very suggestive of enterotoxaemia caused by *Clostridium perfringens* Type D when present together in affected lambs. These authors examined brains from 18 field cases of clinical enterotoxaemia, each of which recorded positive results for the presence of Type D toxin in ileal contents. The diagnosis of this condition is usually based upon characteristic clinical signs and gross autopsy findings and the detection of toxin in intestinal contents. The presence of toxin in the absence of relevant clinical and pathological findings, however, is insufficient

to sustain a diagnosis and failure to detect the presence of toxin does not exclude the diagnosis.

Cerebral Oedema in Water Intoxication

Excessive systemic water intake has been shown to produce cerebral swelling in laboratory animals (Wasterlain and Posner, 1968; Wasterlain and Torack, 1968) and it was proposed to compare the ultrastructural changes in this model of cerebral oedema with those found in epsilon intoxicated brains, in which diffuse cerebral oedema appears to be an early and important change.

Materials and methods:

Mice were injected intraperitoneally with a volume of distilled water equivalent to 30% of their body weight. 15 minutes prior to injection of the water, each animal received 2 units of pitressin (Parke-Davis & Co.) as Wasterlain and Posner (1968) had completely inhibited urinary excretion in rats by this method in a similar experiment. 60 minutes after the water load was administered mice were *in extremis* and were anaesthetized, perfused and the brain prepared routinely for electron microscopic examination.

Results:

Mice became very depressed about 10 minutes after injection of the water with hyperpnoea and head pressing and were moribund at 60 minutes.

Ultrastructural examination of the brain revealed severely dilated perivascular foot processes of astrocytes with a large electron lucent space substantially

devoid of organelles, except for a few mitochondria, most of which showed disruption of cristae. Most tight junctions between astrocytic foot processes appeared to be intact but rupture of astrocytic membranes was sometimes seen. Astrocytes and their processes were also severely oedematous and the extracellular spaces between adjacent structures in the white matter were greatly enlarged. Endothelial cells appeared to be unaltered, however the lumen was often considerably reduced in diameter corresponding to areas of greatest end-feet swelling.

Discussion:

Ultrastructural changes in water intoxicated mice were similar to those found in mice exposed to epsilon toxin and resembled findings by Long *et al* (1966) in human cerebral oedema. Swelling of astrocytes and their processes, especially those in contact with capillaries, was marked and enlargement of extracellular spaces was evident. These findings tend to confirm that the early changes induced in nervous tissue by epsilon toxin are essentially those of oedema and, as endothelial cells in water intoxicated mice appeared relatively normal, the degenerative changes seen in these cells in epsilon intoxicated mice appear to be due to a direct effect of the toxin on the vasculature.

CHAPTER VI

TRACER STUDIES OF THE BRAIN

Horseradish peroxidase

The results obtained from light and electron microscopic studies on intoxicated brains suggested that there was increased vascular permeability and it was decided to use horseradish peroxidase (HRP) as a vascular tracer to determine whether extravasation of this enzyme would occur in toxin treated mice. HRP is a small molecular weight protein (40,000) which is not membrane bound *in vivo* and the half-life of this tracer in the circulation is less than 30 minutes, suggesting also that there is little significant binding to serum proteins (Hirano *et al*, 1969).

Materials and Methods

Mice were subjected to a lethal dose of toxin injected intraperitoneally and 1 hour after toxin administration, 10 mg HRP (Peroxydase Grad II (Lyophilisat), Boehringer Mannheim GmbH, W. Germany) in 0.5 ml of distilled water was injected via a tail vein. Mice were sacrificed 10 minutes after HRP was given.

Brain was immersion fixed in Karnovsky's fixative prepared by dissolving 2 gm of paraformaldehyde powder in 25 ml of water heated to 60-70°C. 1-3 drops of IN NaOH were added until the solution cleared. The mixture was cooled, 5 ml of 50% glutaraldehyde added and the volume made up to 50 ml with 0.2 M cacodylate buffer, pH 7.4 - 7.6. 25 mg $CaCl_2$ anhydrous was also added. The final pH was 7.2. A few brains were also fixed by perfusion but in this case 2.5% glutaraldehyde alone was used as the high osmolality of Karnovsky's fixative may cause tissue shrinkage when perfused; shrinkage, however, is unusual when material is fixed by immersion (Karnovsky, 1965).

After overnight fixation, small blocks of tissue were washed in 0.1M cacodylate buffer and incubated for 60 minutes at room temperature in the dark in 0.05M TrisHCl buffer, at pH 7.6, containing 5 mg of 3-3 diaminobenzidine tetrahydrochloride (DAB) (Sigma Chemical Company) per 10ml of buffer and a final concentration of 0.01% H_2O_2. Tissue was then post-fixed in 2% osmium tetroxide in cacodylate buffer and subsequent steps in preparation for electron microscopy were routine. Ten control mice were, a) injected with HRP in the absence of toxin and b) received no HRP but brain slices were exposed to the incubation medium.

12-20 um frozen sections of coronal slices of brain were also cut, placed on albumin - coated glass slides and incubated for 15 minutes in DAB as above. The sections were then washed and lightly counterstained with haematoxylin.

Results:

When frozen sections were examined by light microscopy, oxidation of DAB had resulted in a light brown to black reaction product which in control mice injected with HRP without toxin filled the lumina of blood vessels but there was no staining of extravascular parenchyma (Fig. 33). In control animals which received no HRP, reaction product was found only in erythrocytes and within neurones. Reese and Karnovsky (1967) attributed staining of these cells to intrinsic peroxidase activity, specifically in lipofuscin granules in neurones. In toxin treated mice, reaction product was widespread in the parenchyma and was seen leaking from blood vessels and in deposits around them (Fig.34,35,36).

In electron microscope preparations, reaction product was easily visualized, the final electron opacity due, in part, to its avid reaction with osmium tetroxide (Graham and Karnovsky, 1966; Reese and Karnovsky, 1967). In immersion fixed control brains, erythrocytes were very electron opaque and exogenous peroxidase was localized in the lumina of vessels and was present in a few micropinocytotic vesicles within endothelial cells (Fig. 75); none was found beyond the vascular endothelium. The endothelial basal lamina was free of reaction product. In perfusion fixed controls, reaction product was confined to micropinocytotic vesicles with a very small residual amount apparently adhering to the luminal surface of the endothelium.

In toxin treated mice reaction product was found in micropinocytotic vesicles within the endothelium but these vesicles did not appear to be any more numerous than in control brains. Reaction product was frequently pooled along the basal lamina (Fig. 76,78) but all structures beyond were free, except for a small amount which sometimes proceeded into the cleft between 2 adjacent astrocytic end-feet (Fig. 77,79). Occasionally tracer was found in junctions between endothelial cells but the filling was only partial and no continuous line of reaction product was evident from the lumen to the basal lamina. The failure to demonstrate extravascular accumulation of reaction product was surprising in view of the extensive extravasation of HRP seen by light microscopy and was unlikely to be due to a sampling defect as tissue prepared for ultrastructural examination was selected from areas of light microscopically evident tracer extravasation.

Discussion

The findings in control mice were in agreement with observations made by Reese and Karnovsky (1967) and Hirano *et al* (1969). These authors found that in normal cerebral endothelium HRP from the lumen penetrated only partly between adjacent endothelial cells and was stopped at tight junctions. HRP - containing pinocytotic vesicles were found to be few in number and confined to the luminal surface or occasionally within the endothelial cytoplasm; they were not seen at the basal surface. The endothelial basal lamina and extracellular spaces were devoid of reaction product. Reese and Karnovsky (1967) considered that cerebral endothelial cells maintained a considerable gradient of this enzyme because the doses used in their study were 3 times the amount sufficient to permeate the extracellular space in myocardium or skeletal muscle of mice. They considered this was probably due to 1) tight junctions (zonulae occludentes) which probably form a continuous belt between adjacent endothelial cells and prevent passage from the vascular compartment to the interstitium of the brain. Endothelial cells in brain capillaries also appear to have more tight junctions than is usual in capillaries in other tissues, and 2) the paucity of vesicles in cerebral endothelium of the type which have been associated with transport of materials across endothelium elsewhere.

In control lambs and mice, Buxton and Morgan (1976) found leakage of reaction product in the choroid plexus and area postrema, regions known to contain fenestrated capillaries. Vessels in these areas (and in pineal gland, hypophysis, hypothalamus) possess an obvious perivascular space and have only an incomplete collar of astrocytes. This anatomical arrangement differs from the majority of central nervous tissue where capillaries are completely invested by the foot processes of astrocytes with no perivascular or Virchow - Robin space (Manz, 1974).

Gardner (1973) found extensive escape of exogenous peroxidase from the vasculature into the extracellular spaces of the brain in intoxicated mice. Morgan (1975) found that HRP leakage could occur within 20 minutes of toxin administration and was present throughout the brain of mice. Buxton and Morgan (1976) found breakdown in the vascular integrity to HRP in brains of lambs only 50 minutes after toxin administration.

Theoretically, there are 3 methods by which tracer could be moved from the vasculature into the parenchymatous extracellular space 1) pinocytosis, 2) between adjacent endothelial junctions or 3) by direct penetration through severely disrupted endothelial cells.

Hirano *et al* (1969, 1970) found that when brain was appropriately injured, leakage of HRP occured by all 3 routes. It is probable in intoxicated mice that most HRP leaks out from the vascular lumen between endothelial cells and although HRP deposits were not demonstrated occupying the entire length of the junction, this direct continuity between luminal and abluminal sites has been shown to occur by Hirano *et al*. In other studies where escape of HRP into extravascular sites in toxin treated mice was extensive, pinocytotic vesicles observed were too few to account for the amount of HRP present in the extracellular spaces, particularly since pinocytosis is generally considered to be a slow process (Brightman *et al*, 1970). Also in these mice, severe disruption of the vascular endothelium did not occur.

Ferritin

It was decided to investigate whether the altered vascular permeability in

epsilon intoxicated mice would result in loss of vascular integrity to injected macromolecules. Ferritin was considered suitable for this study because of its size and electron opacity and because it remains in the circulation at high concentrations for periods up to 2 hours following injection (Tani and Evans, 1965). Ferritin has a molecular weight of 480,000 and the complete molecule measures about 100 A° in diameter. Ferritin has not previously been used to study vascular changes in animals exposed to epsilon toxin.

Materials and Methods

Mice received a lethal dose of toxin and were injected intravenously via a tail vein with 20 mg of ferritin (Calbiochem-Behring Corp) 1-4 hours after toxin administration. Mice were sacrificed 15 minutes after injection of ferritin. The ferritin (equine) was a 2 x crystallized, Cd removed solution in 0.15 M sterile NaCl. The brain was immersion fixed in 2.5% glutaraldehyde and routinely processed for electron microscopy. Unstained sections were sometimes used for better visualization of the ferritin particles. Brain was also processed to paraffin wax and sections stained with Perl's Prussian blue to localize the ferritin tracer.

Results

Prussian blue sections examined by light microscope revealed an abundance of ferrous material in vessel lumina but extravascular deposits of tracer were not found in control or intoxicated brains.

Ultrastructurally, in control brains, a few particles were seen to be entering small vesicles at the luminal surface and were present in a few such vesicles in the endothelial cytoplasm. Only an occasional vesicle was present at the contraluminal side of the endothelial cell, intracellular junctions were free of particles and no ferritin molecules were detected in the endothelial basal lamina (Fig. 81).

In toxin treated brains, there was an increase in the number of particles present in small and large vesicles and vacuoles were sometimes seen containing a significant quantity of ferritin (Fig. 82). A few particles were observed in the intercellular junction on the luminal side but did not penetrate beyond tight junctions. Occasionally, intercellular gaps were considerably widened with apparent loosening of the tight junction but these spaces were conspicuously free of tracer particles (Fig. 83). Few particles were present in the basal lamina of the endothelium and only rarely were ferritin molecules apparent in perivascular glial cells.

Discussion

With respect to the mode of ferritin transfer across cerebral endothelium, 3 routes are possible - via open endothelial junctions, via small (50 mu) vesicles or by direct penetration of the cytoplasmic matrix. Casley-Smith (1964) considered that, in general, all these paths were used to some degree depending upon the substance being transported, the local physicochemical environment and the site and state of the endothelium. Ferritin and thorium dioxide have been seen passing directly through the endothelial cytoplasm, free of encircling membranes, but Casley-Smith (1962) stated that some of these

molecules are displaced by the microtome knife. Casley-Smith (1967) concluded that molecules of molecular weight less than 1000 can readily pass through endothelial tight junctions, but those greater than 20,000 cannot do so and therefore the "meshes" of the zonulae occludentes are impermeable to large molecules. He considered that the slow penetration of large molecules through the endothelial barrier was largely or solely in small vesicles.

Tani and Evans (1965) studied normal and oedematous brain in cats and concluded that intravenously injected ferritin particles passed through the endothelial cell by pinocytosis. In the normal brain the basal lamina appeared to act as a barrier to the passage of ferritin because, even 2-3 hours postinjection, although moderate amounts of ferritin were seen in the endothelial cytoplasm, relatively few particles were found in the cytoplasm of perivascular astrocytes at this time. These findings were in agreement with observations in the present study although fewer ferritin particles were present in cytoplasmic vesicles in normal mouse endothelium, probably because the mice were killed earlier after ferritin administration.

Tani and Evans (1965) produced cerebral oedema by inflation of a balloon which had been placed in the extradural space. Ferritin particles were seen to pass through the basal lamina of the endothelial cell into the cytoplasm of perivascular astrocytes and, in the later stages, particles were seen free in distended extracellular spaces. The present study indicated some breakdown in the integrity of the cerebral endothelium to macromolecules in intoxicated mice but of lesser degree than that found by Tani and Evans (1965). This may have been due to species differences, different methods of oedema production and the longer time interval between ferritin injection and death in the latter experiment.

Raimondi *et al* (1962) found, however, that in the normal cat brain ferritin was free in the basal lamina 12 1/2 minutes post-injection, located in perivascular glial cells within 45 minutes and in extracellular spaces after 3 1/2 hours. These authors used perfusion fixation whereas Tani and Evans fixed the brain by direct injection into the parenchyma which they claimed avoided possible artifacts secondary to perfusion of fixative.

Although vesicular transport of large molecules appears to be a tardy process in cerebral endothelium, Casley-Smith and Carter (1979) demonstrated that in acute inflammation, particles were transported across endothelium in the diaphragm as rapidly as 30-60 seconds after injection. They found that vacuoles which appeared in inflamed endothelium were largely responsible for ferritin transport across these cells since small vesicles did not increase in size or number, no ferritin was seen in intercellular junctions and vacuoles were still present 90 minutes after injection at which time the junctions had closed again.

Thorotrast

To complement studies with ferritin, another large molecule, Thorotrast (Testagar & Co. Inc.) was employed as a vascular tracer. The particle size is 30-100A°.

Materials & Methods

Thorotrast contains 24-26% stabilized colloidal thorium dioxide, 25% aqueous dextrin and 0.15% methyl parasept as a preservative. Five mice were given a

lethal dose of toxin and 30 minutes after administration, 0.2 ml of Thorotrast was injected via a tail vein. Animals were sacrificed 60 minutes later. Brain was immersion fixed in 2.5% glutaraldehyde and routinely processed for electron microscopy.

Results

In control brains, large numbers of electron dense Thorotrast particles were present in the lumen, a few were seen entering small vesicles from the lumen and occasionally larger vesicles contained several particles but particles were rarely found on the abluminal side of the endothelial cell. The basal laminae of the capillaries were almost free of Thorotrast and very infrequently a single particle was observed in a vesicle in the perivascular astrocytic cytoplasm. In toxin treated mice there was a slight increase in the number of particles in cytoplasmic vesicles and the basal lamina and the adjacent astrocytic cytoplasm contained a few particles (Fig. 101). Endothelial junctions appeared not to participate in particle transfer.

Discussion

In a study of experimental allergic encephalomyelitis (EAE), Lampert (1967) used Thorotrast as a vascular tracer and while normal rat cerebral vessels remained impermeable to Thorotrast with no penetration through, or uptake by, endothelial cells, in EAE particles were seen in the gap between endothelial cells, throughout the basal lamina and in adjacent extravascular spaces between glial and neuronal processes.

In the present study, a few particles in vesicles had reached the basal lamina and adjacent glia in controls but the time from tracer injection to death (60 minutes) was longer than Lampert (1967) allowed (30 minutes) and considerably longer than with ferritin (15 minutes). The average particle size was also smaller with Thorotrast than with ferritin.

Colloidal Carbon

Cotran *et al* (1967) demonstrated that when colloidal carbon black was injected intravenously, although most of the particles were rapidly removed by the macrophage-monocyte system, certain vessels when injured retained some particles and were thus "labelled" by them. Particle size is approximately 300 A°.

Materials and Methods

Five mice were exposed to a lethal dose of toxin and 3 hours later 0.1 ml of biological ink (Pelikan Company, batch No C11/1431 a) was injected intravenously into a tail vein of mice. Mice were sacrificed 15 minutes later. Brain was fixed by immersion in 2.5% glutaraldehyde and routinely processed in preparation for ultrastructural examination.

Results

Carbon particles were of slightly varying sizes and moderate electron density. In both control and treated mice the particles were confined entirely within the vessel lumen and no differences were detected between these two experimental situations.

Discussion

Cotran *et al* (1967) reported that in injured vessels the uptake of carbon

was principally due to movement of particles through endothelial gaps rather than by pinocytosis. Carbon was retained at the level of the basal lamina and pinocytosis occurred at a later stage. Cotran *et al* stated that attempts at vascular labelling within the central nervous system have not been successful and the negative results obtained in this study should be viewed in this light.

Monastral blue B

Vascular leakage after local injury to a vessel can occur by a direct effect of an injurious agent, as has been shown to occur in the present study with epsilon toxin, or indirectly via chemical mediators. In the former type of injury, all types of vessels may be involved, whereas venules are predilected for damage in the latter situation due to their concentration of histamine receptors (Joris *et al* 1982). Vascular labelling of leaky vessels *in vivo* may be demonstrated if the endothelial cell is damaged but the basement membrane remains intact as the labelling particles become trapped against this membrane (Cotran *et al* 1967). Although severe toxin-induced endothelial injury was found in the present study, labelling of affected cerebral vessels with colloidal carbon did not occur.

In view of the difficulty of labelling injured vessels in the brain, it was decided to use Monastral blue B as Joris *et al* (1982) successfully labelled rat skeletal muscle venules, after histamine-induced vascular damage, with this substance.

Monastral blue B is a copper phthalocyanine which can be visualized by both light and electron microscopy, is non-toxic when administered at the correct dose, and most of the pigment is removed from the circulation by the macrophage-monocyte system within 1 hour (Joris *et al* 1982).

Materials and Methods

Five control mice received 0.1 ml of a 3% suspension of Monastral Blue B in 0.85% NaCl (Sigma Chemical Company, St. Louis, MO.) via a tail vein and were sacrificed 1 hour after injection. Ten mice were given a lethal dose of toxin, after 3 hours ~~a similar dose~~ 0.1 ml of Monastral blue B was administered, and animals were sacrificed after a further hour. The brain, lung, heart, spleen and kidney were removed and fixed immediately in 10% buffered formalin for 48 hours. Tissues were then embedded in paraffin and 6 um sections cut and stained with haematoxylin and eosin for examination by light microscopy.

Results

The gross findings in both control and toxin-treated mice sacrificed 1 hour after the administration of Monastral blue B were similar. The liver was uniformly blue in colour, the spleen a reddish-blue hue and there were focal areas of bluish discoloration in the lungs. The brain and heart were entirely free of blue pigmentation. There was sometimes also a light blue staining of the capsular and cut surfaces of the kidney.

The microscopic appearance of tissues in intoxicated mice resembled those of control animals, with no labelling of blood vessels occuring in any organ. The most extensive uptake of pigment was by the Kupffer cells of the liver, most of which contained blue deposits, and also by macrophages in the spleen. Capillaries in the alveolar walls of the lung often contained intraluminal deposits of pigment and such deposits were sometimes found in the capillaries of the glomerulus and interstitium of the kidney and occasionally in the brain and heart. No intramural deposits of Monastral blue B, however, were found in cerebral vessels or those of other tissues examined.

Discussion

The unsuccessful labelling of toxin-damaged cerebral vessels in the present study is consistent with findings by other authors with vascular labelling in the brain (Cotran *et al* 1967). Cotran *et al* (1967), in a review of vascular labelling with colloidal carbon, recognized four types of vascular blackening with this substance: 1) intramural deposition due to leakage of plasma-laden carbon between endothelial cells; 2) phagocytosis by endothelial cells; 3) thrombosis, with an admixture of carbon and platelets, associated with endothelial damage; and 4) filling of the vessel lumen with carbon particles.

The efficiency of tight junctions between endothelial cells in the brain probably prevented the passage of Monastral blue B between these cells to the basement membrane, and the paucity of micropinocytotic vesicles in cerebral endothelium would impede the intramural accumulation of sufficient amounts of pigment to be visualized with the light microscope. The failure to label vessels in other organs is consistent with the apparent resistance of these blood vessels in mice, compared to the cerebral vasculature, to epsilon toxin-induced damage which was noted in later experiments in the present study.

Fluorescein Isothiocyanate Albumin

In addition to the egress of water and ions from cerebral capillaries under the influence of epsilon toxin, plasma protein has been found in extravascular sites at both light microscope and ultrastructural levels. An attempt was made to demonstrate exudation of plasma protein using a fluorescent substance bound to albumin.

Materials and Methods

Five mice were given a lethal dose of toxin and 4 hours later were injected with 250 mg/kg of bovine albumin - fluorescein isothiocyanate (FITC - albumin) (Sigma Chemical Company) in 0.5 ml of distilled water via a tail vein . Ten and 30 minutes after injection of FITC - albumin, the brain was rapidly removed and immersion fixed in 10% buffered formalin for 2 hours at room temperature. Two control mice received FITC - albumin alone. Tissues were dehydrated in graded alcohols, cleared in xylol, infiltrated and embedded in paraffin wax and sectioned at 6 um. The FITC fluorescent sections were viewed in a Leitz Ortholux fluorescent microscope fitted with Ploem epi-illumination, an HB 200 mercury lamp as a light source, dichroic mirrors on position 3 and BG 38 and K 510 filters while still in wax. Some sections were subsequently taken through standard haematoxylin and eosin staining for light microscopy.

Results

Under the fluorescence microscope, vessel lumina in control brains were filled with apple-green fluorescing tracer substance which was not present in extravascular sites and background fluorescence was absent. Toxin treated brains presented a similar picture with no extravasation of tracer material detected.

Discussion

The inability to detect exudation of labelled bovine albumin from cerebral vessels exposed to epsilon toxin may have been due to the passage of undetectable amounts of protein out of vessels which were not appreciable under the microscope. The presence of plasma protein in extravascular sites at 4 hours at the ultrastructural level was not constant and small in quantity and copious exudation was infrequently observed 18-24 hours post-injection of toxin.

Evans blue dye

Since extravascular accumulations of plasma protein were observed in intoxicated mice at both light and electron microscope levels, it was decided to use Evans blue dye to examine leakage of albumin since the dye binds strongly and rapidly to this plasma constituent after intravenous injection (Freedman and Johnson, 1969).

Materials and Methods

Fifteen mice were given a lethal dose of toxin and 3 hours after administration, the animals received 0.1 ml via a tail vein of a filtered premixed solution of 4% Evans blue (George T. Gurr, London) and 10% bovine serum albumin (Sigma Chemical Company). 30 minutes after injection of dye, animals were sacrificed and the brains immersion fixed in 10% buffered formalin. The brains were then photographed *in toto* and in coronal slices.

Results

No blueing of the brain parenchyma was found in control mice receiving dye without toxin and the cut surface was the same creamish-white colour as non-Evans blue injected brains (Fig. 37). In intoxicated mice staining of the brain was variable but, in general, animals surviving the longest or showing the most severe clinical signs revealed the most extensive staining of cerebral tissue. Staining was most obvious in the corpus striatum and thalamus and either focal or diffuse in the cerebral cortex (Fig. 38); blueing of white matter tracts was much less apparent and staining of the hippocampus was poor.

Discussion

Since Evans blue dye is bound to albumin when introduced into the circulation and extravasation of this dye occurred in intoxicated, but not control, mice it is evident that epsilon toxin causes sufficient damage to capillary endothelial cells to permit appreciable leakage of plasma proteins into extravascular parenchyma in the brain. Jubb and Kennedy (1970) reported that injection of trypan blue into lambs suffering from enterotoxaemia resulted in diffuse leakage of the dye throughout the brain, with only the heavily myelinated tracts exempted. The most intense staining of the brain in this study was in the corpus striatum, thalamus and cerebral cortex, predilection sites for the development of malacic lesions. The poor staining of the hippocampus is consistent with findings by Buxton (1976) using HRP in mice and the author concluded that blood vessels in this region do not appear to be very susceptible to epsilon toxin-induced injury.

Summary of tracer studies of the brain

Studies on the brain with HRP and Evans blue dye indicated that there was a considerable leakage of these substances in mice exposed to epsilon toxin; such extravasation was absent from control animals. Although no direct continuity of HRP could be demonstrated ultrastructurally between the luminal and abluminal aspects of cerebral capillary endothelium it was, nevertheless, proposed that this was the major route by which HRP escaped from these vessels. This argument is sustainable because complete filling of interendothelial junctions has been demonstrated (Hirano *et al* 1980), the number of pinocytotic vesicles in vessels exposed to toxin was insufficient to account for the amount

of reaction product found extravascularly and no disruption of the vascular endothelium was present to allow direct penetration of tracer from the lumen into extracellular spaces. Since epsilon toxin has a molecular weight of a similar order of magnitude as HRP it is probable that this toxin also leaves cerebral capillaries between adjacent endothelial cells.

The toxin has been shown to bind initially to receptors on the luminal surface of cerebral capillaries (Buxton, 1976) and induce deleterious changes in the endothelium by a mechanism still to be elucidated.

Capillaries in the brain of mice were found to be much less permeable to macromolecules such as ferritin with only a few particles penetrating beyond the basal lamina in affected animals, although the number of molecules in vesicles was increased in toxin treated animals compared to controls. It was considered that vesicular transport in micropinocytotic vesicles was the overwhelmingly important route for transport of these large molecules as particles were never found beyond tight junctions on the contraluminal side of widened interendothelial gaps.

Therefore, although the permeability of brain capillaries to small molecular weight tracers was substantially increased, the vascular integrity to injected macromolecules was comparatively little impaired, mainly as a result of the paucity of vesicles in cerebral capillary endothelium and the effectiveness of tight junctions between these endothelial cells.

CHAPTER VII

MORPHOLOGICAL STUDIES OF LUNG, HEART AND KIDNEY

HISTOPATHOLOGY

Mice

In perfusion fixed *lung* blood vessels were fully patient, usually ovoid in cross section and devoid of erythrocytes. Occasionally a few smaller vessels contained red blood cells which had not been flushed out and in these areas extravasation of erythrocytes into alveolar spaces was sometimes observed. Capillaries were much more obvious in perfused material with their round, open, clear lumina. As a result alveolar walls were increased in thickness. Airways in perfused lung were more regular in outline with fully open lumina. In immersion fixed lung, blood vessels and airways were very irregular in outline and appeared partially collapsed and, in contrast to perfused material where alveolar spaces were open and oval in shape, there was always some degree of atelectasis. There was essentially no difference between pulmonary tissue in control and affected mice with the exception that, in the latter, a small amount of lightly eosinophilic proteinaceous exudate was present in a few alveolar spaces.

In *myocardium* fixed *in vivo* by perfusion the muscle fibres had a uniform eosinophilia and sarcolemmal membranes were well-defined. In heart fixed by immersion, cytoplasmic outlines were blurred, striations more difficult to discern and some fibres showed areas of slight pallor. In affected perfused mice, many blood vessels were separated from the parenchyma by large clear spaces, there was minor haemorrhage into the interstitium and some muscle fibres

showed irregular pale areas in which discontinuity in the fibre was sometimes apparent.

In perfused *kidney* glomerular capillary loops were well defined whereas in immersion fixed tissue the capillary walls tended to be obscured by the erythrocytes in the lumen. In perfused tissue, the glomerular tufts tended to be centrally disposed and surrounded by a larger, more uniform Bowman's space than in immersed tissue. At low magnification, kidney fixed by immersion was compact and cellular whereas perfusion fixed tissue was more open due to clear spaces representing vessel and tubular lumina and Bowman's spaces. With perfusion, lumina of proximal convoluted tubules were open and regular in dimension with generally smooth luminal borders; with immersion fixation these tubules appeared slightly shrunken with indistinct borders at their luminal aspect and irregular, narrowed luminal spaces. In addition, the lumen in proximal tubules contained irregular strands and clumps of eosinophilic material which is an artifact due to apposition and detachment of brush borders caused by constriction of the tubules with immersion fixation. A few tubules were also filled with proteinaceous fluid. With perfusion, tubular lumina were open and clear and only occasionally contained eosinophilic material. No differences were detected in the kidneys of control and toxin-treated mice fixed by perfusion.

Sheep

Tissues from lambs were immersion fixed. In lung examined from control lambs there was little or no space between the adventitia of blood vessels and airways and the surrounding parenchyma and the pleura was thin and closely applied to the underlying pulmonary tissue.

In intoxicated lamb K2-420, there was marked pulmonary congestion and many alveolar spaces were filled with eosinophilic proteinaceous fluid containing extravasated red cells. Most vessels and airways were separated from the parenchyma by large spaces which were either clear or filled with proteinaceous exudate in which the collagenous connective tissue was disrupted. In these spaces, lymphatics were markedly dilated and often filled with eosinophilic fluid and erythrocytes were plentiful. The pleura was greatly thickened by accumulations of proteinaceous fluid, ectatic subpleural lymphatics, filled with this material, and haemorrhage.

The myocardium showed congestion, minor haemorrhage and mild patchy myodegeneration. Renal blood vessels were very congested.

ULTRASTRUCTURAL PATHOLOGY

In control mice, the *myocardium* in longitudinal section showed parallel bundles of myofibrils containing longitudinally disposed myofilaments (Fig. 89). The cross striations seen at the light microscope level had their ultrastructural counterpart in the alternating A and I bands, the latter being less electron dense and crossed by a more dense Z line. The intercalated discs, which represented junctional complexes where the cardiac muscle cells were apposed end-to-end, pursued an irregular course as they crossed each myofibril in a stepwise pattern between adjacent myofibrils. The sarcoplasm was represented by an electron lucent space in which were found abundant mitochondria, cisternae of sarcoplasmic reticulum and numerous glycogen granules.

The mitochondria were arranged in rows, appeared round or elongated and contained tightly packed arrays of membranous cristae. The nucleus of the cardiac muscle cell was elongated and contained evenly dispersed chromatin and a prominent nucleolus. The cytoplasm of the capillary endothelium was moderately electron dense with large numbers of micropinocytotic vesicles and also mitochondria and endoplasmic reticulum. The basal lamina was amorphous, moderately electron dense and of uniform thickness and was closely apposed to the surrounding parenchyma of the myocardium.

In toxin treated mice, nuclear injury in the myocardial cell was reflected by clumping of chromatin at the periphery of the nucleus. In the myofibrils, myofilaments were separated from each other and, in longitudinal section, there were electron lucent spaces in the myofibrils with either completed loss of myofilaments or a few remnants of these structures traversing the spaces as fine, often discontinuous strands (Fig. 90). In affected hearts, areas of apparently normal myocardium could be found. The I bands were enlarged, less electron dense and irregular at their borders with the A bands. The sarcoplasm appeared enlarged with greatly swollen sarcoplasmic reticulum and lipid droplets were sometimes observed; the latter were rarely seen in controls. The mitochondria often appeared swollen with loss of matrix and disorganization of cristae, in marked contrast to their compact arrangement in normal myocardium (Fig. 91). The capillary endothelium was separated from the parenchyma by very large electron lucent spaces. The cytoplasm of these cells was more electron lucent, vesicles were augmented in number and size and there was mitochondrial swelling. The basal lamina was more irregular and less electron dense and in some sites appeared to be interrupted. Interendothelial spaces were partially opened at the luminal and abluminal aspects but tight junctions appeared to be intact.

Discussion

Scant attention has been given to the effect of epsilon toxin on extracranial tissues. Gardner (1973) studied the heart in lambs experimentally intoxicated with Type D toxin and found severe endothelial damage of the type described in the brain of intoxicated mice in this study. The endothelial cytoplasm was attenuated, condensed and electron dense. In contrast, the cytoplasm of endothelial cells in the myocardium of mice was much more electron lucent than normal, probably a reflection of intracellular oedema. In Gardner's lambs there was also severe perivascular oedema with separation of myofibrils and, in addition, bulging of the sarcolemma between the Z lines. Mitochondria were swollen but myofibrils appeared intact.

In experimental myocardial ischaemia, early morphological alterations include swelling of the mitochondria with disruption of cristae, enlargement of the sarcoplasmic reticulum with cisternae swelling into large vesicles, margination of nuclear chromatin in cardiac cells and prominent I bands, the latter indicating evidence of myofibrillar relaxation due to contractile impairment. At this stage myofibrils appeared intact (Scarpelli and Trump, 1971).

Diphtheria is a good example of bacterial toxin-induced myocardial damage and is a well-recognized complication of this disease, the toxin apparently altering protein and fatty acid metabolism in this tissue (Burch *et al*, 1968). Burch (1968) studied ultrastructurally the heart of a child who died of diphtheria on the eighth day of the illness and the most striking change was extensive mitochondrial swelling with disorganization of cristae. Myofibrils were damaged and disrupted at scattered foci, leaving empty, structureless,

pale spaces and numerous lipid droplets were seen in these fibrils. The sarcoplasmic reticulum showed no significant changes.

Pelosi *et al* (1966) examined the effect of diphtheria toxin on the myocardium in guinea pigs and a different pattern of injury emerged. In acute poisoning the ultrastructural changes were minimal but, with longer survival, progressive dilatation of the sarcoplasmic reticulum was observed from day 3 to day 7, modest myofibrillar damage appeared on day 7 but mitochondrial changes almost never occured.

In mice, myofibrillar damage was severe with epsilon toxin and occured early compared to diphtheria. Most of the damage appeared to be related initially to perivascular and intracellular oedema with possibly some contribution by ischaemia. The ultrastructural changes in these two circumstances are similar, except that myofibrils do not show morphological changes early in ischaemia. A direct effect of the toxin on the myocardial cell, however, cannot be dismissed.

In the *lung* of mice, attention was directed to the alveolar septum which is comprised of the inner alveolar lining, the pulmonary capillaries and the interstitial connective tissue space. In control lung, capillary luminal patency was good, though rarely complete, and cytoplasmic organelles (mitochondria, endoplasmic reticulum and Golgi apparatus) were generally well-preserved (Fig. 84). The cytoplasm was attenuated, micropinocytotic vesicles in good supply and tight junctions were evident in most sections. The basal lamina was of moderate electron density and where the endothelium came into close contact with type 1 cells, their basal laminae appeared to fuse. The squamous or type 1 cell presented with an attenuated cytoplasm, poor in

organelles, but containing pinocytotic vesicles and nuclei were rarely seen in sections. The cuboidal or type 2 cells, on the other hand, possessed a conspicuous ovoid nucleus. In the cytoplasm, mitochondria were numerous with endoplasmic reticulum, a few lysosomes, glycogen granules and large, osmiophilic reticulated lamellar bodies (which are believed to synthesize and secrete surfactant) (Fig. 84). Short microvilli were sometimes observed projecting from these type 2 cells into the lumen. In alveolar spaces were not uncommonly found irregularly laminated structures known as tubular myelin, which are thought to be released into air spaces by extrusion of the lamellar body. In the interstitial space were bundles of collagen fibrils and elastic fibres with a fibroblast sometimes discernible.

In toxin treated mice, changes in the lung were minimal (Fig. 85, 86) and largely restricted to capillaries. The cytoplasm in some of these vessels appeared more electron lucent, mitochondria were often swollen with disruption of cristae (also seen in type 2 cells) and vesicles were sometimes increased in size (Fig. 88). Occasionally, apposition between adjacent endothelial cells appeared to be less close than normal and projections of endothelial cytoplasm into the lumen, similar but larger than the "blebs" seen in cerebral capillaries, were not uncommon. In a few lungs fixed by immersion, capillary lumina were irregular and less patent than in perfused material and no exuded plasma protein was found.

Sections of lung removed from lamb K2-94, which died 1 1/4 hours after toxin administration revealed capillary endothelium whose cytoplasm was reduced to an electron dense band (Fig. 87). The nucleus of the endothelial cell was shrunken and very electron dense. Alveolar spaces contained copious amounts of fibrin which was composed of moderately electron dense strands in which a fibrillary pattern was sometimes discernible (Fig. 87).

Discussion

Gardner (1973) examined lungs from epsilon intoxicated lambs and found severe capillary endothelial damage with adhesion of thrombocytes, mild swelling of alveolar epithelial cells, proteinaceous fluid in alveolar spaces and fluid accumulation in interstitial connective tissue. Severe capillary endothelial damage was also found in the lamb examined in the present study and alveolar spaces contained a fibrin-rich exudate. Pulmonary changes in similarly intoxicated mice, however, were minimal.

These ultrastructural findings were consistent with light microscope observations and it appeared that pulmonary capillaries in mice were much less susceptible than in sheep and also apparently more resistant to the action of epsilon toxin than cerebral capillaries. Pulmonary congestion and oedema, characteristic findings in intoxicated sheep, were very rarely observed in mice and, when present, were exceedingly mild.

The role of vesicular transport in pulmonary oedema is still unresolved but a frequent observation in the capillary network of the lung is attenuation of the endothelial cytoplasm which is thinner than the vesicular diameter and devoid of vesicles. Therefore, if vesicles are important for the transport of substances across these cells, these areas would restrict permeability. It is generally accepted, however, that when capillary pressures greatly increase to about 3 times normal, endothelial junctions in the lung widen and allow easy access of blood proteins to the interstitial space. At higher pressurers, or when pressures of the above order are maintained, intersititial oedema is succeeded by alveolar oedema (Fishman and Renkin, 1979). Pulmonary endothelial junctions are of the so-called "leaky" type, in contradistinction to the much tighter

zonulae occludentes in the cerebral capillaries.

In *kidneys* removed from control mice, nuclei of proximal convoluted tubule cells were round to oval in shape with dense areas of chromatin and surrounded by a considerable amount of granular endoplasmic reticulum; individual tubule cells were cuboidal in shape. Mitochondria were numerous and tended to be vertically oriented in the basal portion of the cell. The cytoplasm also contained pinocytotic vesicles, vacuoles and a number of lysosomes. Long, thin microvilli were closely packed at the luminal surface, collectively forming the brush border, and short invaginations of the cell membrane were present between the bases of neighbouring microvilli. The basal surface of the cell was deeply invaginated extending up between the mitochondria, but the invaginations of these cells at their lateral borders were more difficult to appreciate.

In toxin treated mice, the cytoplasm of the proximal tubule cells was more electron lucent with clear spaces almost devoid of organelles or containing vague outlines of these structures; mitochondria, however, were generally well-preserved (Fig. 94). Degenerative changes in the brush border were sometimes evident (Fig. 95). There appeared to be a reduction in the number of lysosomes. Occasionally, capillaries in the interstitium showed severe endothelial damage with the cytoplasm very attenuated and electron dense (Fig. 95).

The renal corpuscles from control mice were similar to previous descriptions. The glomerular filtration membrane was composed of the capillary endothelium, the basal lamina and the visceral layer of Bowman's capsule. The endothelial cytoplasm was markedly attenuated and perforated by fenestrae. An occasional mesangial cell was associated with the deep surface of capillaries.

The epithelial cells or podocytes were composed of highly branched cytoplasmic extensions which attached to the capillary basal lamina as foot processes or pedicels where they interdigitated with their fellows forming slit pores. The basal lamina was considerably thicker in glomerular capillaries than in other endothelia examined.

The glomeruli from intoxicated mice appeared normal with no evidence of capillary damage (Fig. 93).

Discussion

Gardner (1973) examined kidney from mice and lambs exposed to epsilon toxin and found no detectable differences ultrastructurally between control and intoxicated animals, except capillaries in the interstitium often showed major endothelial damage.

In this study mild degenerative changes were present in proximal tubule epithelium and widespread necrosis of these cells has often been described in lambs dying of enterotoxaemia, however the latter changes should be viewed with caution as body temperatures are usually high when death is preceded by convulsions and the body of sheep is well-insulated, both these conditions engendering rapid autolysis.

Gardner (1973) examined changes in proximal tubules at the ultrastructural level in kidneys left *in situ* after death. Progressive degenerative changes occurred in the epithelium of these tubules with autolysis but changes in control lambs were less severe than in intoxicated animals.

CHAPTER VIII

TRACER STUDIES OF LUNG, HEART AND KIDNEY

The integrity of the vascular endothelium to injected ferritin in epsilon intoxicated mice (or sheep) has not previously been investigated and since pathological changes in these organs constitute an essential part of enterotoxaemia as a disease entity, alterations in vascular permeability in these sites were considered both relevant and important.

Materials and Methods

Mice were administered a lethal dose of toxin intraperitoneally and 4 hours later, 20 mg of ferritin (Calbiochem-Behring Corp.) was injected via a tail vein. Animals were sacrificed 15 minutes post-injection of ferritin. Pieces of tissue were removed from the apical lobe of the lung, left ventricle of the heart and renal cortex, immersion fixed in 2.5% glutaraldehyde and processed routinely for electron microscopy.

Results

In control lung, ferritin particles were largely confined to the lumen, a very small number of particles were seen in large and small vesicles, occasionally in the basal lamina and a few particles had penetrated into the adjacent alveolar space (Fig. 96). In lung exposed to toxin there was a slight increase in the number of tracer particles in small and large vesicles but the distribution in the basal lamina and alveolar spaces was similar to control sections (Fig. 97).

The capillary endothelium in control sections of myocardium was characterized by numerous vesicles. Many of these large vesicles contained ferritin particles and tracer was also seen to be traversing the endothelium in smaller vesicles. In addition, particles were quite commonly found in the pericapillary connective tissue (Fig. 98). In intoxicated mice, large vesicles were not uncommonly seen open to the capillary lumen with ferritin particles entering and vesicles at the contraluminal side were occasionally observed to be discharging their contents. Tracer particles were frequently noted in large and small vesicles in the endothelium, were more numerous in pericapillary regions and had penetrated a greater distance from blood vessels compared to controls (Fig. 99).

In sections of glomerulus examined from control mice, ferritin particles were in high concentration in the lumen of capillaries, were commonly seen to be passing through fenestrae of the endothelium and were rarely present in cytoplasmic vesicles. Particles were rather numerous in the basal lamina but noticeably concentrated at the side closest to the lumen of the vessel. A few particles were seen in the foot processes of the epithelial layer but were rarely observed in the capsular space. Glomerular capillaries in toxin treated mice revealed a similar quantity of ferritin in the basal lamina and foot processes of podocytes but these particles were more evenly distributed in the former site (Fig. 100). Only an occasional particle was present in Bowman's space.

Discussion

Capillaries differ in their structural details from one tissue to another These differences primarily affect the endothelial and adventitial layers, which

may be discontinuous or absent, but the basal lamina generally persists as an uninterrupted layer and is thus the structural feature common to this type of vessel. 3 types of capillaries are generally recognized: 1) continuous thick endothelium, the type found in cardiac muscle, and generously provided with micropinocytotic vesicles; 2) continuous thin endothelium, present in lung and central nervous system, and containing a smaller number of vesicles; 3) fenestrated thin endothelium, slightly modified in glomerular capillaries where the majority of fenestrations are open and not spanned by a thin membrane. Only occasional micropinocytotic vesicles are found in the endothelial cytoplasm.

The distribution of ferritin particles was essentially the same in pulmonary and renal capillaries in both control and toxin treated mice, but the passage of tracer molecules across capillary endothelium in the myocardium appeared to be enhanced by the exposure of these vessels to epsilon toxin. The lack of vascular permeability change found in the lung and kidney correlates with the minimal light microscope and ultrastructural pathology in these tissues, whereas lesions were consistently present in the heart in toxin treated mice and appeared to be mainly vessel-related. These observations however, should also be considered with reference to the larger number of pinocytotic vesicles present in the type of endothelium found in the heart and the fact that vesicular transport is considered to be the major route for the passage of macromolecules across endothelia.

The findings in lung capillaries were consistent with observations made by Schneeberger and Karnovsky (1971). These authors found that ferritin particles were numerous in the lumen of lung capillaries in normal mice, a few particles were seen in pinocytotic vesicles and, rarely, in the basal lamina 1 hour post-

inoculation; ferritin was never found in endothelial clefts.

Palade (1961) studied the distribution of micelles of colloidal gold (ranging from 30 to 250 A° in diameter) in rat myocardial capillaries 60 minutes after injection. Particles were found in large numbers in the lumen and in considerably smaller numbers in endothelium (largely in vesicles), basal lamina and pericapillary spaces. Bruns and Palade (1968) examined the passage of intravenously administered ferritin across the capillary wall in the muscle of rat diaphragm (skeletal muscle has the same type of capillary as myocardium). 10 minutes after injection a small number of particles had reached the adventitia, they were numerous at this level by 60 minutes and the amount of ferritin in the adventitia and pericapillary areas gradually increased until, at 24 hours, it approached the concentration in the lumen.

Farquhar *et al* (1961) also used ferritin as a tracer to investigate the transfer of this substance across the 3 layers of glomerular capillaries in normal rats, namely the capillary endothelium, basal lamina and foot processes of the visceral epithelium. 2-15 minutes post-injection, ferritin molecules were found in high concentration in the lumen and fenestrae, at low concentration in the basal lamina and in very small numbers within the epithelium. By 1-2 hours, tracer particles had accumulated on the luminal side of the basal lamina and larger numbers were also found in the epithelium. These observations paralleled those in this study and suggested that the endothelial fenestrae offered very little impedance to the passage of ferritin but the basal lamina significantly retarded movement of these particles out of the endothelium. The filtration barrier offered by the basal lamina, however, appeared to be

imperfect because a detectable amount of tracer was present in the foot processes of the epithelium. It is thought that the epithelium recovers these leaked particles from the filtrate and thus acts as a second line of defence compensating for any deficiencies in the barrier function of the basal lamina.

Some disquiet has been expressed about evidence provided by vascular tracers on the grounds that during fixation there must be gradation in the penetration of fixative and therefore vesicles are preserved at different levels in the endothelial cytoplasm at varying times and interpretation of tracer transport, especially when this movement is rapid, may become difficult or even invalid. In addition, if labelling occurs in interstitial space it could be argued that tracer material initially penetrated the interstitium (presumably at a different level in the vascular network from a particular vessel under consideration) and was secondarily taken up by vesicles in the endothelium.

Summary of studies of extracranial tissues

The integrity of capillaries in the pulmonary alveolar walls and renal glomeruli of intoxicated mice to ferritin remained largely intact but particles moved quite freely out of capillaries in the myocardium in both control and treated animals, the passage considerably augmented by exposure to toxin. Leakage of this tracer in the heart may be partly attributed to the fact that capillaries here are well endowed with pinocytotic vesicles. Extensive perivascular oedema in the myocardium and intracellular oedema in the capillary endothelium probably reflected a direct action of the toxin on these vessels.

Capillaries in the lung and renal corpuscle of toxin-treated mice were morphologically little affected and it appears in this species that there is a

spectrum of susceptibility to epsilon toxin between vessels in different tissues. Cerebral capillaries seem to be particularly vulnerable, myocardial vessels to a lesser degree and pulmonary and glomerular capillaries quite resistant to intoxication; intertubular capillaries in the kidney, however, were occasionally severely affected. In sheep there appears to be a more uniform response by the microvasculature to epsilon toxin as Gardner (1973) found severe generalized endothelial damage in the brain, heart, lung and renal interstitium (glomerular capillaries, however, were apparently unaffected) in intoxicated lambs. Capillaries in the brain and lung in intoxicated lambs examined in this study also showed degenerative changes of the same type observed in the brain of affected mice. This species difference is underlined by the paucity of significant lesions in visceral organs in mice, with the exception of the myocardium, and in the heart lesions were only readily appreciable at the ultrastructural level. In sheep, gross findings of pulmonary congestion and oedema, myocardial oedema and haemorrhage and pericardial effusion are characteristic of the acute clinical disease induced by epsilon toxin. Myocardial degeneration in mice, although patchy, was focally severe in affected fibres ultrastructurally and may contribute to the demise of intoxicated animals probably due to conduction defects as cardiac function was not affected to a degree sufficient to result in secondary pulmonary changes. There was, however, at the ultrastructural level, evidence to suggest impairment of contractility.

CHAPTER IX

CLINICAL PATHOLOGY

Clostridium perfringens Type D enterotoxaemia in sheep is associated with a number of alterations in biochemical and haematological parameters (Kellaway *et al* 1940; Gordon *et al* 1940, Gardner, 1973) and as an adjunct to morphological studies it was proposed to investigate these changes in intoxicated sheep and mice.

Materials and Methods

Three, 6 month old lambs, of unknown vaccination status, were obtained from SAMCOR and injected via a jugular vein with 10 ml of undiluted toxin. Heparinized venous blood samples were collected at intervals until death for blood gas analysis and blood was also collected into fluoride - E.D.T.A. for blood glucose estimation and dipotassium - E.D.T.A. for haematological examination. The following methods were used to obtain these measurements: blood gas analyses (Corning 168 pH/Blood Gas Analyzer), blood glucose (Calbiochem - Behring Glucose - S.V.R. reagents), haemoglobin (cyanmethaemoglobin method), haematocrit (microhaematocrit), total red and white cell counts (Coulter counter) and plasma proteins (refractometer).

Mice were also subjected to lethal and sublethal doses of toxin and at varying times post-injection were decapitated and blood collected into fluoride - E.D.T.A. for blood glucose estimation.

Liver samples were removed from mice given a lethal dose of toxin and sacrificed 4 hours post-inoculation. These tissues were immersion fixed in 10% buffered formalin, routinely prepared for light microscopy and stained with

periodic acid Schiff (PAS) to detect the presence of glycogen. Liver sections were also pre-treated with diastase to confirm the presence of glycogen in control animals.

Results

Lambs rapidly became incoordinated with increased respiratory movements and progressed to recumbency with convulsions, paddling and ophistotonos. Dyspnoea, ptyalism and cyanosis were pronounced when the animals were *in extremis*. Death occurred 15-60 minutes post-injection of toxin.

The alterations in biochemical and haematological parameters are shown in Tables 5, 6 and 7.

A consistent pattern was observed in the analysis of blood gases. There was a progressive decline in PO_2 to less than half the pre-injection level and PCO_2 values rose substantially. The pH showed a uniform fall in all 3 lambs. The hydrogen ion concentration increased markedly while the level of actual bicarbonate declined steadily. There was a rapid rise in blood glucose levels to 2 to 3 times the preinoculation value.

Haematological changes were more difficult to interpret as alterations in values were small. There was a slight rise in the total red cell count and haemoglobin level in all 3 lambs and an increase in the haematocrit in lambs 1 and 2. Lambs 1 and 2 registered a fall in the total leucocyte count but this was not substantial. No consistent pattern was observed in the differential white cell count. There was a minor decline in the plasma protein concentration.

Mice showed a rapid increase in blood glucose levels after exposure to epsilon toxin to nearly double the normal value.

In control sections of liver stained with PAS, the cytoplasm of hepatocytes was densely packed with magenta coloured granules (Fig. 39). The hepatocytes were devoid of these granules when pre-treated with diastase, confirming that the granules represented glycogen. At 4 hours post-administration of toxin, there was a marked depletion of glycogen and entire acini could be found with only a few liver cells containing granules (Fig. 40). In other acini, the diminution in granules was more patchy with some cells showing a reduced concentration of granules and the occasional hepatocyte apparently retaining the full complement of glycogen.

Discussion

An examination of blood gases in this study revealed a significant and consistent change in all indices. The rise in PCO_2 due to decreased ventilation as a result of pulmonary oedema resulted in a respiratory acidosis. If the acidosis was purely respiratory, however, the HCO_3- level would be expected to increase but, in fact, this value decreased indicating also a major contribution by metabolic acidosis. Similar results were recorded by Gardner (1973) who found sheep with pulmonary oedema developed high PCO_2 values; in the absence of oedema in the lungs the acidosis was entirely of metabolic origin. It should be noted that the PCO_2 is higher and the pH lower in venous blood because it contains the CO_2 being carried from the tissues to the lungs for excretion.

The outstanding biochemical findings in sheep dying of acute enterotoxaemia are a marked hyperglycaemia and glycosuria (Blood *et al* 1979) and sheep

injected with a lethal dose of epsilon toxin also develop a pronounced hyperglycaemia, the blood glucose level more than doubling in the period between the onset of clinical signs and death (Gardner, 1973). Elevation of blood glucose of this order was found in this study. This alteration in blood glucose levels, however, is not unique to enterotoxaemia and may be found in sheep dying of other diseases (Blood *et al* 1979), but it is a useful diagnostic aid when correlated with relevant symptomatology or autopsy findings. A negative urine test for glucose does not exclude the diagnosis if the interval between death and necropsy has been prolonged as glucose is rapidly degraded postmortem in the urine. The hyperglycaemia results from a rapid mobilization of hepatic glycogen and no increase in blood glucose occurs in animals in which glycogen has been depleted from the liver by starvation before intoxication (Gardner, 1973). Hyperglycaemia and glycosuria are reported not to be a feature of sheep suffering from FSE (Gay *et al* 1975)

Gordon *et al* (1940) found in sheep injected with Type D toxin haemoconcentration with a raised haematocrit value. Some sheep also showed an elevation of the haemoglobin concentration and a decrease in granulocytes, lymphocytes and monocytes resulting in leucopenia. Gardner (1973) also examined haematological changes in intoxicated sheep and found a rapid and substantial rise in haematocrit and haemoglobin levels and haemoconcentration was most marked in lambs with severe pulmonary oedema. The total white cell count rose slightly but only to a degree which reflected the haemoconcentration and the decline in plasma protein values was minimal. The rise in haematocrit (in lambs 1 and 2) and fall in plasma protein levels in this study were small, possibly a result of the relatively short interval between intoxication and death.

CHAPTER X

DISCUSSION

The early lesions induced in the brain of mice and lambs by epsilon toxin were essentially those of oedema, which was more severe in the white matter. White matter is known to be more susceptible than grey matter to damage in oedema states (Manz, 1974). The vulnerability of white matter may be related to the relative paucity of capillaries and the lack of extensive anastomoses in this area, predisposing to stasis and oedema; to the parallel course of myelinated fibres, which is conducive to fluid spread; or to the greater size of the extracellular space in white matter compared to grey matter, allowing accumulation of larger amounts of fluid (Bakay and Lee, 1965). This oedema corresponds to Klatzo's (1967) classification of vasogenic oedema with extravasation of fluid secondary to severe endothelial damage. At the ultrastructural level, affected cerebral capillary endothelium was attenuated, vacuolated and very electron dense, obscuring organelle detail. It is reasonable to assume that the progressive development to diffuse cerebral oedema was due to oedematization of perivascular tissue first and these perivascular areas rapidly coalesced with increasing toxin dose, time or host susceptibility. The originally swollen white matter compressed adjacent veins which in turn raised the capillary pressure and this capillary hypertension lead to exudation or transudation of plasma into the brain tissue, resulting in oedema in neighbouring white matter. This now enlarged oedematous area compressed even more vessels at its periphery and in this manner oedema fluid spread rapidly from the initial site of injury. The greater susceptibility of lambs to acute epsilon-intoxication may be, in part, related to the fact that young animals (and children) are considered more prone to develop cerebral oedema than adults (Bakay and Lee, 1965).

The initial ultrastructural change in toxin-treated mice, which preceded morphological damage in endothelial cells by a short time interval, was swelling of astrocytes and their processes, especially the extensions of these cells investing capillaries. These changes in astrocytes resemble alterations in this glial element described by Long *et al* (1966) in human cerebral oedema and Ishii and Tani (1962) in experimentally induced brain oedema in cats. Long *et al* (1966) concluded that the first ultrastructural change in brain oedema was an increase in the size of the perivascular processes of astrocytes. Capillary endothelial cytoplasmic swelling and vacuolation occasionally occured at the same time, but attenuation and increased electron density of the cytoplasm, seen early in intoxicated mice in the present study, was not found (these latter changes were also not observed in the model of cerebral oedema described in the present study). This suggests that endothelial damage in epsilon-intoxicated brains was not simply the result of oedema but probably due to a direct effect of the toxin on these cells, after binding to specific receptor sites on vascular endothelium (Buxton, 1976). According to Long *et al* (1966) the next abnormality to become manifest was enlargement of astrocytic processes throughout the neuropil and an increase in the extracellular space of the white matter. If this process continued, there was a further increase in the volume of astrocytes and other cellular elements with rupture of unit membranes and the eventual development of frank necrosis. This sequence of events also occured in the white matter of intoxicated mice and is a feasible mechanism for the production of macroscopic malacic foci in FSE while not, however, explaining their characteristic topographical distribution. As in the present study, hypoxic changes in neurones were an insignificant finding by Long *et al* (1966).

In epsilon-intoxicated mice, perivascular end-feet were often greatly swollen resulting in collapse of the enclosed capillary. Chiang *et al* (1968)

examined post-ischaemic vascular changes in rabbits ultrastructurally and found the most important alteration was swelling of perivascular glia which appeared to impinge upon the capillary lumen causing stenosis, thus reducing the blood flow. Blood clotting and platelet thrombosis were not significant contributing factors to vascular obstruction in their study and they were rarely observed in the present study. No such reduction in capillary luminal diameter has been described in studies of cerebral oedema (Long *et al*, 1966) so it appears that a period of ischaemia may be a prerequisite for this vascular change reported by Chiang *et al* (1968).

It was proposed by Lindenberg (1955) that any condition causing increased intracranial pressure may result in secondary ischaemia of the brain by arterial compression. Cerebral oedema has special significance because the brain is contained in a non-expandable bony compartment whose volume exceeds that of the brain by only 5% (Garcia *et al*, 1980). Thus, any sizable increase in the volume of the brain will be reflected in a reciprocal decrease in the volume of intravascular blood and cerebrospinal fluid. Since blood vessels are the only readily compressible structure in the brain they are predisposed to collapse whenever another cerebral element undergoes a rapid increase in volume, as occurs in cerebral oedema. The cell which swells so prominently in oedematous conditions is the astrocyte (Hirano, 1980), particularly the processes in intimate contact with cerebral capillaries, and hence it might be anticipated that a reduction in the diameter of the capillary lumen could be a sequel to end-feet enlargement. It has been suggested that the susceptibility of astrocytes to intracellular fluid accumulation is due to the presence of sodium in relatively high concentration in these glial cells. Under these conditions astrocytes would swell rapidly with inhibition of their vectorial cationic pump (Manz, 1974).

The following hypothesis may, therefore, be advanced to explain the

genesis of malacic lesions, at least at the ultrastructural level. In epsilon-intoxicated brains damage to capillary endothelium results in increased vascular permeability leading to a net movement of water and electrolytes from the extracellular to the intracellular phase and cellular swelling occurs, being most marked in the astrocytic end-feet. This movement of fluid from the blood into perivascular glia leads to stenosis of the capillary lumen, haemoconcentration and stasis. Localized tissue necrosis may occur in areas where the vascular supply is compromised in this manner. Platelet aggregations, occasionally observed in this study, may further contribute to the embarrassment of blood supply to such a region. These changes ultimately constitute a failure of brain perfusion in a localized area and Brierley (1977) considered that, in the human brain, the commonest cause of damage was related to some failure of perfusion.

In addition to narrowing of luminal dimensions by swollen astrocytic end-feet, Chiang *et al* (1968) also observed endothelial 'blebs' which caused a degree of luminal obstruction. Blebbing was often prominent in the present study but had probably not reached its full potential as lesions were examined at an early stage and perivascular glia are known to be more susceptible to hypoxia than endothelial cells (Blackwood and Corsellis, 1976). Blebbing has also been observed in many types of cells under a variety of pathological conditions (and in improperly fixed tissue) and probably represents a diffuse type of endothelial swelling resulting in cellular projections which may present obstruction to flow and, if detachment from the endothelium occurs, result in embolism.

The central nervous system derives its energy for normal metabolism from the oxidation of glucose. Thus a deficiency of oxygen or glucose will impair brain function and lead to irreversible damage if of sufficient severity or duration (Brierley, 1977). The most rapid interference with brain function follows impairment of the oxygen supply. Anoxic-ischaemic

changes in the brain all have hypoxia as their final common pathway whether it is produced by hypotension (with or without hypoxaemia), circulatory arrest or primary hypoxaemia with secondary myocardial depression (Brierley *et al*, 1973).

Brierley *et al* (1973) stated that 'no hypothesis purporting to account for the neuropathology of any type of hypoxia merits serious consideration unless it can offer a reasonable explanation for the pattern of selective vulnerability'. While the hypothesis outlined above may be formulated from ultrastructural changes in intoxicated mice to explain the production of focal necrotic lesions, it offers no satisfactory explanation for the distribution of malacic foci found in FSE, and it must be acknowledged that no convincing argument has been advanced to account for the apparent selective vulnerability of certain regions in the brain in the vast majority of diseases in animals and man.

The distribution and symmetry of the lesions of FSE are of particular interest and two major hypotheses have been advanced to explain the phenomenon of selective vulnerability in the brain (Blackwood and Corsellis, 1976). The 'vascular theory' of Speilmeyer invoked anatomical features such as the length and tortuosity of a particular vessel as well as factors such as stasis and vasospasm. On the other hand, the concept of 'pathoclisis' of Vogt and Vogt highlighted the role of physicochemical or metabolic properties as a basis for local vulnerability. It is probable that both regional circulatory and metabolic differences underlie the concept of selective vulnerability in most conditions.

Furthermore, the production of lesions in individual epsilon-intoxicated mice probably is complex and was reflected in the variable distribution, severity and occurence of pathological changes in response to a given dose of toxin. While the blood supply to a particular region in the brain is largely determined by the metabolic requirements of dependent tissues, a number of other factors determine the oxygen tension at a given site. These factors

include the oxygen tension in arterial blood, the perfusion rate, the rate of oxygen consumption; and architectural factors such as the intercapillary distance, capillary length, and the disposition of capillaries with respect to the tissue being supplied. Vulnerability of a given tissue is also determined by the anastomotic network which can be called upon, alternative metabolic pathways which can be utilized, the level of tissue activity at the time of the insult and variations in species and individual responses to a given deleterious influence. All these factors mitigate against a uniform response to a given insult.

The anatomical arrangements in the arterial supply to the brain differ somewhat between species and may be a modifying factor in the response of the brain to changes in perfusion. In the sheep (and ox), blood destined for the Circle of Willis must first traverse a well-developed intracranial carotid rete. The main source of blood supply to the rete in sheep is from the external carotid artery, via branches of the internal maxillary artery. The internal carotid is poorly developed in immature sheep and the segment proximal to the carotid rete is absent in adults. Furthermore, unlike most other species, the basilar artery has few connections with the vertebrals (Baldwin, 1964).

In a consideration of the pathogenetic mechanisms causing malacic lesions in intoxicated mice and lambs, experiments by Ames *et al* (1968), Cantu and Ames (1969) and Kowada *et al* (1968) require attention. These authors found that when rabbit brain was submitted to periods of ischaemia exceeding 5 minutes and blood flow was allowed to return, localized areas of brain failed to reperfuse as assessed by post-ischaemic, intra arterial injection of a suspension of carbon black. It was apparent that obstruction to blood flow had developed (the 'no-reflow' phenomenon) and entertained the possibility that irreversible damage to the parenchyma may occur as a secondary response to ischaemic vascular damage. Vascular obstruction was most severe in the

cerebellum, pons and medulla and caudate, fornix and lenticular nuclei, and thalamus. The cerebral cortex was much less frequently involved, but obstruction was often widespread in the cerebellar cortex.

In intoxicated lambs in the present study there was a rapid decline in blood oxygen levels, due mainly to severe pulmonary congestion and oedema. This hypoxia could conceivably have lead to further alterations in cardio-respiratory function resulting in impaired brain perfusion and ischaemic brain damage by the mechanism of 'no-reflow'.

Pure hypoxic hypoxia (i.e. reduced arterial oxygen tension with normal cerebral blood flow) cannot, however, produce brain damage unaided. Systemic hypoxaemia produces brain damage via a secondary reduction in perfusion pressure (Brierley, 1977). The initial pure hypoxia gives rise to secondary impairment of circulation and respiration and it is this inhibition of cardiorespiratory function that reduces the tolerance of the brain to hypoxia, not a diminution of the energy reserves of the brain *per se*.

Myocardial haemorrhage and oedema, pericardial effusion and severe pulmonary congestion and oedema in acutely intoxicated lambs undoubtedly contributed to cardiorespiratory distress. Electrocardiographic abnormalities have also been reported in lambs suffering from acute enterotoxaemia (Kellaway *et al*, 1940; Worthington *et al*, 1979; Gardner, PhD thesis, 1971). Myocardial damage and impaired contractility were also found at the ultra-structural level in epsilon-intoxicated mice in the present study. This cardiac and pulmonary pathology would impair the capacity of the heart to maintain a high level of blood flow through a cerebral vascular bed initially fully dilated by hypoxia and impede the rapid restoration of normal blood flow should the cardiorespiratory crisis subside.

The cerebral circulation is very efficient in the presence of a well-maintained systolic blood pressure and flow remains constant despite wide variations in arterial blood pressure. Within this range, cerebral blood

flow is kept at a constant level by alterations in cerebrovascular resistance. This autoregulation depends initially on the ability of brain arterioles to dilate as perfusion pressure falls. With increasing time, slower adjustments occur which appear to be mediated by metabolic factors such as a reduction in local oxygen tension and accumulation of carbon dioxide and acid metabolites. A localized reduction in intraluminal pressure is largely responsible for dilatation of vessels. Important anastomoses exist between cerebral arteries of all sizes and when there is a localized fall in intraluminal pressure, increased flow occurs from neighbouring collaterals which are at a higher pressure. When vasodilation is maximal throughout the brain, however, adjustments are no longer possible and cerebral blood flow then becomes linearly related to perfusion pressure. This threshold is at about 50mm of mercury and below this level the collateral circulation fails and infarction results (Meyer and Denny-Brown, 1957; Brierley, 1970).

In addition to the hypoxia in affected lambs, there was a severe respiratory and metabolic acidosis with hypercapnia. These changes probably contributed to alterations in central nervous tissue as hypercapnia itself may cause temporary barrier dysfunction to a number of tracers and considerable swelling of astrocytic processes has been demonstrated in hypercapnic hypoxia with acidosis. Hypercapnic hypoxia has been associated with generalized brain oedema. Brain tissue swells if exposed to a lowered blood pH of 7.3 to 6.0. (Manz, 1974).

The validity of the 'no-reflow' phenomenon has, however, been challenged on a number of grounds. This hypothesis implies that blood vessels in the brain are the structures initially vulnerable to ischaemia, whereas neurones are conventionally accepted as being most sensitive to hypoxia (Levy *et al*, 1975). It was assumed by Ames *et al* (1968) that the brain parenchyma was still viable as a whole when blood flow was allowed to return and that certain areas subsequently became ischaemic (when the interruption of blood

flow exceeded 5 minutes) due to local failure to reperfuse. This assumption of the survival of brain tissue up to 5 minutes was not supported by histopathological examination of affected brains (Brierley, 1973). Salford *et al* (1973) examined brains from Levine rat models of cerebral ischaemia which had been perfusion fixed immediately after exposure to nitrogen for 5 and 15 minutes. Microvacuolation of neurones was the only morphological alteration in the neocortex and hippocampus and no alterations in blood vessels or astrocytes were found. These findings are not consistent with the concept of 'no-reflow'. Levy *et al* (1975) examined gerbil brains following unilateral carotid artery occlusion and found impaired reperfusion ('no-reflow') rarely occured and, in their opinion, could not therefore be implicated in the pathogenesis of ischaemic brain damage. Studies with intravenously injected carbon further suggested that the route of administration may have been responsible for different results from those obtained by Ames *et al* (1968), who employed the arterial route. It was considered possible that carbon black injection resulted in intravascular aggregates of particles that were filtered in the lung after intravenous, but in the brain following intra arterial injection.

Finally, the zones of 'no-reflow' do not conform to the distribution of lesions found in most studies of cerebral ischaemia. These zones are also not directly comparable to areas of predilection in FSE. The regions of the brain predominently selectively vulnerable to hypoxia are layers 3, 5 and 6 of the cerebral cortex, parts of the hippocampus and the Purkinje cells of the cerebellum, with variable involvement of the basal ganglia (Brierley *et al*, 1973). It is therefore unlikely that the phenomenon of 'no-reflow' is central to the pathogenesis of FSE lesions and these lesions cannot be attributed solely to toxin-induced anoxic-ischaemic cell damage as the above pattern of changes was different from those seen in intoxicated mice. Ischaemic neuronal change, the common denominator in all changes resulting in

cerebral hypoxia, was an uncommon and late alteration in affected regions of epsilon-intoxicated brains.

No purely vascular hypothesis can explain the vulnerability of certain cortical laminae, the hippocampus and cerebellar Purkinje cells to ischaemia-anoxia (Brierley *et al*, 1973). The 'no-reflow' phenomenon is open to the same criticism.

The basal ganglia, corpus striatum and thalamus, the regions often involved in intoxicated brains in this study are, however, quite highly vulnerable to hypoxia although the occurence of lesions in these areas in hypoxic states is variable. The vulnerability of the basal ganglia has been related to its relatively less rich blood supply, longer arterioles, and high and continuous rate of metabolism (Cantu and Ames, 1969). The basal ganglia are also considered to be supplied by end-arteries (Brierley, 1977).

The distribution of lesions in mice in this study was also substantially different from the pattern observed in Levine's (1960) model of ischaemic-anoxic encephalopathy in rats induced by carotid ligation and nitrogen or nitrous oxide administration. The hippocampus was the most vulnerable area in Levine's study (followed by the neocortex, striatum and thalamus) but the white matter of the fimbria and alveus often escaped; in intoxicated mice, malacic lesions were not uncommonly found in the fimbria and alveus but the hippocampus remained undamaged. The callosal radiations and anterior commissures were never affected as isolated structures in Levine's model but only with contiguous grey matter; in mice focal lesions sometimes occured in these sites. Lesions in the corpus callosum in these rats were rare but since the carotid ligation was unilateral and the callosum is a midline structure, it may have suffered little or no loss of blood supply. Pulsinelli and Brierley (1979) found a similar pattern of selective vulnerability in their improved model of ischaemia-anoxia. Vulnerable regions were parts of the hippocampus, layers 3, 5 and 6 of the cerebral cortex and striatum. These

authors produced transient, bilateral hemispheric ischaemia in rats by permanent occlusion of the vertebral arteries and ligation of the common carotid arteries. The model was uncomplicated by anaesthesia, systemic hypoxia or hypotension, without interference with purely cerebral changes by ischaemic damage to other organs, especially the heart, which may attend the latter two situations.

The bilateral symmetry of lesions in FSE is one of the hallmarks of this condition. Since oedema in the brain causes increased intracranial pressure and may secondarily produce local lesions by compression of arteries (Lindenberg, 1955), and because the pressure exerted by oedema in this manner is symmetrical, it is not surprising that the location of lesions in this condition are also symmetrical. It is difficult to explain, however, why other conditions causing diffuse cerebral oedema and vascular collapse do not also produce lesions resembling FSE. There is, nevertheless, some degree of selective vulnerability, with certain areas more severely involved, in generalized cerebral oedema of differing aetiology in man. In these oedema states involving the whole brain, for example, the hippocampus is most susceptible in hypoxia-related oedema, the cerebral and cerebellar cortex and basal ganglia in oedema of heat stroke, and the hypothalamus and cortex are most vulnerable in oedema resulting from severe burns (Bakay and Lee, 1975).

Lesions were not always, however, bilaterally symmetrical or present in all selectively vulnerable areas in all animals in this study. In this context, Courville (1958) stated that 'in spite of the basic agencies at work in the production of a given cerebral lesion and regardless of the means by which it is produced, the pathological effects on the central nervous system are as remarkable for their diversity as for their complexity'. The wide variation in the damage produced by cerebral hypoxia, for example, implies that only some fraction of all selectively vulnerable regions are involved in any one case and some of the usually damaged territories are

spared. Damage in the cerebral cortex, which is particularly susceptible to hypoxia, may range from slight loss of neurones in the third layer to subtotal destruction in which remnants of the second and fourth layers are just recognizable.

With respect to the distribution of malacic lesions, the nature of the softening *per se*, in man, gives little or no indication of aetiology, but the location and distribution pattern are often of greatest assistance in identifying a causative factor (Innes and Saunders, 1962).

While no unifying pathogenesis can be advanced to embrace all the cerebral lesions found in intoxicated mice, mechanisms proposed to explain lesions in other conditions involving some of the same areas are relevant to the discussion of epsilon-induced lesions. Most of these mechanisms implicate vascular factors.

Lesions in the cerebral cortex of intoxicated mice were unlikely to be due to hypoxia alone as one of the hallmarks of this type of injury to the brain is laminar cortical necrosis. In toxin-treated mice, cortical lesions were focal and generally well-circumscribed. It should be emphasized, however, that destruction of the cerebral cortex in hypoxia is never complete and within each damaged lamina there may be large numbers of normal neurones.

The brain is a relatively impoverished tissue in terms of capillary density and, in an idealized mid-intercapillary region, doubling the inter-capillary distance would reduce to nil the oxygen tension by extending the oxygen diffusion path length (Bourke *et al*, 1980). Astrocytes are in a potentially strategic location to alter the concentration of blood-borne solutes and gas to and from dependent neurones because their processes are disposed as satellites around neurones and end-feet cover most of the surface area of capillaries. In oedematous conditions, with astrocytic swelling, the diffusion path length between vessels and neurones may be exceeded in focal scattered areas of grey matter and result in cortical lesions of the type

found in this study. Similarly, focal necrosis in the internal granular layer of the cerebellum may be due to the supply of nutrients to these cells being compromised by early and severe swelling of astrocytes in this region. The granular layer is much more apt to show an oedematous response to injury than the molecular layer or Purkinje cells. In hypoxia-related cerebral oedema, the most vulnerable cells are those with low oxidative enzymes, particularly the granule cells and astrocytes of the cerebellum (Bakay and Lee, 1965). These cells showed very early and severe changes in intoxicated mice in the present study. In diffuse cerebral oedema resulting from heat stroke and from certain types of radiation injury, these cells were also shown to be selectively vulnerable (Bakay and Lee, 1965). These focal cerebellar lesions in the present study were quite different from cerebellar damage induced by ischaemia-hypoxia, where the typical 'boundary zone' lesion is triangular with its base at the cortical surface and its apex in the central white matter (Brierley, 1970).

In lower animals, the cortical grey matter is supplied by copious, poorly differentiated leptomeningeal anastomoses which are capable of diverting large quantities of blood and may be responsible for the relative preservation of this region in intoxicated mice. By contrast, the leptomeningeal anastomotic network in the mature human cerebrum is a well-differentiated system of fragile and incomplete arterial loops which predispose to local stasis. In these circumstances, the cortical border zones of the 3 major cerebral arteries are predilected for ischaemia (De Reuck *et al*, 1972), as these territories are most remote from the arterial trunk.

The consistent and often extensive involvement of the more compactly arranged myelinated fibre tracts such as the corpus callosum, internal capsule and, to a lesser degree, the anterior commissures was unexpected as these tracts are considered to be relatively resistant to the destructive effects of oedema (Manz, 1974). Furthermore, Jubb and Kennedy (1970) stated

that the altered permeability of vessels to trypan blue in lambs with acute enterotoxaemia was diffuse throughout the brain, but the heavily myelinated tracts such as the corpus callosum and optic tracts were spared. These tracts also tended not to be stained by Evans blue in toxin-treated mice in the present study. These findings suggest that necrosis in these tracts may be due to direct vascular involvement and not simply the result of passive accumulation of oedema fluid. The internal capsule, for example, is supplied by end-arteries (Brierley, 1977).

The hippocampus and substantia nigra are recognized as regions which are poorly vascularized (Hicks, 1950) and are commonly damaged by ischaemic-anoxic insults. The substantia nigra is a common site for lesions in ovine FSE (Jubb and Kennedy, 1970) and intoxicated mice sometimes showed malacic changes in this area. In intoxicated mice, however, the hippocampus was undamaged and blood vessels in this region are apparently not very susceptible to the action of epsilon toxin as Buxton (1976) found the hippocampus to be almost devoid of reaction product when extravasation of horseradish peroxidase was diffuse throughout the rest of the brain in mice exposed to this toxin.

In toxin-treated mice, lesions were commonly found in paraventricular areas adjacent to the lateral ventricles. In periventricular leukomalacia of infancy in man, related to cardiorespiratory stress in the neonatal period, lesions are similar and consist of bilateral infarcts located in peri-ventricular end-zones adjacent to the external angles of the lateral ventricles (Abramowicz, 1964; De Reuck *et al*, 1972). The periventricular regions in lower animals and immature human brains are predilected for ischaemia as they derive their main blood supply from a system of primitive penetrating arteries whose straight and long channels have few collaterals and no true anastomoses and are, therefore, essentially end-arteries (De Reuck *et al*, 1972).

In a review of 13 cases of this neonatal condition, De Reuck *et al* (1972) found one case where the periventricular lesions involved immediately

subjacent portions of thalamus and lenticular nuclei and, in another case, the basal ganglia, all regions commonly incriminated in intoxicated mice. Abramowicz (1964) used the cat as an experimental model for this condition because its cerebral vascular structure closely resembles that seen in the human foetus in the last months of gestation and produced similar lesions to the human disease by ligation of the basilar artery, together with one or both carotid arteries. Some infarcts were also produced in the internal capsule at the level of the caudate nucleus and in the corpus callosum and callosal radiations, again predilection sites in mice. The presence of numerous foci of liquefaction necrosis in these cats supported the role of vascular factors in the genesis of the lesions.

Bilaterally symmetrical malacic lesions were commonly found in the vestibular area of intoxicated mice. Microscopic haemorrhages are sometimes found in the vestibular nuclei in Wernicke's encephalopathy in man (attributed to thiamine deficiency) but the pathogenesis of this syndrome is unclear. Focal capillary haemorrhage was often found in early lesions in epsilon-treated mice. Vascular changes are usually regarded as the primary lesion in Wernicke's syndrome followed by secondary degeneration of neurones (Blackwood and Corsellis, 1976). Bilaterally symmetrical lesions occur in the medial vestibular nuclei, among other sites, in Chastek's paralysis of carnivores. This condition is due also to thiamine deficiency and has been compared to Wernicke's syndrome in man. The pathogenesis of lesions in carnivores in sequence is oedema, vascular dilation, haemorrhage and necrosis (Jubb and Kennedy, 1970), similar to the progression of events seen in epsilon-intoxicated mice, but an explanation for the topographical distribution of lesions in Chastek's paralysis has not been forthcoming.

In addition to FSE, there are several other disease entities in animals where malacic lesions in the brain are bilaterally symmetrical and in which vascular factors have been implicated in the pathogenesis. In

polioencephalomalacia (PEM) of sheep and cattle, associated with thiamine deficiency, the initial change is a diffuse cerebral oedema (as occurs early in epsilon-intoxicated brains), which proceeds to bilateral laminar necrosis in the cerebral cortex and, less frequently, bilaterally symmetrical malacic foci in the thalamus, lateral geniculate bodies, basal ganglia and anterior and posterior colliculi. The cause of the oedema in PEM is unknown but the resulting lesions appear to be related to interference with cerebral circulation as the distribution of the laminar cortical necrosis corresponds to the boundary zone of the middle cerebral artery. Furthermore, when the cerebral oedema is severe resulting in tentorial herniation, compression of the posterior cerebral artery may occur with additional cortical lesions in the boundary zone of this vessel (Jubb and Kennedy, 1970).

In focal symmetrical spinal poliomalacia of sheep, lesions are bilaterally symmetrical and restricted to the ventral grey matter of the spinal cord. The lesion is consistent with an obstruction of the ventral spinal artery (Jubb and Kennedy, 1970). Bilaterally symmetrical malacic lesions have been found in the globus pallidus and substantia nigra of horses in California following ingestion of the plant, *Centaurea solstitialis*, but the pathogenesis of this condition is unknown (Innes and Saunders, 1962).

It was considered that malacic lesions in this study were caused primarily by toxin-induced vascular changes but the possibility of a direct effect of epsilon toxin on the brain parenchyma has not been investigated and cannot, therefore, be dismissed.

Hicks (1950) investigated metabolic aspects of cerebral lesions induced experimentally with a number of compounds and suggested that different parts of the brain possess qualitative and quantitative differences in metabolism. This author considered that the vascular supply to a given region was only partially responsible for its vulnerability because the cerebral cortex, for example, which has a rich blood supply, is easily

damaged by hypoxia (this region does, however, have greater metabolic needs). White matter has about 20% of the capillary length per unit volume of tissue compared to cerebral cortical grey matter (Hicks, 1950).

Hicks (1950) produced bilaterally symmetrical lesions in the corpus striatum (especially the white matter), corpus callosum and cerebral cortex, with a tendency to destruction of white matter, by the administration of cyanide and sodium azide to rats. These areas commonly were damaged in intoxicated mice in this study. Hicks attributed white matter damage to inhibition of cytochrome oxidase by these compounds. White matter has a paucity of this enzyme but is heavily dependent upon it for its energy production. Sodium azide, however, also causes a rapid fall in systemic blood pressure and therefore, in some of the above lesions, hypotension may have been a contributing factor (Blackwood and Corsellis, 1976).

Carbon monoxide causes both a hypoxic and histotoxic hypoxia, the latter due to inhibition of cytochrome oxidase. In acute poisoning, haemorrhages occur which may be petechial, with an affinity for white matter (especially the corpus callosum), or diffuse and less well-defined in distribution. Damage to white matter is a common and prominent sequel to carbon monoxide poisoning. Myelin destruction in the corpus callosum may be focal or diffuse, the latter showing a 'butterfly-like' distribution in coronal section (Blackwood and Corsellis, 1976), similar to extensive destruction of the callosum often seen in epsilon-intoxicated mice. The action of epsilon toxin at the biochemical level has, however, been little studied.

The precise pathogenetic mechanisms giving rise to specific disease entities in the brain are often complex and underline the paucity of knowledge in many areas of neuropathology. This study has advanced a hypothesis for the development of necrosis based upon observations in the early stages of intoxication at the ultrastructural level, but a cogent explanation for the topographical distribution of malacic foci at the light microscope level was

not possible. The mechanisms proposed for the development of malacic lesions in some of these areas in other conditions were examined and may provide a partial explanation of lesions in individual sites, but do not encompass the full range of lesions induced by epsilon toxin.

Mice were found to be of considerable value in the study of the neurotoxic effects of epsilon toxin and both the nature and distribution of malacic lesions were comparable with those observed in sheep with FSE. Mice are, therefore, a useful model for the ovine disease.

SUMMARY

Lethal and sublethal doses of epsilon toxin prepared from filtrates of broth cultures of *Clostridium perfringens* Type D were administered to mice and sheep. Their brains were examined by light and electron microscopy after varying intervals post-inoculation. Both perfusion and immersion fixation techniques were employed.

The earliest change in the brain of mice exposed to epsilon toxin was increased vascular permeability leading to vasogenic oedema. The initial ultrastructural finding was swelling of astrocytes and their processes, notably the perivascular extensions of these cells, and this alteration imparted a spongy appearance to the neuropil at the light microscope level. Marked swelling of astrocytic end-feet sometimes caused stenosis of some capillary lumina. Swelling of astrocytes in the cerebellum was prominent at this stage and the cerebellar granular layer may be the area where necrotic foci are first manifest. Capillary haemorrhage and exudation of copious amounts of plasma protein was associated with the oedema in some areas. Morphological evidence of severe damage to the capillary endothelium closely followed astrocytic swelling with the endothelial cytoplasm becoming attenuated, vacuolated and very electron dense. "Blebs" of endothelial cytoplasm often projected into the lumen of affected vessels contributing to luminal obstruction. Axonal swelling with separation of myelin lamellae and a moderate increase in the size of the extracellular space in the white matter also occured relatively early in the disease process. Neuronal degeneration appeared to be secondary to oedematization of the neuropil.

In mice which survived the acute intoxication or were subacutely affected the oedema sometimes progressed to frank necrosis. The lesions were focal in nature and usually bilaterally symmetrical. A pathogenetic sequence of events leading to malacia, derived from ultrastructural observations, is proposed and possible mechanisms which could be invoked to explain the topographical distribution of the lesions are discussed. These necrotic foci were eventually

invaded by macrophages, becoming compound granular corpuscles with ingestion of myelin debris, and capillaries leading to resolution by astrocytic scarring. The distribution of malacic foci in mice closely resembled those found in naturally occuring cases of ovine focal symmetrical encephalomalacia, and the early changes in the brain of experimentally intoxicated lambs were similar to those described in mice.

The integrity of cerebral vessels to macromolecules such as ferritin remained largely unchanged, but widespread leakage of smaller vascular tracers such as horseradish peroxidase and Evans blue into the brain of intoxicated mice occured, confirming the alteration in vascular permeability in many affected areas. However, increased permeability of vessels was minimal or absent in the hippocampus and heavily myelinated fibre tracts, where malacic lesions were also detected.

Histological and ultrastructural changes in the lung and kidney of intoxicated mice were minimal but severe myocardial damage was sometimes observed when the heart was examined electron microscopically. It appears that murine cerebral vessels are more susceptible to the action of epsilon toxin as evidence of endothelial damage of the type found in the brain was usually lacking in visceral organs. Tracer studies with ferritin indicated little change in the integrity of pulmonary and glomerular vessels in mice to this large molecular weight protein but transendothelial movement of tracer material was augmented in micropinocytotic vesicles of myocardial vessels exposed to epsilon toxin. Severe endothelial degeneration was present in lungs examined from intoxicated lambs and evidence from this and other studies suggests that, while capillary damage appears to be generalized in sheep, there appears to be a range of susceptibility of blood vessels in different organs in mice to epsilon toxin. Cerebral vessels in the latter species are especially vulnerable.

The prominent biochemical alterations in blood from intoxicated lambs were a respiratory and metabolic acidosis with a marked elevation of blood glucose.

TABLE 1

ASSAY FOR EPSILON ANTITOXIN IN SERUM OF LAMBS

Lamb identification	Antitoxin titre
K2 - 126	> 32.0 µ/ml.
K2 - 147	2.0 "
K2 - 274	8.0 "
K2 - 314	> 32.0 "
K2 - 387	8.0 "
K2 - 460	4.0 "
K2 - 558	16.0 "
K2 - 643	32.0 "
K2 - 663	32.0 "

TABLE 2

CLOSTRIDIUM PERFRINGENS TOXINS

TYPE	alpha	beta	epsilon	iota
A	++	-	-	-
B	+	++	+	-
C	+	++	-	-
D	+	-	++	-
E	+	-	-	++

++ produced as the predominant toxic fraction

+ produced in smaller quantities

- not produced

TABLE 3

RESPONSE OF LAMBS TO EPSILON TOXIN

Lamb identification	Weight (kg.)	Age (days)	Toxin dose (mls)	Toxin dilution	Time of death post-inoculation (hrs)
K2-104	7.7	16	Control	-	-
K2-94	8.3	16	5	undiluted	1.25
K2-100	7.2	16	10	undiluted	0.08
K2-420	3.1	6	0.5	1/10	3.00
K2-98	5.5	16	20*	undiluted	3.50
K2-93	5.9	16	25*	undiluted	6.00
K2-96	7.5	16	25*	undiluted	6.00
K2-97	8.0	16	25*	undiluted	6.50

* administered in divided doses

TABLE 4

DISTRIBUTION AND SEVERITY OF BRAIN LESIONS IN MICE

	MULTIPLE SUBLETHAL DOSES OF TOXIN ADMINISTERED				SINGLE SUBLETHAL DOSE OF TOXIN ADMINISTERED			
	GRADED SEVERITY OF LESIONS			NUMBERS OF ANIMALS AFFECTED	GRADED SEVERITY OF LESIONS			NUMBERS OF ANIMALS AFFECTED
	+	++	+++		+	++	+++	
Cerebral cortex	9	4	1	14	3	–	–	3
Corpus callosum	4	3	6	13	–	–	–	–
Corpus striatum	2	9	3	14	1	–	–	1
Thalamus	4	1	1	6	–	–	–	–
Paraventricular area of lateral ventricles	5	1	–	6	–	–	–	–
Vestibular area	7	7	–	14	1	–	–	1
Corpus medullare cerebelli	4	6	1	11	1	–	–	1
Granular layer of cerebellum	2	2	–	4	1	4	–	5
Substantia nigra	–	1	–	1	2	–	–	2
Anterior commissure	–	1	–	1	–	–	–	–
Number of animals injected	60				30			
Number of animals with lesions	32				7			

Degree of severity of lesions: + minimal; ++ moderate; +++ severe

+ = mild vacuolation of the neuropil and macroglial reaction

++ = moderate vacuolation with necrosis of a few glial cells

+++ = severe vacuolation with necrosis of most glial elements

TABLE 5

ALTERATION IN BLOOD BIOCHEMICAL PARAMETERS FOLLOWING ADMINISTRATION OF EPSILON TOXIN TO LAMBS

Lamb No.	Time from toxin administration (Minutes)	PO_2 (mm Hg)	PCO_2 (mm Hg)	pH	H+Ion conc. (NMOL/L)	Actual HCO_3^- (MMOL/L)	Blood Glucose (MMOL/L)
1	0	37	39	7.39	41	24	6.7
	60	16	80	6.90	126	16	12.8
2	0	43	49	7.37	42	28	3.5
	30	39	44	7.38	42	23	9.7
	45	23	50	7.19	64	20	13.9
	60	18	62	7.03	92	16	12.4
3	0	46	37	7.42	38	24	4.8
	15	21	53	7.19	64	20	7.7

TABLE 6

ALTERATION IN HAEMATOLOGICAL VALUES IN LAMBS FOLLOWING EPSILON TOXIN ADMINISTRATION

Lamb No.	Time from toxin administration (mins.)	RBC $x10^6/mm^3$	Hb %	PCV %	MCV μ^3	MCHC %	Total WBC $x10^3/mm^3$	Neutrophils %	Lymphocytes %	Monocytes %	Eosinophils %	Plasma Protein gm %
1	0	9.2	10.0	29.0	32.0	34.5	5.5	30	70	-	-	7.0
	60	10.8	12.0	35.0	32.0	34.3	3.7	41	53	5	1	6.5
2	0	10.1	10.8	31.5	32.0	34.3	12.2	56	34	-	10	6.1
	30	11.6	13.1	38.5	33.0	34.0	9.8	55	42	-	3	7.3
	45	11.0	12.4	37.0	34.0	32.4	7.6	42	57	-	1	5.8
	60	11.1	12.4	33.0	30.0	37.6	8.0	67	32	-	1	5.8
3	0	9.4	7.8	55.0	27.0	30.6	5.3	20	77	1	2	12.0
	15	11.1	9.5	32.0	29.0	29.7	5.8	7	93	-	-	11.9

TABLE 7

BLOOD GLUCOSE LEVELS IN INTOXICATED MICE

TOXIN DOSE	TIME FROM TOXIN ADMINISTRATION (HOURS)	BLOOD GLUCOSE (MMOL/L)
Control	0	8.83
Control	0	8.92
Lethal	½	16.78
Lethal	½	18.71
Lethal	½	15.36
Lethal	1	15.60
Sublethal	2	15.39
Sublethal	4	16.50
Sublethal	4	17.03

BIBLIOGRAPHY

Abramowicz, A. 1964. The Pathogenesis of Experimental Periventricular Cerebral Necrosis and its Possible Relation to the Periventricular Leukomalacia of Birth Trauma. J. Neurol. Neurosurg. Psychiat. 27: 85-95.

Adornato, B. and Lampert, P. 1971. Status Spongiosus of Nervous Tissue: Electron Microscopic Studies. Acta Neuropathol. 19: 271-289.

Ames, A., Wright, L., Kowada, M., Thurston, J.M. and Majno, G. 1968. Cerebral Ischaemia. II. The No-Reflow Phenomenon. Am. J. Pathol. 52: 437-453.

Baldwin, B.A. 1964. The Anatomy of the Arterial Supply to the Cranial Regions of the Sheep and Ox. Am. J. Anat. 115: 101-118.

Banker, B.Q. and Larroch, J.C. 1962. Periventricular Leukomalacia of Infancy: A Form of Neonatal Anoxic Encephalopathy. Arch. Neurol. 7: 386-410.

Barlow, R.M. 1958. Focal Symmetrical Encephalomalacia in Lambs. Vet. Rec. 70: 884.

Bennetts, H.W. 1932. Infectious Enterotoxaemia of Sheep in Western Australia. Comm. Sci. Ind. Res. Aust. Bull. No. 57.

Bourke, R.S., Kimelberg, H.K., Nelson, L.R., Barron, K.D., Auen, E.L., Popp, A.J. and Waldman, J.B. 1980. Biology of Glial Swelling in Experimental Brain Oedema. In Advances in Neurology, Vol. 28, Raven Press, New York. P. 100.

Brierley, J.B. 1970. Systemic Hypotension - Neurological and Neuropathological Aspects. Mod. Trends. Neurol. 5: 164-167.

Brierley, J.B., Meldrum, B.S. and Brown, A.W. 1973. The Threshold and Neuropathology of Cerebral "Anoxic - Ischaemic" Cell Change. Arch. Neurol. 29: 367-374.

Brierley, J.B. 1977. Experimental Hypoxic Brain Damage. J. Clin. Pa th., 30, Suppl., 11: 181-187.

Brierley, J.B. 1979. Ischaemic Necrosis Along Brain Arterial Boundary Zones: Some Aspects of its Aetiology. Adv. Neurol. 26: 155-162.

Brightman, M.W., Klatzo, I., Olsson, Y. and Reese, T.S. 1970. The Blood-Brain Barrier to Proteins Under Normal and Pathological Conditions. J. Neurol. Sci. 10: 215-239.

Bruns, R.R. and Palade, G.E. 1968. Studies on Blood Capillaries. II. Transport of Ferritin Molecules Across the Wall of Muscle Capillaries. J. Cell. Biol. 37: 277-299.

Bullen, J.J. 1970. Role of Toxins in Host-Parasite Relationships. In Microbial Toxins, Vol. 1, S.J. Ajl, S. Kadis and T.C. Montie (Eds), Academic Press, New York, pp. 233-276.

Bullen, J.J. and Scarisbrick, R. 1953. Enterotoxaemia of Sheep: The Fate of Washed Suspensions of *Clostridium welchii* Type D Introduced into the Rumen of Normal Sheep. J. Pathol. Bacteriol. 65: 209-219.

Bullen, J.J. and Scarisbrick, R. 1957. Enterotoxaemia of Sheep: Experimental Reproduction of the Disease. J. Pathol. Bacteriol. 73: 493-509.

Burch, G.E., Shih-Chien Sun, Sohral, R.S., Kang-Chu Chu and Colcolough, H.L. 1968. Diphtheritic Myocarditis - A Histochemical and Electron Microscopic Study. Am. J. Cardiol. 21: 261-268.

Buxton, D. 1976. Use of Horseradish Peroxidase to Study the Antagonism of *Clostridium welchii (Cl. perfringens)* Type D Epsilon Toxin in Mice by the Formalinized Epsilon Prototoxin. J. Comp. Pathol. 86: 67-72.

Buxton, D. and Morgan, K.T. 1976. Studies of Lesions Produced in the Brains of Colostrum Deprived Lambs by *Clostridium welchii (Cl. perfringens)* Type D Toxin. J. Comp. Pathol. 86: 435-447.

Buxton, D. 1978. Further Studies on the Mode of Action of *Clostridium welchii* Type D Epsilon Toxin. J. Med. Microbiol. 11: 293-302.

Buxton, D. 1978. The Use of an Immunoperoxidase Technique to Investigate by Light and Electron Microscopy the Sites of Binding of *Clostridium welchii* Type D Toxin in Mice. J. Med. Microbiol. 11: 289-298.

Cantu, R.C. and Ames, A. 1969. Distribution of Vascular Lesions Caused by Cerebral Ischaemia. Relation to Survival. Neurology. 19: 128-132.

Casley-Smith, J.R. 1962. The Displacement of Ferritin Molecules by the Microtome Knife. J. Microscopie. 1: 335-342.

Casley-Smith, J.R. 1964. Endothelial Permeability - The Passage of Particles Into and Out of Diaphragmatic Lymphatics. Quart. J. Exp. Physiol. 49: 365-383.

Casley-Smith, J.R. 1967. An Electron Microscopical Study of the Passage of Ions Through the Endothelium of Lymphatic and Blood Capillaries, and Through the Mesothelium. Quart. J. Exp. Physiol. 52: 105-113.

Casley-Smith, J.R. and Carter D.B. 1979. The Passage of Macromolecules Across Inflamed Capillary Endothelium via Large Vacuoles. Microvasc. Res. 18: 319-324.

Casley-Smith, J.R. and Chin, J.C. 1971. The Passage of Cytoplasmic Vesicles Across Endothelial and Mesothelial Cells. J. Microscopy. 93: 167-189.

Cervos-Navarro, J. and Ferstz, R. 1980. Brain Oedema-Pathology, Diagnosis and Therapy. In Advances in Neurology, Vol. 28, Raven Press, New York, p. 24.

Chiang, J., Kowada, M., Ames, A., Wright, R.L. and Majno, G. 1968. Cerebral Ischaemia. III. Vascular Changes. Am. J. Pathol. 52: 455-476.

Cotran, R.S., Suter, E.R. and Majno, G. 1967. The Use of Colloidal Carbon as a Tracer for Vascular Injury. Vasc. Dis. 4: 107-127.

Courville, C.B. 1958. Aetiology and Pathogenesis of Laminar Cortical Necrosis. Arch. Neurol. Psychiat. 79: 7-30.

De Reuck, J. 1971. The Human Periventricular Arterial Blood Supply and The Anatomy of Cerebral Infarctions. Eur. Neurol. 5: 321-334.

De Reuck, J., Chattha, A.S. and Richardson, E.P. 1972. Pathogenesis and Evolution of Periventricular Leukomalacia in Infancy. Arch. Neurol. 27: 229-236.

Elder, J.M. and Miles, A.A. 1957. The Action of the Lethal Toxins of Gas-Gangrene *Clostridia* on Capillary Permeability. J. Pathol. Bacteriol. 74: 133-145.

Ellner, P.D. 1961. Fate of Partially-Purified C^{14}-labelled Toxin of *Clostridium perfringens*. J. Bacteriol. 82: 275-283.

Farquhar, M.G., Wissig, S.L. and Palade, G.E. 1961. Glomerular Permeability. I. Ferritin Transfer Across the Normal Glomerular Capillary Wall. J. Exp. Med. 113: 47-66.

Feigin, I. and Popoff, N. 1962. Neuropathological Observations on Cerebral Oedema. Arch. Neurol. Psychiat. 6: 151.

Fishman, A.P. and Renkin, E.M. 1979. Pulmonary Oedema. American Physiological Society, Bethesda, Maryland, pp. 17, 20.

Freedman, F.B. and Johnson, J.A. 1969. Equilibrium and Kinetic Properties of the Evans blue-Albumin System. Am. J. Physiol. 216: 675-681.

Garcia, J.H., Conger, K.A., Morawetz, R. and Halsey, J.H. 1980. Post-Ischaemic Brain Oedema: Quantitation and Evolution. In Advances in Neurology, Vol. 28., Raven Press, New York, p. 147.

Gardner, D.E. 1973. Pathology of *Clostridium welchii* Type D Enterotoxaemia I. Biochemical and Haematological Alterations in Lambs. J. Comp. Pathol. 83: 499-507.

Gardner, D.E. 1973. Pathology of *Clostridium welchii* Type D Enterotoxaemia. II. Structural and Ultrastructural Alterations in the Tissues of Lambs and Mice. J. Comp. Pathol. 83: 509-524.

Gardner, D.E. 1973. Pathology of *Clostridium welchii* Type D Enterotoxaemia III. Basis of the Hyperglycaemic Response. J. Comp. Pathol. 83: 525-529.

Gardner, D.E. 1972. The Stability of *Clostridium perfringens* Type D Epsilon Toxin in Intestinal Contents *in vitro*. N.Z. Vet. J. 20: 167-168.

Gardner, D.E. 1974. Brain Oedema: An Experimental Model. Br. J. Exp. Pathol. 55: 453-457.

Gay, C.C., Blood, D.C. and Wilkinson, J.S. 1975. Clinical Observations of Sheep with Focal Symmetrical Encephalomalacia. Aust. Vet. J. 20: 266-269.

Gill, D.A. 1927. "Pulpy Kidney" Disease of Lambs. N.Z. J. Agric. 35: 217-230.

Gonatas, N.K., Zimmermann, H.M. and Levine, S. 1963. Ultrastructure of Inflammation with Oedema in the Rat Brain. Am. J. Pathol. 42: 455-469.

Gordon, W.S., Stewart, J., Holman, H.H. and Taylor, A.W. 1940. Blood Changes and Post-Mortem Findings Following Intravenous Inoculation of Sheep with Culture Filtrates of *Cl. welchii*, Types A, C and D. J. Pathol. 50: 251-269.

Graham, R.C. and Karnovsky, M.J. 1966. The Early Stages of Absorption of Injected Horseradish Peroxidase in the Proximal Tubules of the Mouse Kidney: Ultrastructural Cytochemistry by a New Technique. J. Histochem. Cytochem. 14: 291-302.

Greenfield's Neuropathology. W. Blackwood and J.A.N. Corsellis (Eds), 3rd Edn, Edward Arnolds, London, pp. 68-70, 77, 196-198.

Griner, L.A. 1961. Enterotoxaemia of Sheep. I. Effects of *Clostridium perfringens* Type D Toxin on the Brains of Sheep and Mice. Am. J. Vet. Res. 22: 429-442.

Griner, L.A. and Carlson, W.D. 1961. Enterotoxaemia of Sheep. II. Distribution of I^{131} Radioiodinated Serum Albumin in Brains of *Clostridium perfringens* Type D Intoxicated Lambs. Am. J. Vet. Res. 22: 443-448.

Habeeb, A.F.S.A. 1969. Studies on Epsilon-Prototoxin of *Clostridium perfringens* Type D. I. Purification Methods and Evidence for Multiple Forms of Epsilon-Prototoxin. Arch. Biochem. Biophysics. 130: 430-440.

Hartley, W.J. 1956. A Focal Symmetrical Encephalomalacia of Lambs. N.Z. Vet. J. 4: 129-135.

Hauschild, A.H.W. 1971. *Clostridium perfringens* Toxins Types B, C, D and E. In Microbial Toxins, S. Kadis, T.C. Montie and S.J. Ajl (Eds), Vol. IIA, Academic Press, New York, p. 170-182.

Hicks, S.P. 1950. Brain Metabolism *in vivo*. I. The Distribution of Lesions Caused by Cyanide psg., Insulin Hypoglycaemia, Asphyxia in Nitrogen and Fluoroacetate psg. in Rats. Arch. Pathol. 49: 111-137.

Hicks, S.P. (1950). Brain Metabolism *in vivo*. II. The Distribution of Lesions Caused by Azide, Malononitrile, Plasmocid and Dinitrophenol Poisoning in Rats. Arch. Pathol. 50: 545-561.

Hirano, A., Becker, N.H. and Zimmermann, H.M. 1969. Pathological Alterations in the Cerebral Endothelial Cell Barrier to Peroxidase. Arch. Neurol. 20: 300-303.

Hirano, A., Becker, N.H. and Zimmerman, H.M. 1970. The Use of Peroxidase as a Tracer in Studies of Alterations in the Blood-Brain Barrier. J. Neurol. Sci. 10: 205-213.

Hirano, A. 1980. Fine Structure of Oedematous Encephalopathy. In: Advances in Neurology, Vol. 28, Raven Press, New York, pp. 83-97.

Innes, J.R.M. and Saunders, L.Z. 1962. Encephalomalacia and Myelomalacia. In Comparative Neuropathology, Academic Press, New York, p. 607-623.

Ishii, S. and Tani, E. 1962. Electron Microscopic Study of the Blood-Brain Barrier in Brain Swelling. Acta Neuropath. 1: 474-488.

Jorris, I., De Girolami, U., Wortham, K. and Majno, G. 1982. Vascular Labelling with Monastral blue B. Stain Tech. 57: 177-183.

Jubb, K.V.F. and Kennedy, P.C. 1970. Pathology of Domestic Animals, Vol. II, Academic Press, New York, pp. 114-120, 377-387.

Karnovsky, M.J. 1965. A Formaldehyde-Glutaraldehyde Fixative of High Osmolality for Use in Electron Microscopy. J. Cell. Biol. 27: 137.

Karnovsky, M.J. 1967. The Ultrastructural Basis of Capillary Permeability Studied With Peroxidase as a Tracer. J. Cell. Biol. 35: 213-236.

Kellaway, C.H., Trethewie, E.R. and Turner, A.W. 1940. Neurotoxic and Circulatory Effects of the Toxin of *Clostridium welchii* Type D. Aust. J. Exp. Biol. Med. Sci. 18: 225-252.

Klatzo, I. 1967. Neuropathological Aspects of Brain Oedema. J. Neuropathol. Exp. Neurol. 26: 1-14.

Klatzo, I. and Seitelberger, F. 1967. Brain Oedema, Springer-Verlag, New York.

Klatzo, I., Chui, E., Fujiwara, K. and Spatz, M. 1980. Resolution of Vasogenic Brain Oedema. In: Advances in Neurology, Vol. 28, Raven Press, New York, pp. 359-374.

Kohler, B. and Friemuth, U. 1971. Stability of *Clostridium perfringens* Toxins in Post-Mortem Material From Dead Animals. Monatsh. Veterinarmed. 26 Heft. 16: 620-625.

Kowada, M., Ames, A., Majno, G. and Wright, R.L. 1968. Cerebral Ischaemia. I. An Improved Experimental Method for Study; Cardiovascular Effects and Demonstration of an Early Vascular Lesion in the Rabbit. J. Neurosurg. 28: 150-157.

Levine, S. 1960. Anoxic-Ischaemic Encephalopathy in Rats. Am. J. Pathol. 36: 1-17.

Levy, D.E., Brierley, J.B. and Plum, F. 1975. Ischaemic Brain Damage in the Gerbil in the Absence of "No-Reflow". J. Neurol. Neurosurg. Psychiat. 38: 1197-1205.

Lindenberg, R. 1955. Compression of Brain Arteries as Pathogenetic Factor for Tissue Necroses and Their Areas of Predilection. J. Neuropathol. Exp. Neurol. 14: 223-243.

Long, D.M., Hartmann, J.F. and French, L.A. 1966. The Ultrastructure of Human Cerebral Oedema. J. Neuropathol. Exp. Neurol. 25: 373-395.

Manz, H.J. 1974. The Pathology of Cerebral Oedema. Hum. Pathol. 5: 291-313.

Meyer, J.S. and Denny-Brown, D. 1957. The Cerebral Collateral Circulation. I. Factors Influencing Collateral Blood Flow. Neurology. 7: 447-458.

Morgan, K.T. and Kelly, B.G. 1974. Ultrastructural Study of Brain Lesions Produced in Mice by the Administration of *Clostridium welchii* Type D Toxin. J. Comp. Pathol. 84: 181-191.

Morgan, K.T., Kelly, B.G. and Buxton, D. 1975. Vascular Leakage Produced in the Brains of Mice by *Clostridium welchii* Type D Toxin. J. Comp. Pathol. 85: 461-466.

Niilo, L. 1965. Bovine "Enterotoxaemia". III. Factors Affecting The Stability of the Toxins of *Clostridium perfringens* Types A, C and D. Can. Vet. J. 6: 38-42.

Niilo, L. 1980. *Clostridium perfringens* in Animal Disease: Review of Current Knowledge. Can. Vet. J. 21: 141-148.

Orlans, E.S., Richards, C.B. and Jones, V.E. 1960. *Clostridium welchii* Epsilon-Toxin and Antitoxin. Immunology. 3: 28-44.

Palade, G.E. 1961. Blood Capillaries of the Heart and Other Organs. Circulation. 24: 368-388.

Pelosi, G., Meldolesi, J. and Nidiri, J. 1966. Ultrastructural and Biochemical Aspects of the Myocardium in Guinea-Pigs Treated with Diphtheria Toxin. Med. Pharm. Exp. 14: 537-549.

Peters, A., Palay, S.L. and Webster, H. DeF. 1970. The Fine Structure of the Nervous System, Harper and Row, New York.

Pienaar, J.G. and Thornton, D.J. 1964. Focal Symmetrical Encephalomalacia in Sheep in South Africa. J. S. Afr. Vet. Med. Assoc. 35: 351-358.

Pulsinelli, W.A. and Brierley, J.B. 1979. A New Model of Bilateral Hemispheric Ischaemia in the Unanaesthetized Rat. Stroke. 10: 267-272.

Raimondi, A.J. Evans, J.P. and Mullen, S. 1962. Studies of Cerebral Oedema. III. Alterations in the White Matter: An Electron Microscopic Study Using Ferritin as a Labelling Compound. Acta Neuropathol. 2: 177-197.

Reed, L.V. and Muench, H. 1938. A Simple Method of Estimating Fifty Per Cent Endpoints. Am. J. Hyg. 27: 493.

Reese, T.S. and Karnovsky, M.J. 1967. Fine Structural Localization of a Blood-Brain Barrier to Exogenous Peroxidase. J. Cell. Biol. 34: 207-217.

Salford, L.G., Plum, F. and Brierley, J.B. 1973. Graded Hypoxia - Oligaemia in Rat Brain. II. Neuropathological Alterations and Their Implications. Arch. Neurol. 29: 234-238.

Scarpelli, D.G. and Trump, B.F. 1971. Cell Injury. The Upjohn Co., Michigan, pp. 13-24.

Schade, J.P. and McMenemey, W.H. 1963. Selective Vulnerability of the Brain in Hypoxaemia. Blackwell Scientific Publications, Oxford.

Schneeberger, E.E. and Karnovsky, M.J. 1971. The Influence of Intravascular Fluid Volume on the Permeability of Newborn and Adult Mouse Lungs to Ultrastructural Protein Tracers. J. Cell. Biol. 49: 319-334.

Sidman, R.L., Angevine, J.B. and Pierce, E.T. 1971. Atlas of the Mouse Brain and Spinal Cord. Harvard University Press, Cambridge, Massachussetts.

Smith, L.D.S. 1957. *Clostridial* Diseases of Animals. Adv. Vet. Sci. 3: 463-524.

Smith, U. and Ryan, J.W. 1973. Electron Microscopy of Endothelial and Epithelial Components of the Lungs: Correlations of Structure and Function. Fed. Proc. 32: 1957-1966.

Tani, E. and Evans, J.P. 1965. Electron Microscopic Studies of Cerebral Swelling. I. Studies on the Permeability of Brain Capillaries, Using Ferritin Molecules as Tracers. Acta Neuropathol. 4: 507-526.

Thomson, R.O. 1963. The Fractionation of *Clostridium welchii* Epsilon-Antigen on Cellulose Ion Exchangers. J. Gen. Microbiol. 31: 79-90.

Tschirgi, R.D. 1962. Blood-Brain Barrier: Fact or Fancy? Fed. Proc. 21: 665-671.

Wasterlain, C.G. and Posner, J.B. 1968. Cerebral Oedema in Water Intoxication. I. Clinical and Chemical Observations. Arch. Neurol. 19: 71-78.

Wasterlain, C.G. and Torack, R.M. 1968. Cerebral Oedema in Water Intoxication. II. An Ultrastructural Study. Arch. Neurol. 19: 79-87.

Willis, A.T. 1977. Anaerobic Bacteriology: Clinical and Laboratory Practice. 3rd Edn., Butterworths, London, pp. 138.

Worthington, R.W., Mulders, M.S.G. and Van Rensberg, J.J. 1973. Enzymatic Activation of *Clostridium perfringens* Epsilon Prototoxin and Some Biological Properties of Activated Toxin. Onderstepoort J. Vet. Res. 40: 153-156.

Worthington, R.W., Mulders, M.S.G. and Van Rensberg, J.J. 1973. *Clostridium perfringens* Type D Epsilon Prototoxin. Some Chemical, Immunological and Biological Properties of a Highly Purified Prototoxin. Onderstepoort J. Vet. Res. 40: 145-152.

Worthington, R.W. and Mulders, M.S.G. 1975. The Effect of *Clostridium perfringens* Epsilon Toxin on the Blood-Brain Barrier of Mice. Onderstepoort J. Vet. Res. 42: 25-28.

Worthington, R.W., Bertschinger, H.S., Mulders, M.S.G. 1979. Catecholamine and Cyclic Nucleotide Responses of Sheep to the Injection of *Clostridium welchii* Type D Epsilon Toxin. J. Med. Microbiol. 12: 497-502.

Addendum:

Bakay, L. and Lee, J.C. 1965. Cerebral Oedema. Charles C. Thomas, Springfield, Illinois, U.S.A. p. 72.

Buxton, D., Linklater, K.A., and Dyson, D.A. 1978. Pulpy Kidney Disease and its Diagnosis by Histological Examination. Vet.Rec. 102:241.

ILLUSTRATIONS

Figure 1. Coronal section of mouse brain. 24 hours post-inoculation. Malacic foci in corpus callosum, area lateral to the lateral ventricle and thalamus. (arrows)
H & E x 10.

Figure 2. Coronal section of mouse brain. 24 hours post-inoculation. Bilaterally symmetrical lesions in corpus callosum, paraventricular area, corpus striatum, thalamus, fimbria of the hippocampus and focal lesion in the cerebral cortex. (arrows)
H & E x 10.

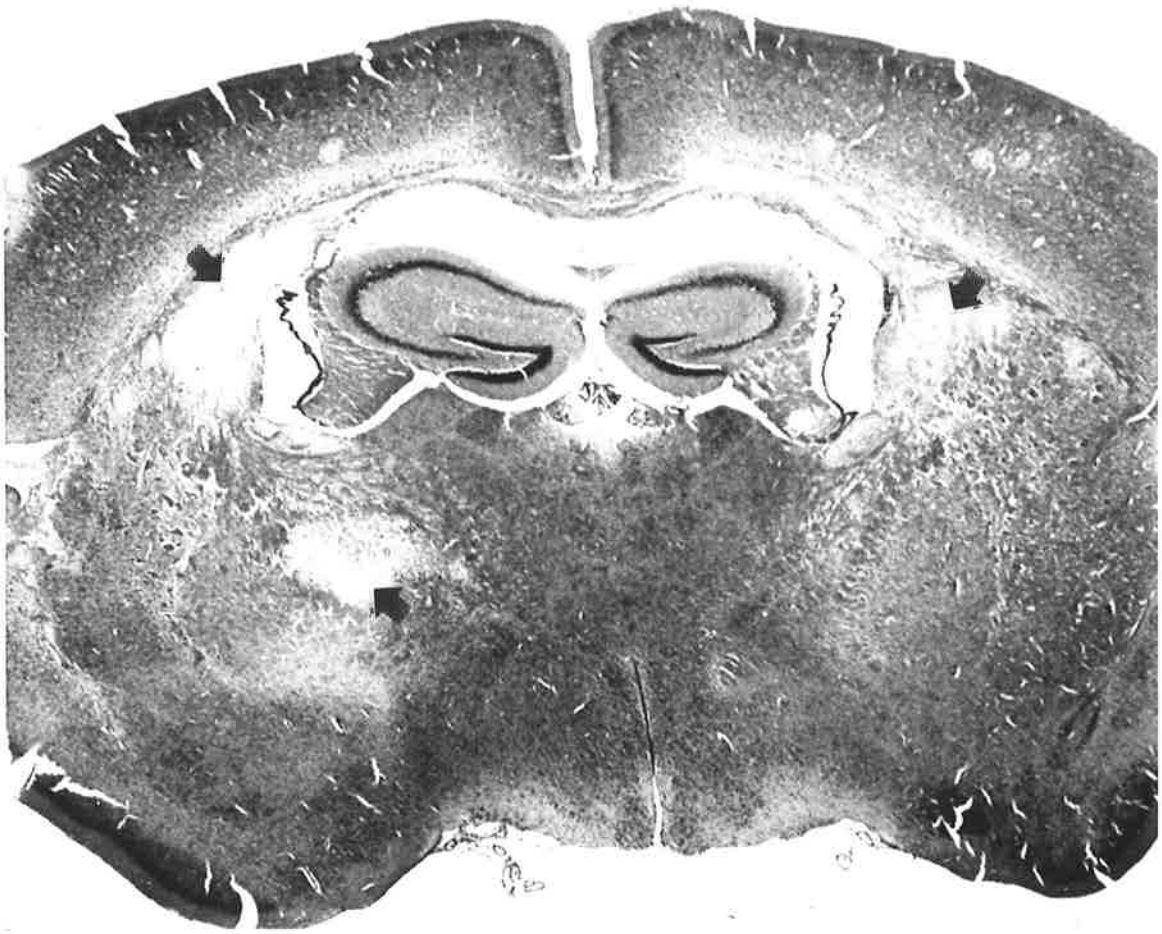

Figure 1.

Figure 2.

Figure 3. Normal mouse brain. Coronal section showing distribution of heavily myelinated fibre tracts. (arrows) Compare with distribution of lesions in Fig.2.
Luxol fast blue x 10.

Figure 4. Coronal section of mouse brain. 24 hours post-inoculation. Bilaterally symmetrical malacic foci in vestibular area. (arrows)
H & E x 10.

Figure 3.

Figure 4.

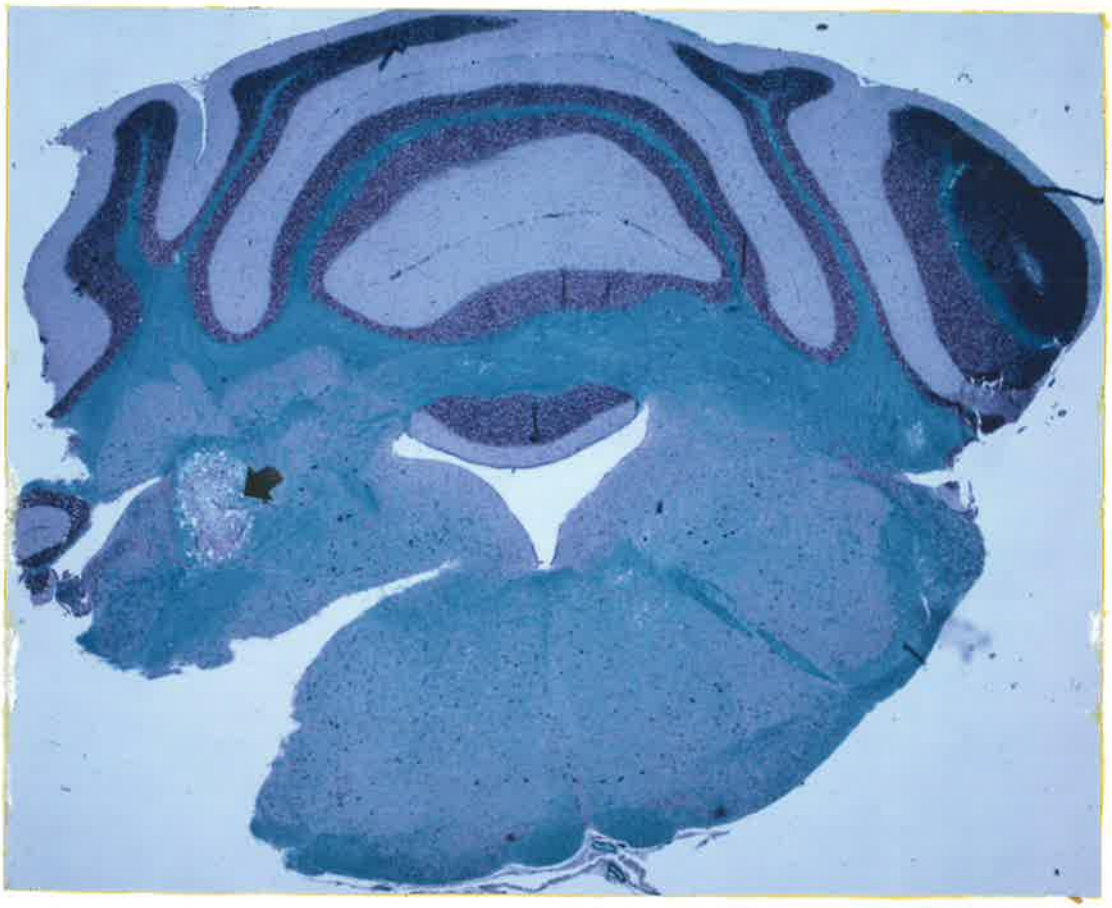

Figure 5.

Figure 6.

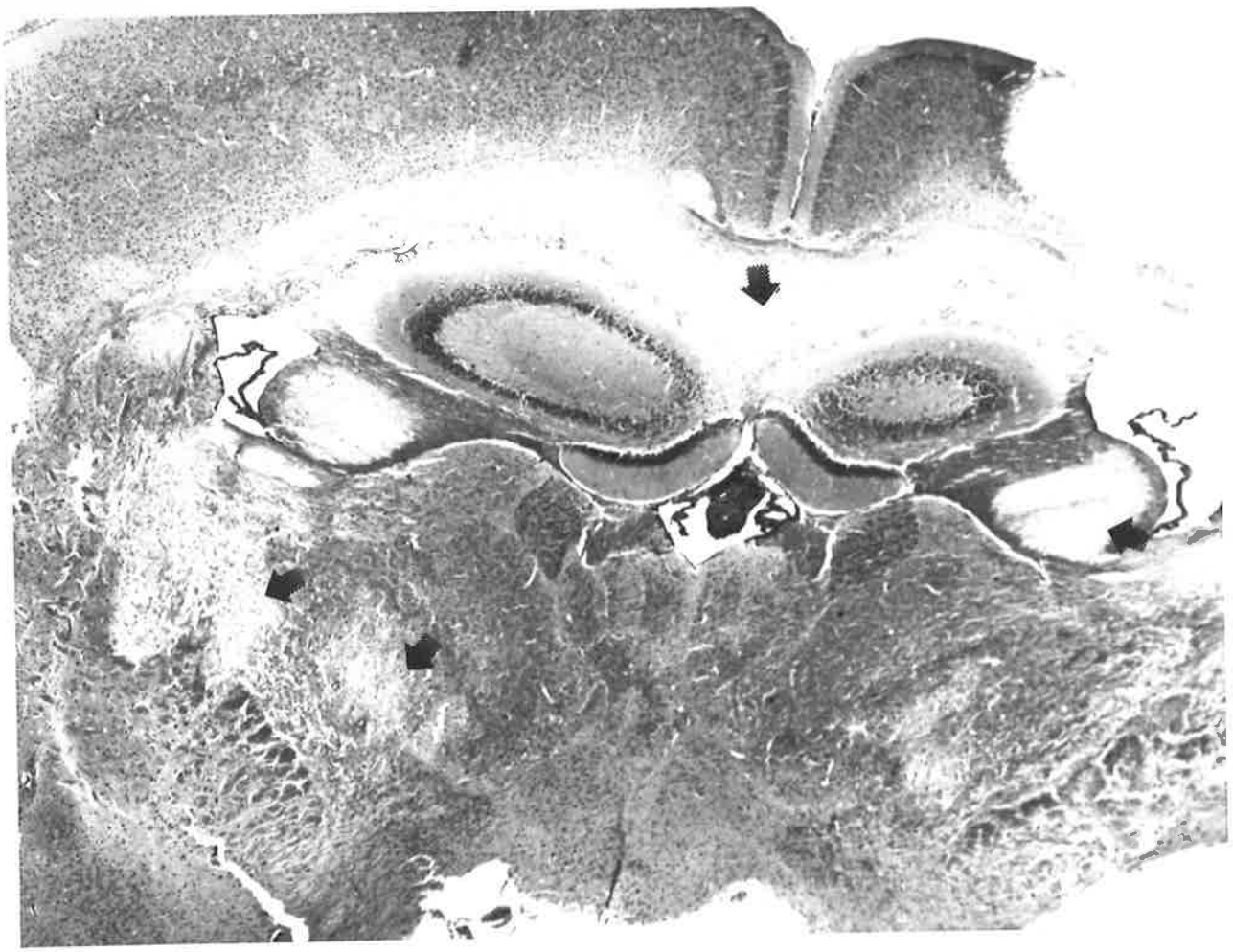

Figure 7.

Figure 8.

Figure 7. Coronal section of mouse brain. 36 hours post-inoculation. Extensive liquefaction necrosis in corpus callosum and bilaterally symmetrical malacic foci in corpus striatum, thalamus and fimbria of the hippocampus. (arrows)
H&E x 10.

Figure 8. Coronal section of mouse brain. 24 hours post-inoculation. Necrosis in corpus medullare cerebelli and vestibular area. (arrows)
H&E x 10.

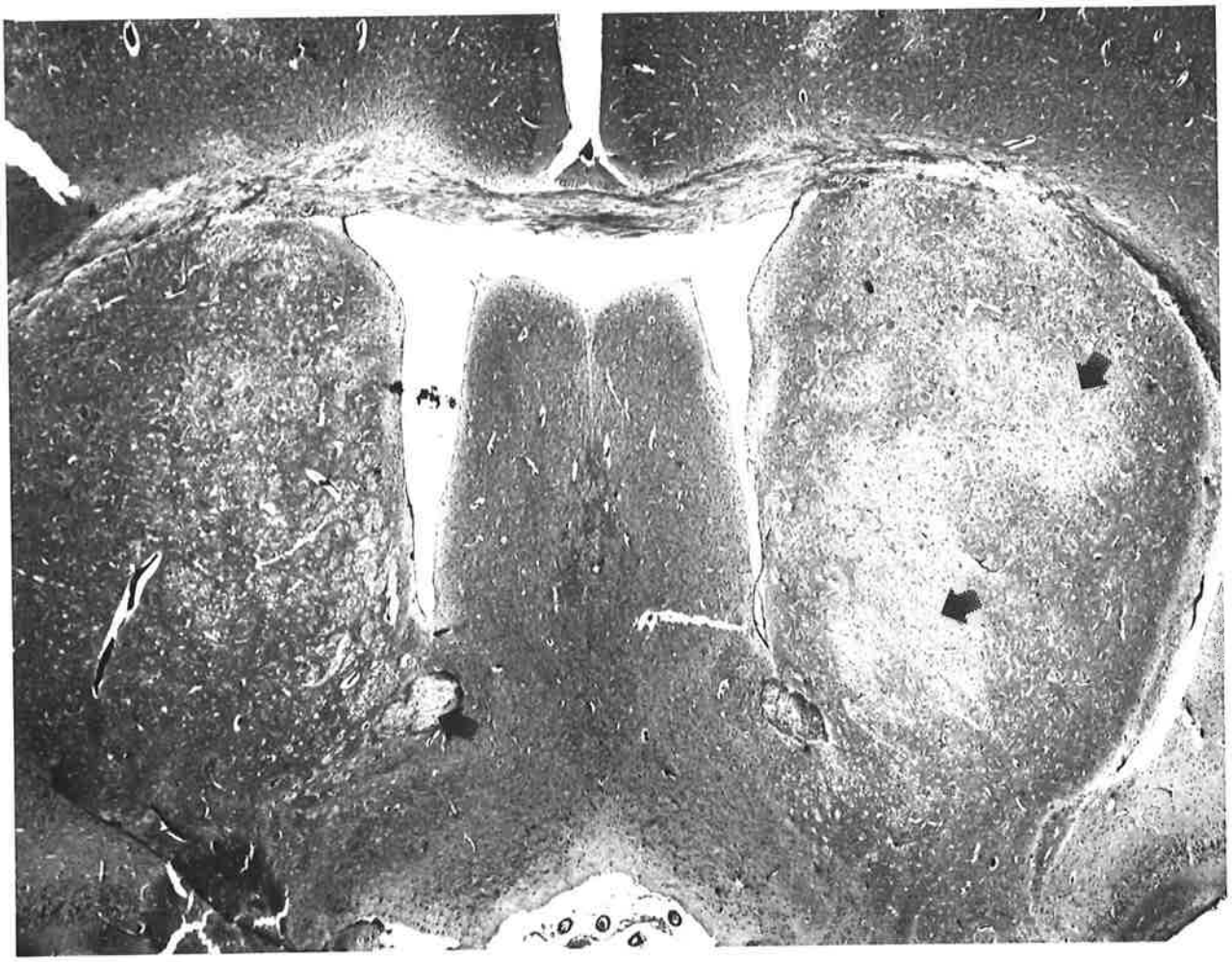

Figure 9.

Figure 10.

Figure 9. Coronal section of mouse brain. 24 hours post-inoculation. Necrotic foci in caudate nucleus and putamen, corpus callosum and anterior commissures. (arrows) H&E x 10.

Figure 10. Coronal section of mouse brain. 18 hours post-inoculation. Malacic lesions in callosal radiations, caudate nucleus, putamen, claustrum and anterior commissure. (arrows) H&E x 10.

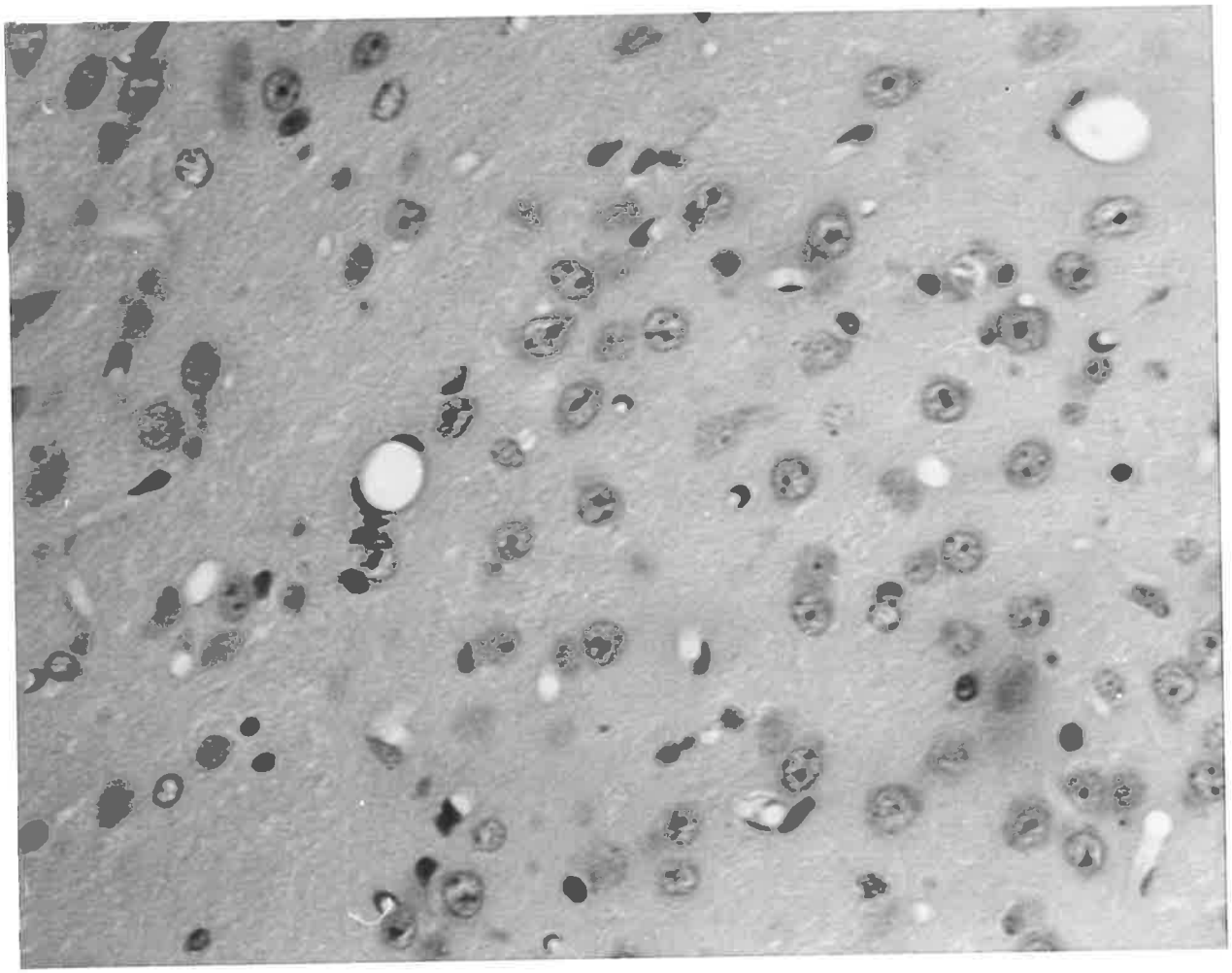

Figure 11.

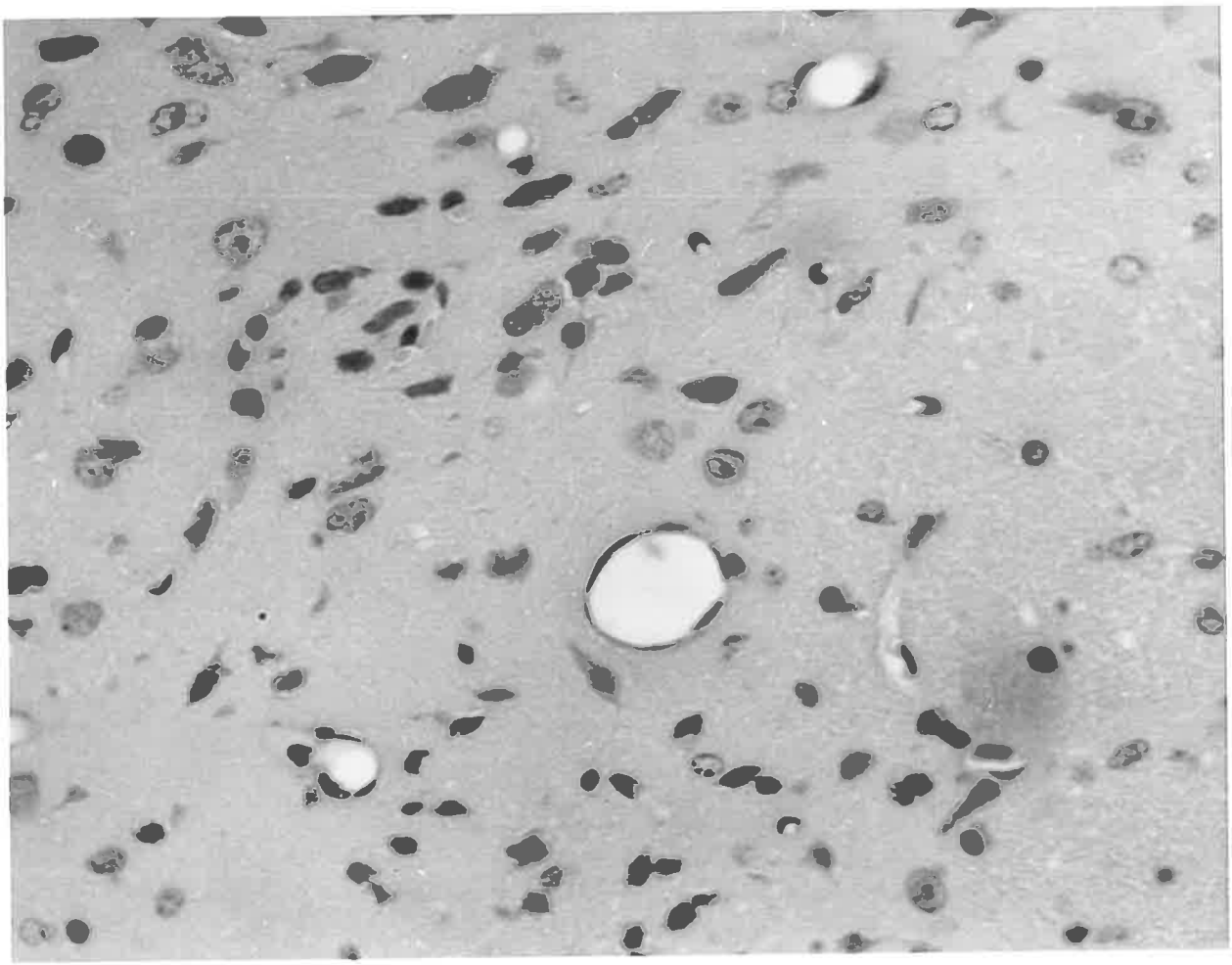

Figure 12.

Figures 11 & 12. Control mouse. Cerebral cortex. Perfusion fixation showing neuronal preservation and close apposition of capillary endothelium to the surrounding neuropil.

H&E x 200.

Figure 14. Toxin treated mouse. Corpus callosum. 2 hours post-inoculation. Early vacuolar appearance of spongy change in the neuropil.
H & E x 100.

Figure 13. Toxin treated lamb. Cerebral cortex. 1 hour post-inoculation. Marked enlargement of perivascular spaces.
H & E x 200.

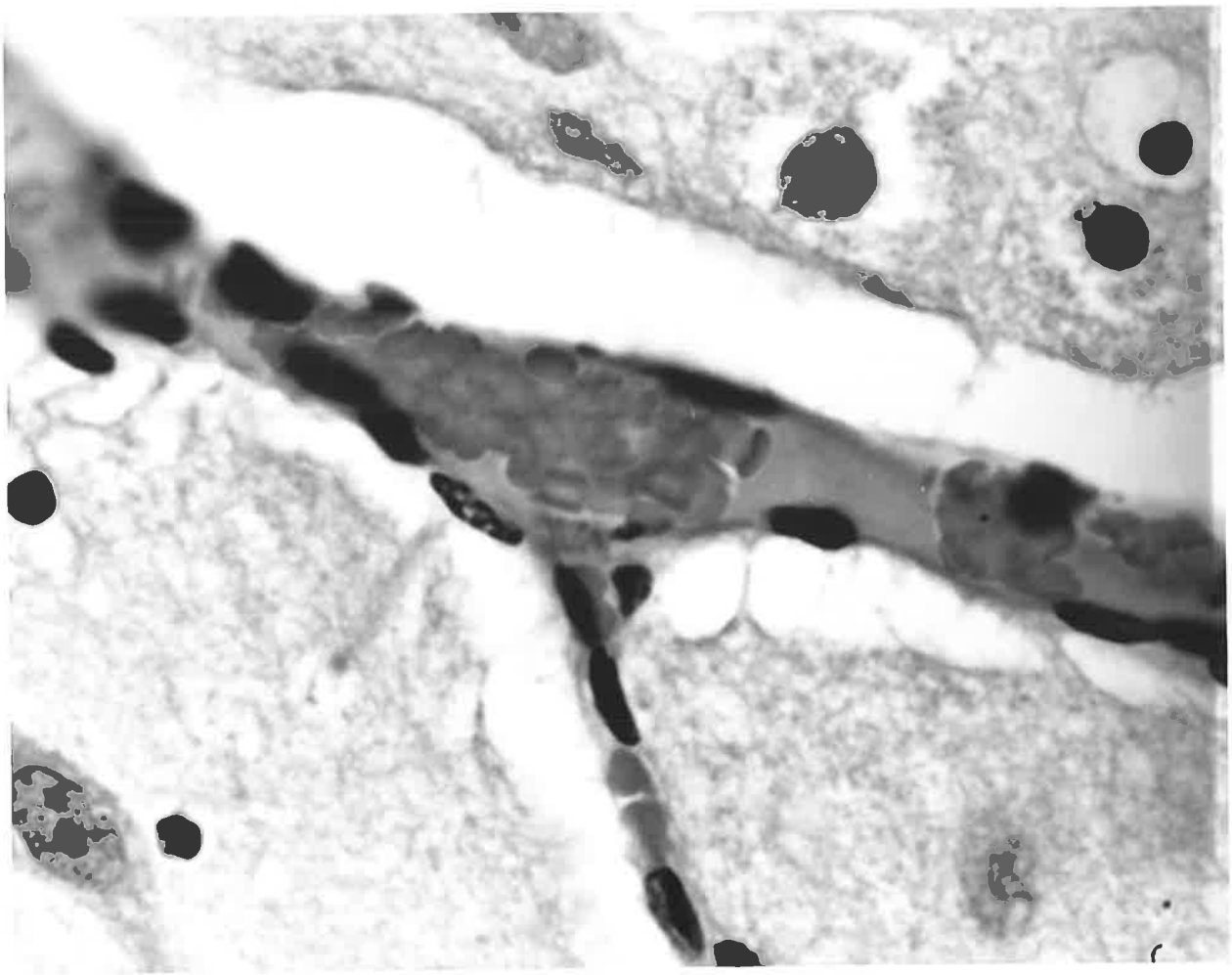

Figure 13.

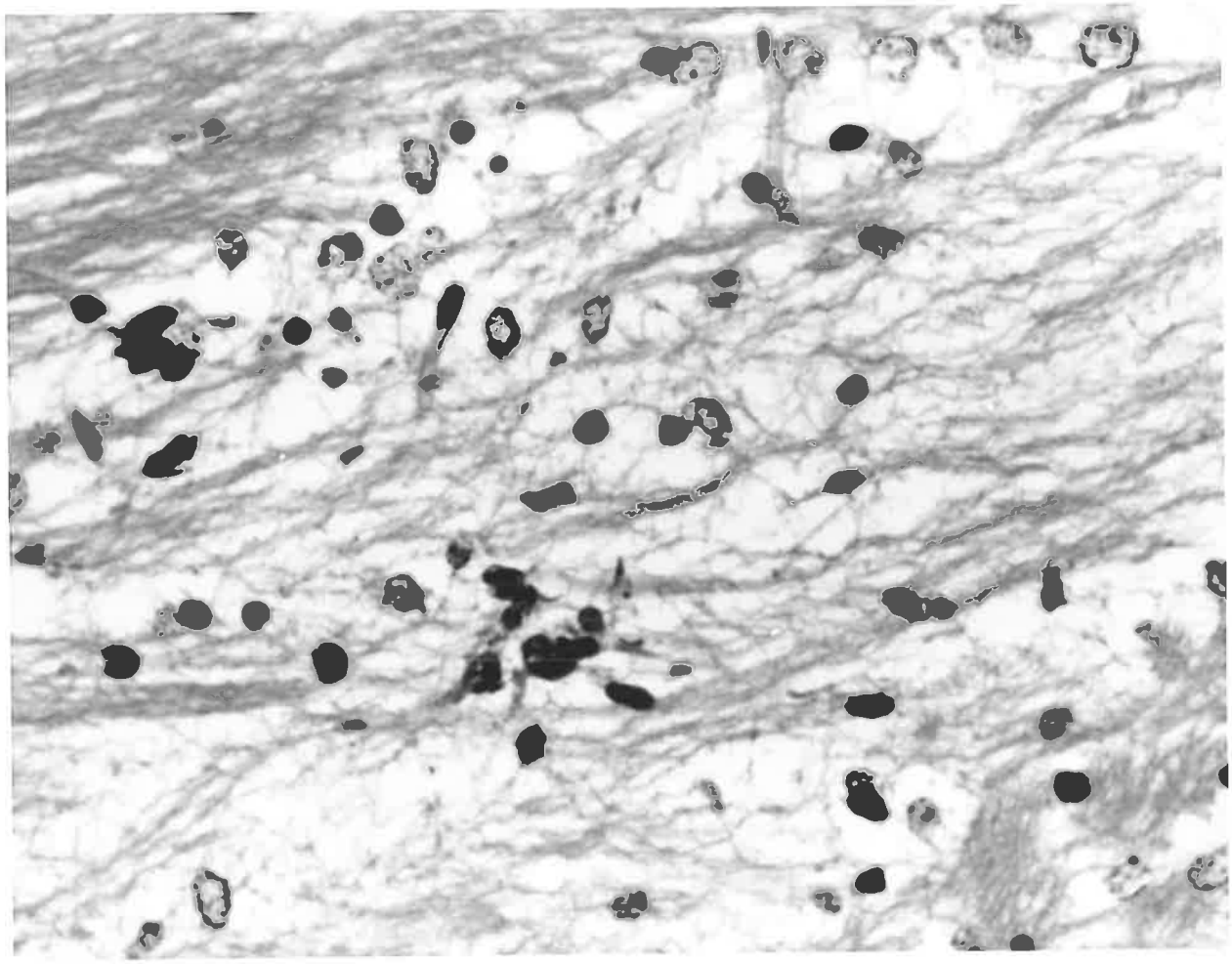

Figure 14.

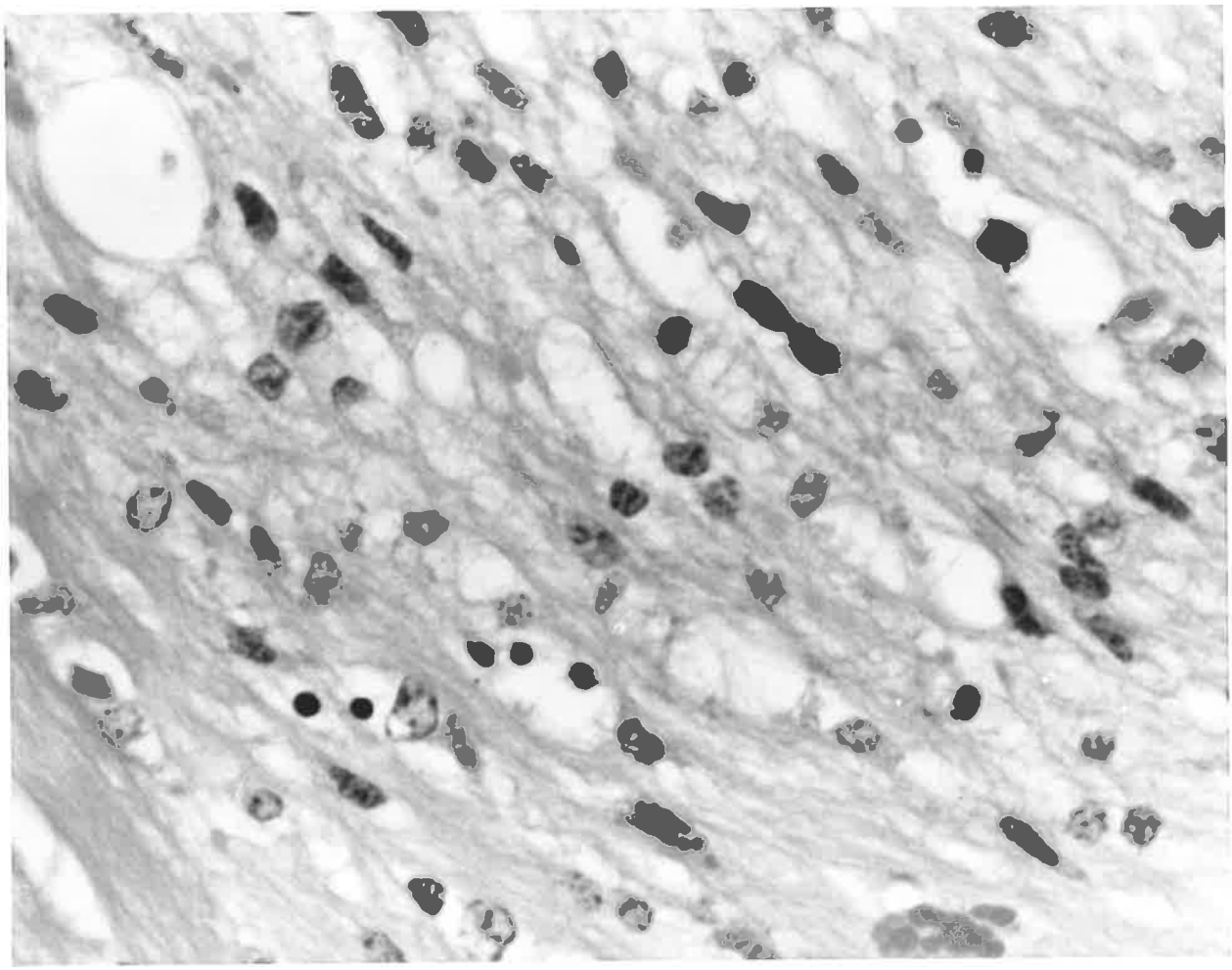

Figure 15.

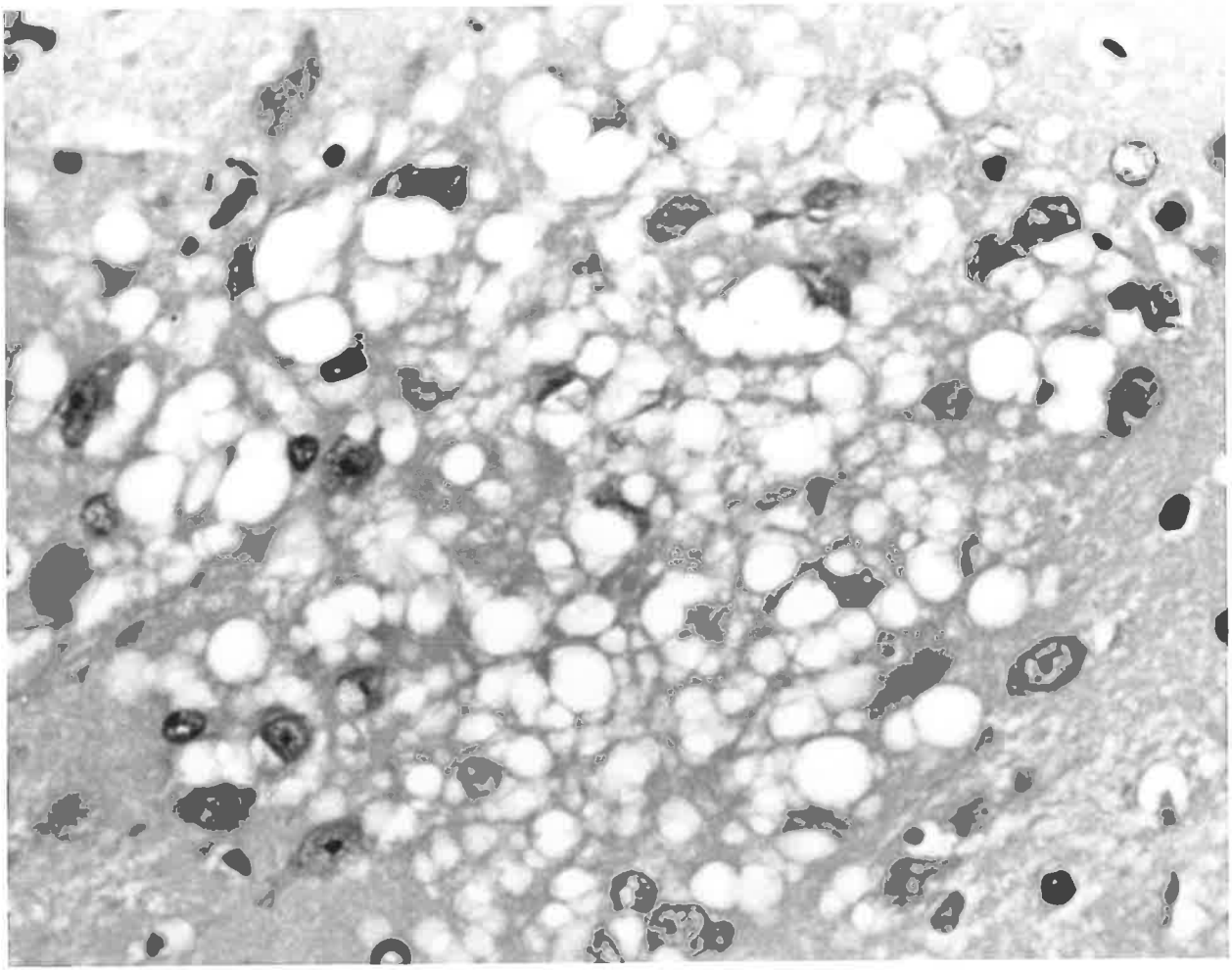

Figure 16.

Figure 15. Toxin treated mouse. Paraventricular area. 4 hours post-inoculation. Vacuolation of neuropil with lacy appearance of separated fibres. A few pyknotic astrocytic nuclei.
H&E x 100.

Figure 16. Toxin treated mouse. Cerebral cortex. 6 hours post-inoculation. Focal area of severe vacuolation. Neurones generally well preserved.
H&E x 100.

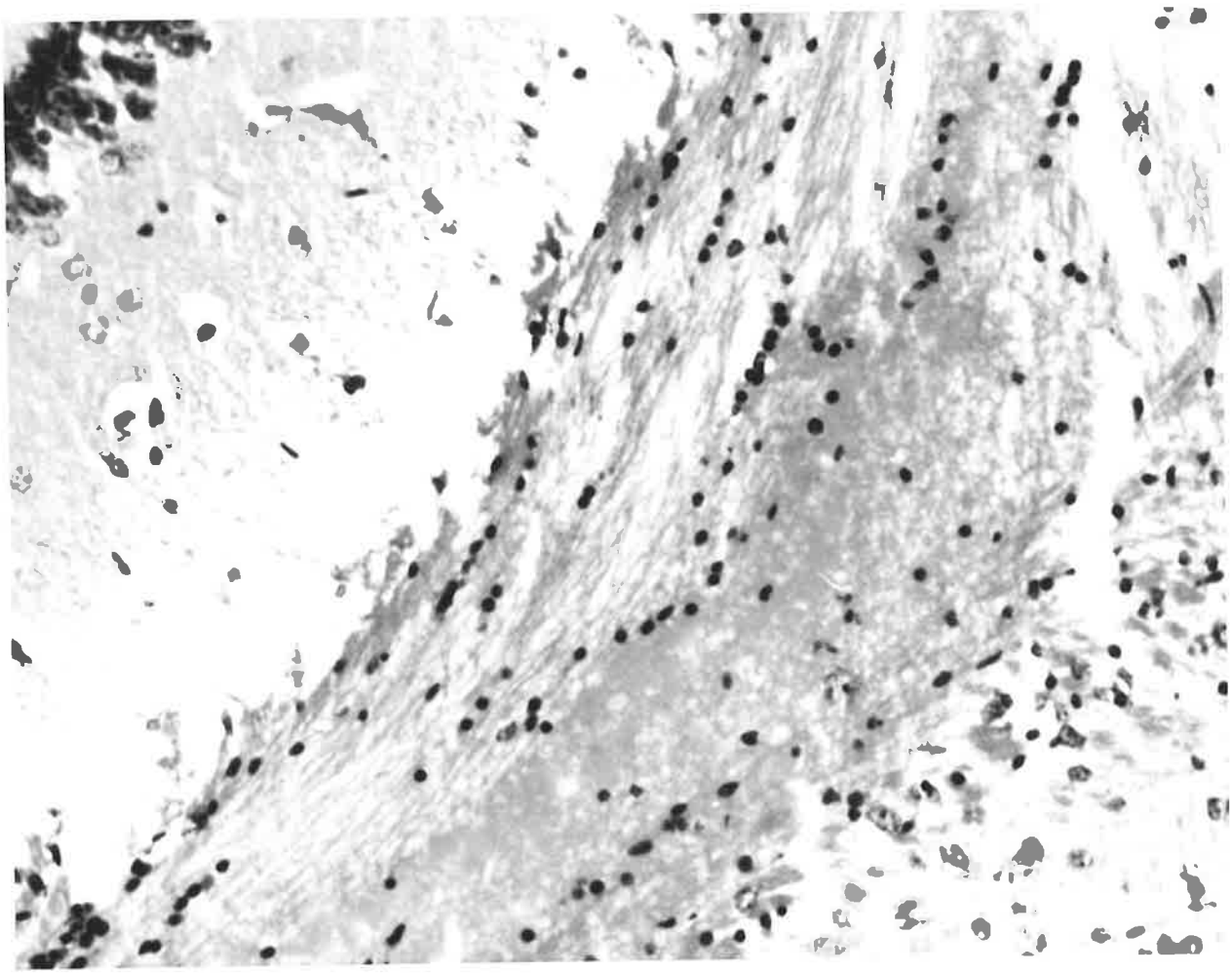

Figure 17.

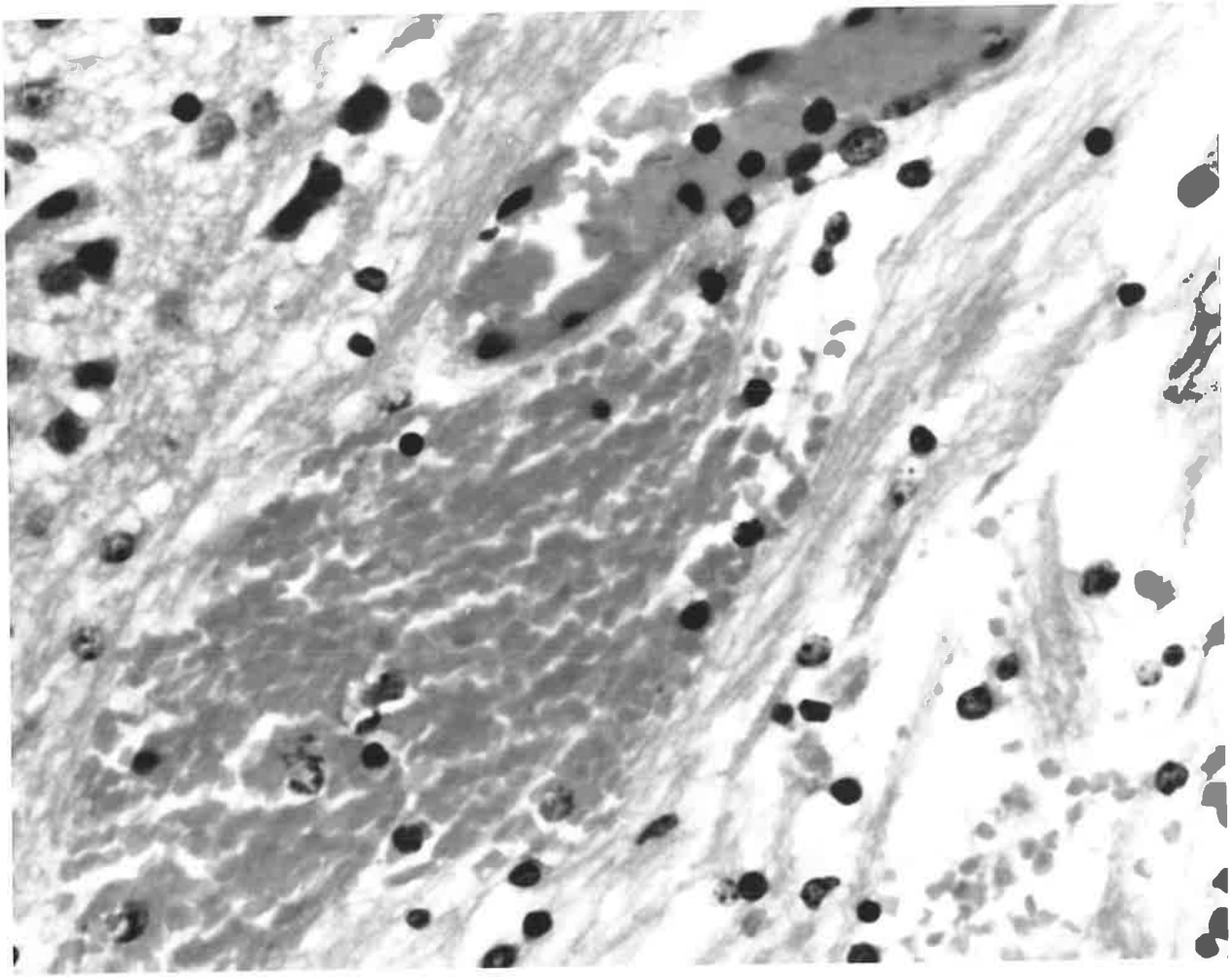

Figure 18.

Figure 17. Toxin treated mouse. Corpus callosum. 18 hours post-inoculation. Accumulation of copious plasma exudate in white matter with necrosis of many glial elements.
H&E x 50.

Figure 18. Toxin treated mouse. Corpus callosum. 6 hours post-inoculation. Oedematous white matter with extensive capillary haemorrhage.
H&E x 100.

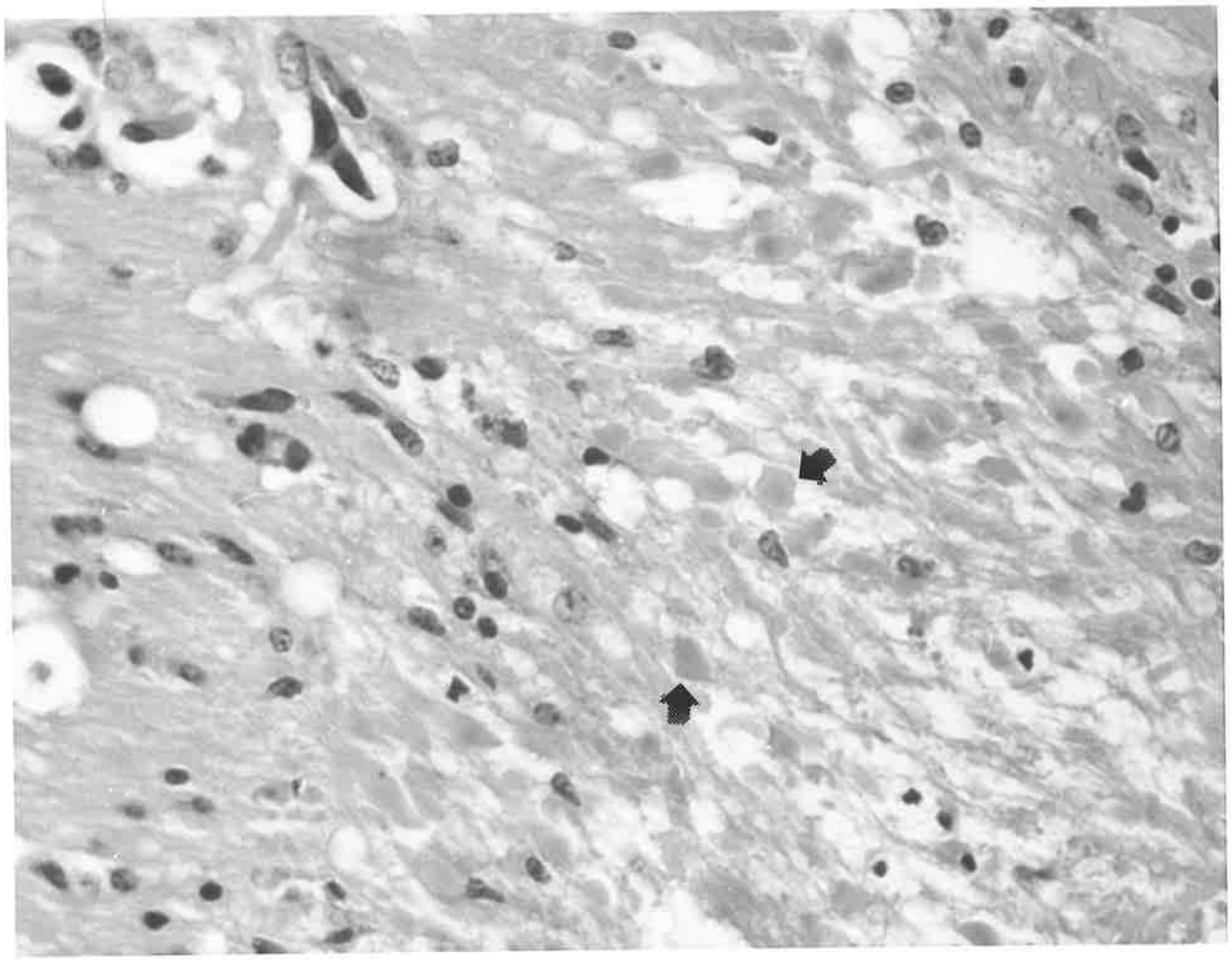

Figure 19.

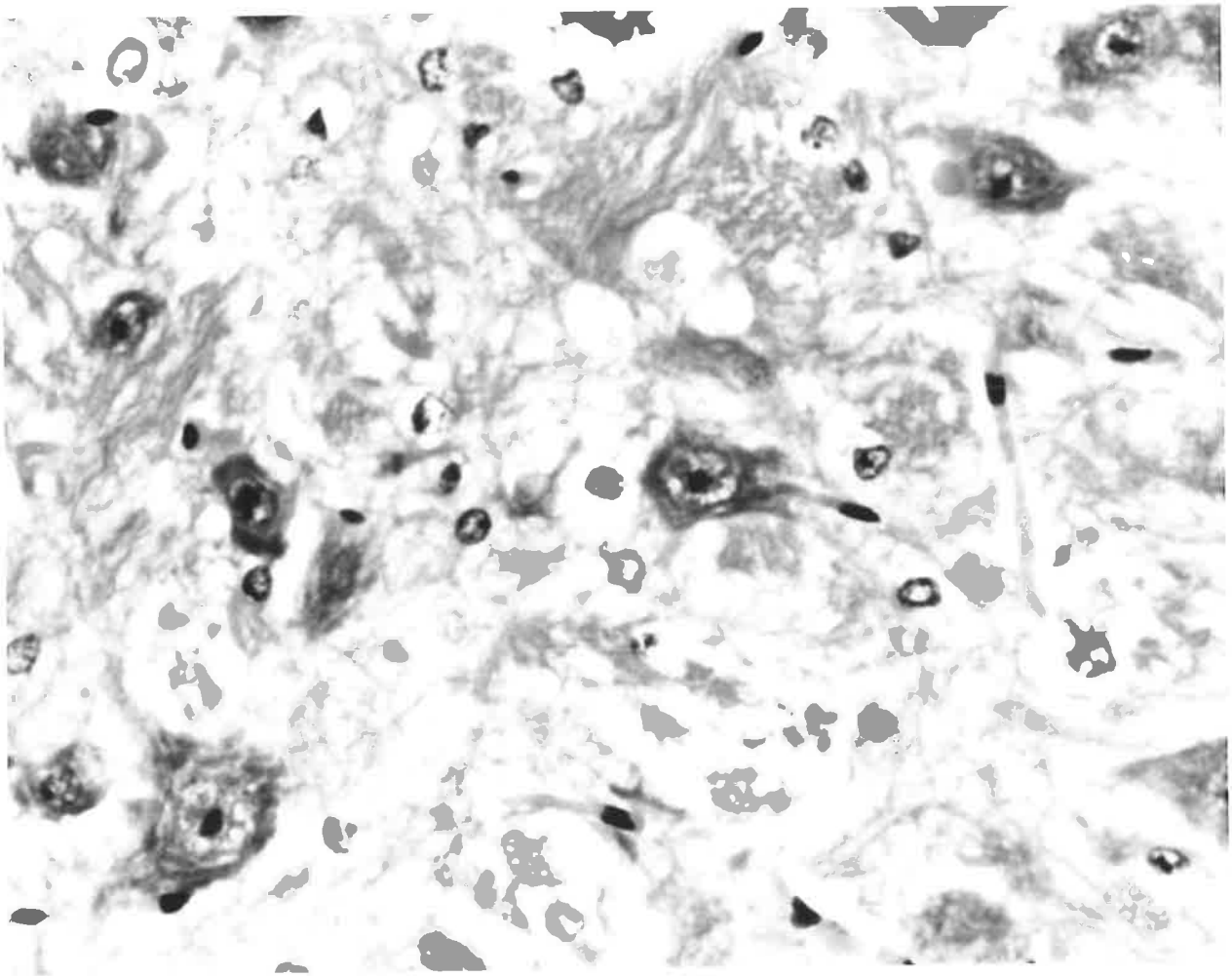

Figure 20.

Figure 19. Toxin treated mouse. 18 hours post-inoculation. Vestibular area. Vacuolation of neuropil, necrosis of glial cells and numerous swollen degenerating axons (arrows).
H&E x 100.

Figure 20. Toxin treated mouse. Corpus striatum. 12 hours post-inoculation. Status spongiosus of white matter and mild vacuolar degeneration of neurones.
H&E x 100.

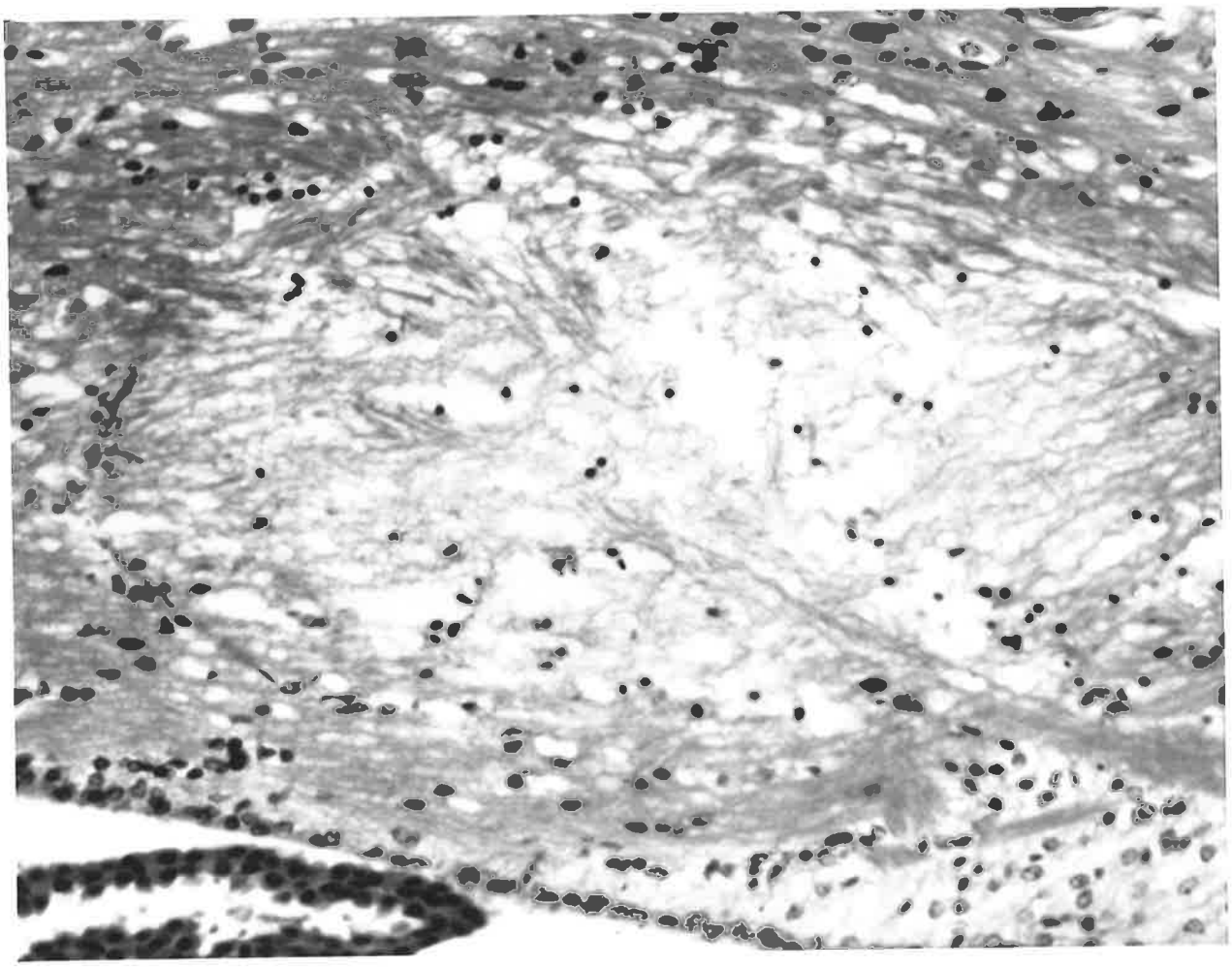

Figure 21.

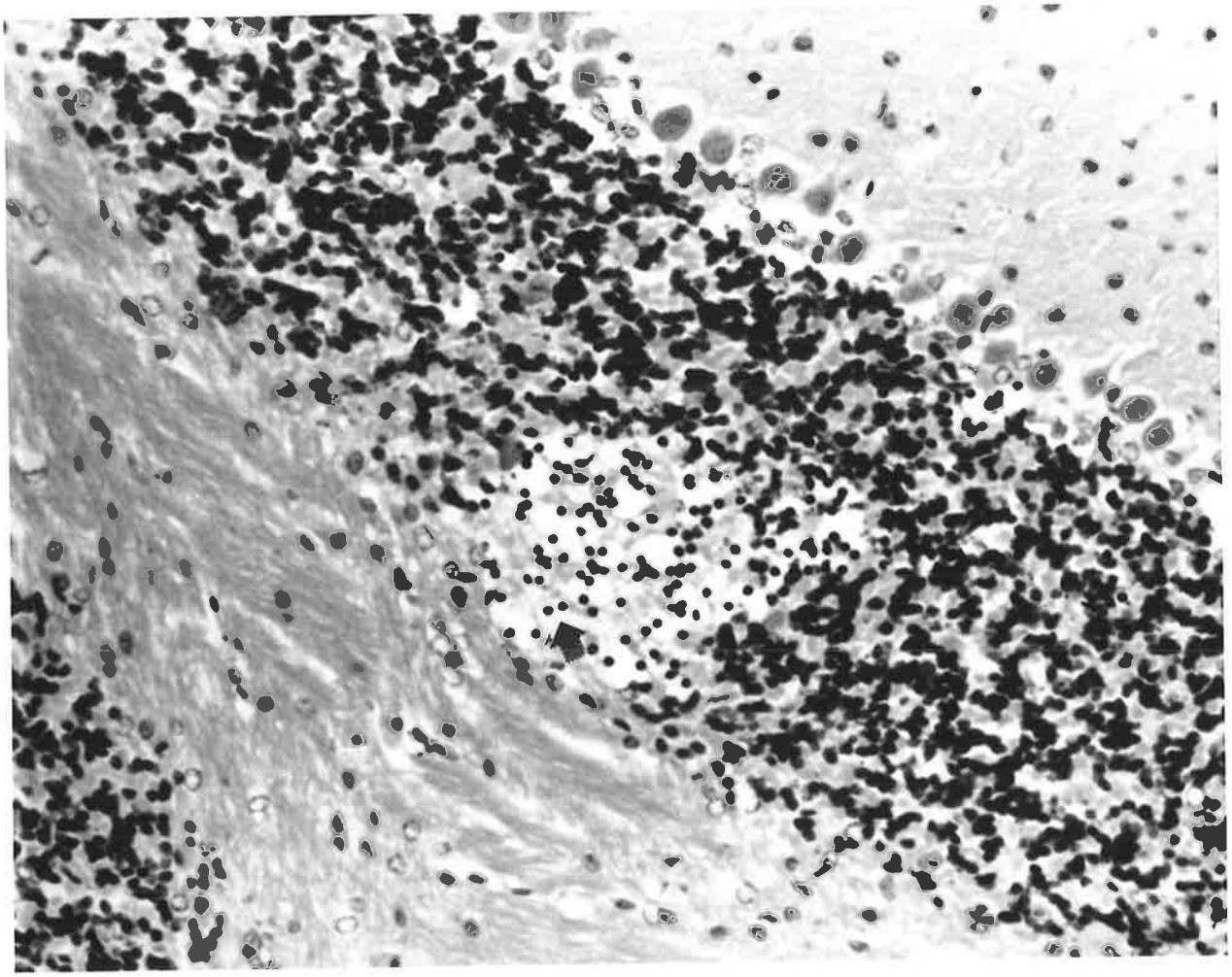

Figure 22.

Figure 21. Toxin treated mouse. 24 hours post-inoculation. Focal area of malacia in area lateral to lateral ventricle.
H&E x 50.

Figure 22. Toxin treated mouse. 12 hours post-inoculation. Focal necrosis in granule cell layer of the cerebellum. (arrow)
H&E x 50.

Figure 23. Toxin treated mouse. 24 hours post-inoculation. Focal lesion in the cerebral cortex showing vacuolation of the neuropil and neuronal necrosis.
H & E x 20.

Figure 24. Toxin treated mouse. 24 hours post-inoculation.
Necrosis of large area of corpus callosum. (arrow)
H & E x 20.

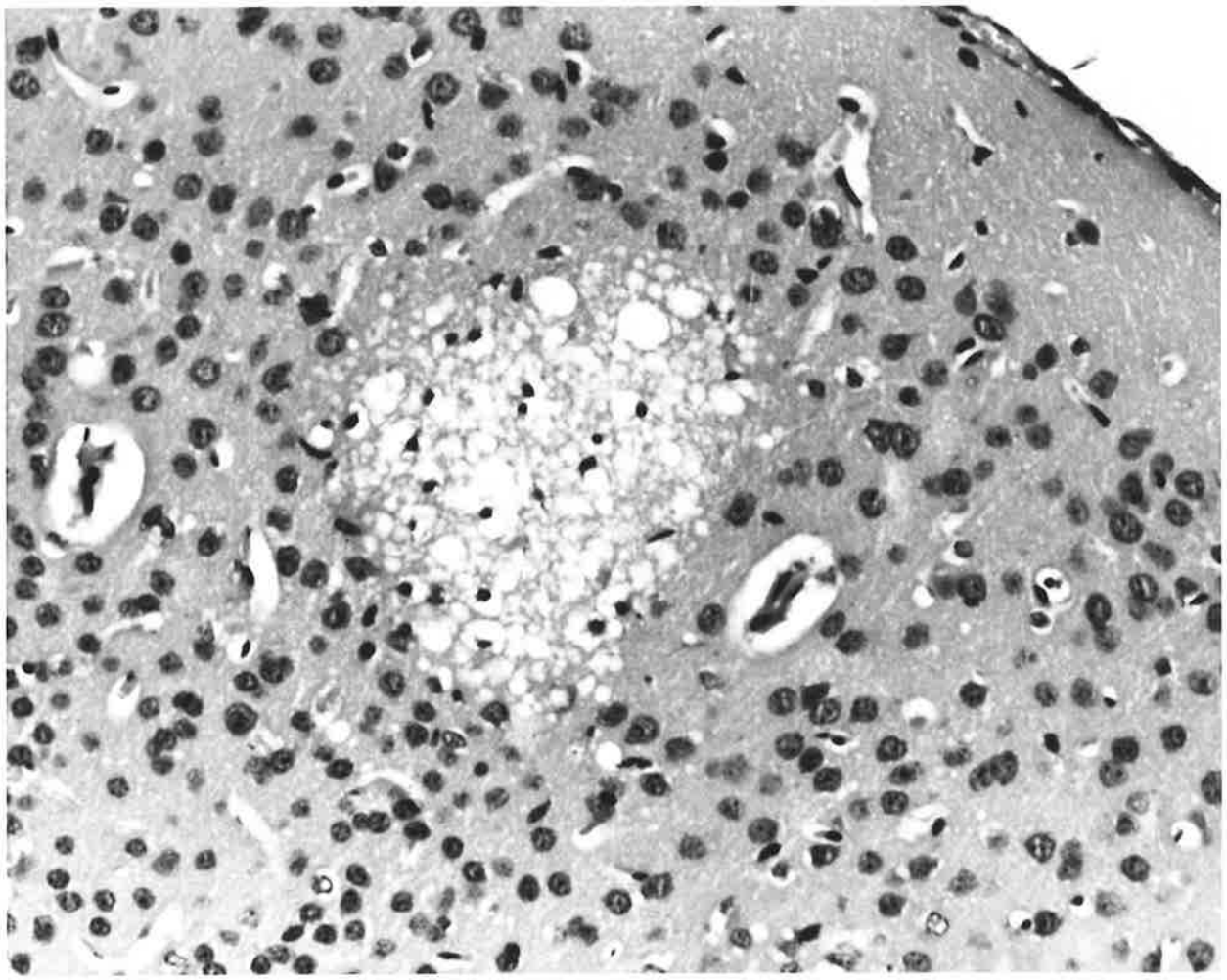

Figure 23.

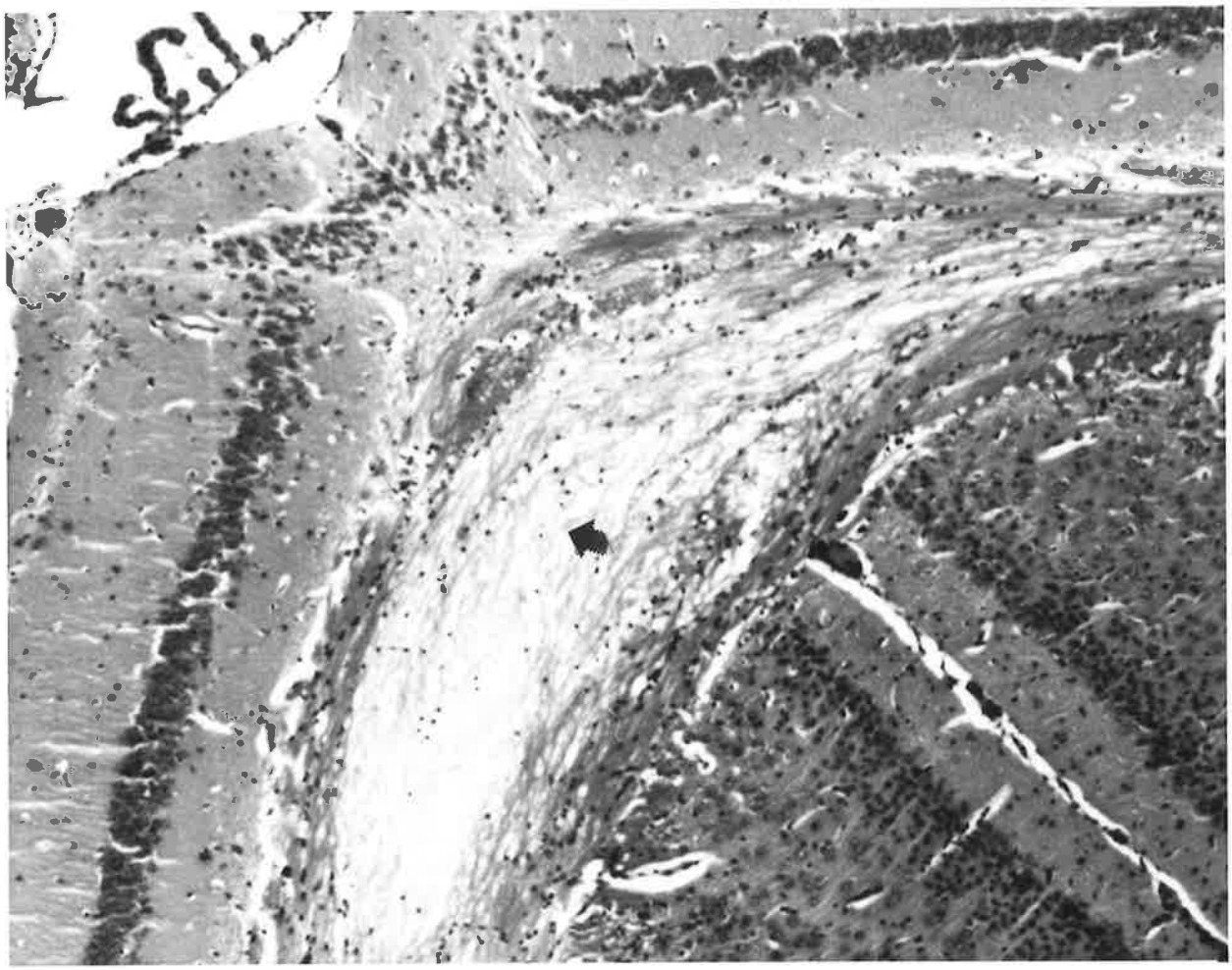

Figure 24.

Figure 25. Toxin treated mouse. Vestibular area. 18 hours post-inoculation. Vacuolation corresponding to myelin loss and fragments of axonal debris in large vacuoles (digestion chambers) (arrows). A few gitter cells present and early peripheral capillary invasion.
H&E x 100.

Figure 26. Toxin treated mouse. 18 hours post-inoculation. Vestibular area. Lower magnification of Figure 25. Circumscribed focus of early malacia.
H&E x 50.

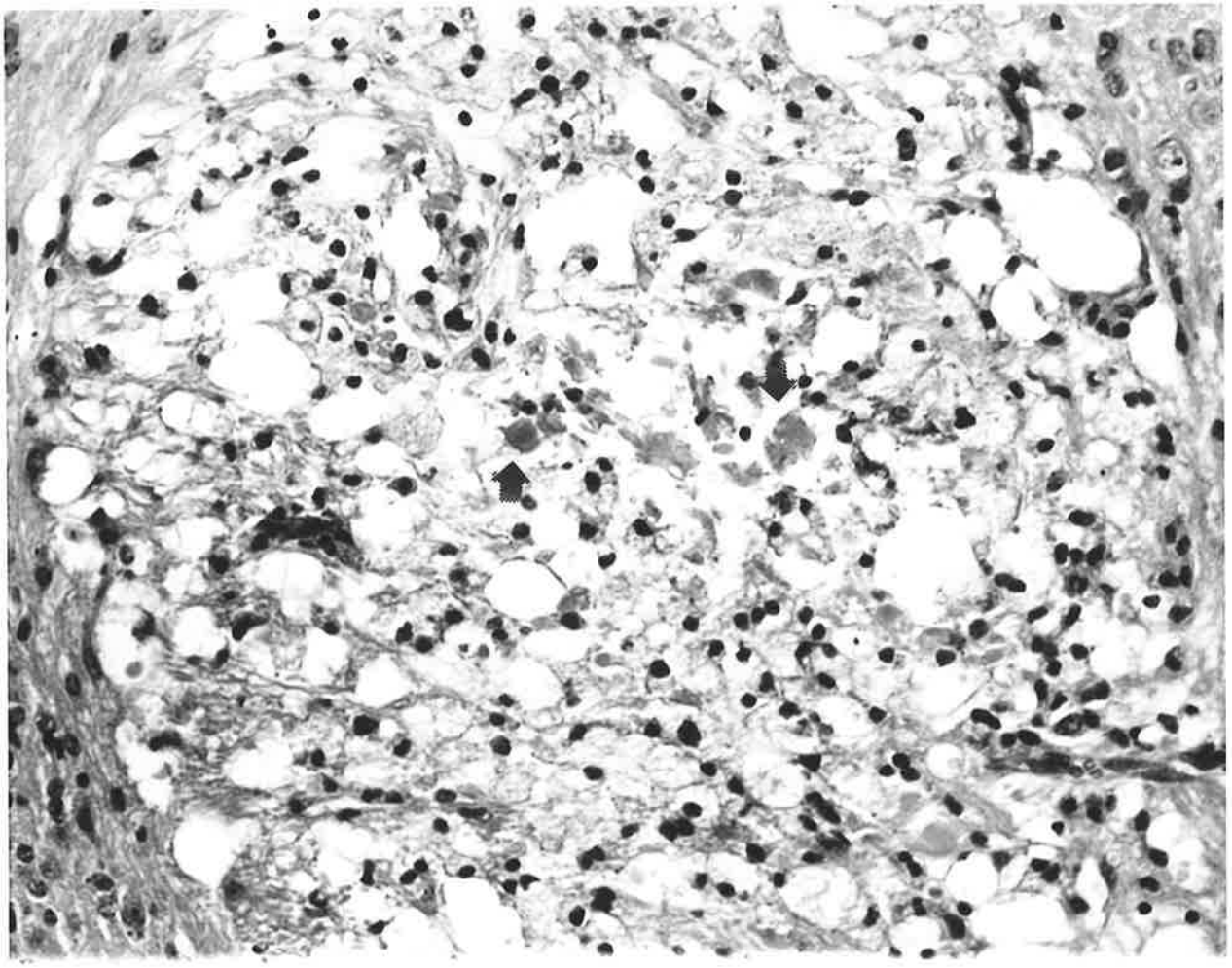

Figure 25.

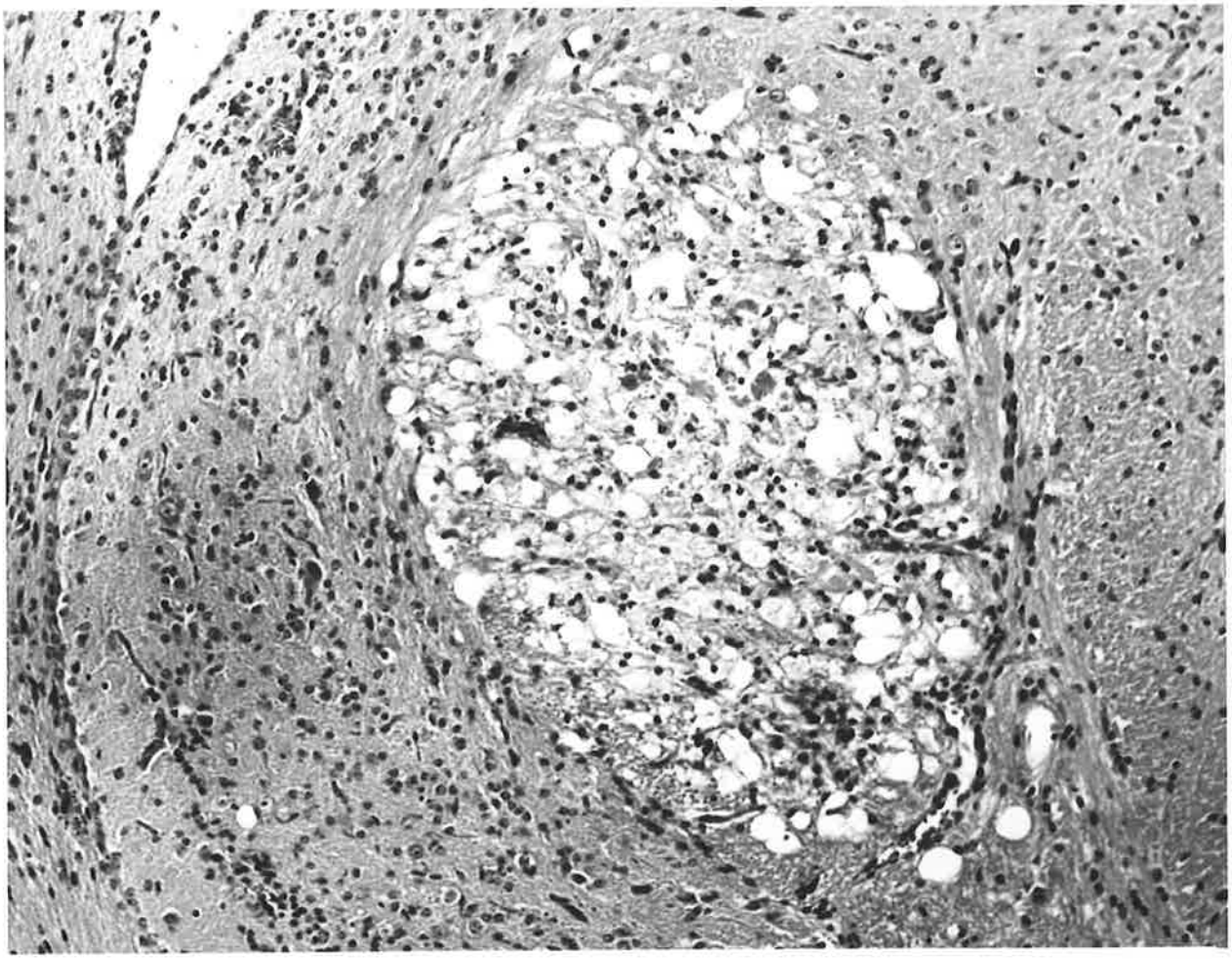

Figure 26.

Figure 27. Toxin treated mouse. Paraventricular area. 7 days post-inoculation. Marked astrocytic proliferation and numerous gitter cells.
H & E x 100.

Figure 28. Toxin treated mouse. Vestibular area. 18 hours post-inoculation. Vacuolation of the neuropil due to extensive myelin loss in vestibular tracts.
H & E x 100.

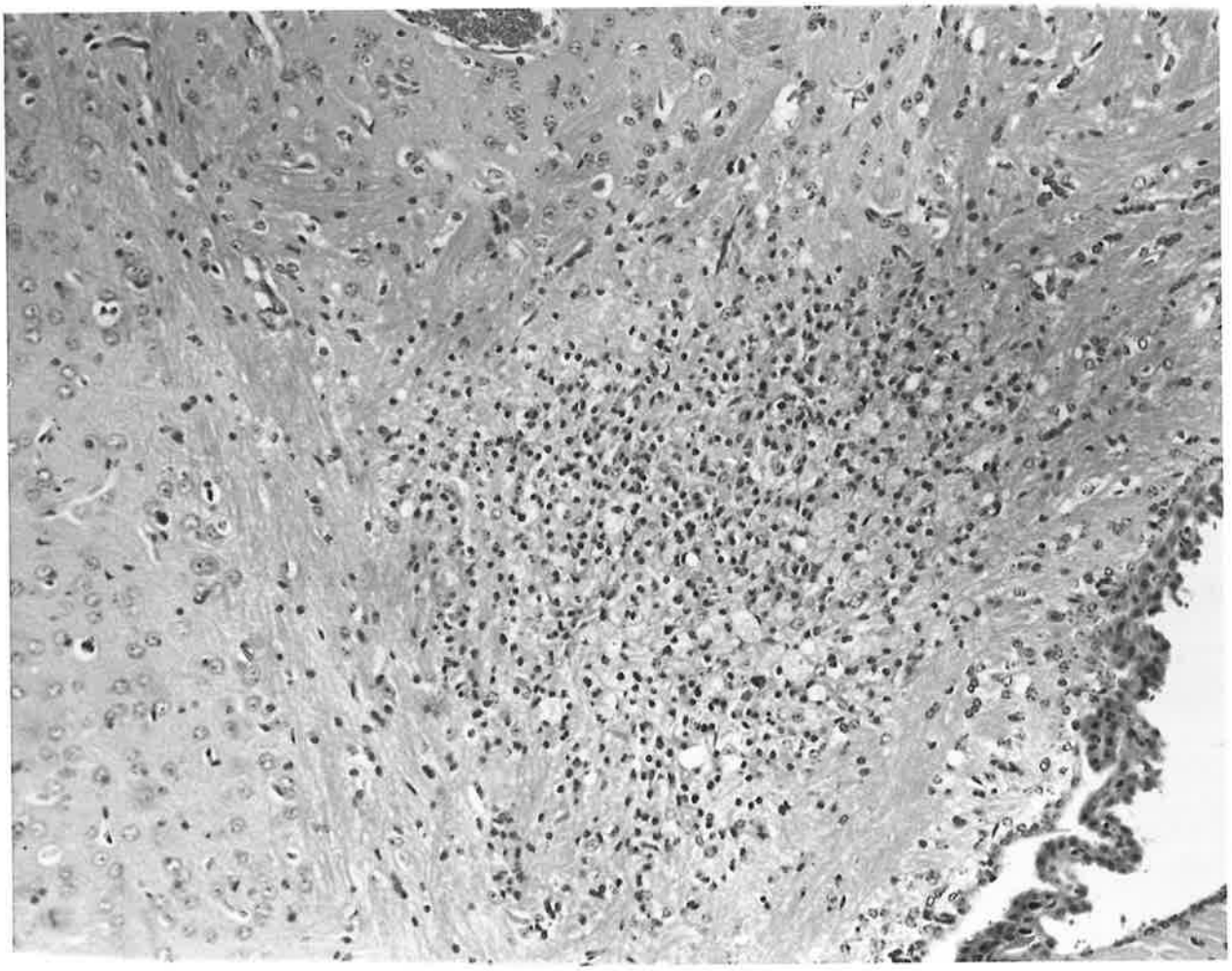

Figure 27.

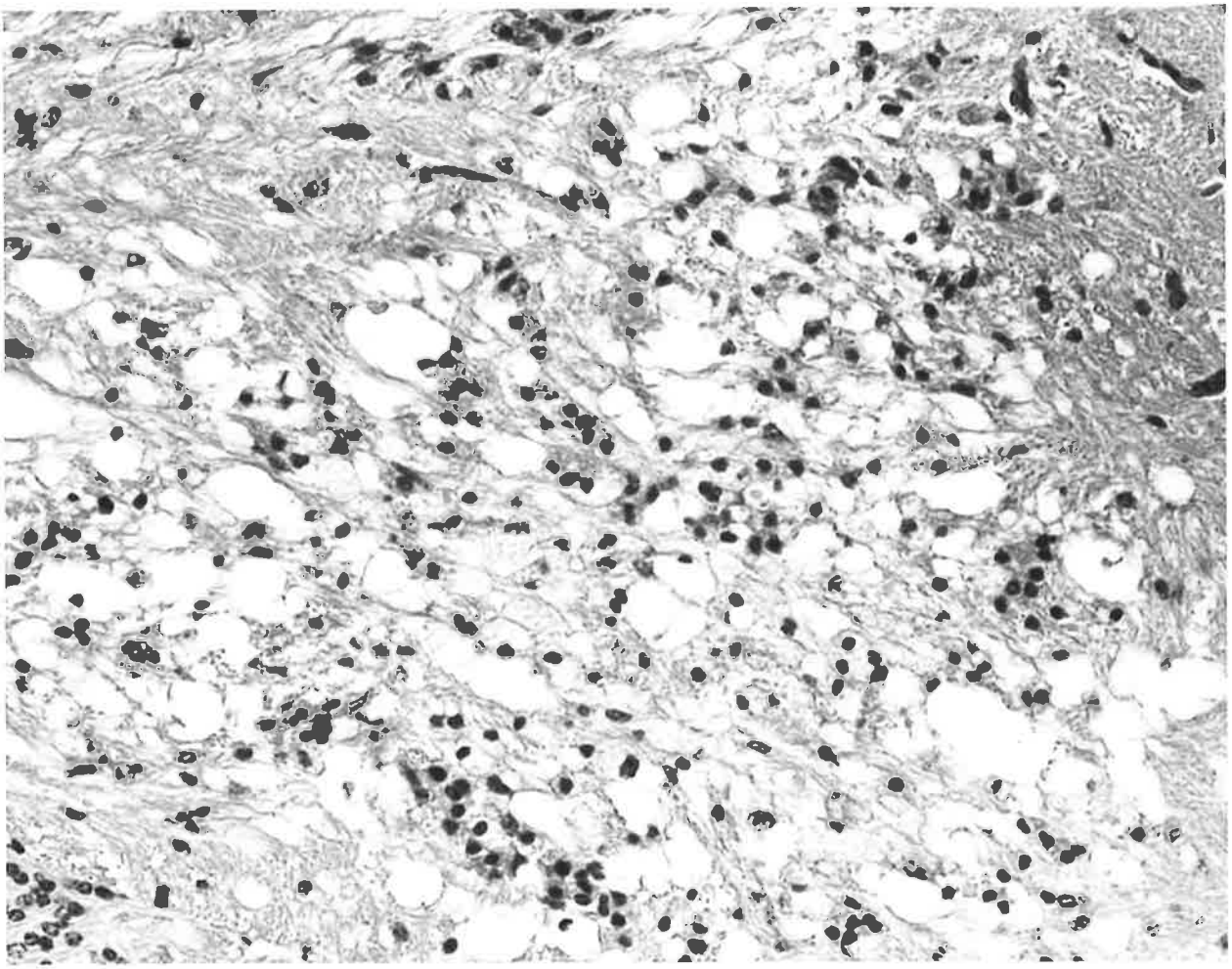

Figure 28.

Figure 29. Toxin treated mouse. Anterior commissure. 7 days post-inoculation. Similar changes to Figure 27. (arrows)
H & E x 100.

Figure 30. Toxin treated mouse. Corpus callosum. 7 days post-inoculation. Malacic area containing compound granular corpuscles (gitter cells) and proliferating astrocytes. (arrows)
H & E x 100.

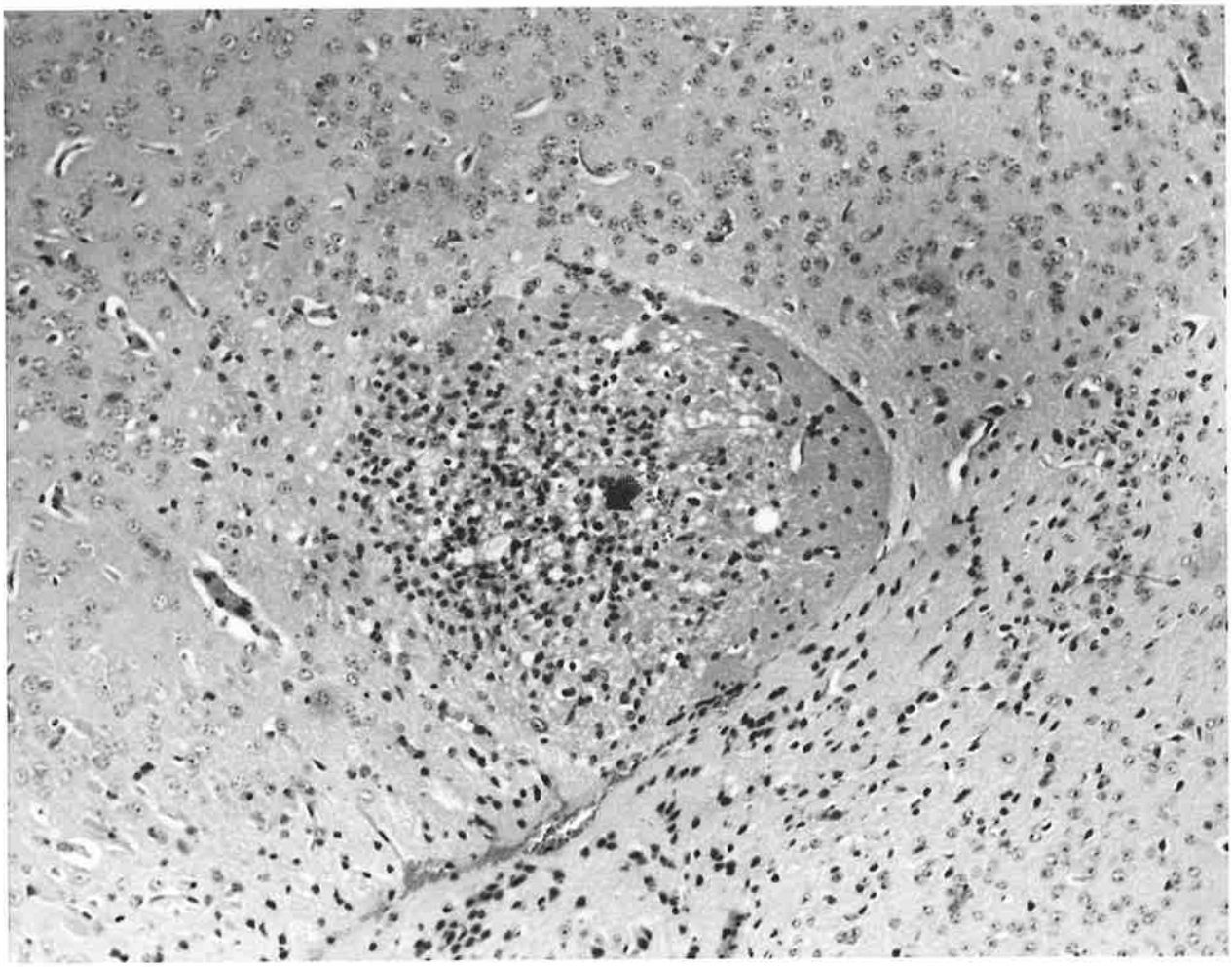

Figure 29.

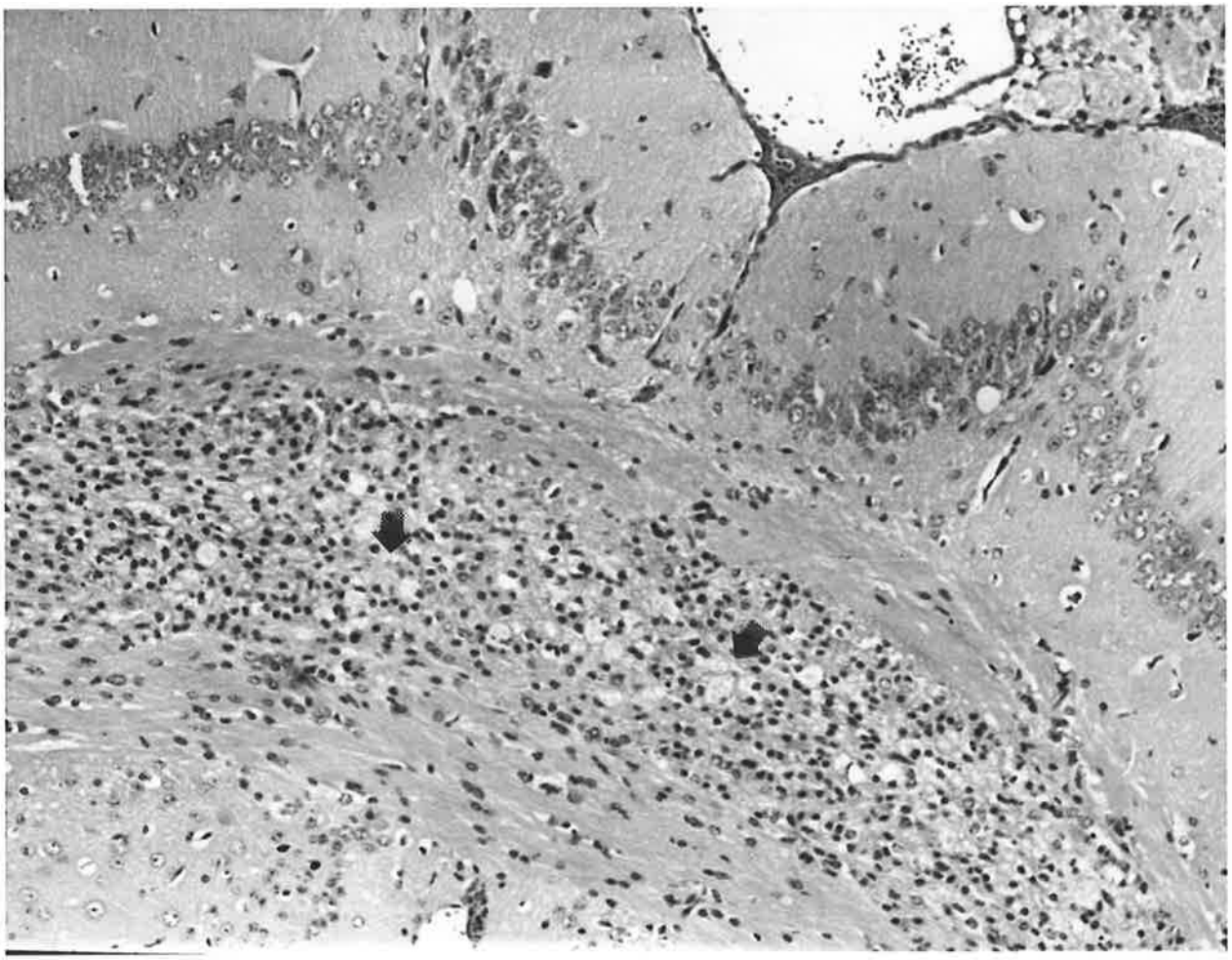

Figure 30.

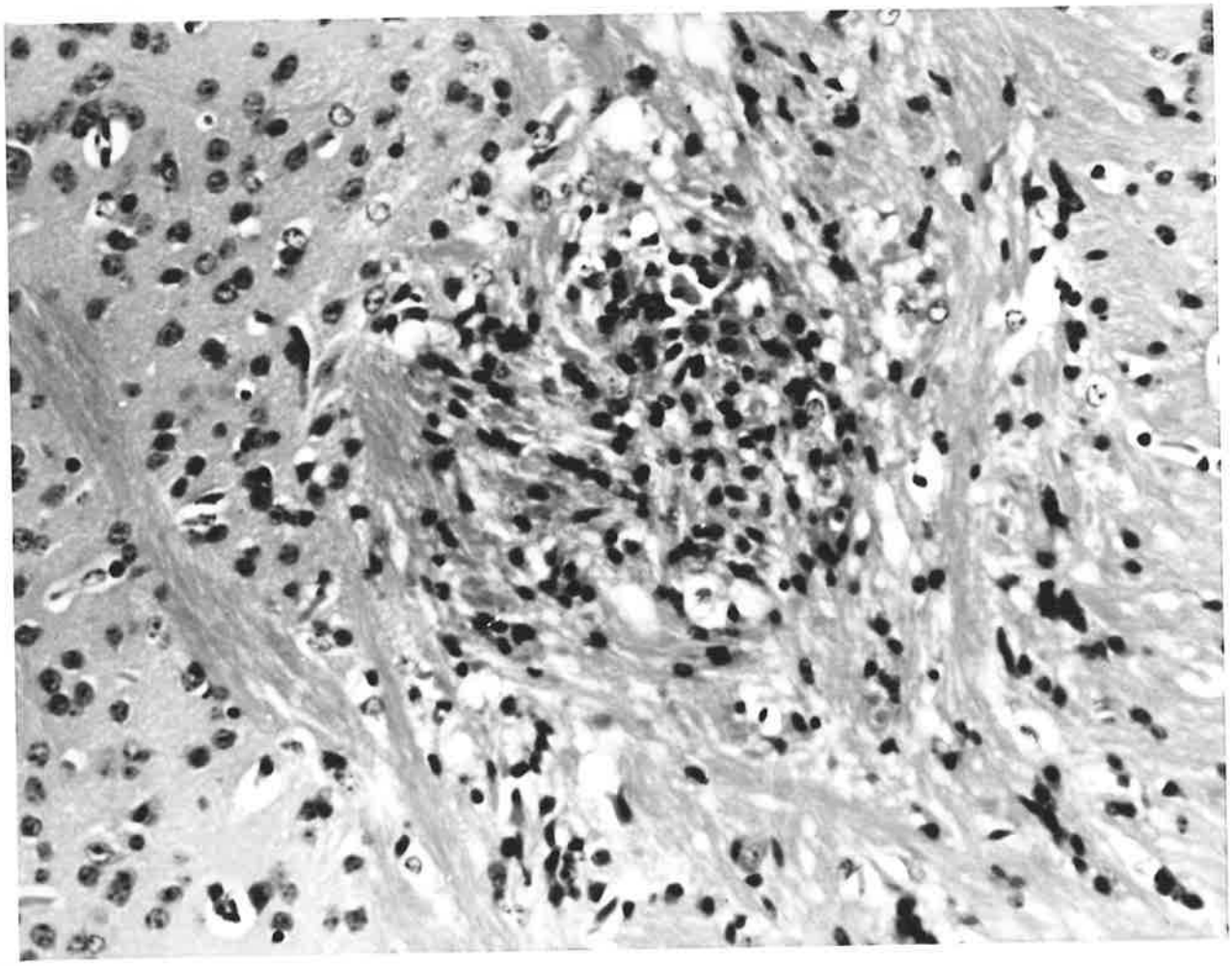

Figure 31.

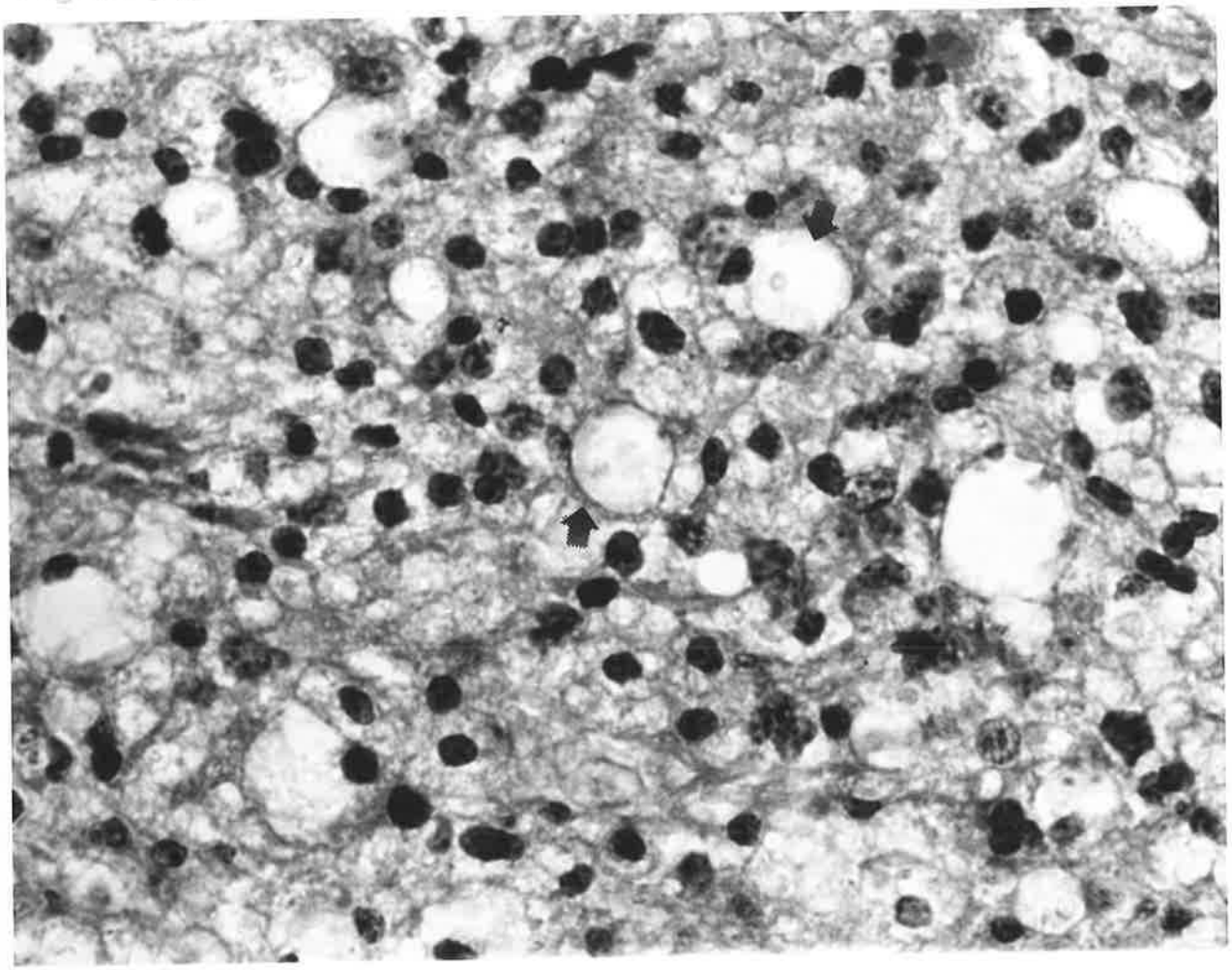

Figure 32.

Figure 31. Toxin treated mouse. Thalamus. 10 days post-inoculation. Organizing necrotic focus showing intense astrogliosis and capillary invasion. H&E x 50.

Figure 32. Toxin treated mouse. Corpus callosum. 7 days post-inoculation. Higher magnification of Figure 30. Numerous gitter cells (arrows) with foamy, lipid-laden cytoplasm and astrocytes. H&E x 200.

Figure 33. Control mouse. Coronal section of brain injected with HRP. Reaction product confined within cerebral vasculature.
Haematoxylin x 10.

Figure 34. Toxin treated mouse. Coronal section of brain injected with HRP. Diffuse leakage of reaction product, especially in the thalamic region and corpus callosum.
Haematoxylin x 10.

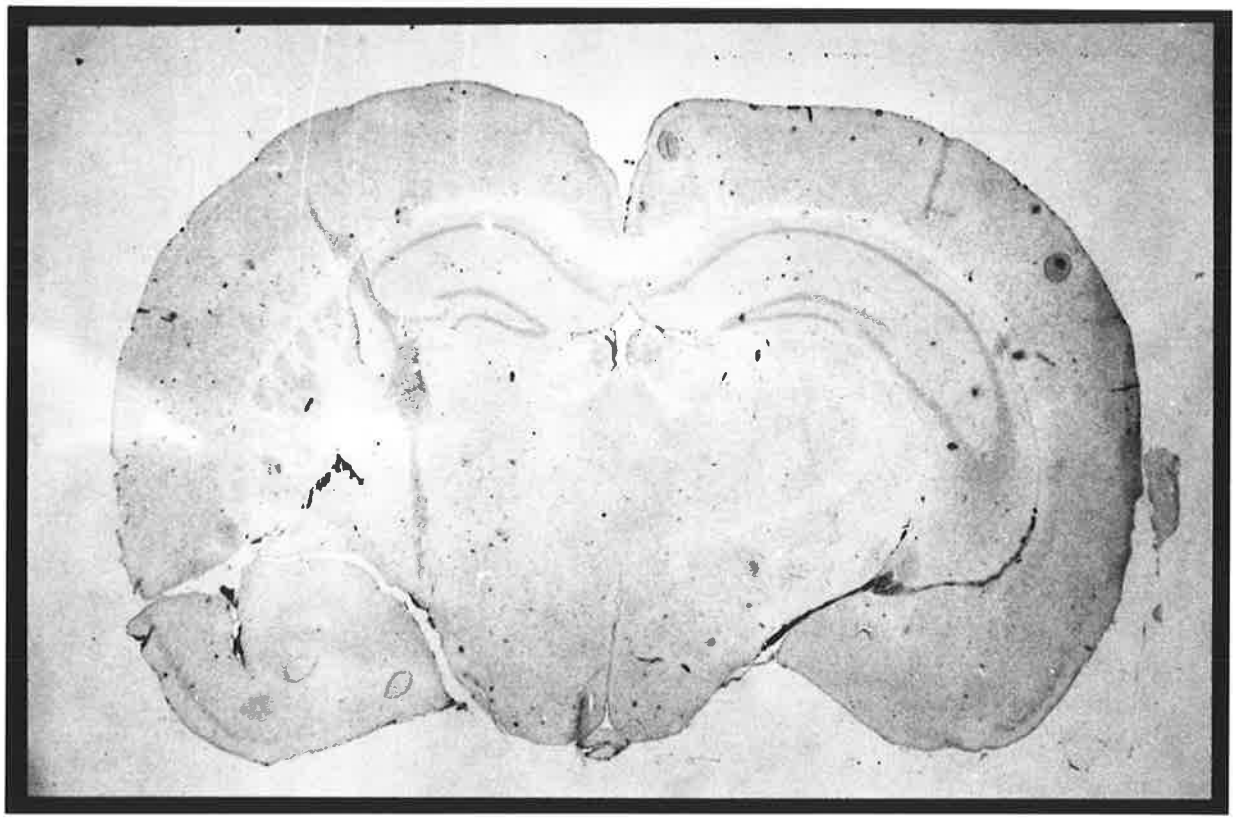

Figure 33.

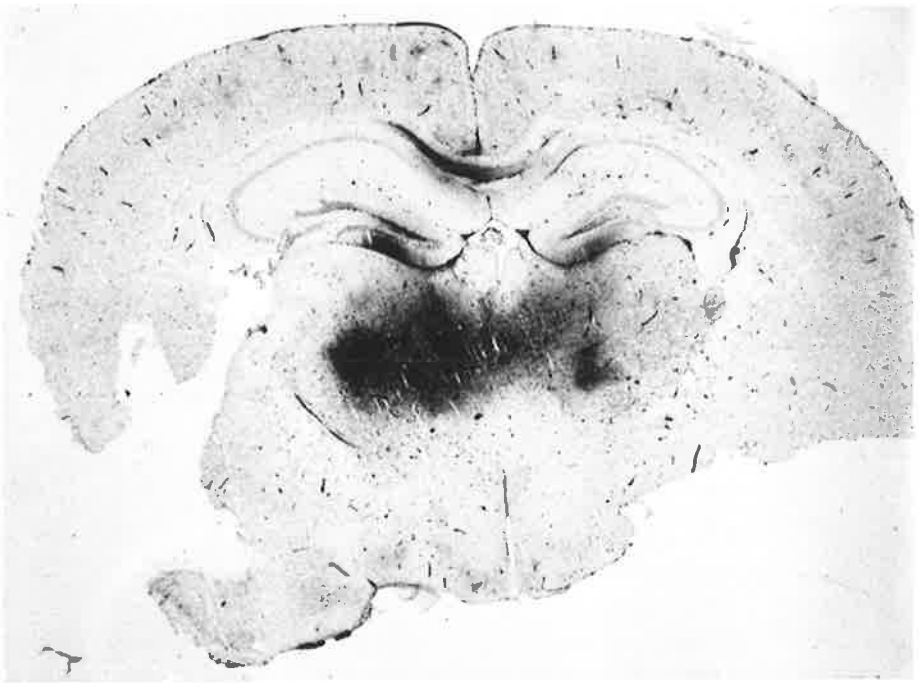

Figure 34.

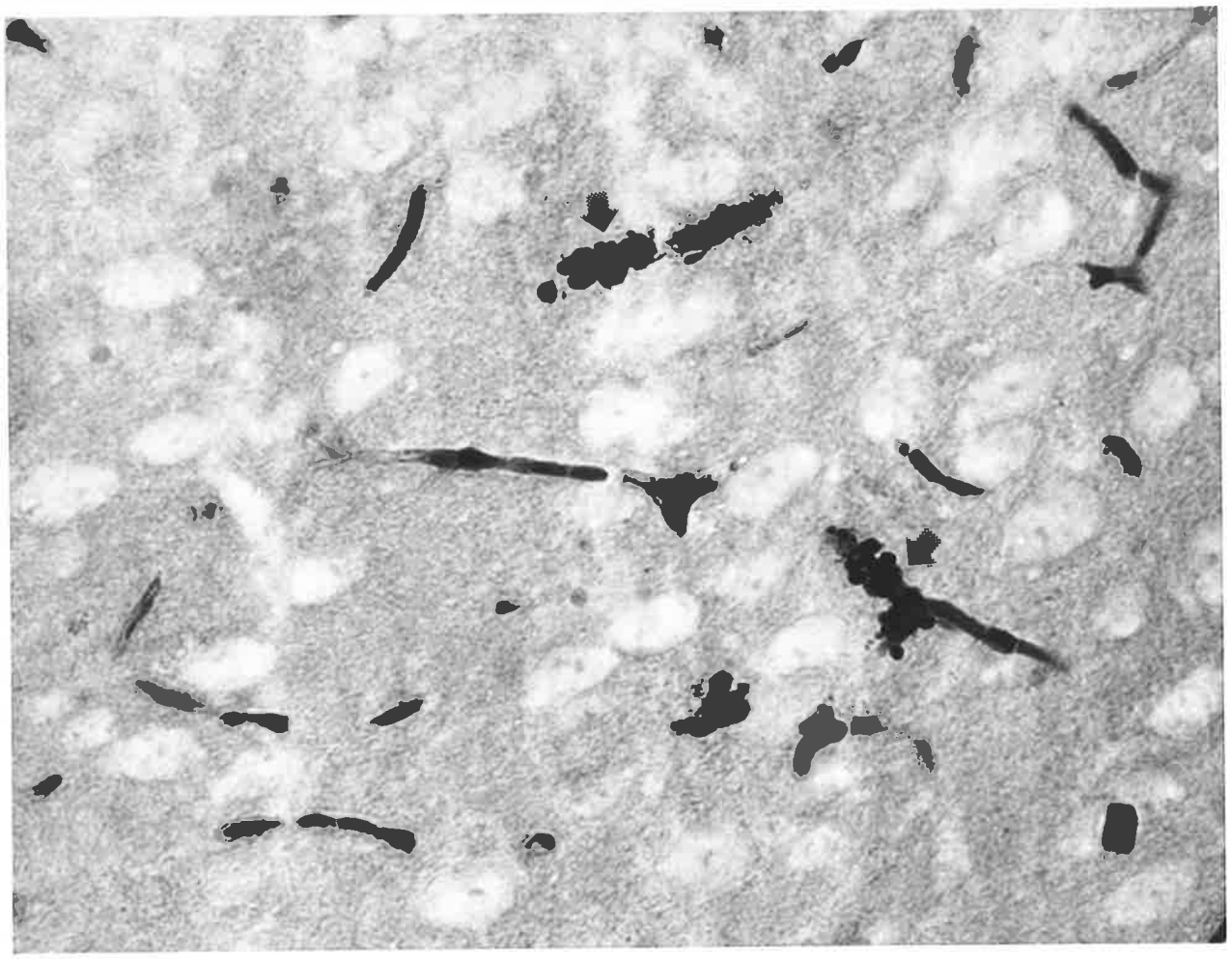

Figure 35.

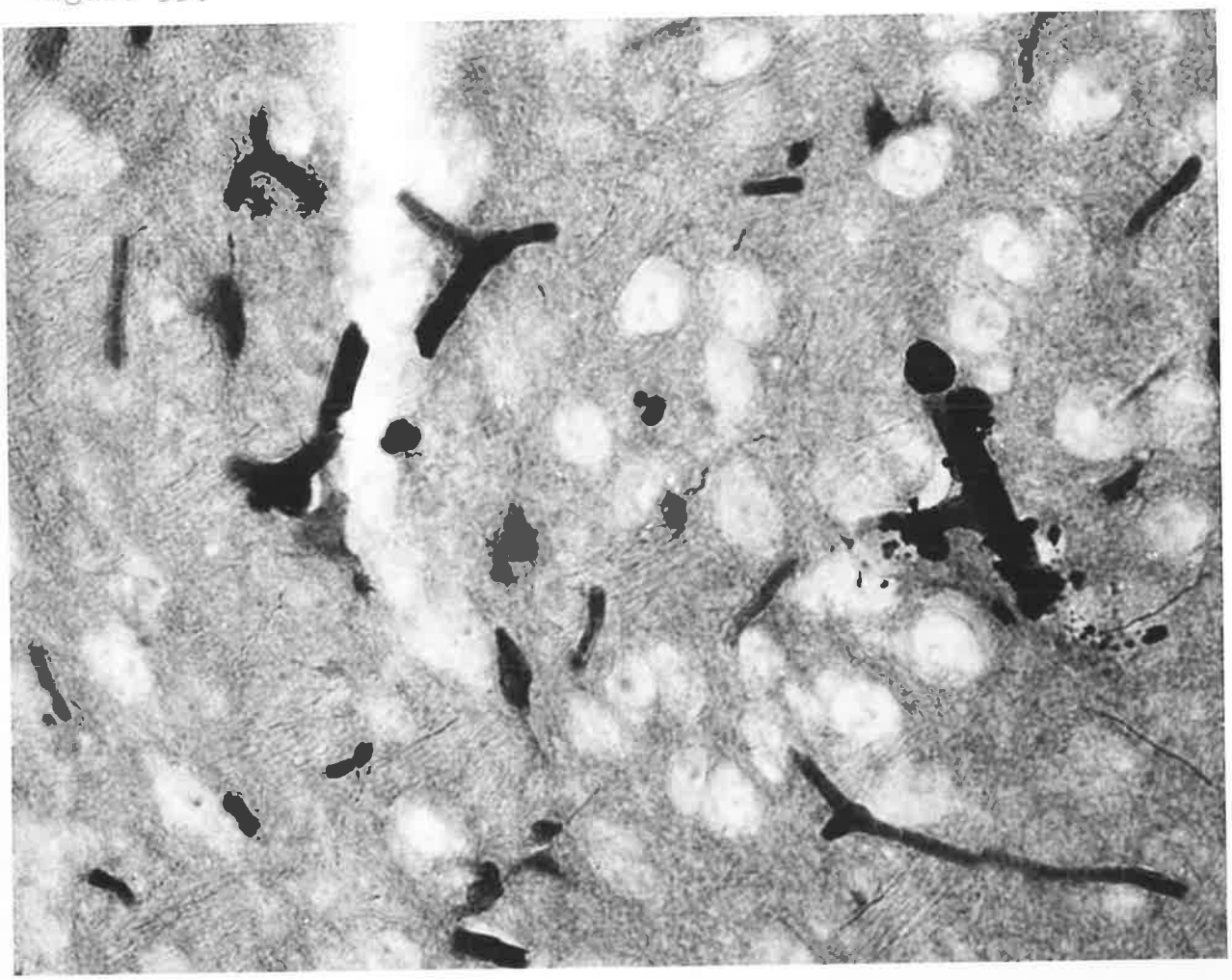

Figure 36.

Figure 35. Toxin treated mouse. Frozen section of brain injected with HRP showing escape of reaction product from capillaries (arrows).
x 200.

Figure 36. Toxin treated mouse. Frozen section of brain injected with HRP. Dense perivascular accumulation of reaction product and lighter diffuse staining of the parenchyma.
x 200.

Figure 37. Control mouse. Coronal section of brain injected with Evans blue. There is no evidence of dye extravasation.

Figure 38. Toxin treated mouse. Coronal section of brain injected with Evans blue. Extensive extravasation of dye in region of thalamus and corpus striatum and focal areas of cerebral cortex. Note the relative sparing of the hippocampus and large white matter tracts.

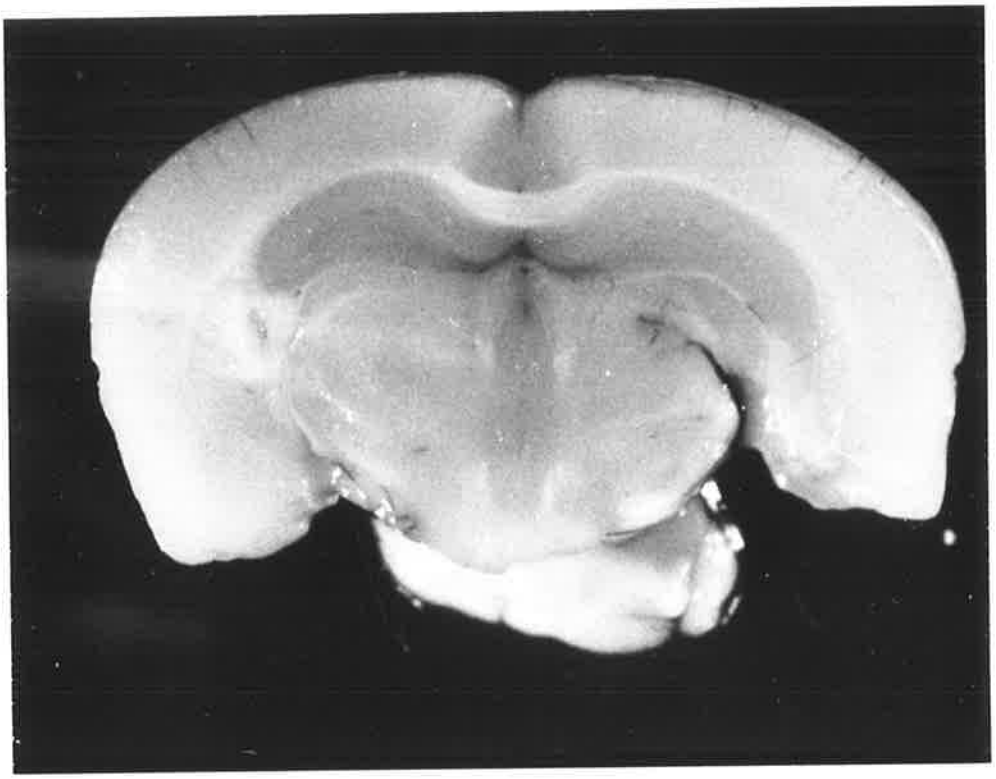

Figure 37.

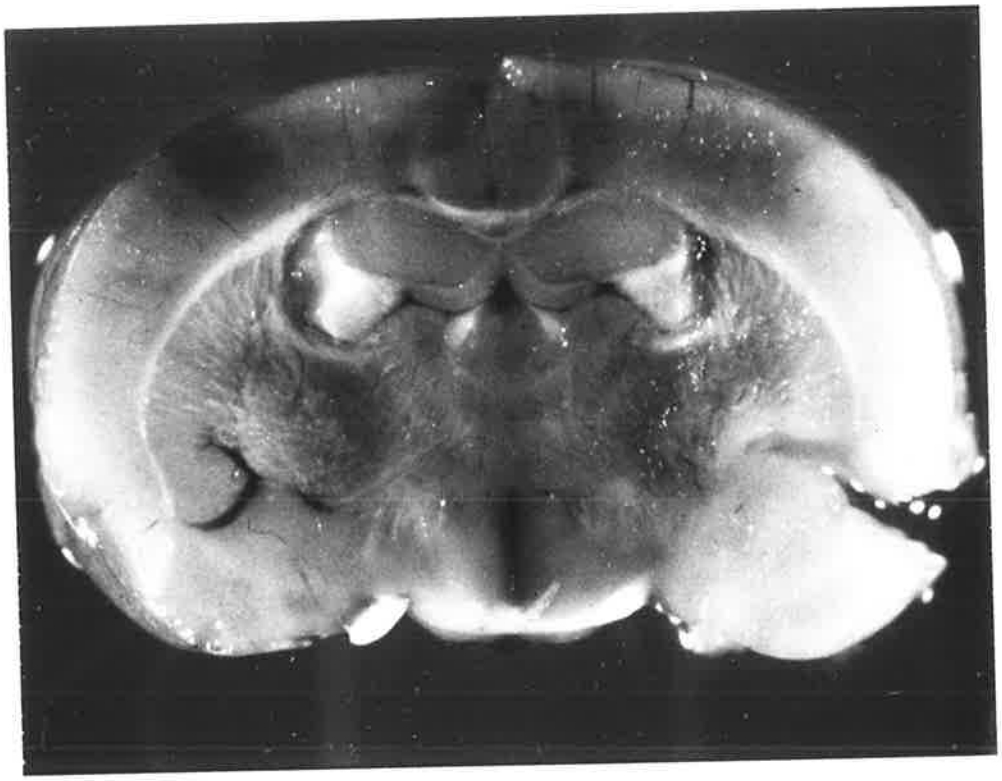

Figure 38.

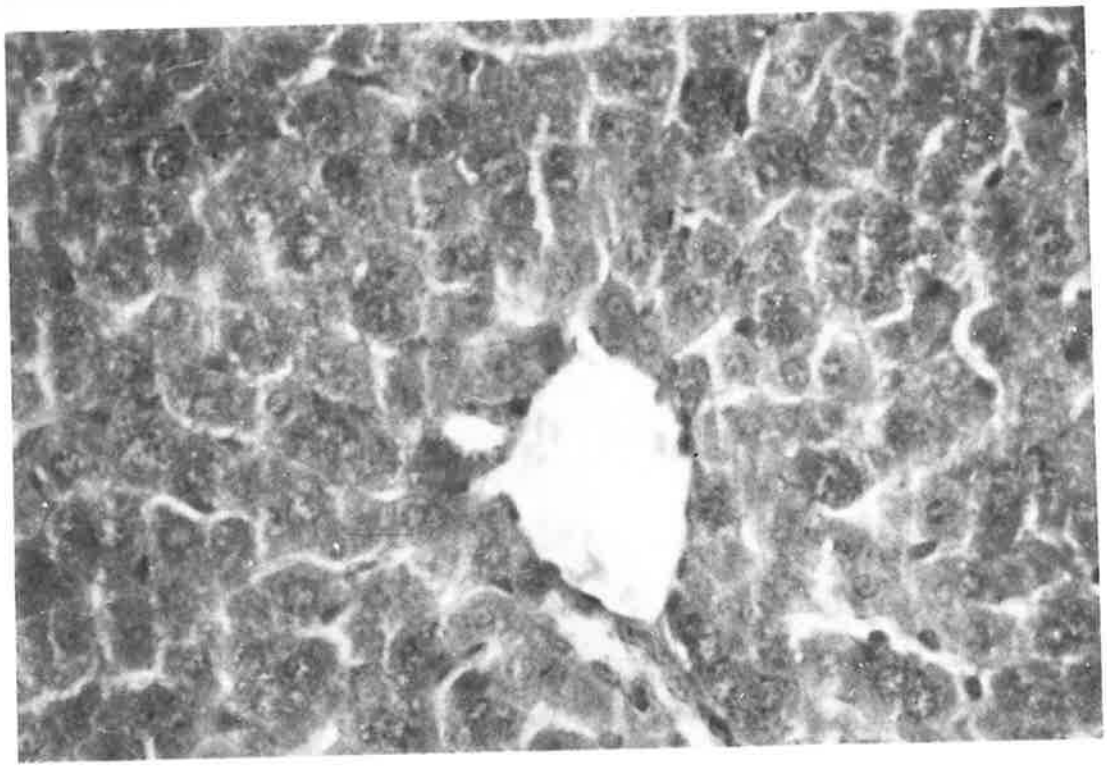

Figure 39.

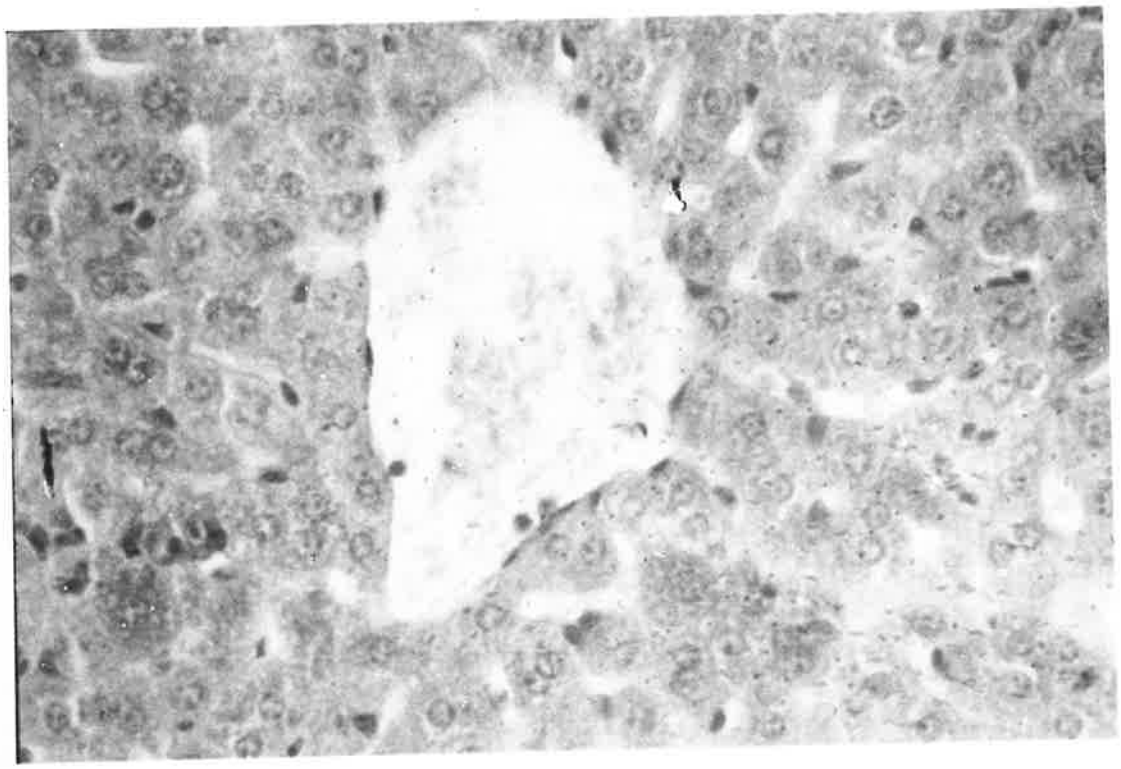

Figure 40.

Figure 39. Control mouse. Liver. Hepatocytes showing densely packed glycogen granules in the cytoplasm.
P.A.S. x 200.

Figure 40. Toxin treated mouse. Liver. 4 hours post-inoculation. Hepatocytes in periacinar zone show marked depletion of glycogen.
P.A.S. x 200.

ALL TISSUES FOR ULTRASTRUCTURAL EXAMINATION WERE PERFUSION FIXED IN VIVO UNLESS OTHERWISE INDICATED.

Figure 41. Control mouse. Cerebral cortex. The neuropil is compact with close apposition of the capillary basal lamina to the surrounding parenchyma.
x 10,250.

Figure 42. Control mouse. Cerebral cortex. Very mild focal astrocytic end-foot swelling (arrow) and a few cytoplasmic "blebs" projecting into the vessel lumen.
x 6765.

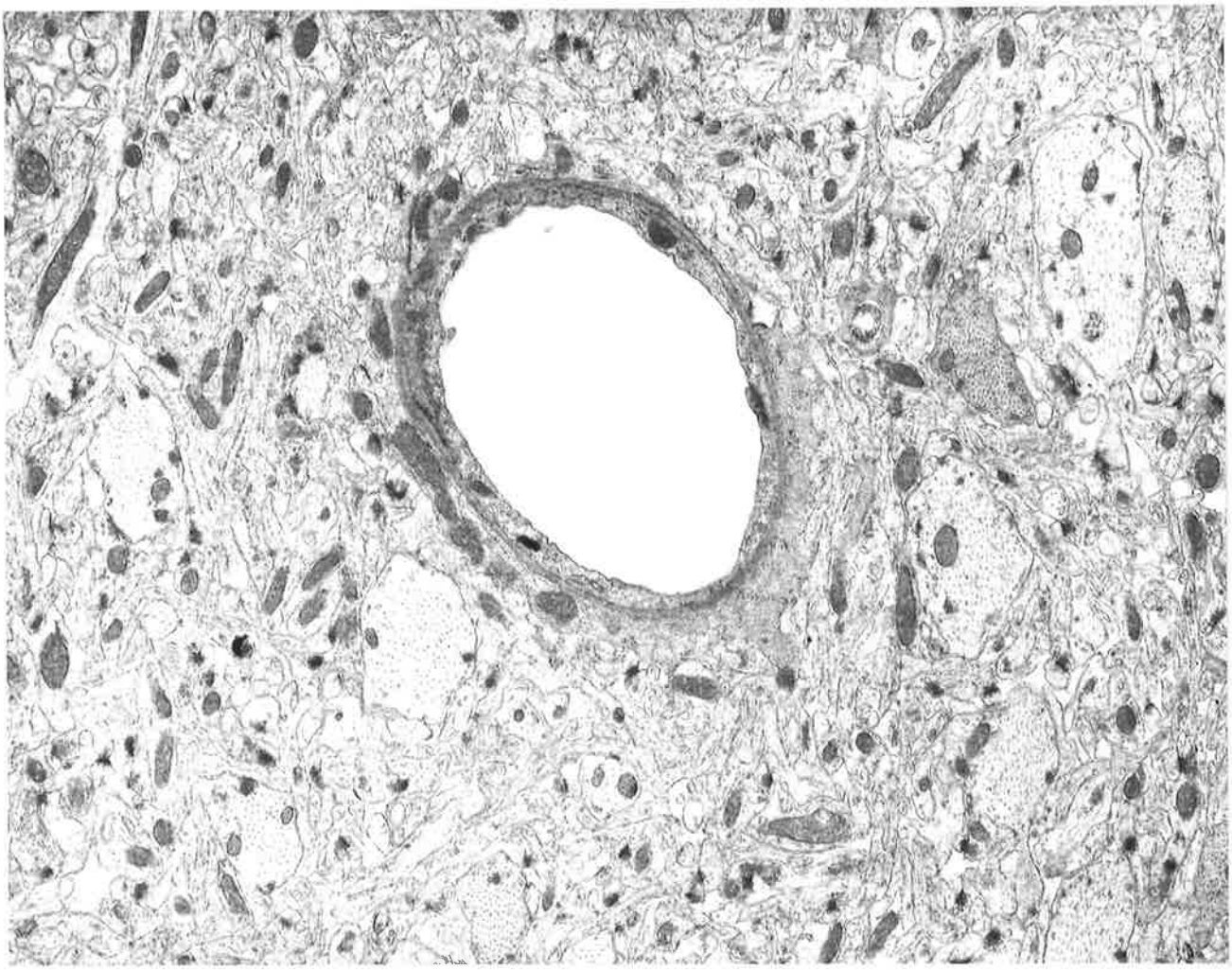

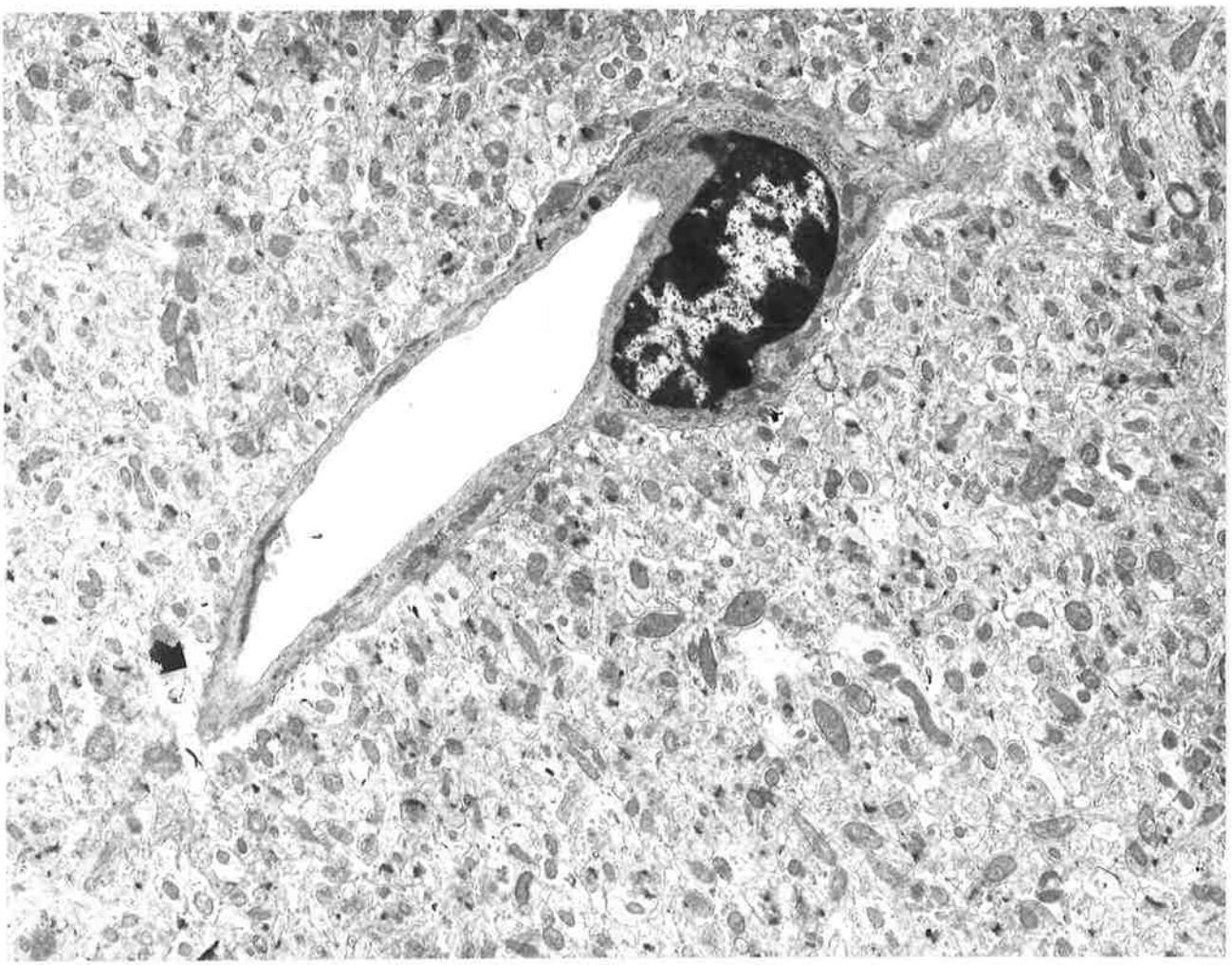

Figure 43. Control mouse. Cerebral cortex. Immersion fixation. Artifactual swelling of astrocytic end-feet around capillaries and of astrocyte cell bodies and their processes in the neuropil. In the endothelial cytoplasm, mitochondrial swelling is evident with loss of internal structure (arrows).
x 5330.

Figure 44. Control mouse. Cerebellum. Purkinje cell, astrocytes and granule cells are shown with mild swelling of astrocytic processes around the Purkinje cell.
x 10,250.

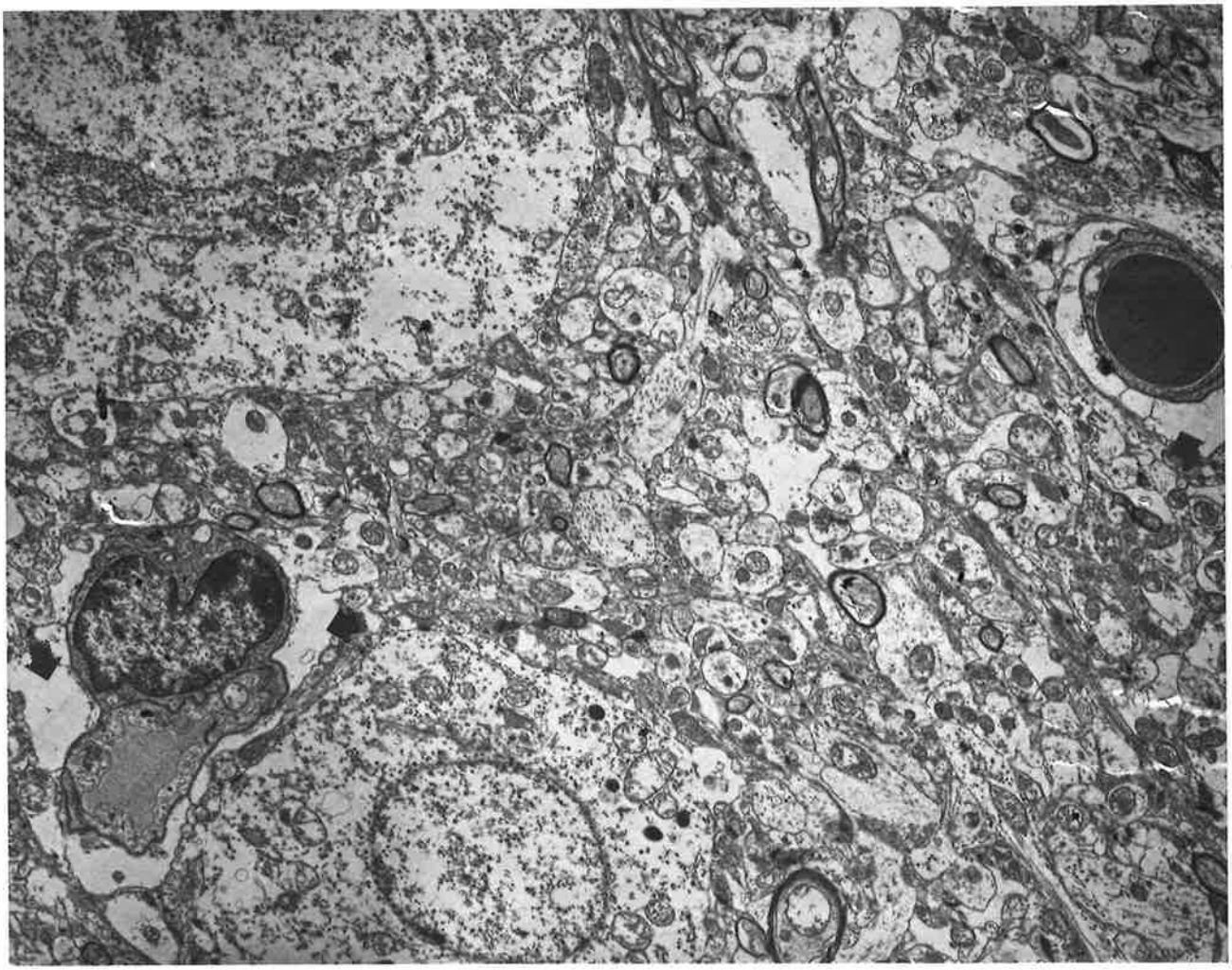

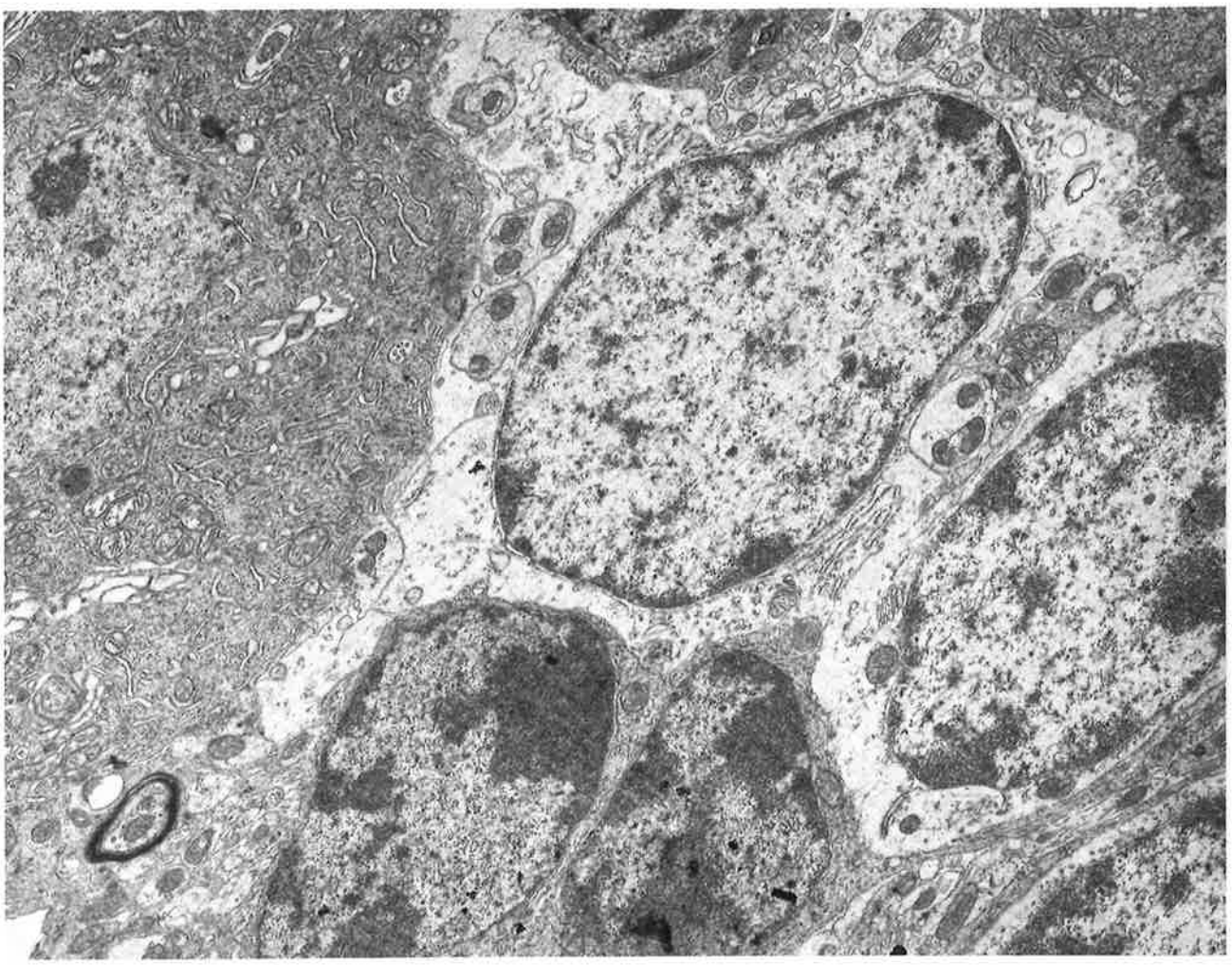

Figure 45. Control mouse. Corpus callosum. Focal separation of myelin lamellae in many myelinated axons (arrows) and an oligodendrocyte is present.
x 6765.

Figure 46. Toxin treated mouse. Cerebellum. 30 minutes post-inoculation. Swelling of protoplasmic astrocytes and granule cells with remnants of cytoplasmic organelles (arrow).
x 6765.

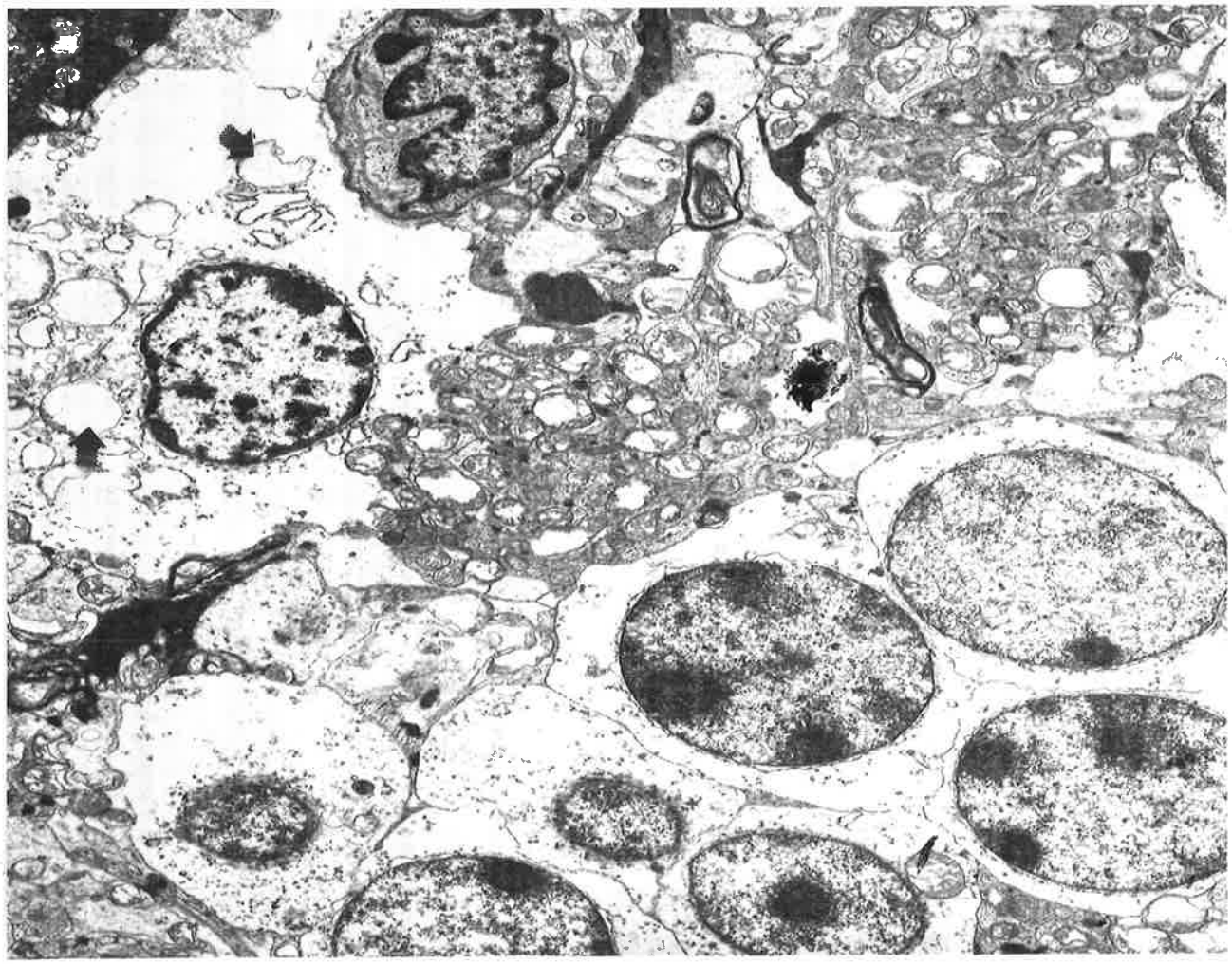

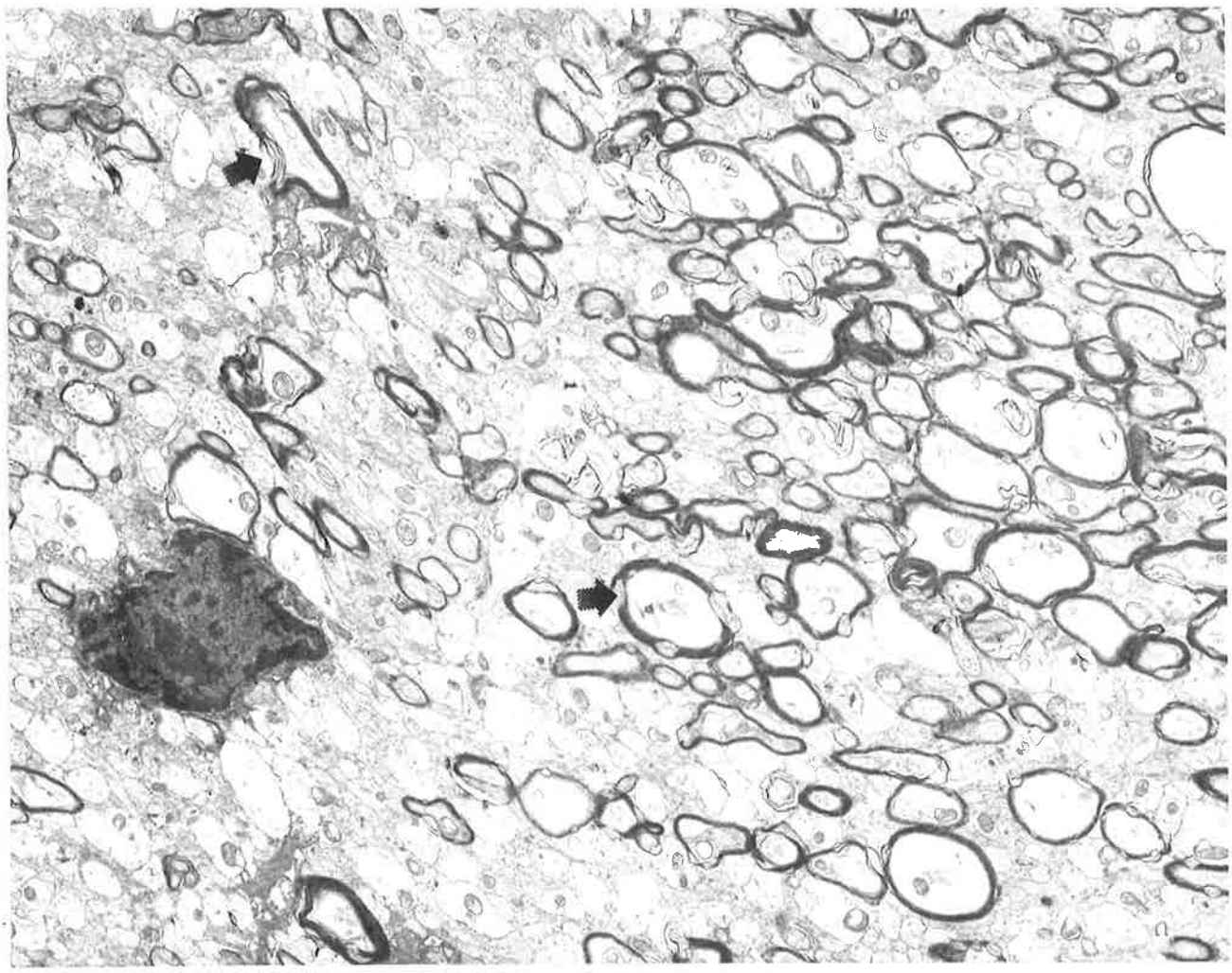

Figure 47. Toxin treated mouse. Cerebral cortex. 30 minutes post-inoculation. Swelling of astrocytic end-feet (arrows) and adjacent astrocyte cell bodies.

x 10,250.

Figure 48. Toxin treated mouse. Cerebral cortex. 30 minutes post-inoculation. Severe astrocytic end-feet swelling with rupture of cell membranes and dissolution of cytoplasmic organelles and collapse of the capillary. The peripheral basal lamina of the vessel is demarcated by arrows.

x 10,250.

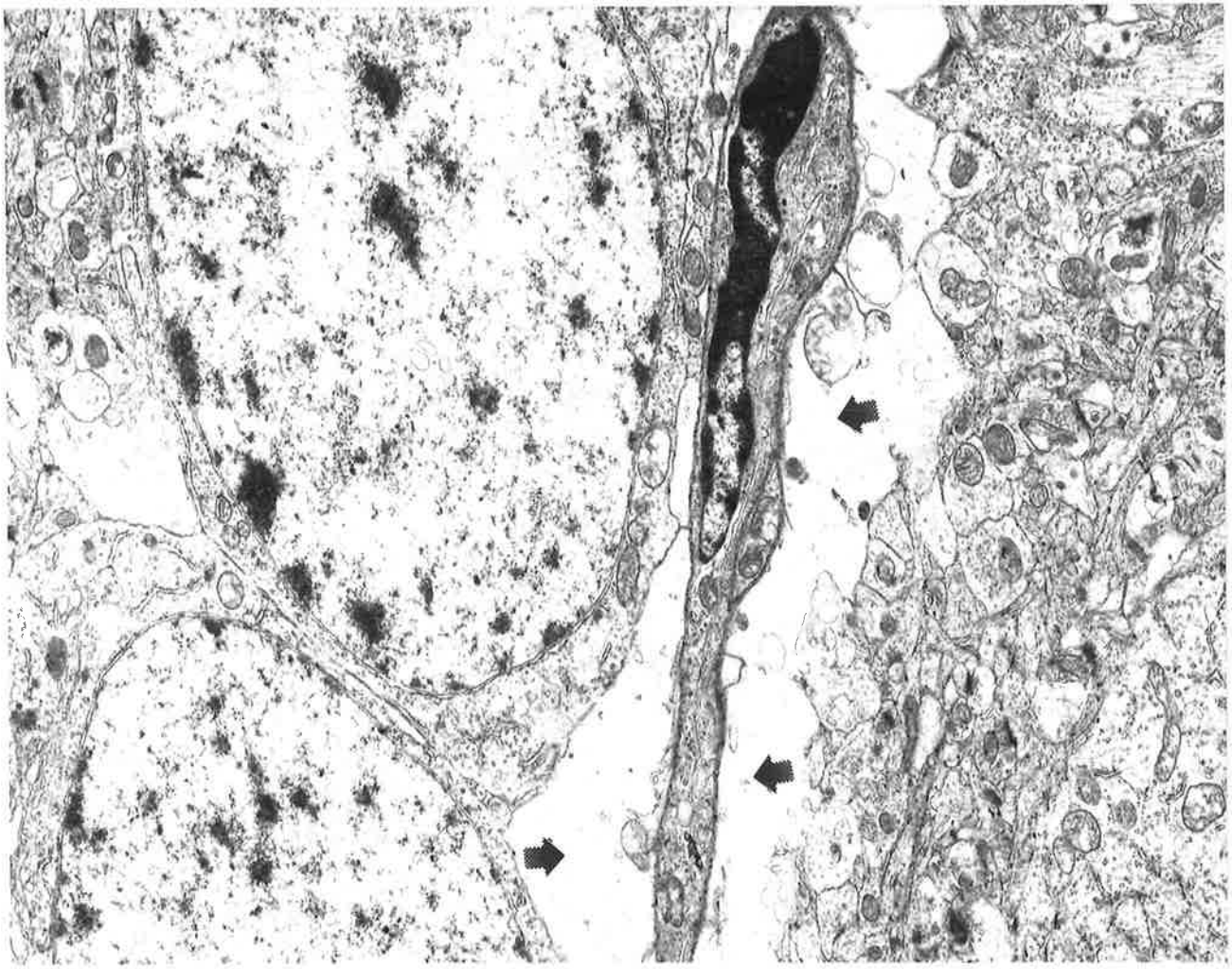

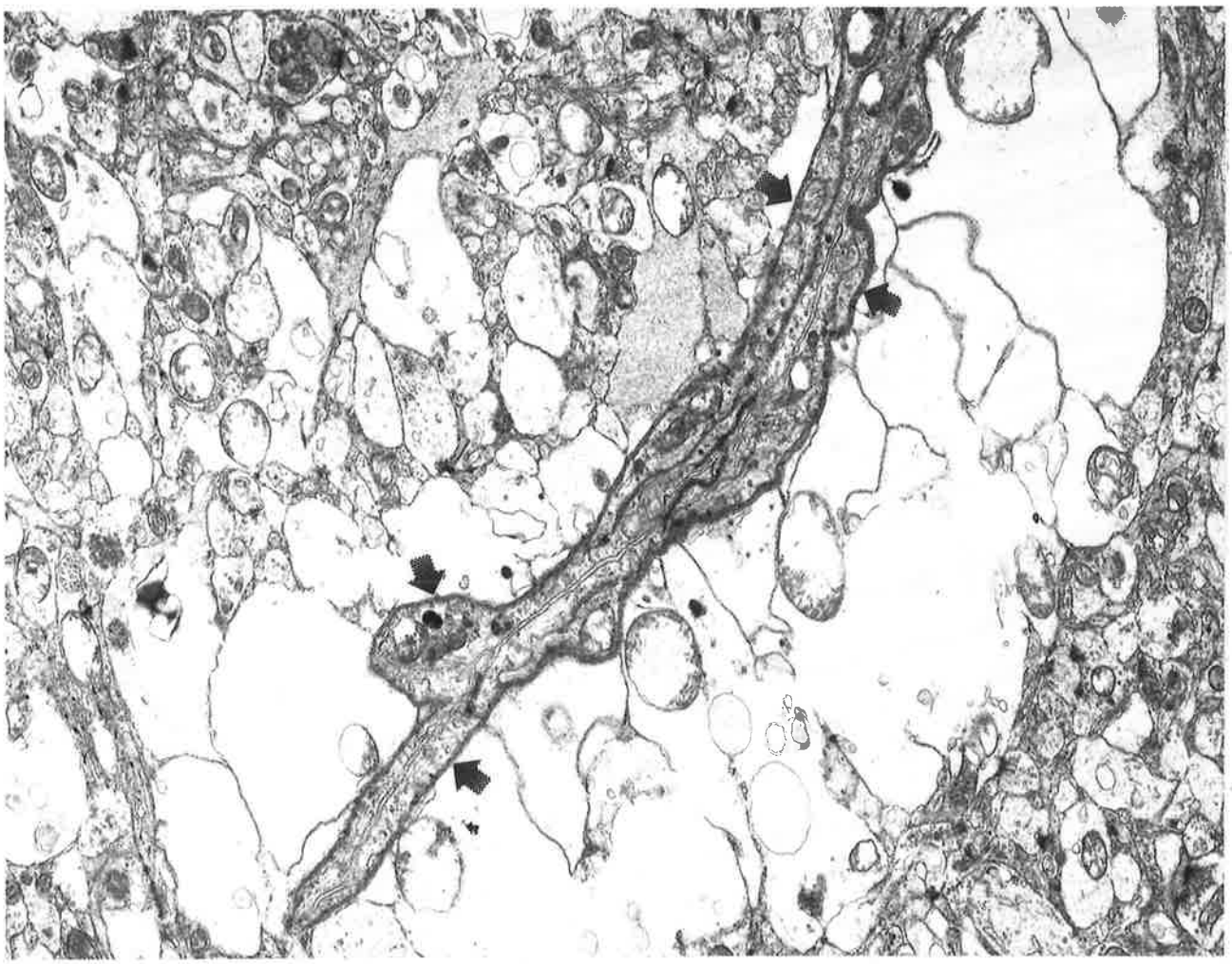

Figure 49. Toxin treated mouse. Cerebellum. 1 hour post-inoculation. Swelling of astrocytes with loss of cytoplasmic organelles leaving behind clear spaces. x 5330.

Figure 50. Toxin treated mouse. Cerebral cortex. 1 hour post-inoculation. The capillary endothelial cytoplasm is highly condensed as shown by increased electron opacity and attenuated and vacuolated. Severe end-feet swelling is evident with a small accumulation of proteinaceous exudate in the pericapillary region (arrow). x 10,250.

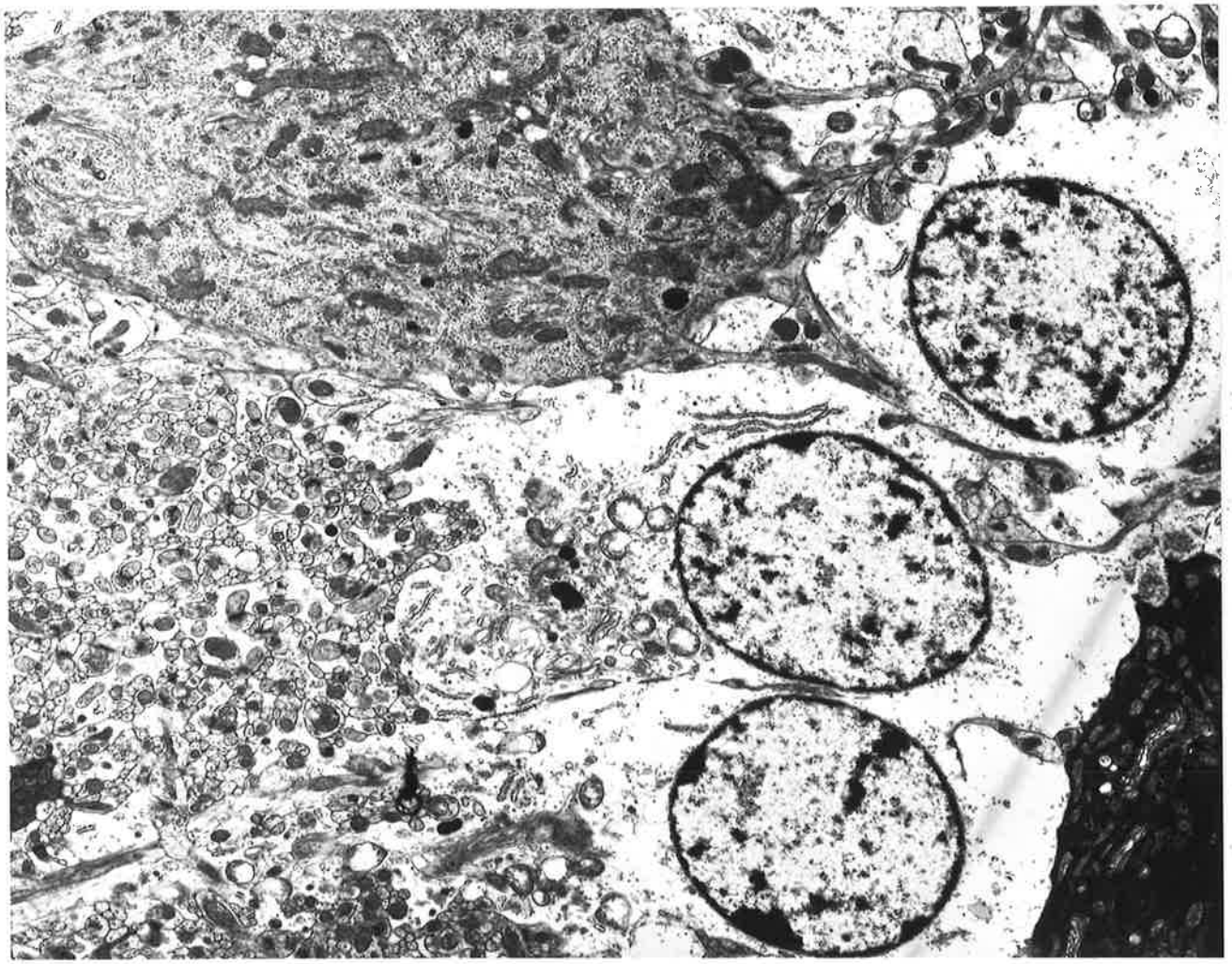

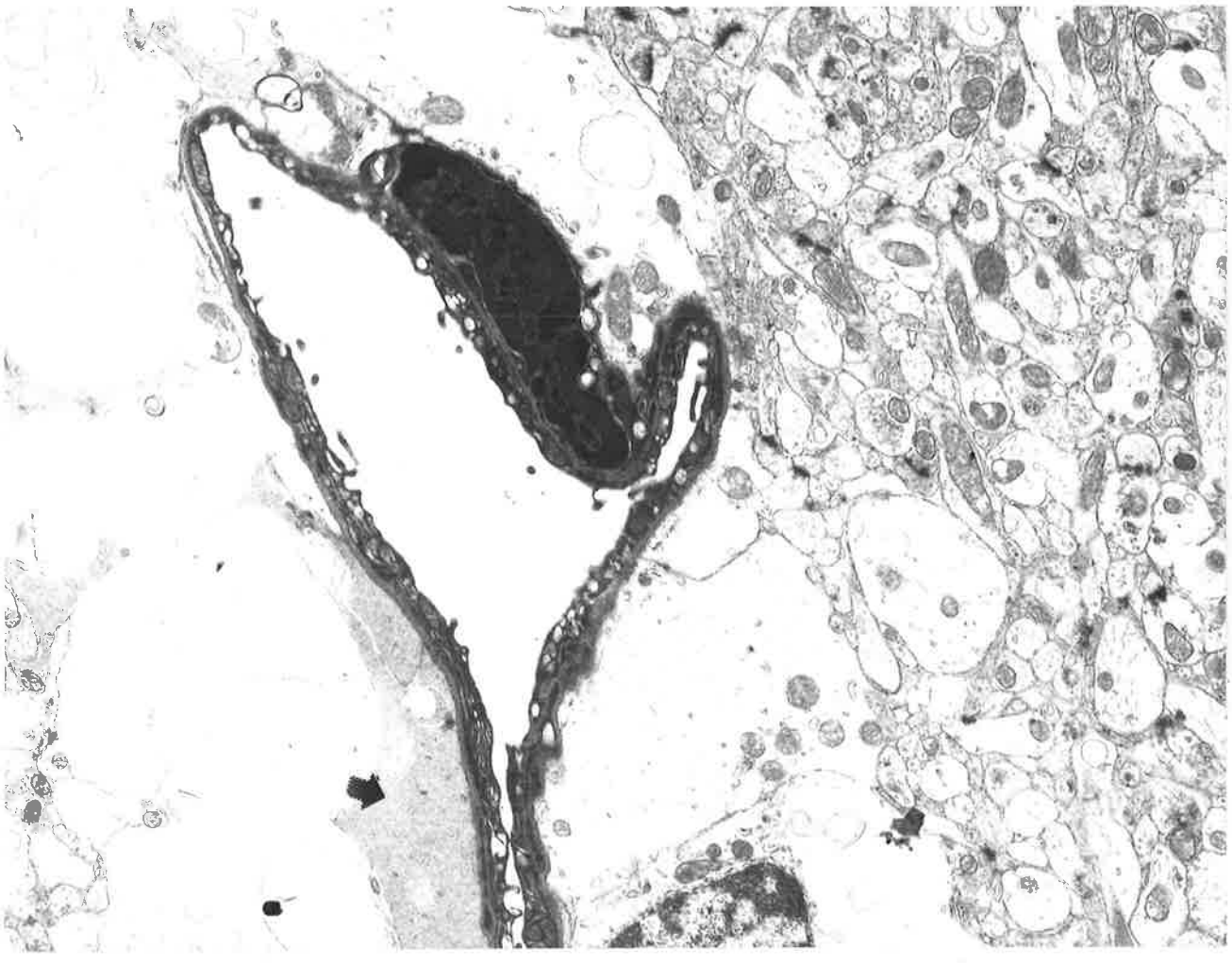

Figure 51. Toxin treated mouse. Cerebral cortex. 1 hour post-inoculation. Marked distension of end-feet and collapse of the capillary. The electron density of the endothelial cytoplasm obscures organelle detail. x 4100.

Figure 52. Toxin treated mouse. Cerebellum. 3 hours post-inoculation. Enhanced attenuation and electron-density of the capillary endothelium. The endothelial nucleus is pyknotic but part of the pericyte nucleus shown appears normal. Numerous granule cells are present. x 5330.

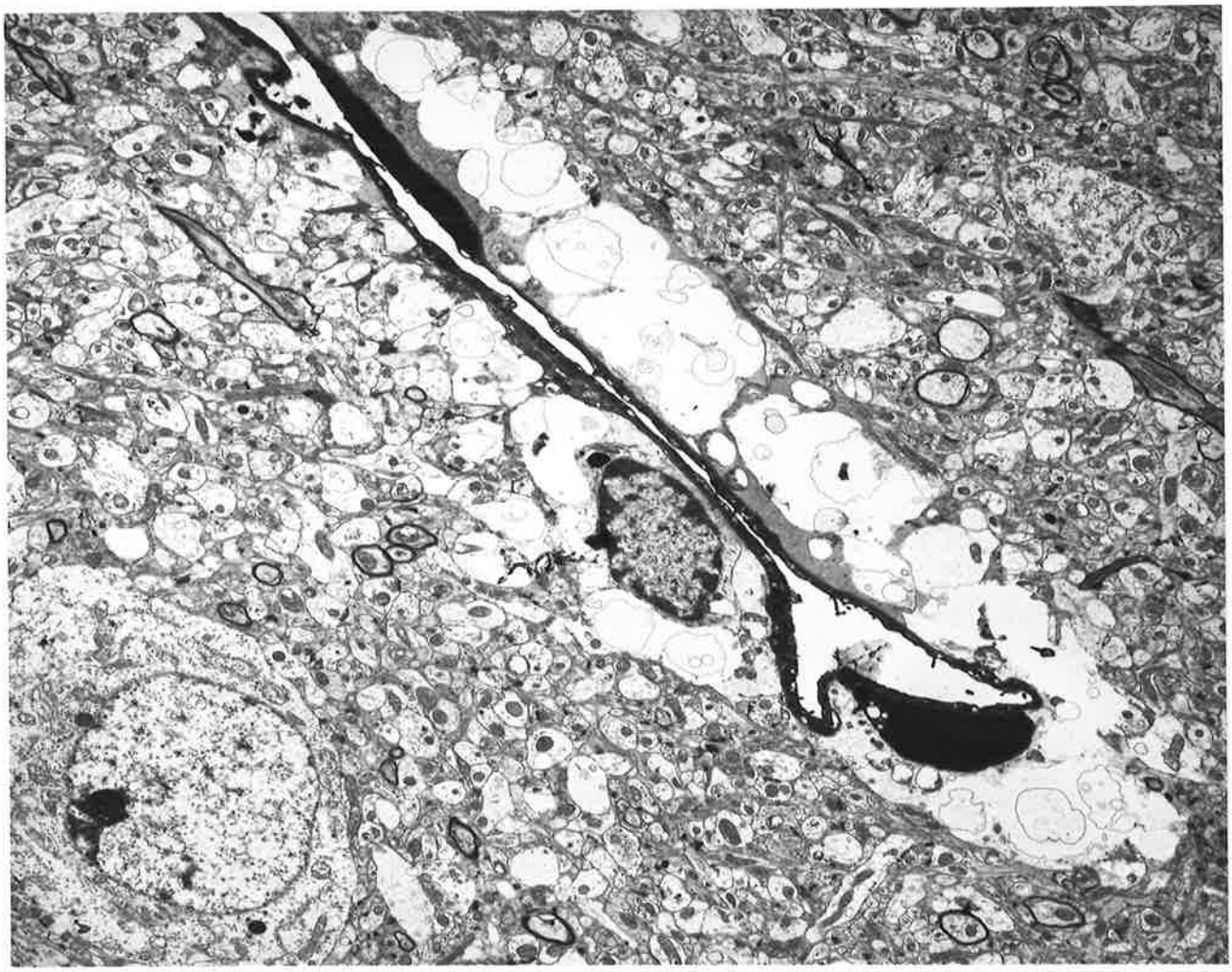

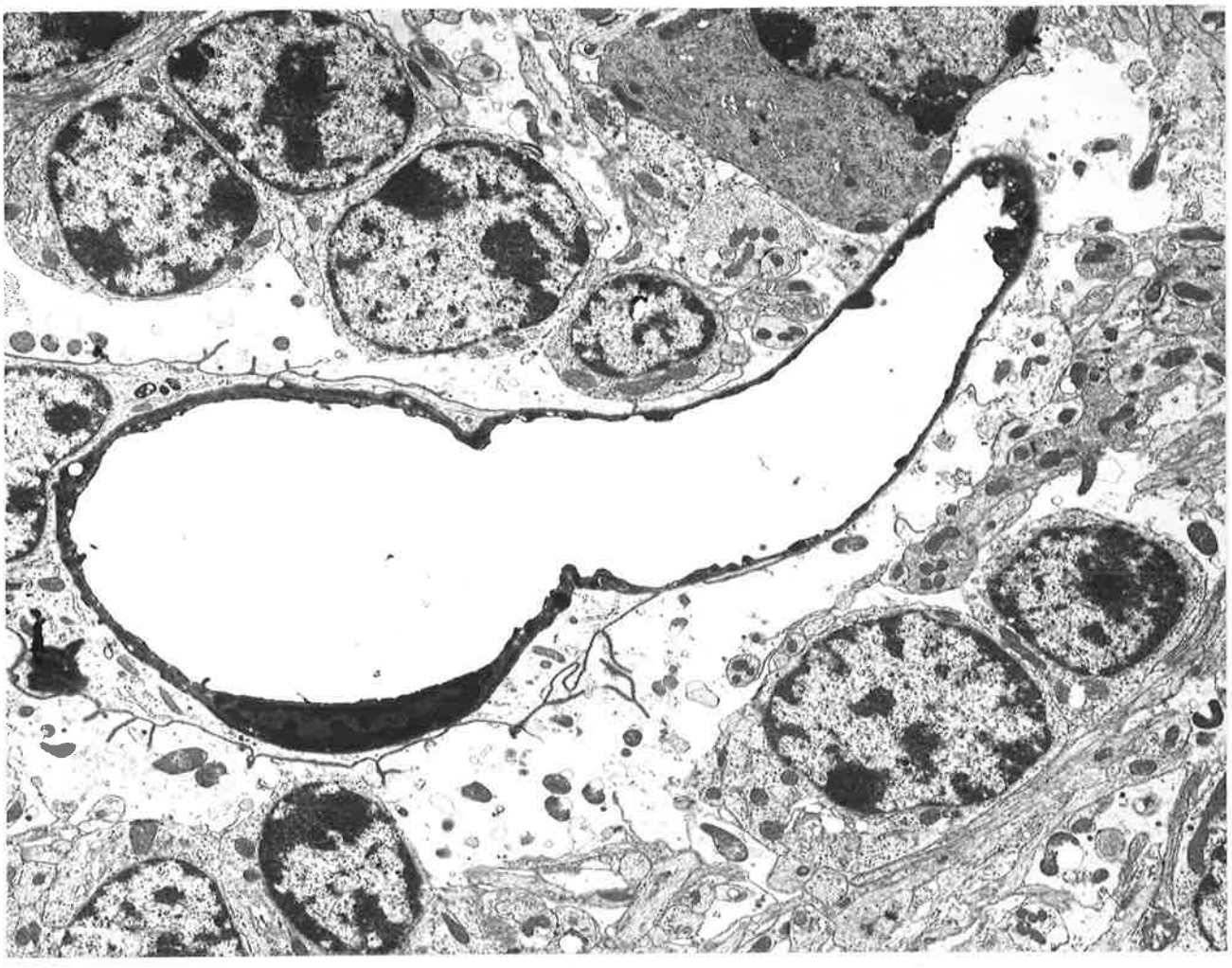

Figure 53. Toxin treated mouse. Cerebellum. 3 hours post-inoculation. Swelling of astrocytes and granule cells. The Purkinje cell (arrow) appears relatively normal. x 4100.

Figure 54. Toxin treated mouse. Cerebellum. 3 hours post-inoculation. Marked swelling of granule cells with loss of organelle detail and cellular outlines. Compare with Figure 44. A capillary shows a "dark" endothelial cell. x 5330.

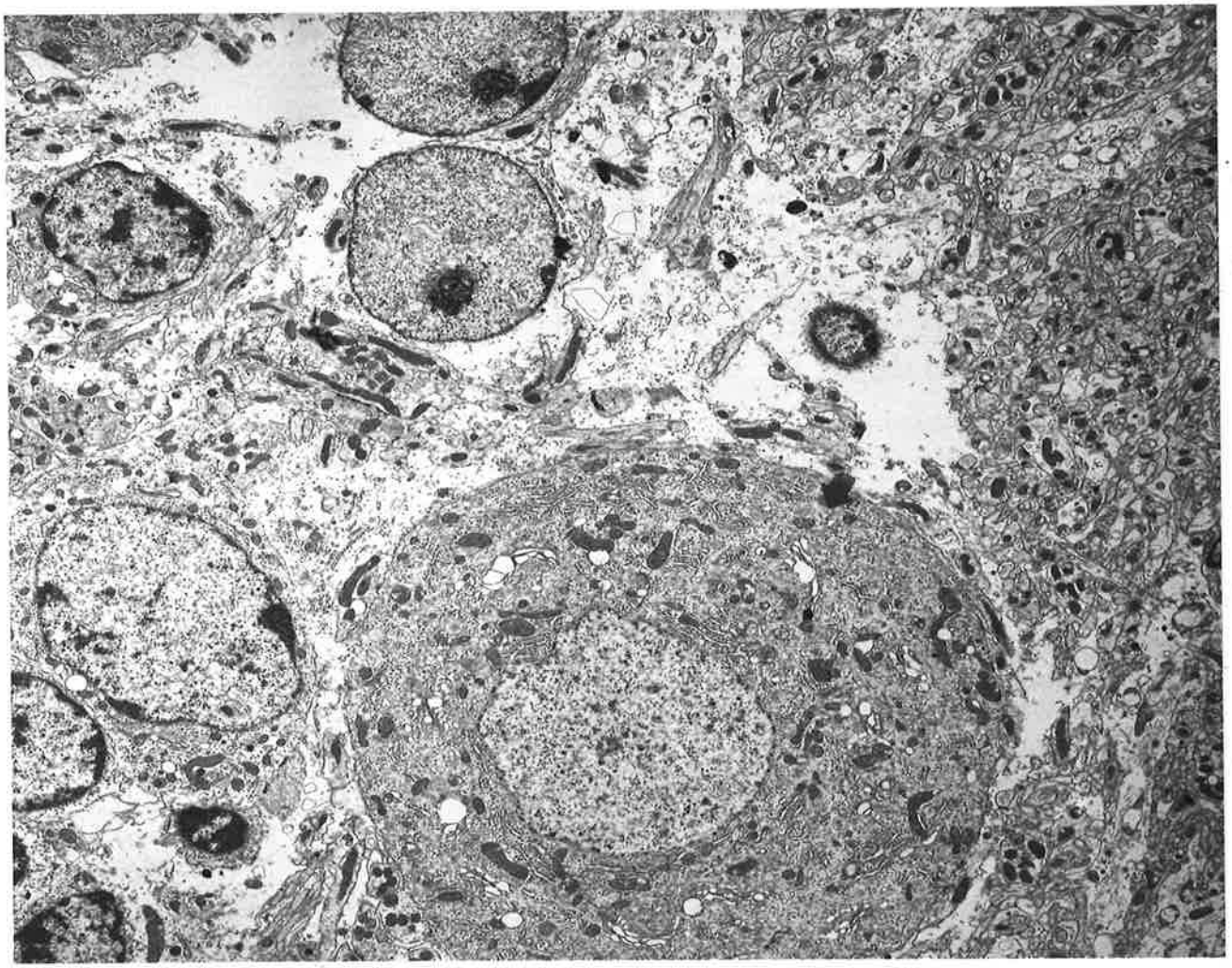

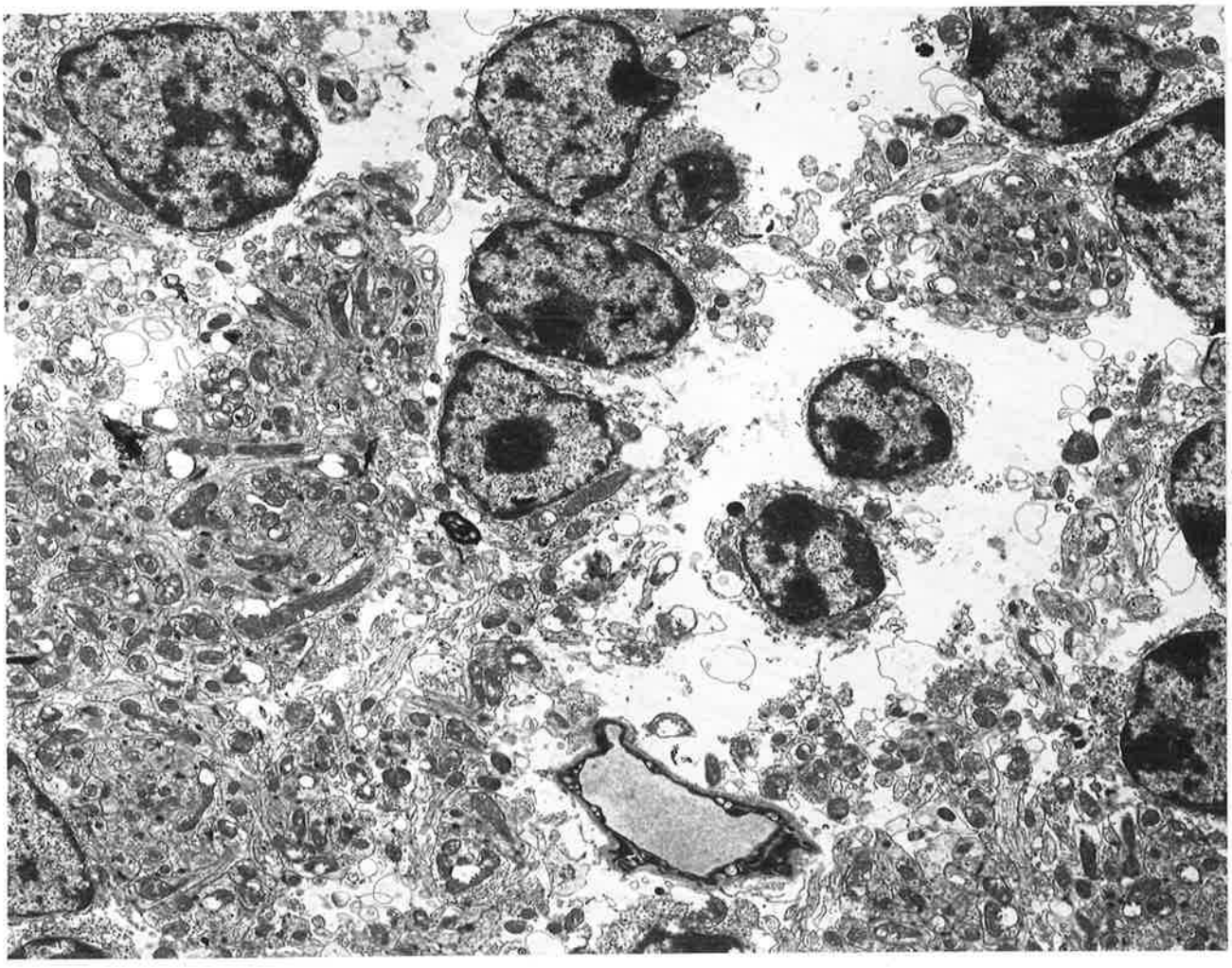

Figure 55. Toxin treated mouse. Cerebellum. 3 hours post-inoculation. The capillary endothelium is very electron dense and vacuolated, Endothelial "blebbing" is prominent.
x 10,250.

Figure 56. Toxin treated mouse. Cerebellum. 3 hours post-inoculation. Swelling of astrocytes with remnants of cytoplasmic organelles and indistinct plasma membranes.
x 6765.

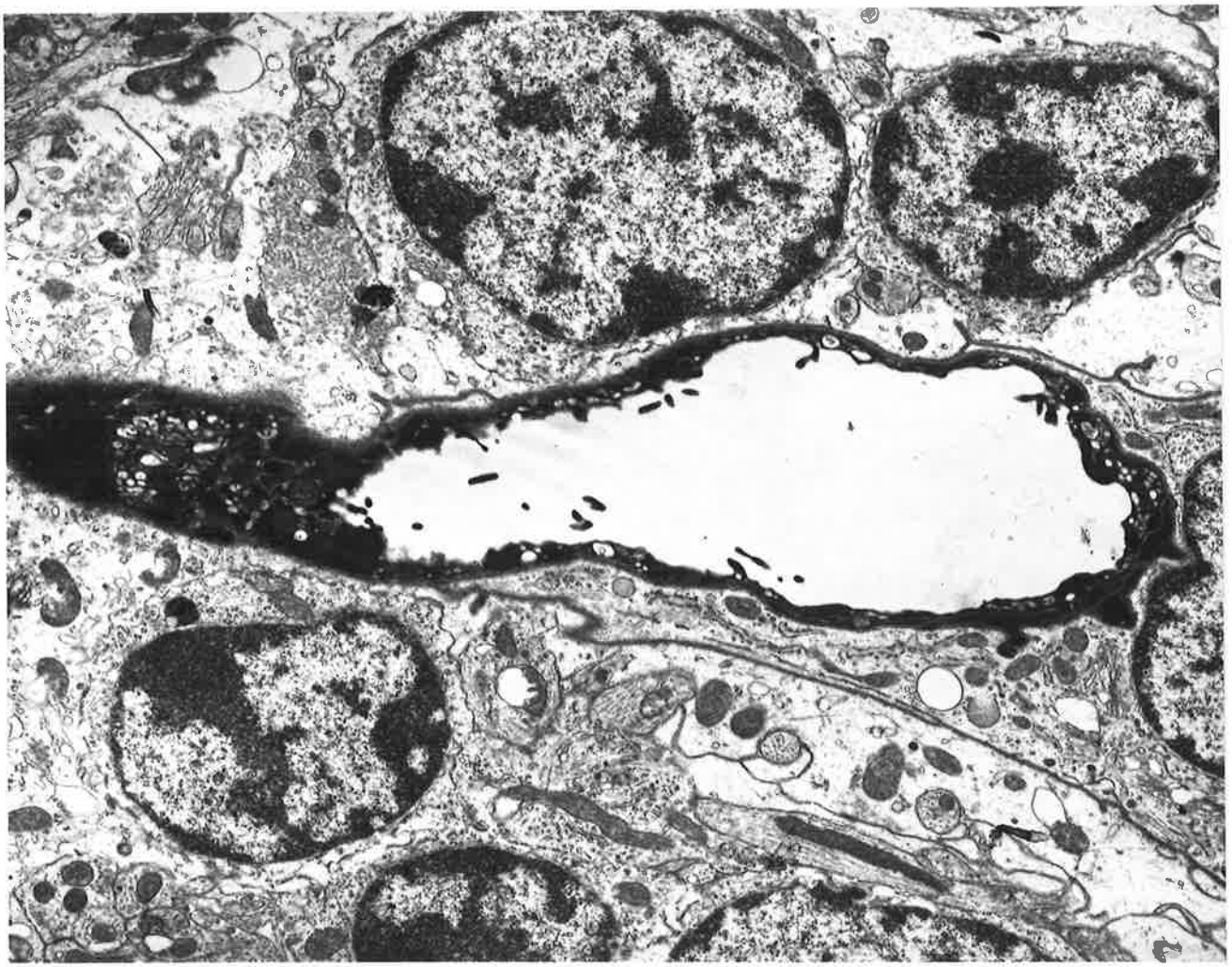

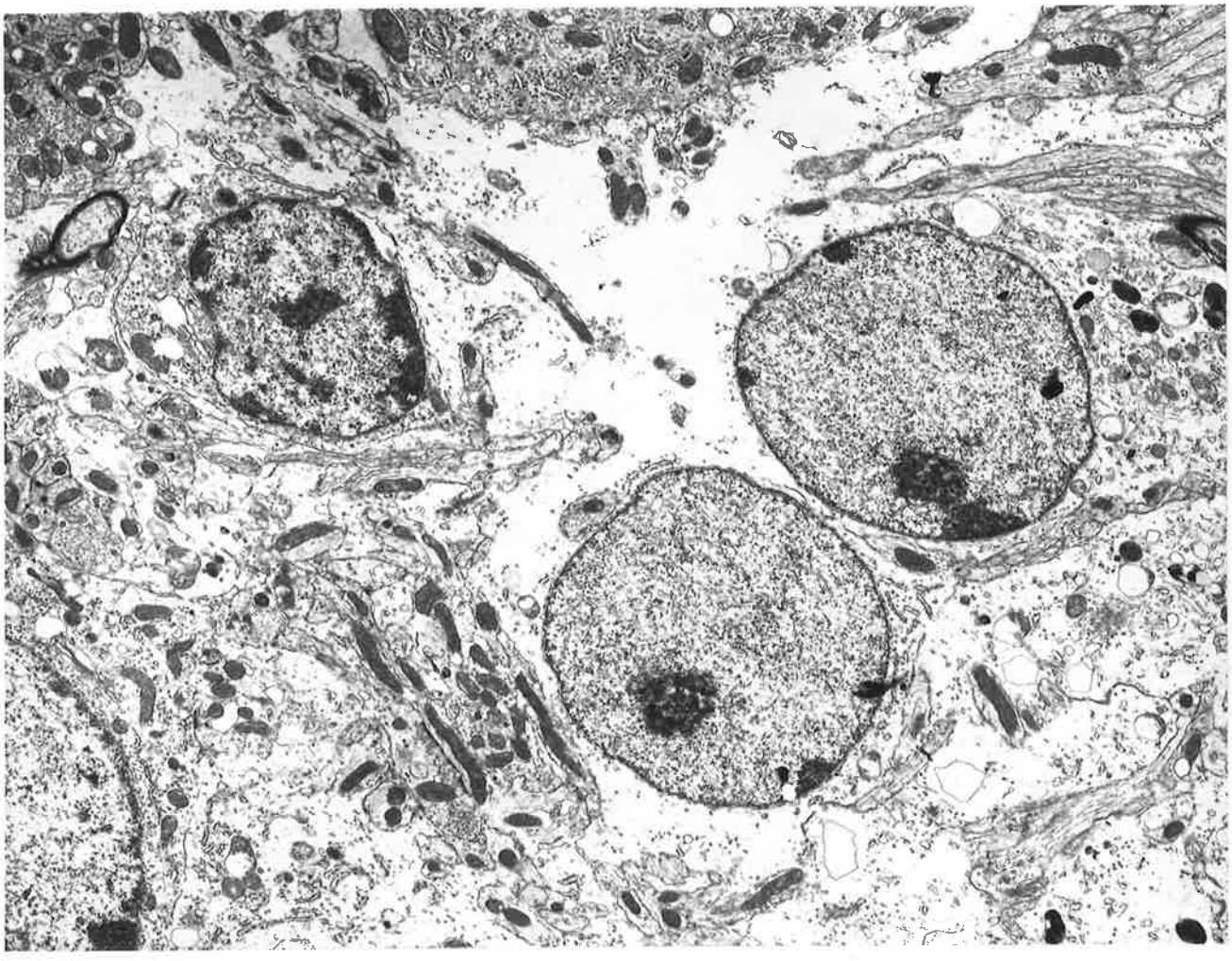

Figure 57. Toxin treated mouse. Cerebellum. 4 hours post-inoculation. Marked astrocytic swelling with an expanded electron lucent cytoplasm, almost devoid of organelles. The parts of Purkinje cells shown appear largely unaffected.
x 10,250.

Figure 58. Toxin treated mouse. Cerebellum. 4 hours post-inoculation. Lower magnification of a similar area to Figure 57 showing marked swelling of astrocytes.
x 5330.

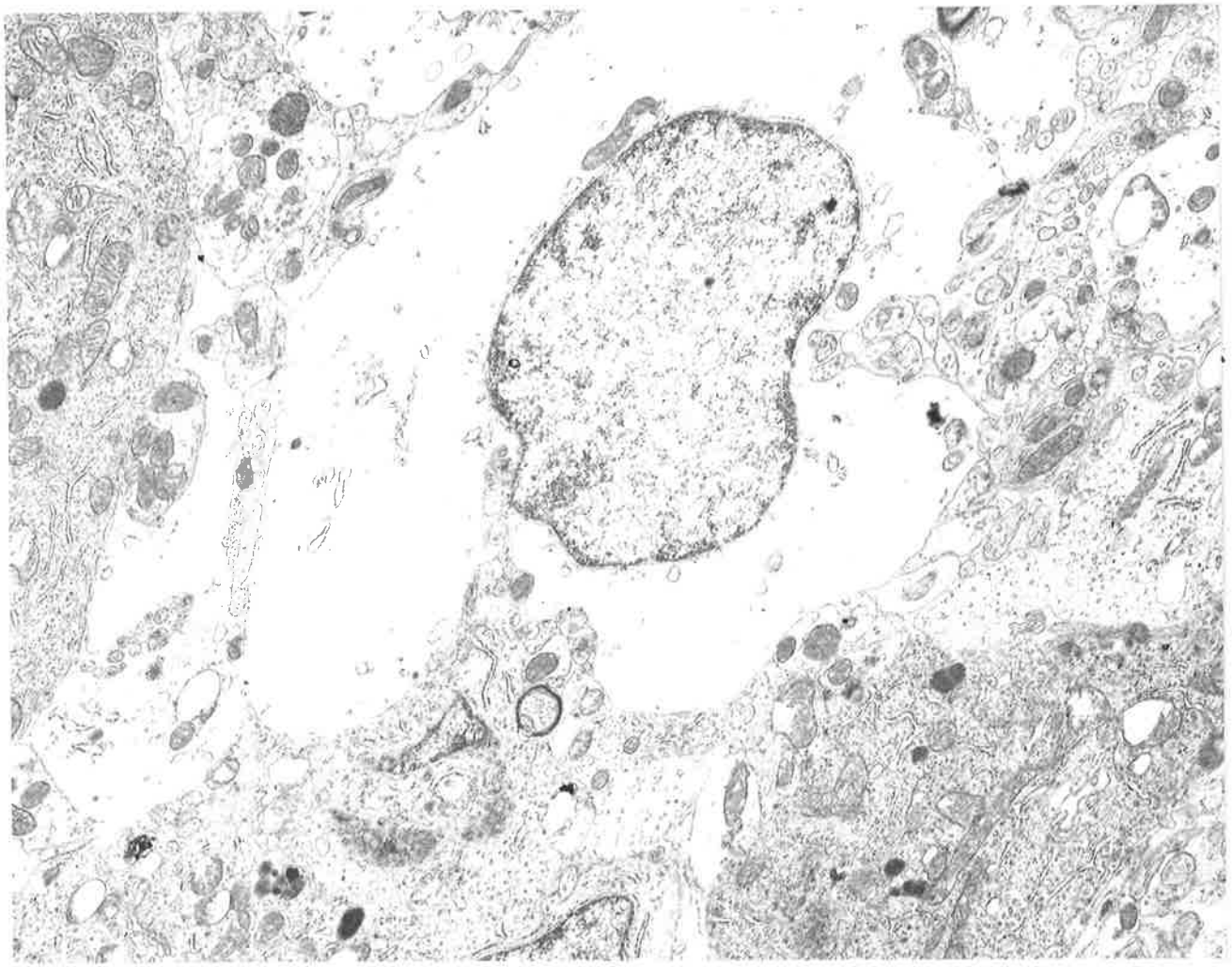

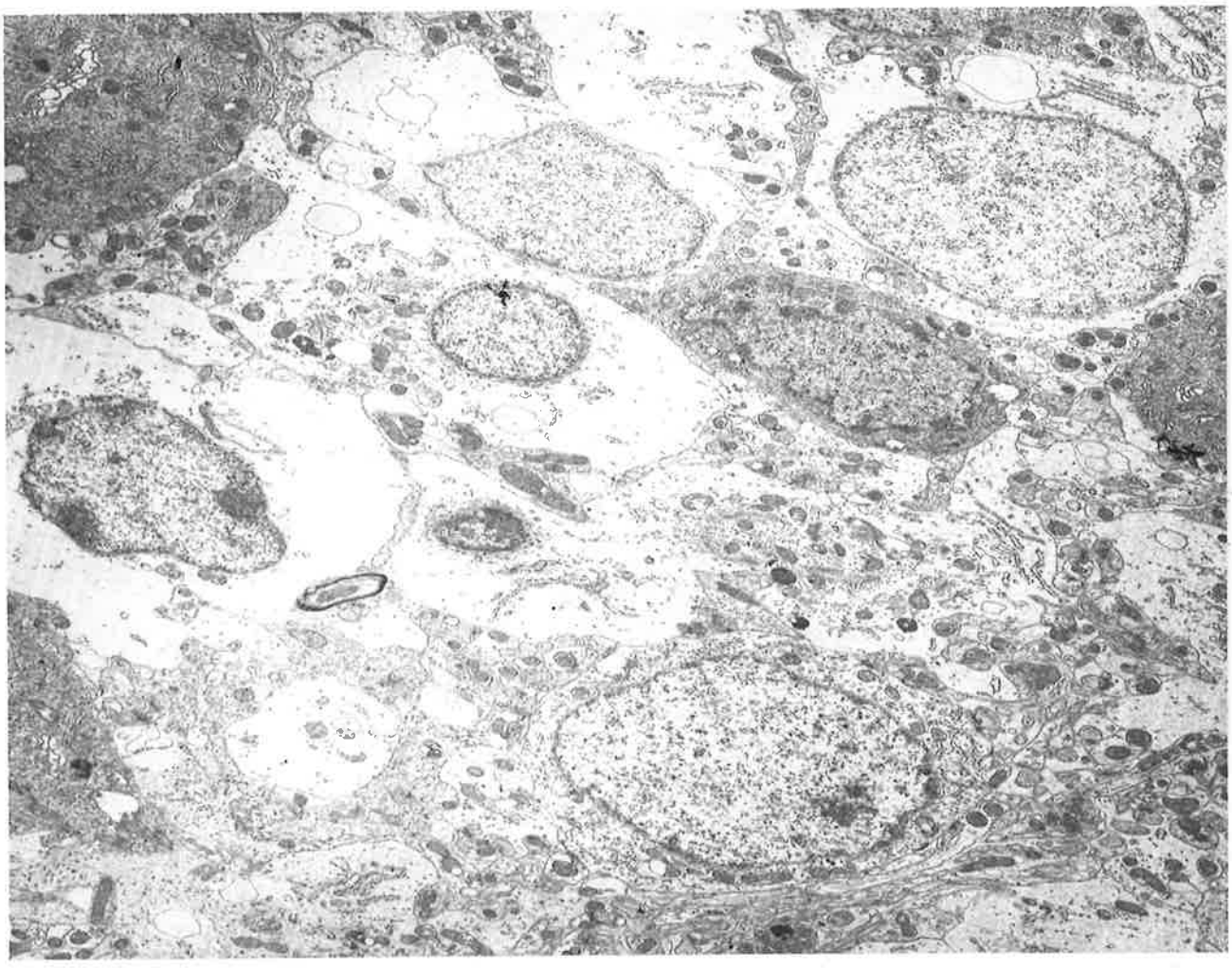

Figure 59. Toxin treated mouse. Cerebellum. 4 hours post-inoculation. Severe endothelial degeneration but astrocytic end-feet enlargement is minimal. Numerous granule cells are present.
x 13,530.

Figure 60. Toxin treated mouse. Cerebellum. 2 hours post-inoculation. Marked astrocytic swelling with "ghost" outlines of cytoplasmic organelles. The Purkinje cell (arrow) appears normal.
x 4100.

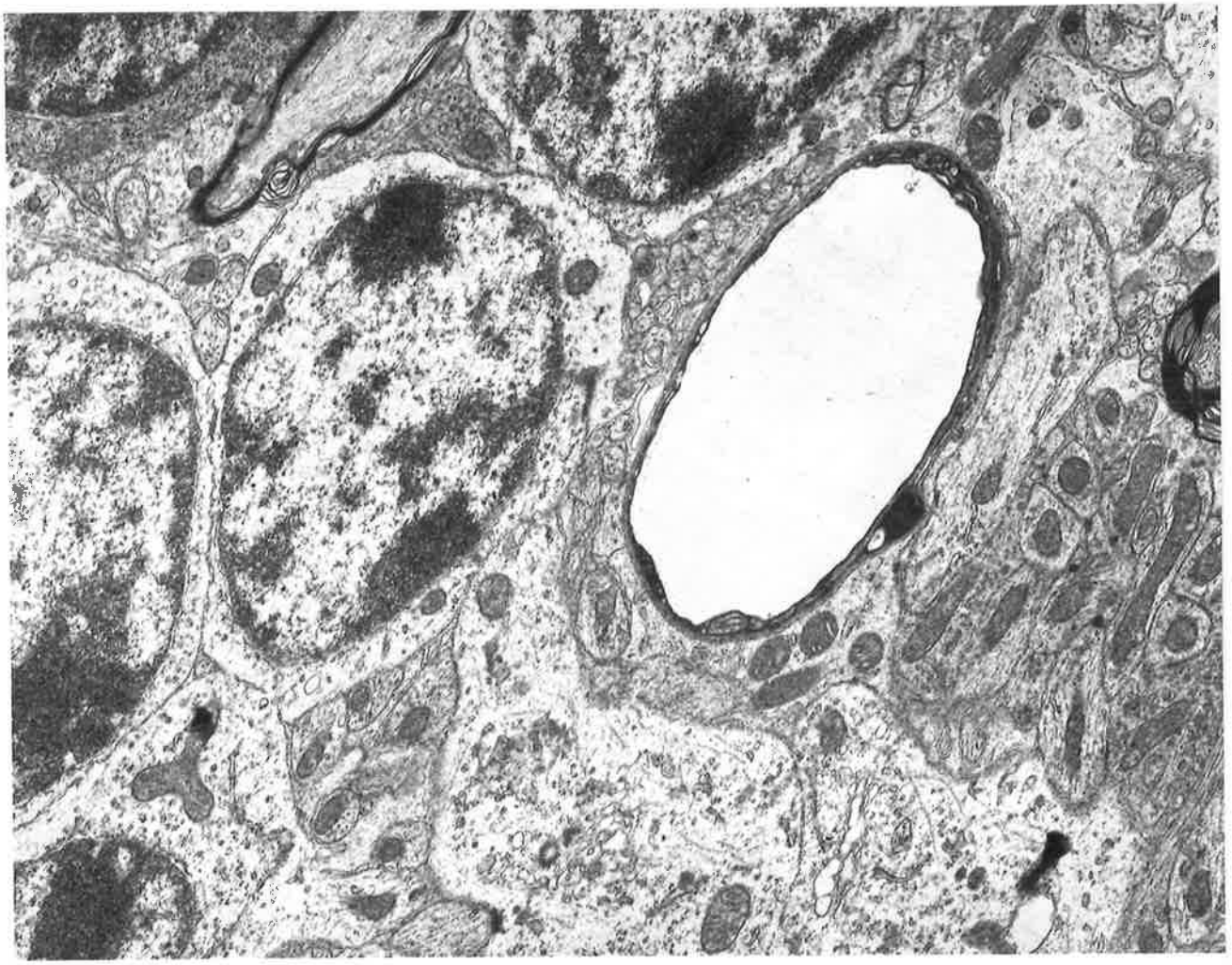

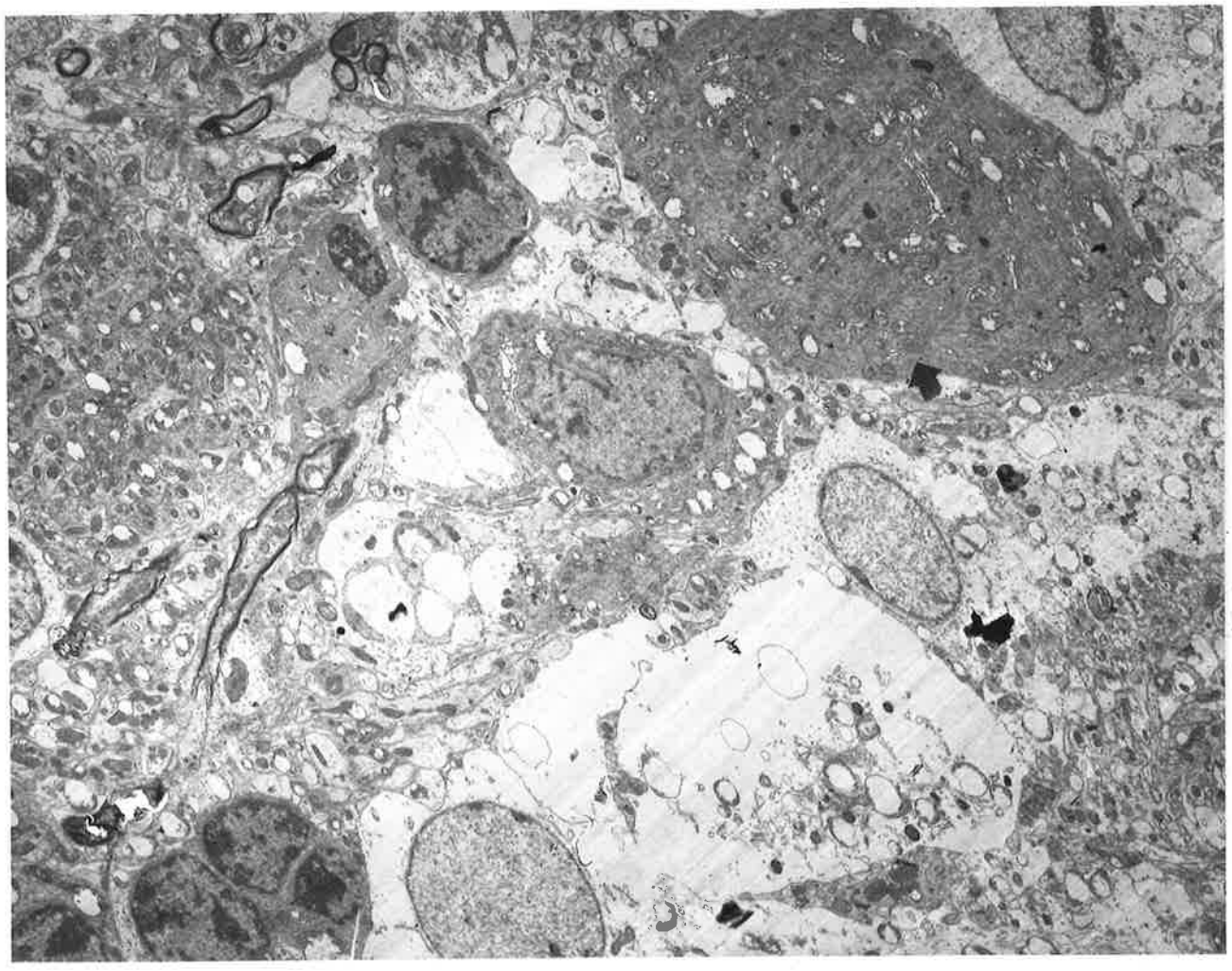

Figure 61. Toxin treated mouse. Cerebellum. 6 hours post-inoculation. The capillary endothelium is electron dense with marked perivascular end-feet swelling (arrow). Swelling of astrocytes and astrocytic processes around a Purkinje cell. Granule cells appear relatively normal. x 5330.

Figure 62. Toxin treated mouse. Cerebral cortex. 24 hours post-inoculation. Mild swelling of cellular elements in the neuropil and perivascular extensions of astrocytes. The capillary lumen appears collapsed only where foot processes are very distended (arrows). x 6765.

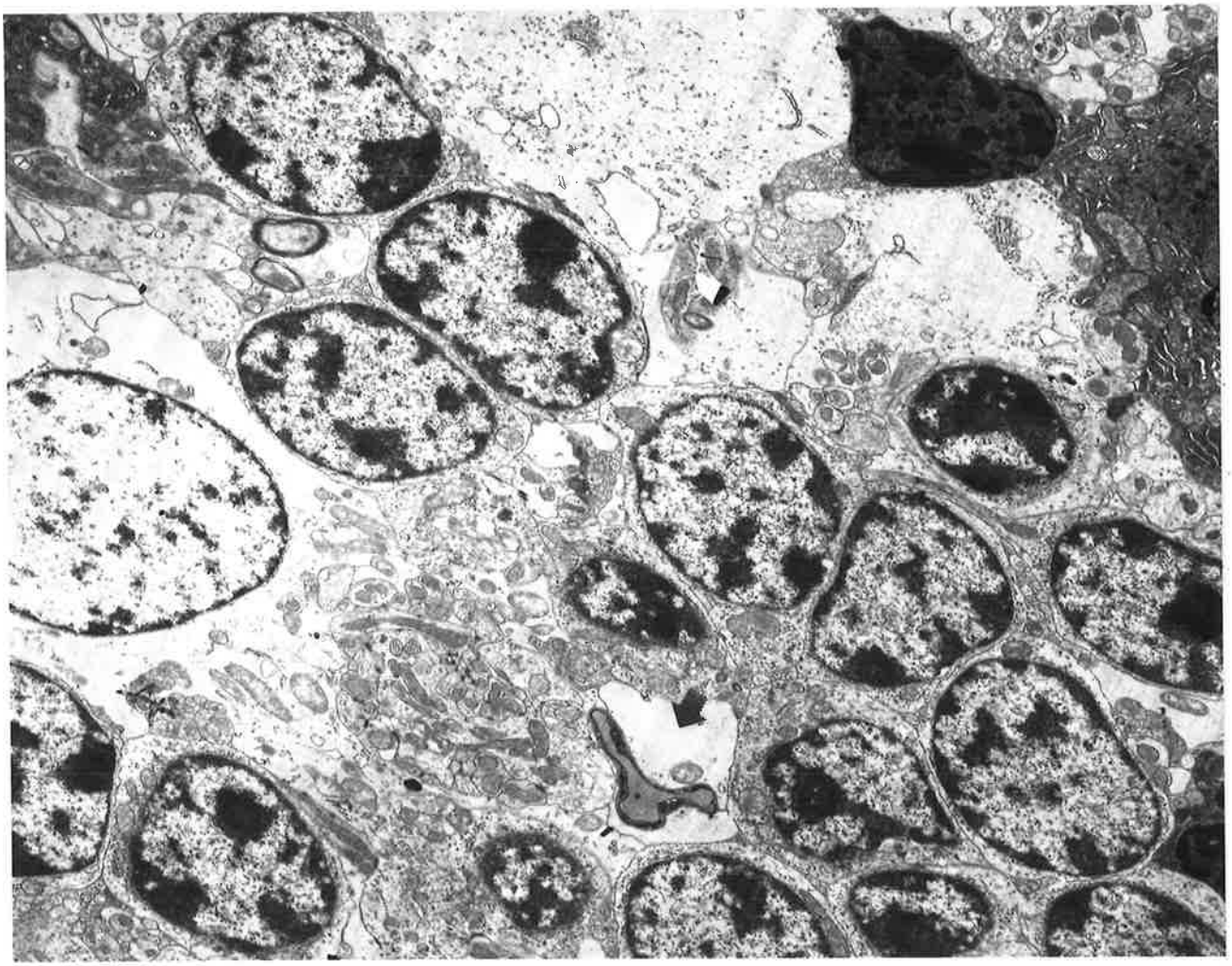

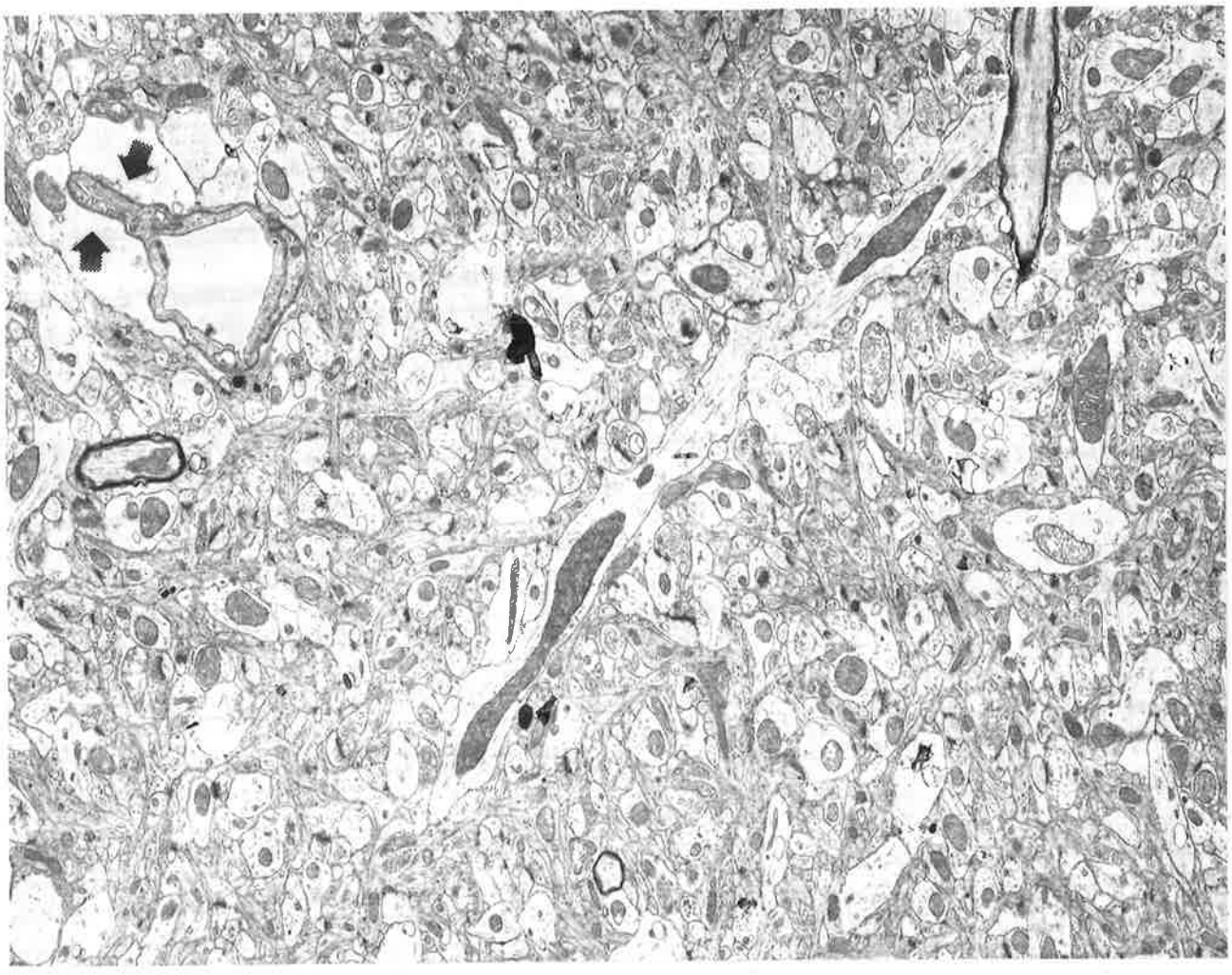

Figure 63. Toxin treated mouse. Corpus callosum. 4 hours post-inoculation. Extracellular space is expanded and axons are dilated with extensive disruption of myelin lamellation (arrows).
x 6765.

Figure 64. Toxin treated mouse. Corpus callosum. Immersion fixation. 6 hours post-inoculation. The endothelial cytoplasm is condensed into electron dense bands with numerous vacuoles evident. Swelling of astrocytic end-feet and astrocytic processes in the neuropil.
x 13,530.

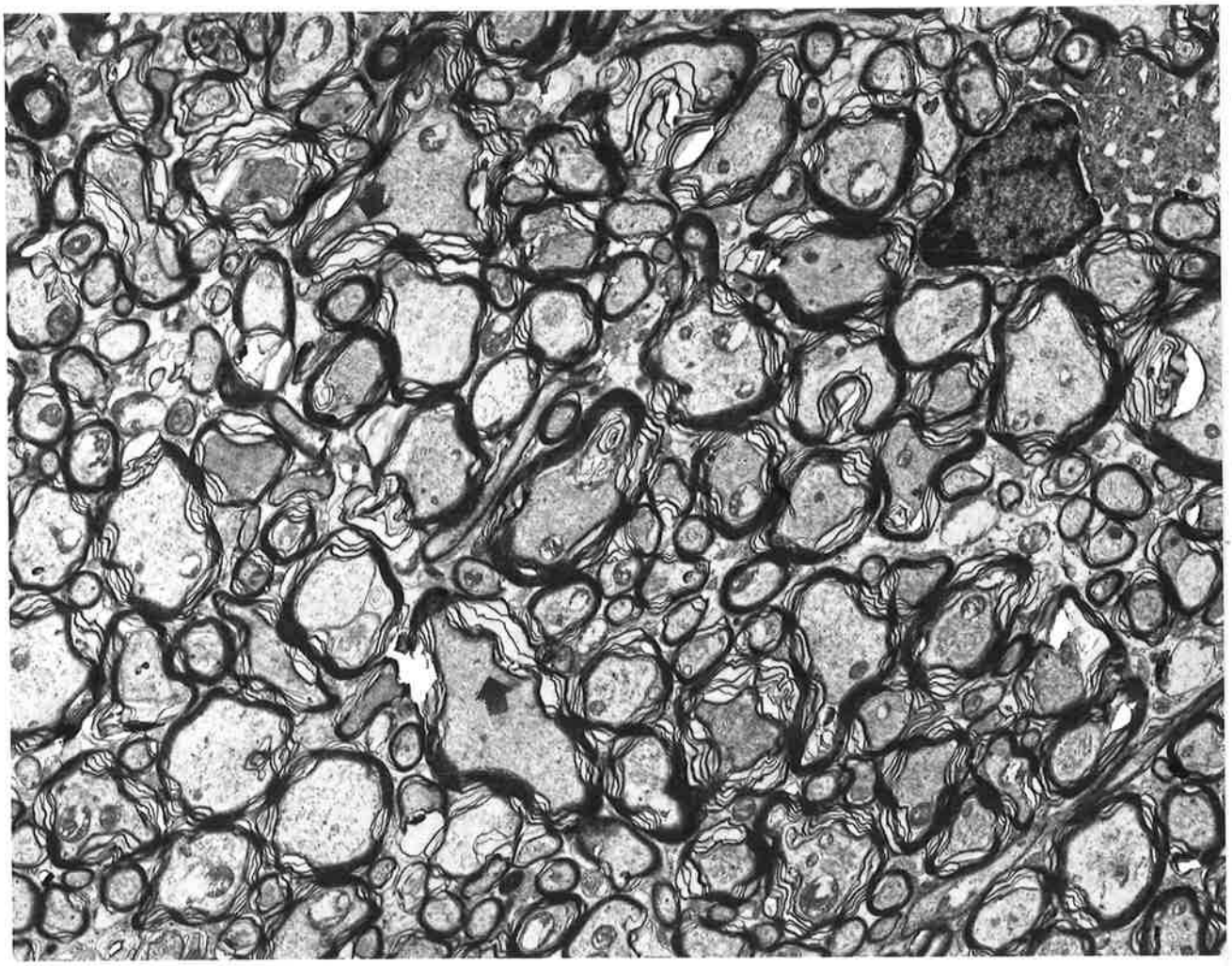

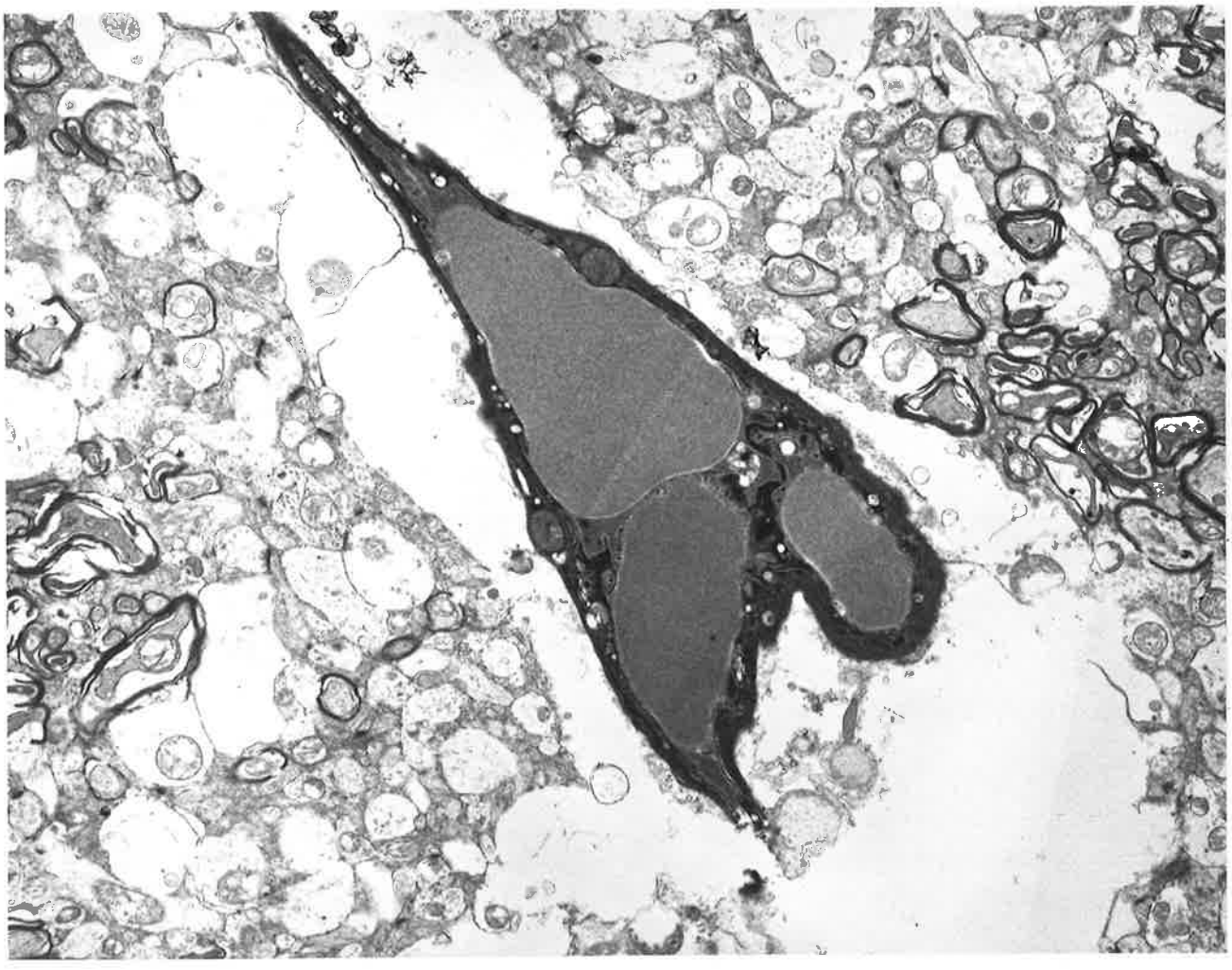

Figure 65. Toxin treated mouse. Cerebral cortex. Immersion fixation. 6 hours post-inoculation. The endothelial cytoplasm is reduced to electron dense bands. Severe swelling and breakdown of astrocytic end-feet. An erythrocyte is visible in the capillary lumen.
x 13,530.

Figure 66. Toxin treated mouse. Corpus callosum. Immersion fixation. 36 hours post-inoculation. Prominent swelling of myelinated axons (arrows) and astrocytic processes.
x 5330.

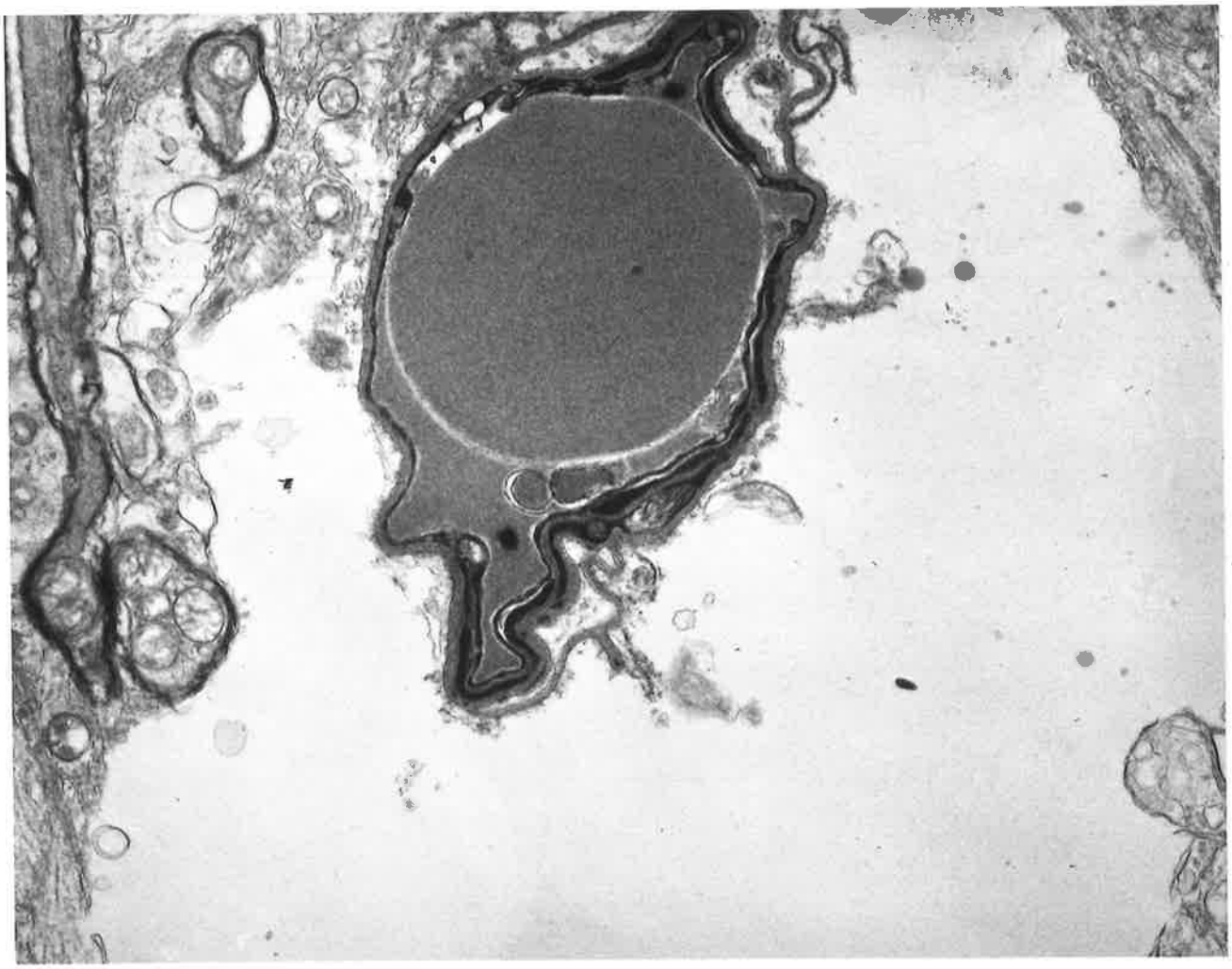

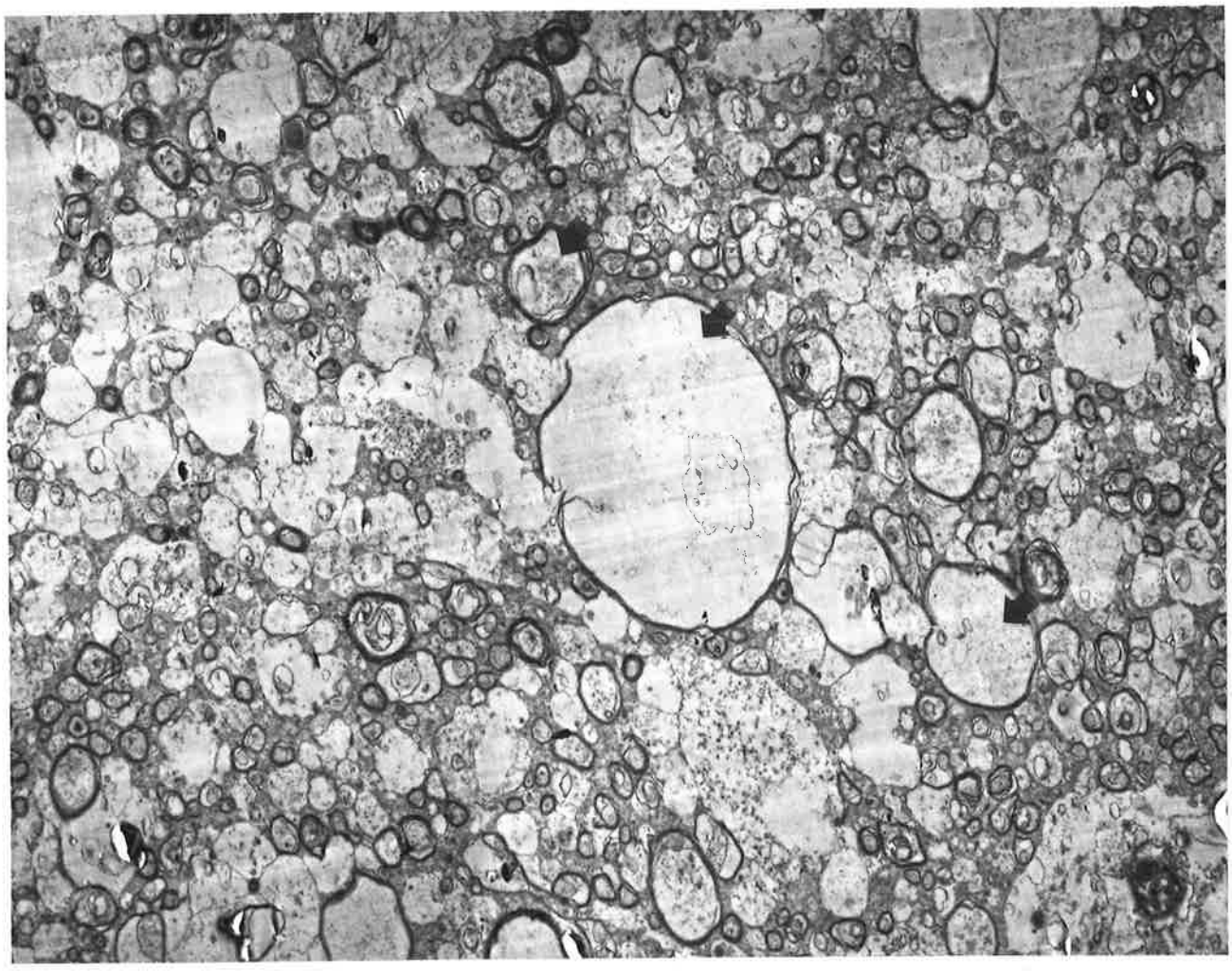

Figure 67. Toxin treated mouse. Corpus callosum. Immersion fixation. 36 hours post-inoculation. Swelling of myelinated axons and astrocytic processes in white matter tracts. Oligodendroglial swelling is also evident.
x 5330.

Figure 68. Toxin treated mouse. Corpus callosum. Immersion fixation. 4 hours post-inoculation. Axonal swelling, disruption of myelin lamellation (arrow) and enlargement of the extracellular space.
x 13,530.

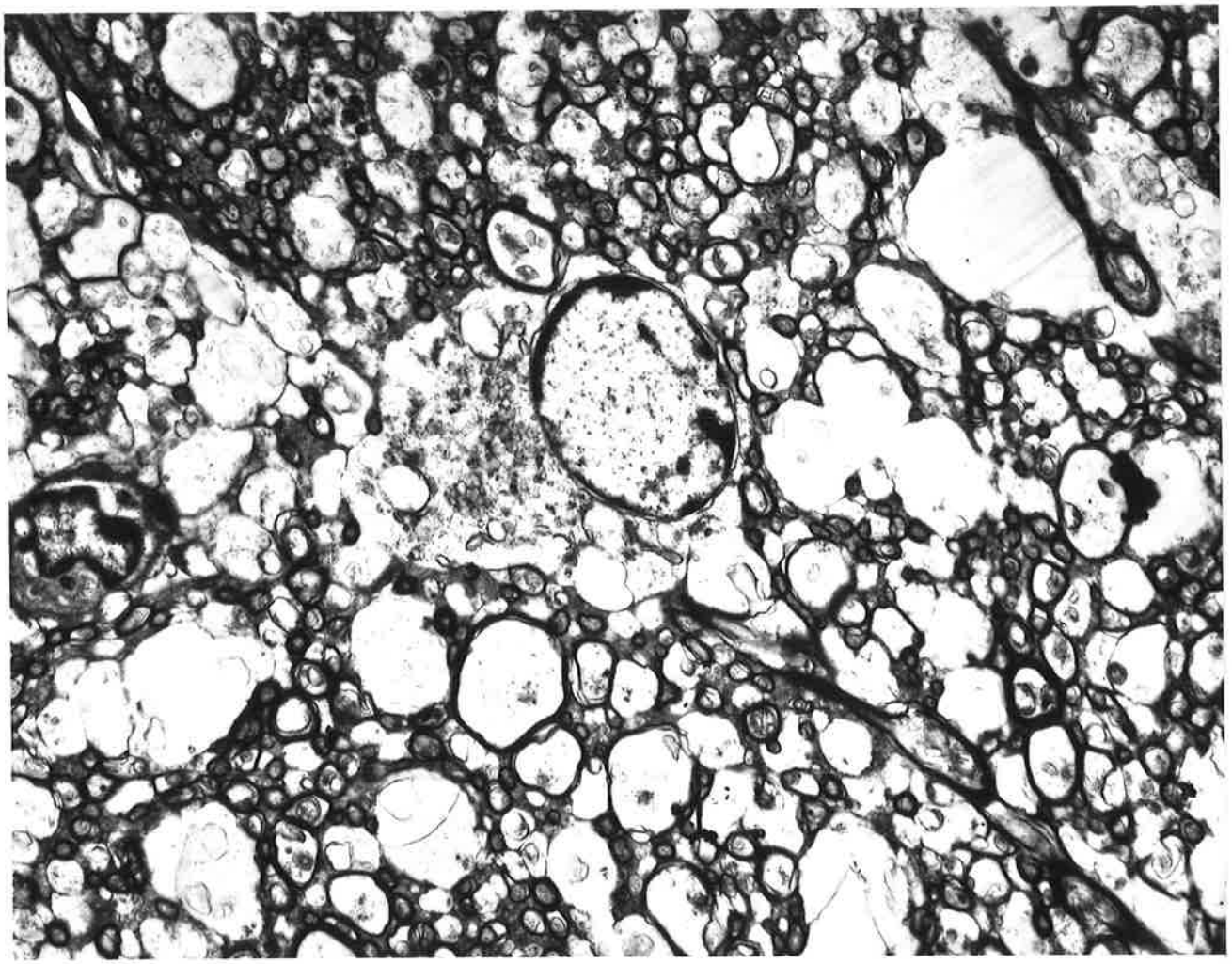

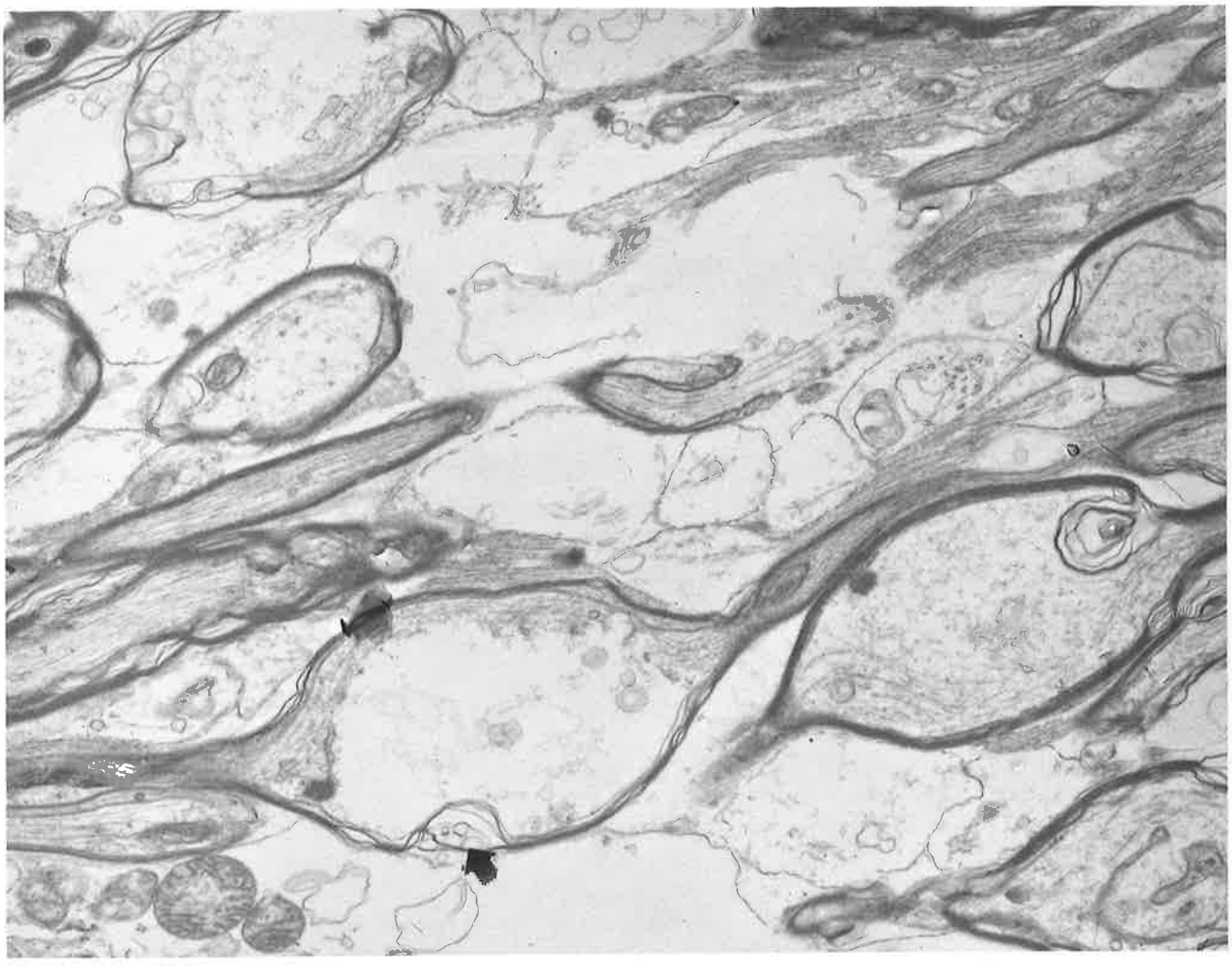

Figure 69. Toxin treated mouse. Cerebral cortex. Immersion fixation. 72 hours post-inoculation. Marked swelling of perivascular foot processes and astrocytic processes in the neuropil. A neuron appears slightly shrunken and more electron dense with cytoplasmic vacuolation. The blood vessel appears normal except for mitochondrial swelling. A pericyte is also shown (arrow).
x 4100.

Figure 70. Toxin treated mouse. Cerebral cortex. Immersion fixation. 36 hours post-inoculation. Severe swelling of cellular elements in the neuropil with loss of organelles. The blood vessel appears morphologically unaffected, however microthrombus visible in lumen.
x 13,530.

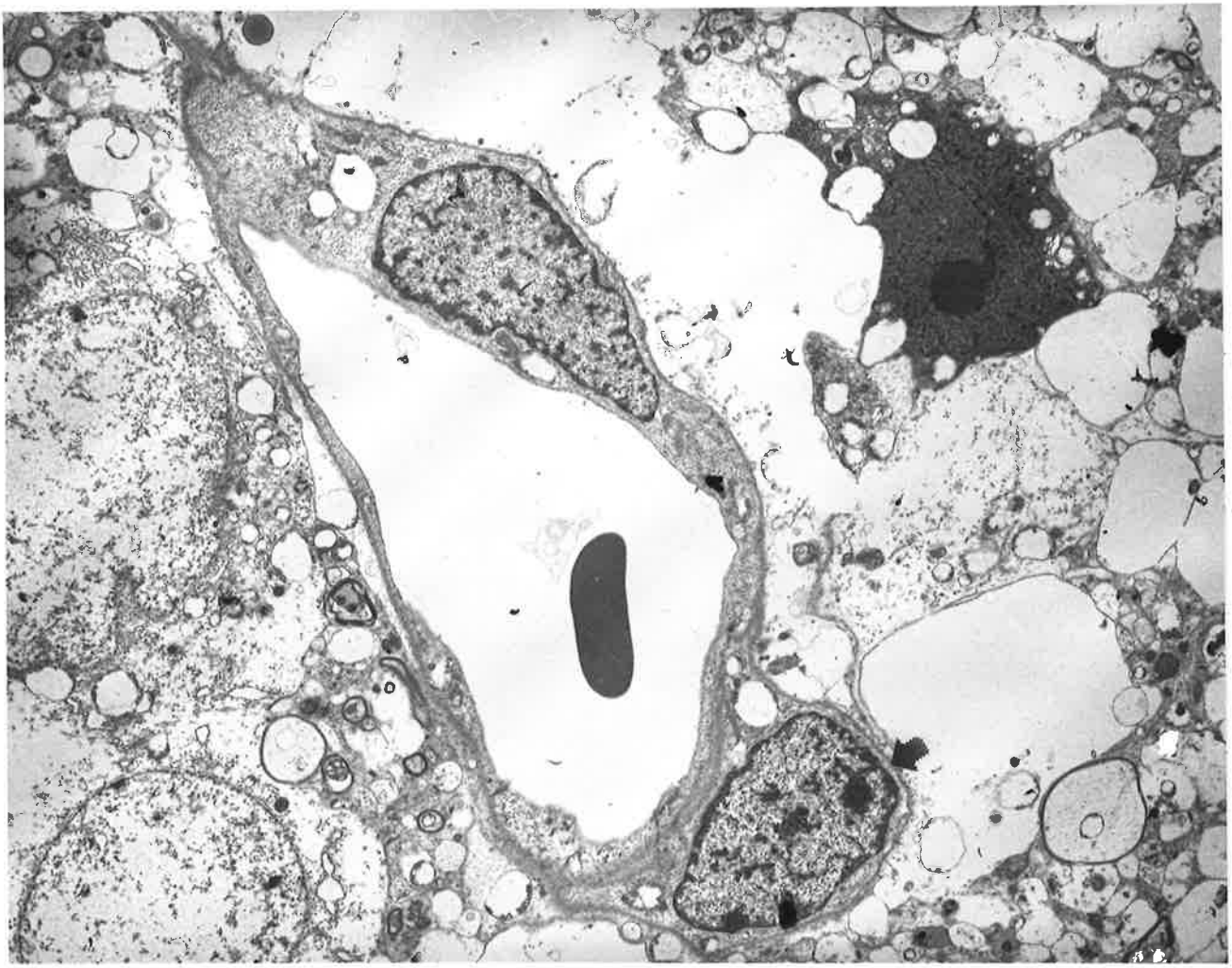

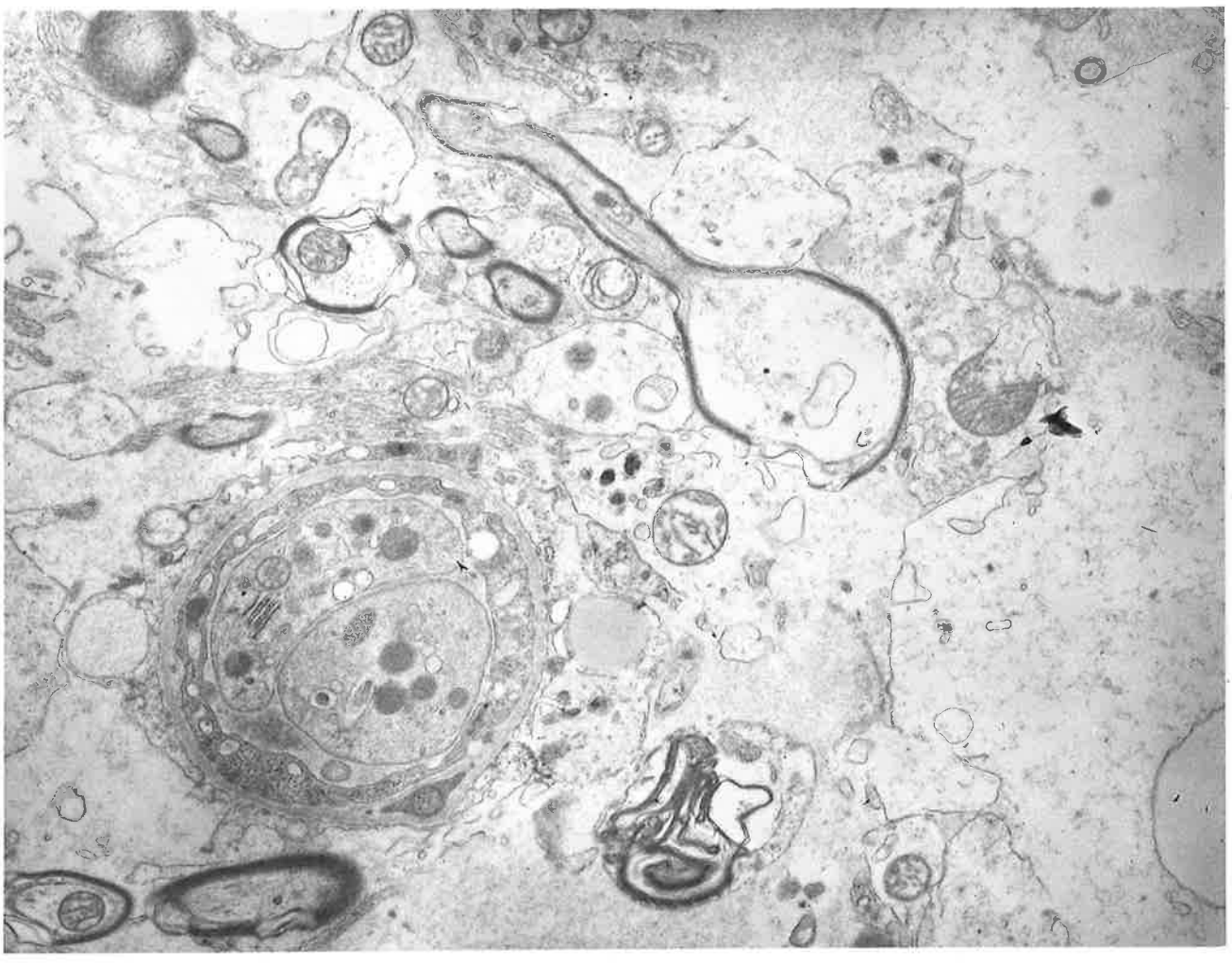

Figure 71. Toxin treated mouse. Corpus callosum. Immersion fixation. 36 hours post-inoculation. A much enlarged extracellular space containing copious amounts of extravasated plasma protein.
x 5330.

Figure 72. Toxin treated mouse. Corpus callosum. Immersion fixation. 36 hours post-inoculation. Cellular remnants are scattered in a large pool of exuded plasma protein. An oligodendrocyte shows modest swelling.
x 5330.

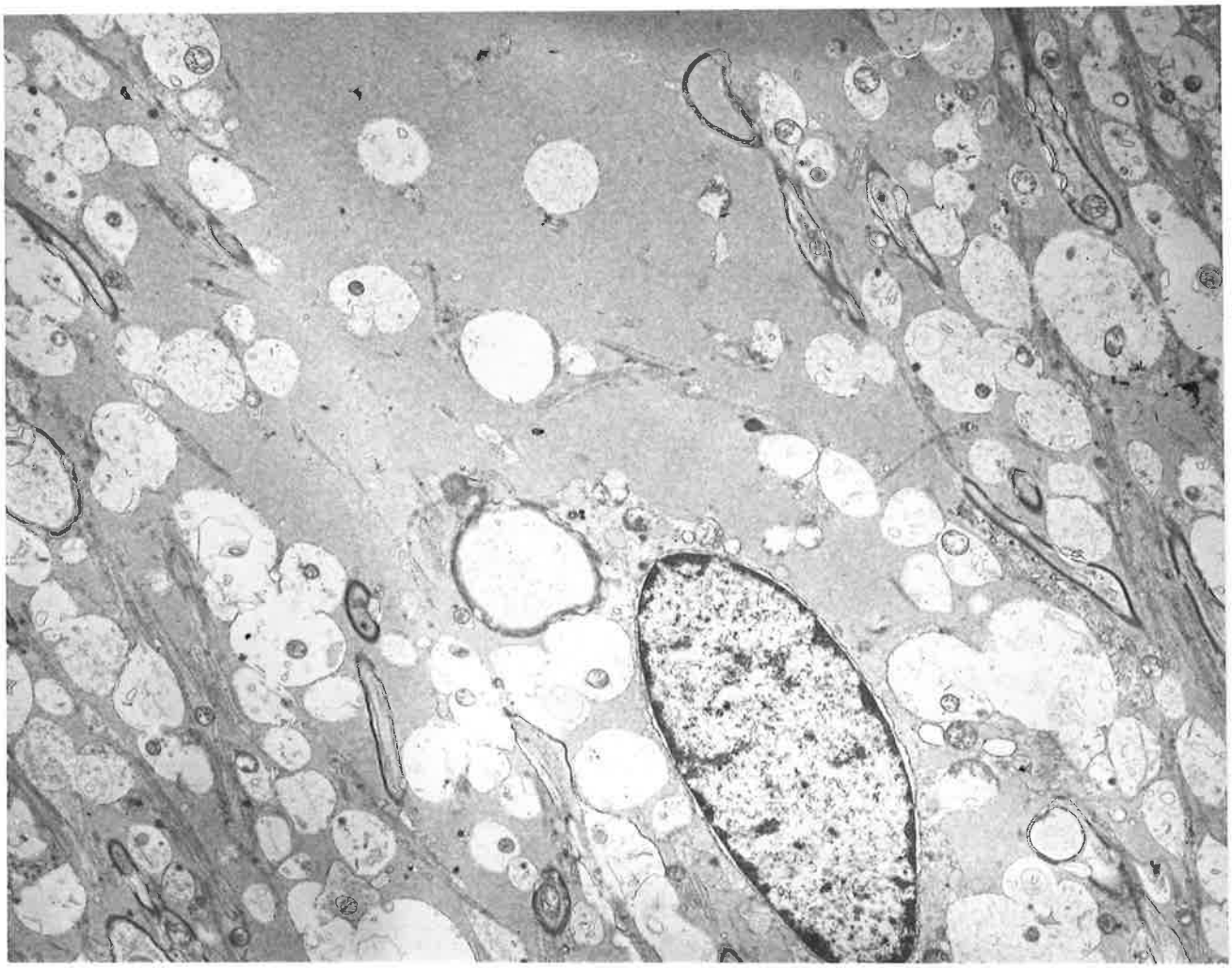

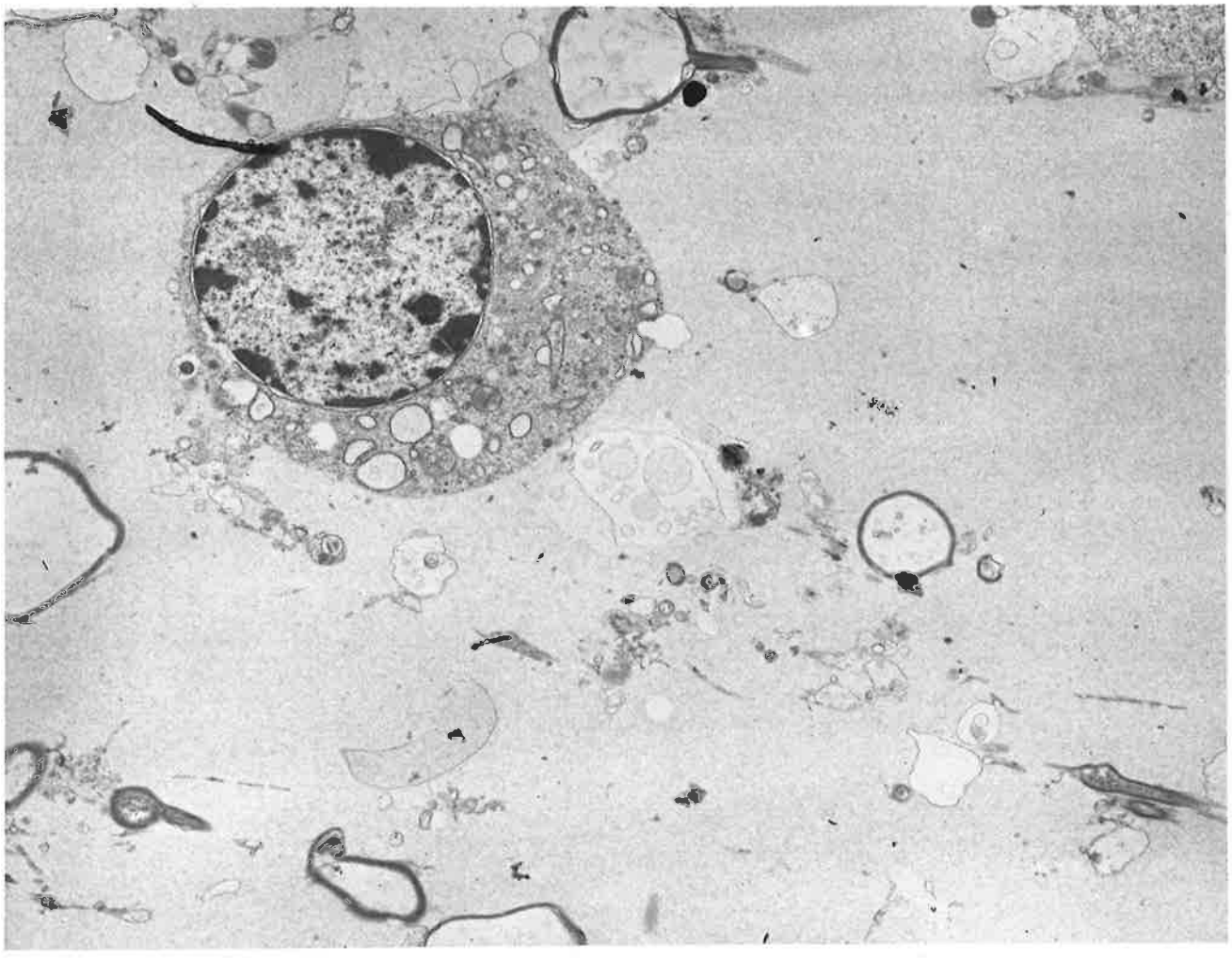

Figure 73. Toxin treated mouse. Cerebral cortex. Immersion fixation. 4 hours post-inoculation. The capillary endothelial cytoplasm is reduced to an electron-dense band and the astrocytic end-feet are severely swollen with rupture of cell membranes.
x 13,530.

Figure 74. Toxin treated mouse. Corpus callosum. Immersion fixation. 3 hours post-inoculation. Marked swelling of astrocytic processes and non-myelinated axons in the neuropil. The blood vessel shows electron dense bands of cellular condensation in the endothelial cytoplasm and the endothelial cell nucleus is very electron dense.
x 6765.

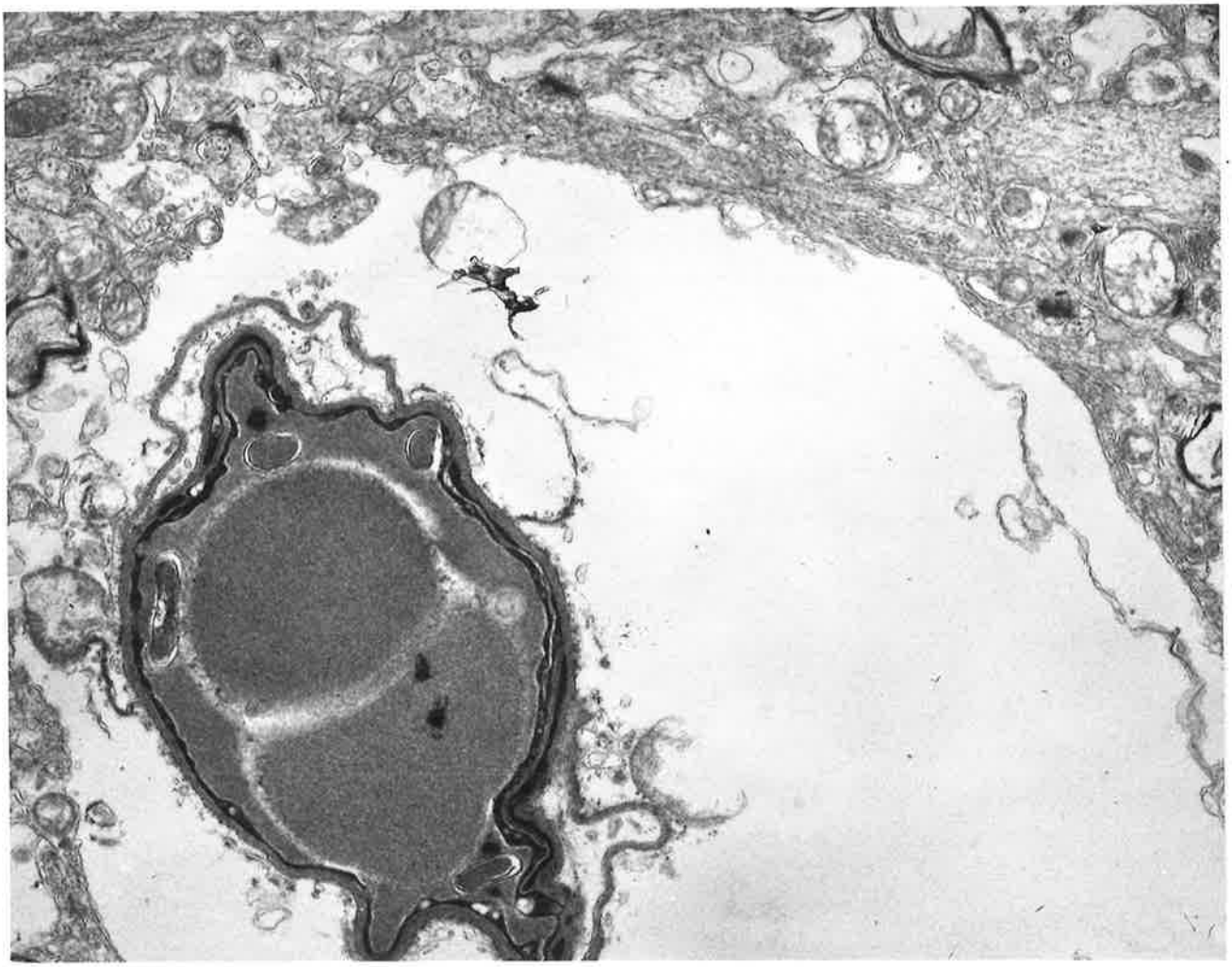

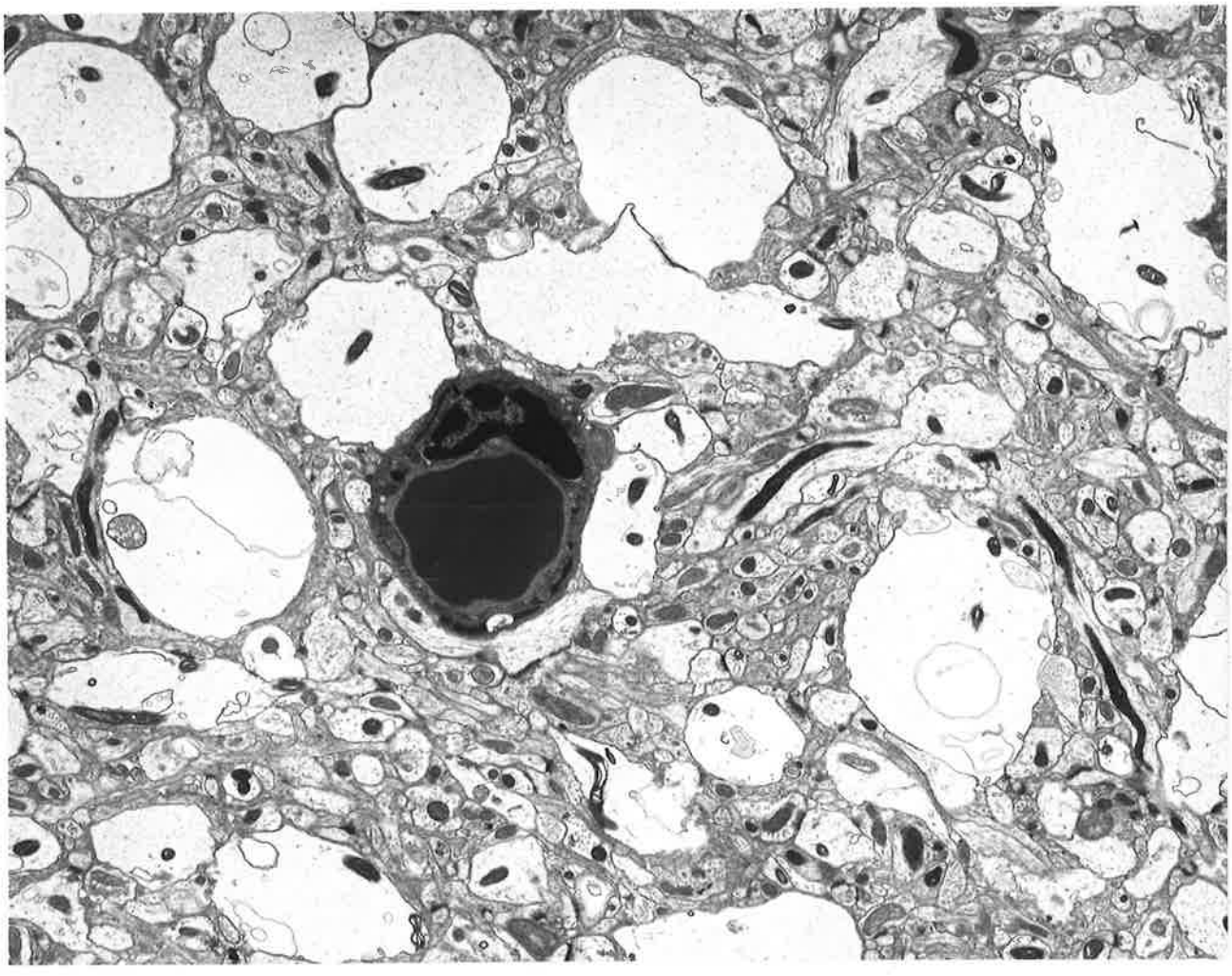

Figure 75. Control mouse. Brain. HRP is confined to the vascular lumen and in a few micropinocytotic vesicles within the endothelial cell (arrows). Reaction product is shown in an erythrocyte due to endogenous peroxidase activity.
x 10,250.

Figure 76. Toxin treated mouse. Brain. Pooling of HRP along the basal lamina (arrows) but structures beyond are free of reaction product.
x 10,250.

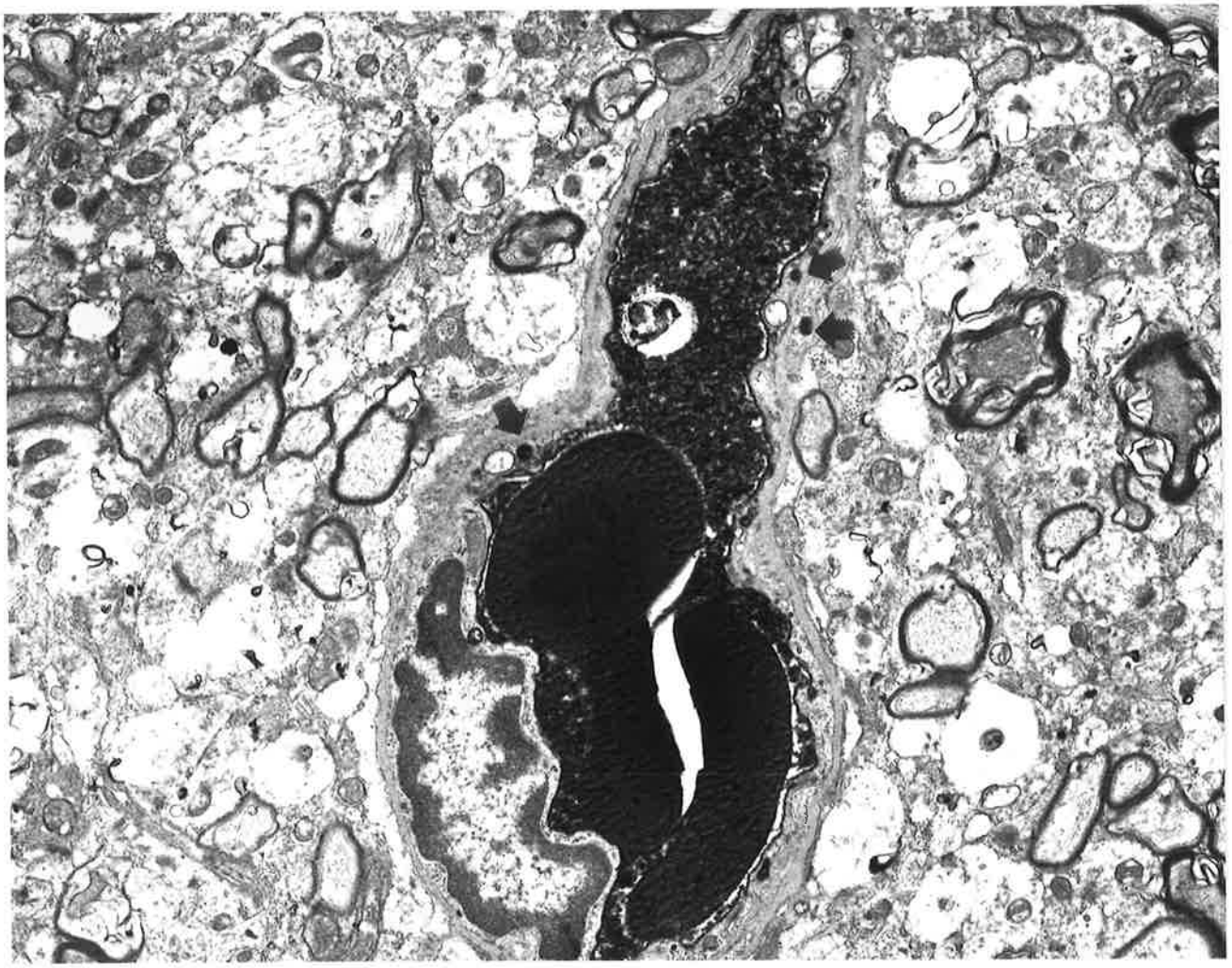

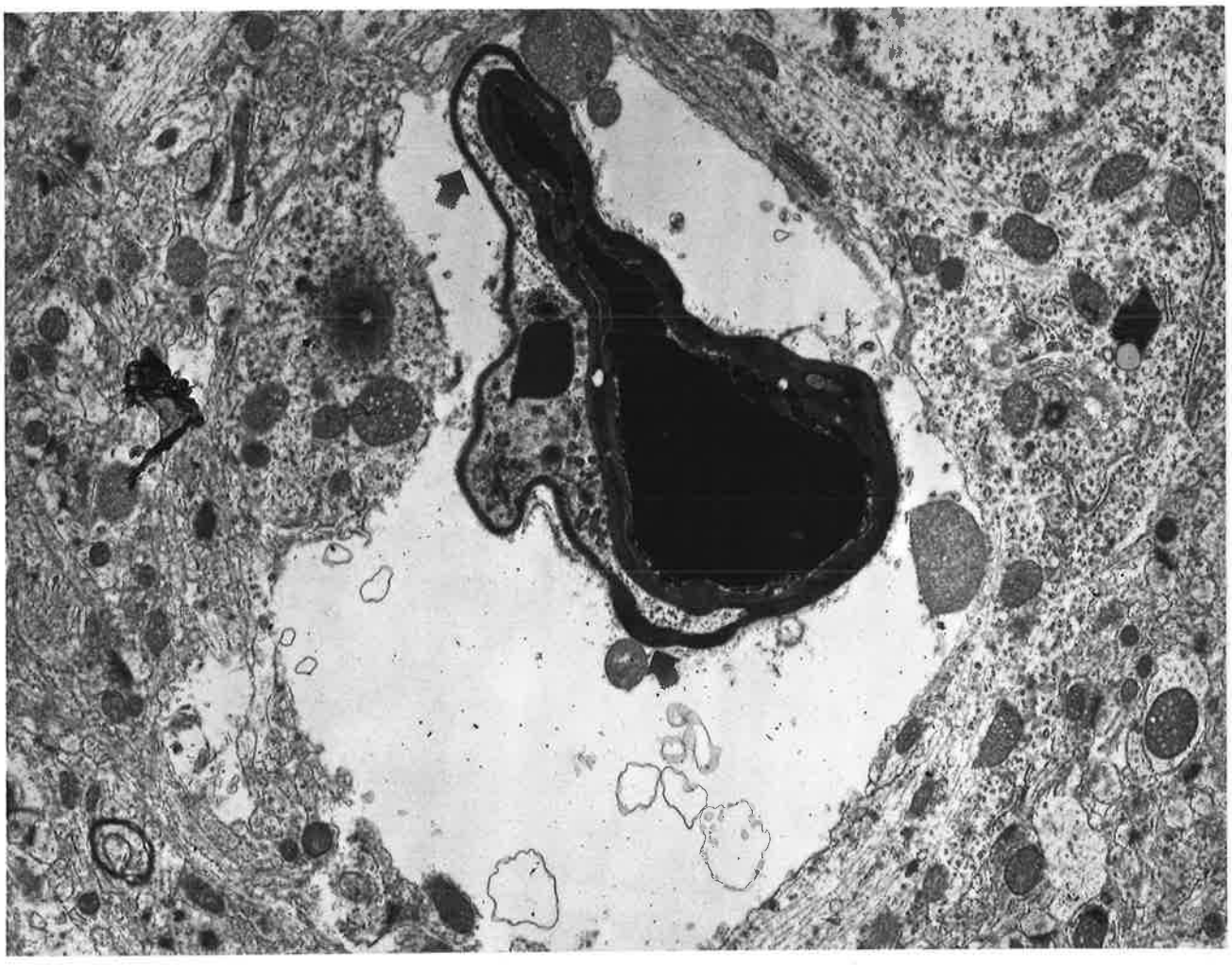

Figure 77. Toxin treated mouse. Brain. Accumulation of HRP along the capillary basal lamina with a small amount in clefts between two adjacent astrocytic end-feet (arrows). x 4100

Figure 78. Toxin treated mouse. Brain. A capillary showing accumulation of HRP along the basal lamina but extravascular tissues are free of reaction product. x 6765.

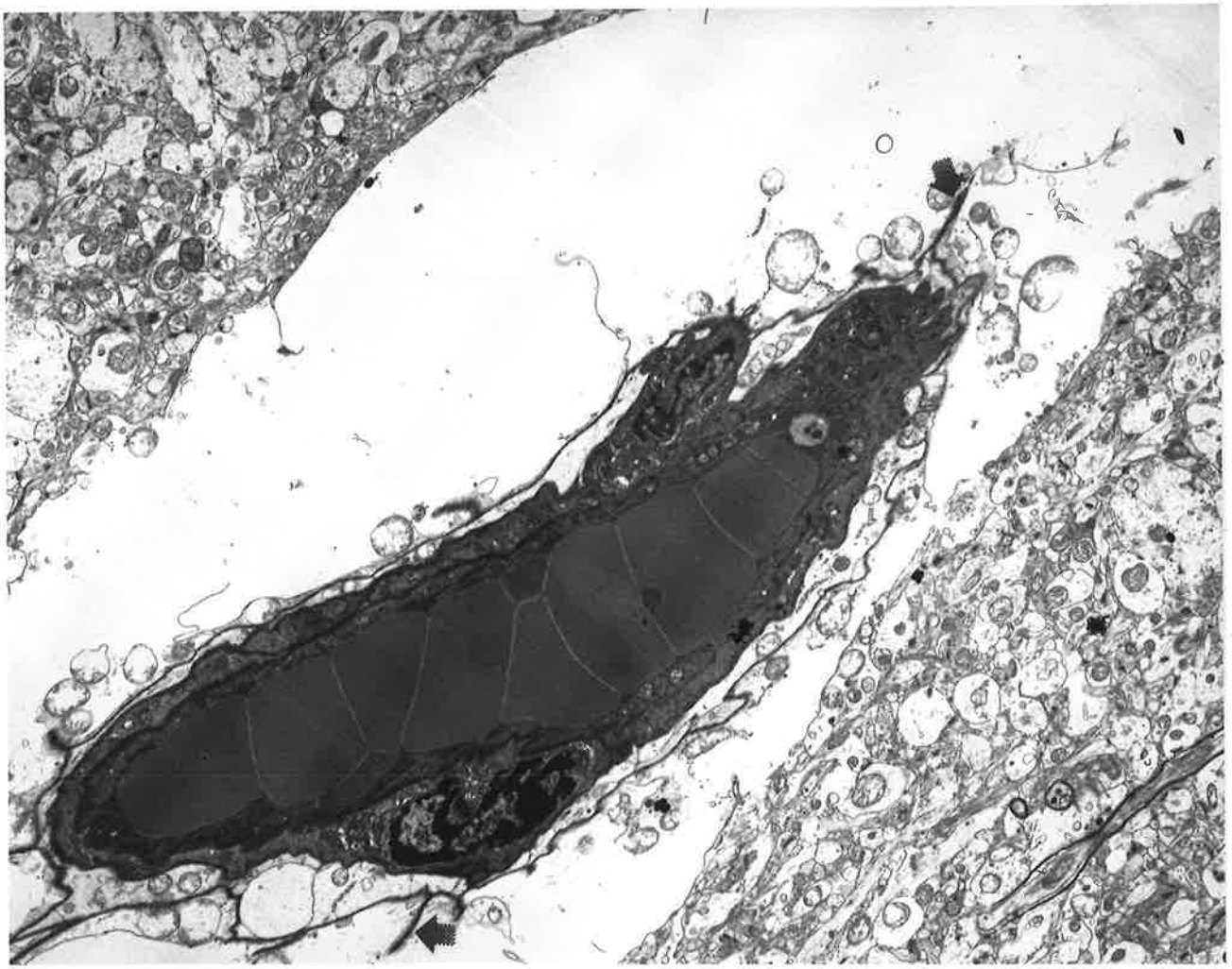

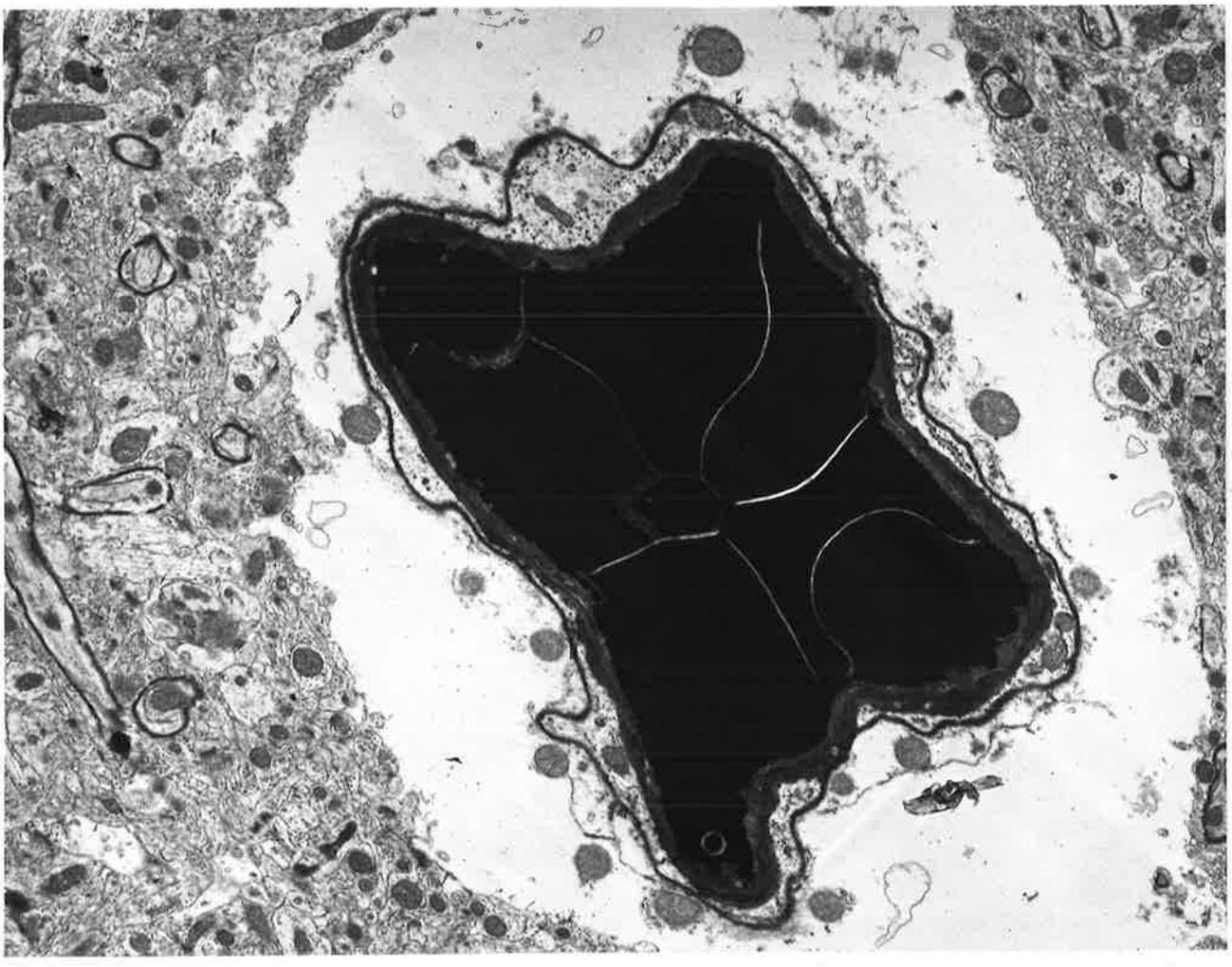

Figure 79. Toxin treated mouse. Brain. Accumulation of HRP along the basal lamina with some penetration between astrocytic end-feet (arrow).
x 10,250.

Figure 80. Toxin treated mouse. Brain. 3 hours post-inoculation. A blood vessel is occluded by platelet aggregates and the endothelial cytoplasm is condensed into electron opaque bands. This animal had been injected with HRP.
x 6765.

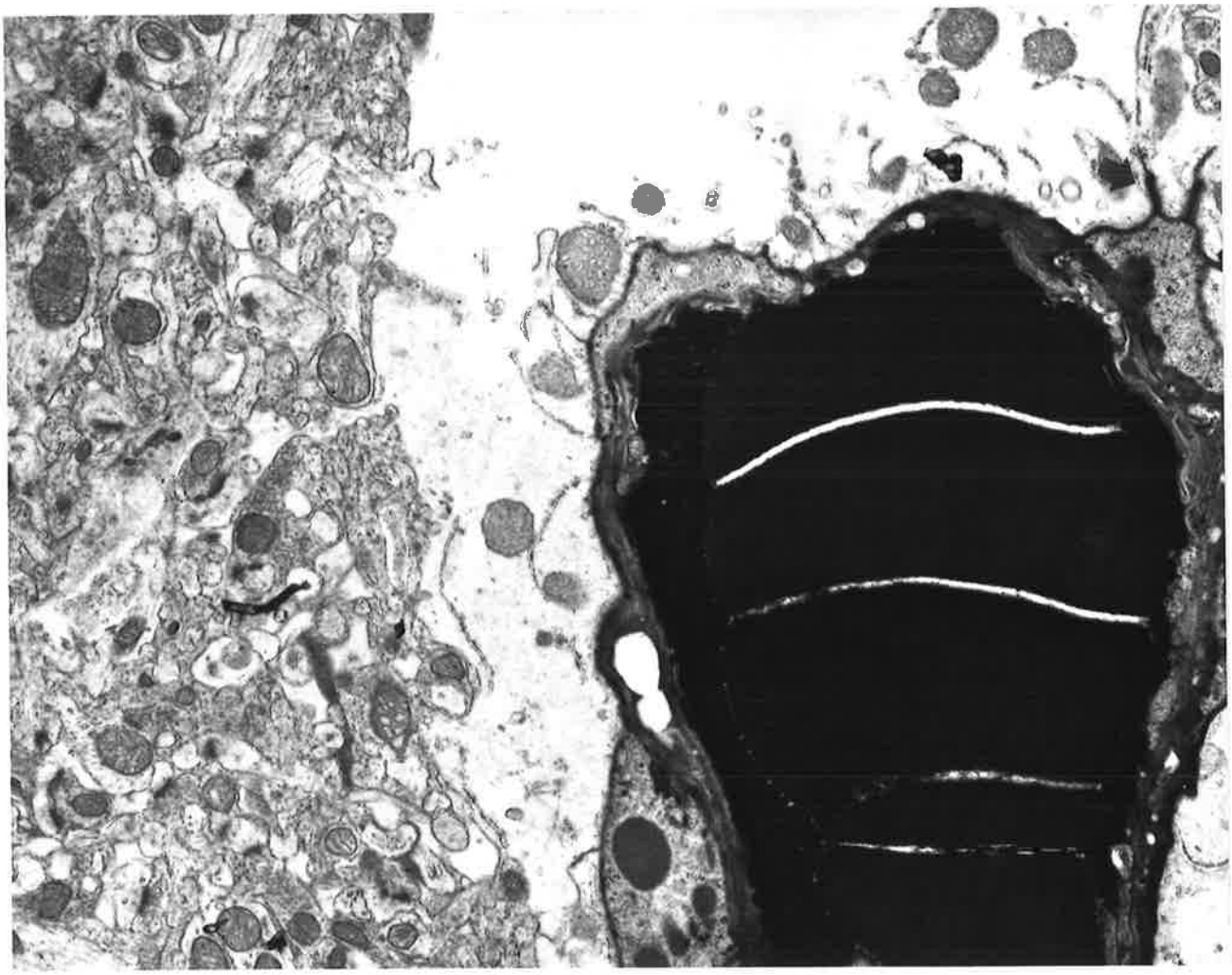

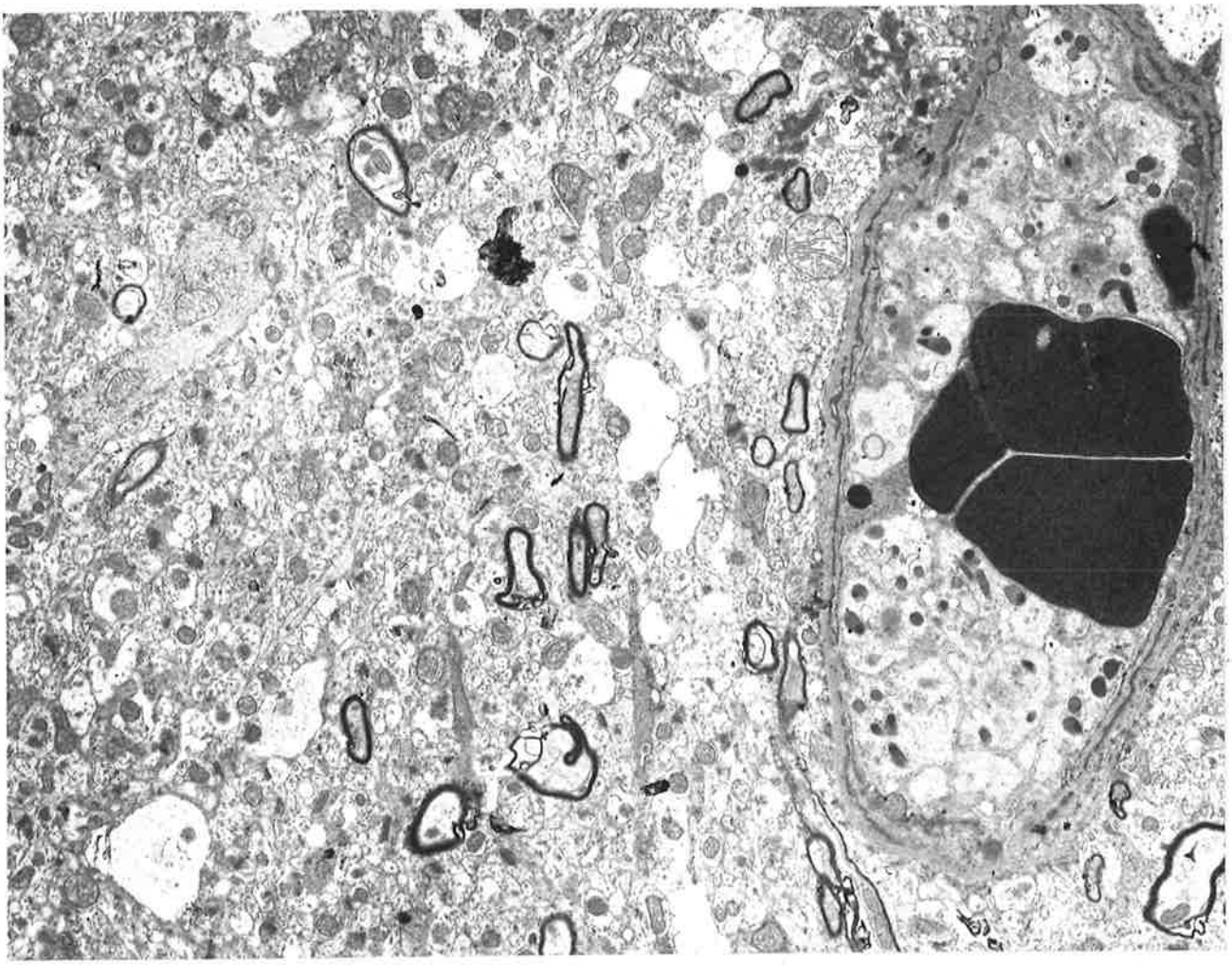

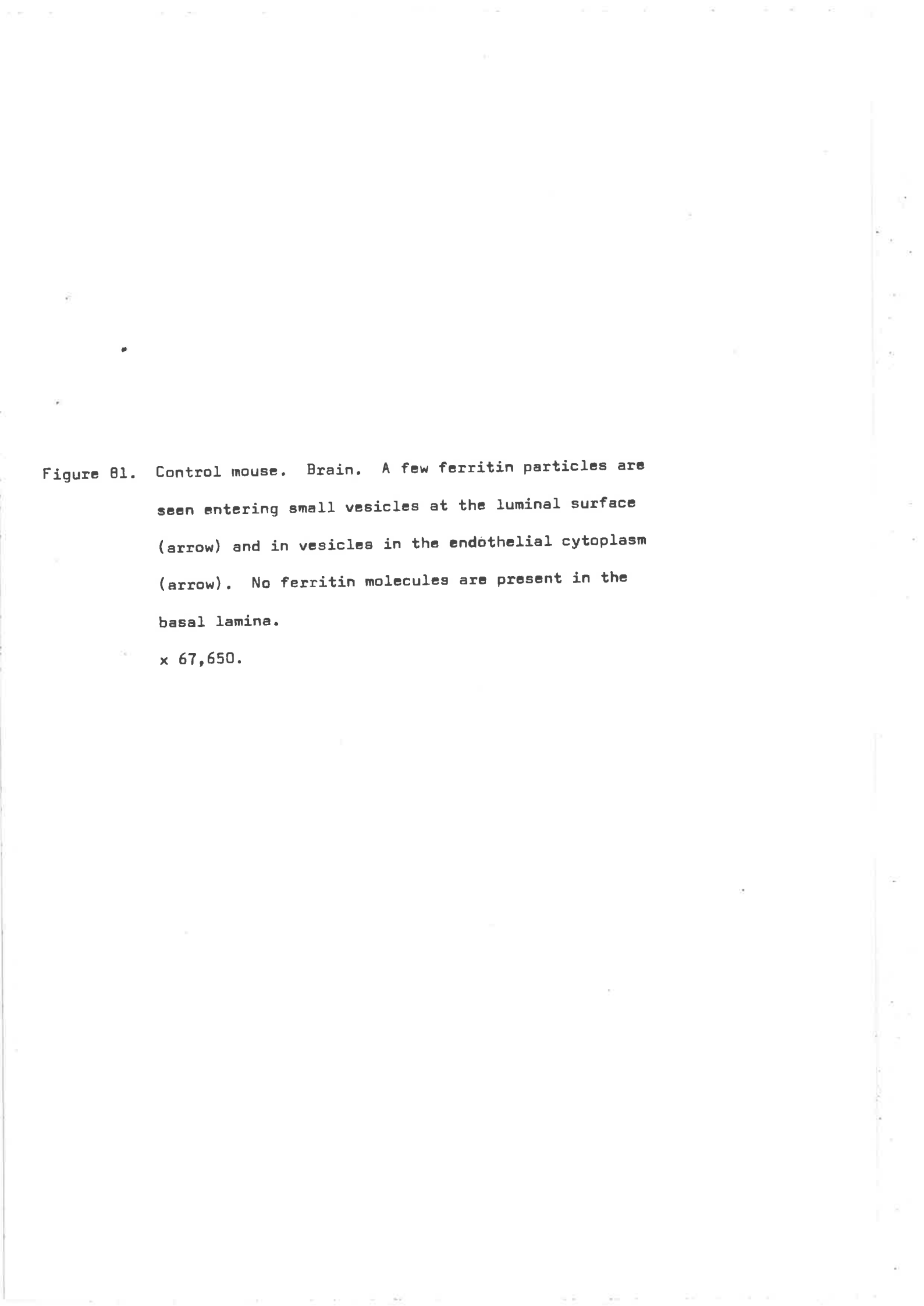

Figure 81. Control mouse. Brain. A few ferritin particles are seen entering small vesicles at the luminal surface (arrow) and in vesicles in the endothelial cytoplasm (arrow). No ferritin molecules are present in the basal lamina.
x 67,650.

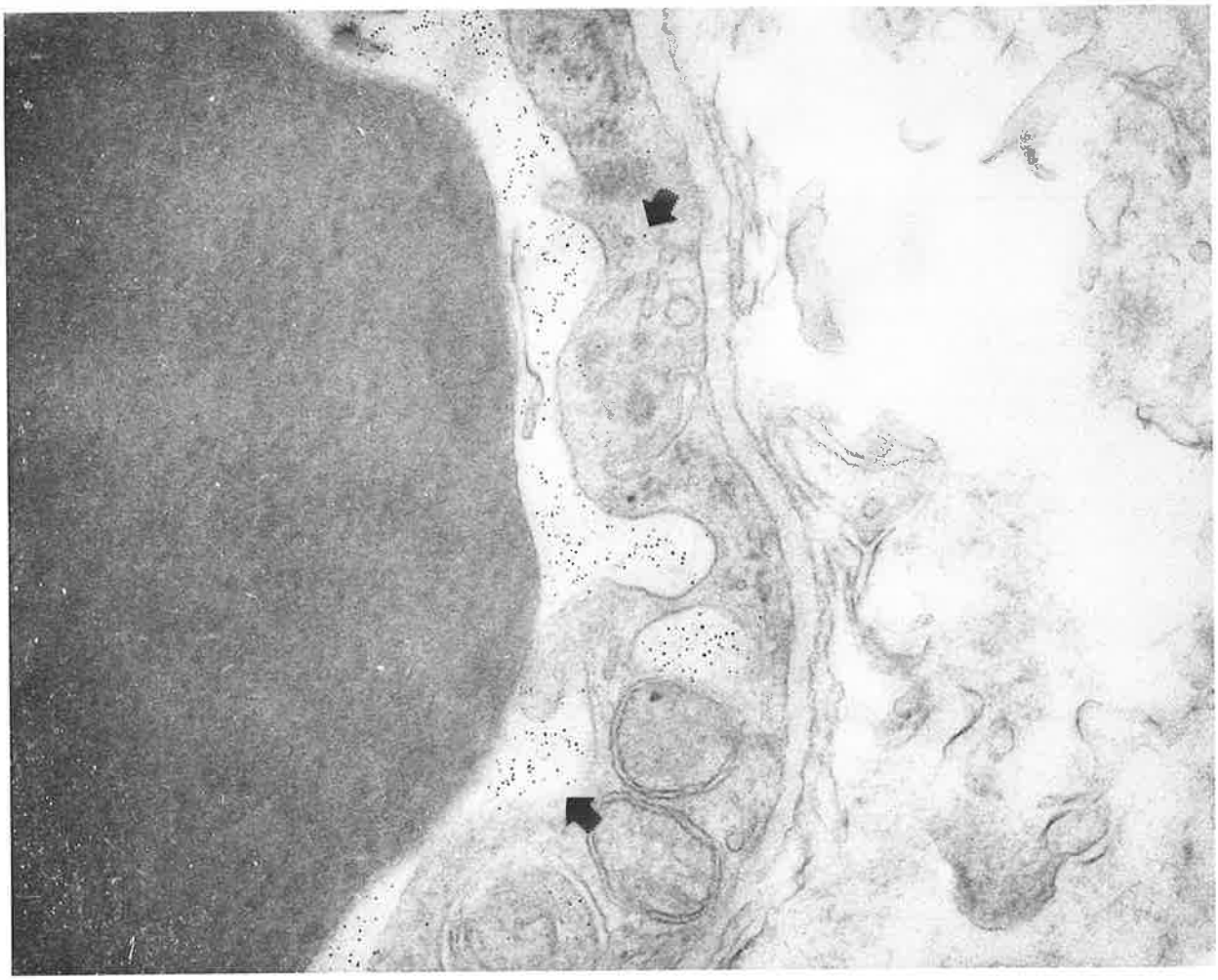

Figure 81.

Figure 82. Toxin treated mouse. Brain. An increased number of ferritin particles in cytoplasmic vesicles, a few in the basal lamina and an occasional particle in perivascular sites.
x 67,650.

Figure 83. Toxin treated mouse. Brain. Widening of the gap between endothelial cells with loosening of the tight junction but this space is conspicuously free of ferritin tracer material (arrow).
x 67,650.

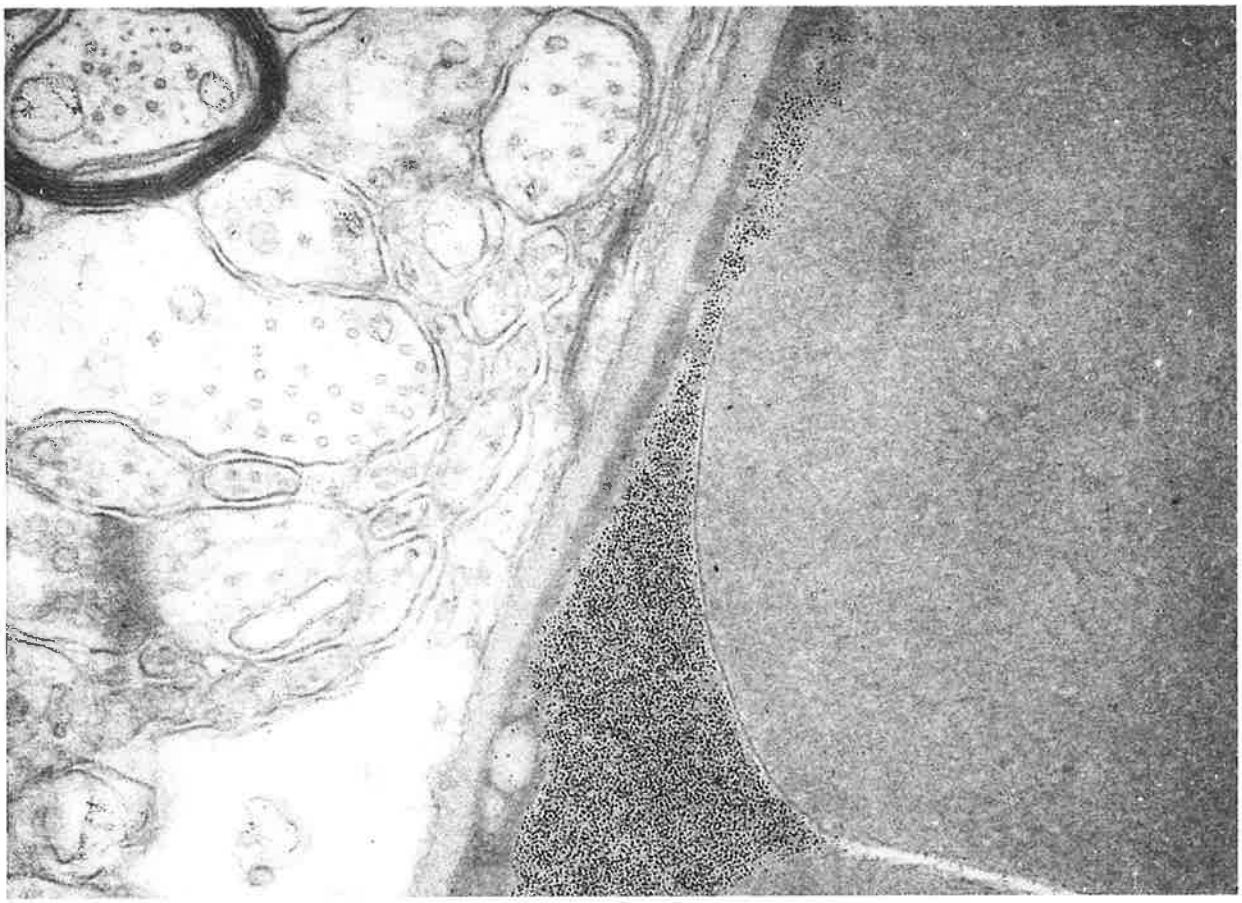

Figure 82.

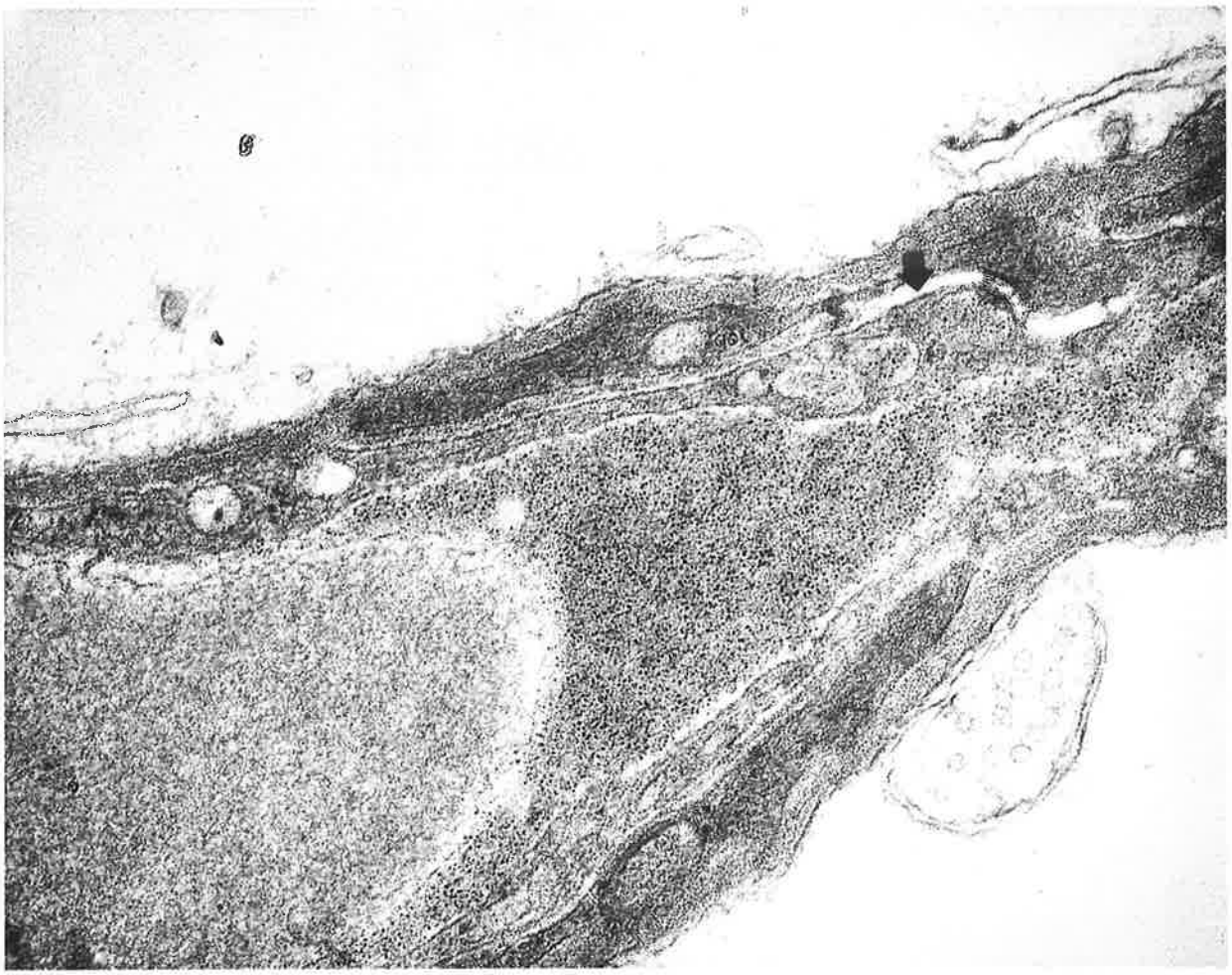

Figure 83.

Figure 84. Control mouse. Lung. Capillaries are fixed in an open state and a type 2 pneumocyte is shown with prominent lamellar bodies and a few short microvilli.
x 6765.

Figure 85. Toxin treated mouse. Lung. 4 hours post-inoculation. A modest increase in the size and number of micropinocytotic vesicles (arrows) in capillary endothelium is shown with mitochondrial swelling. Compare with the paucity of these vesicles in Figure 84. An alveolar macrophage is interposed between the capillaries. Tubular myelin is arrowed.
x 10,250.

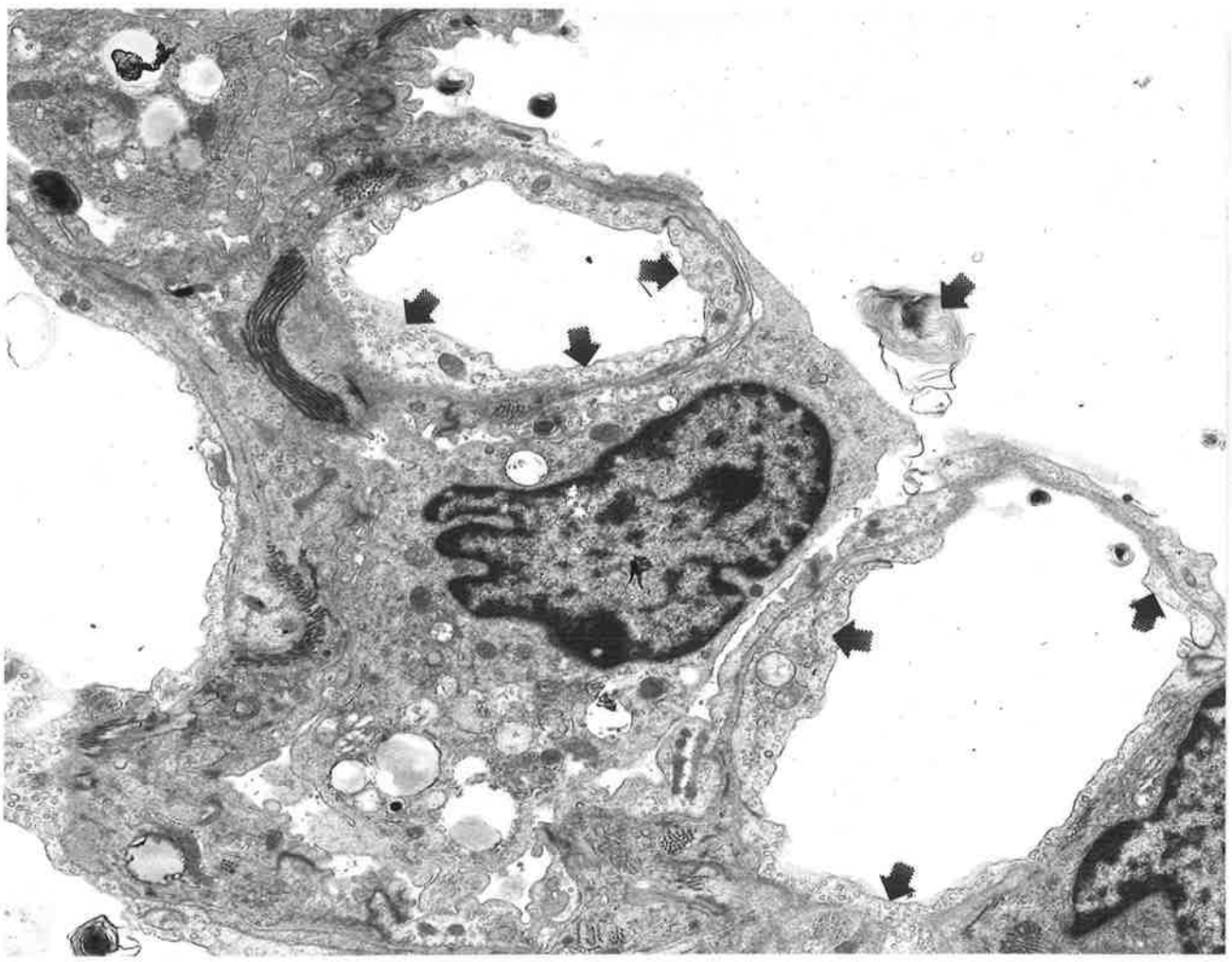

Figure 86. Toxin treated mouse. Lung. 4 hours post-inoculation. Capillaries appear normal.
x 10,250.

Figure 87. Toxin treated lamb. Lung. Immersion fixation. 1½ hours post-inoculation. The capillary endothelium is reduced to an electron dense band (arrows); the nucleus is condensed and electron opaque. Compare with Figure 86. A copious amount of fibrin is present in the alveolar space.
x 10,250.

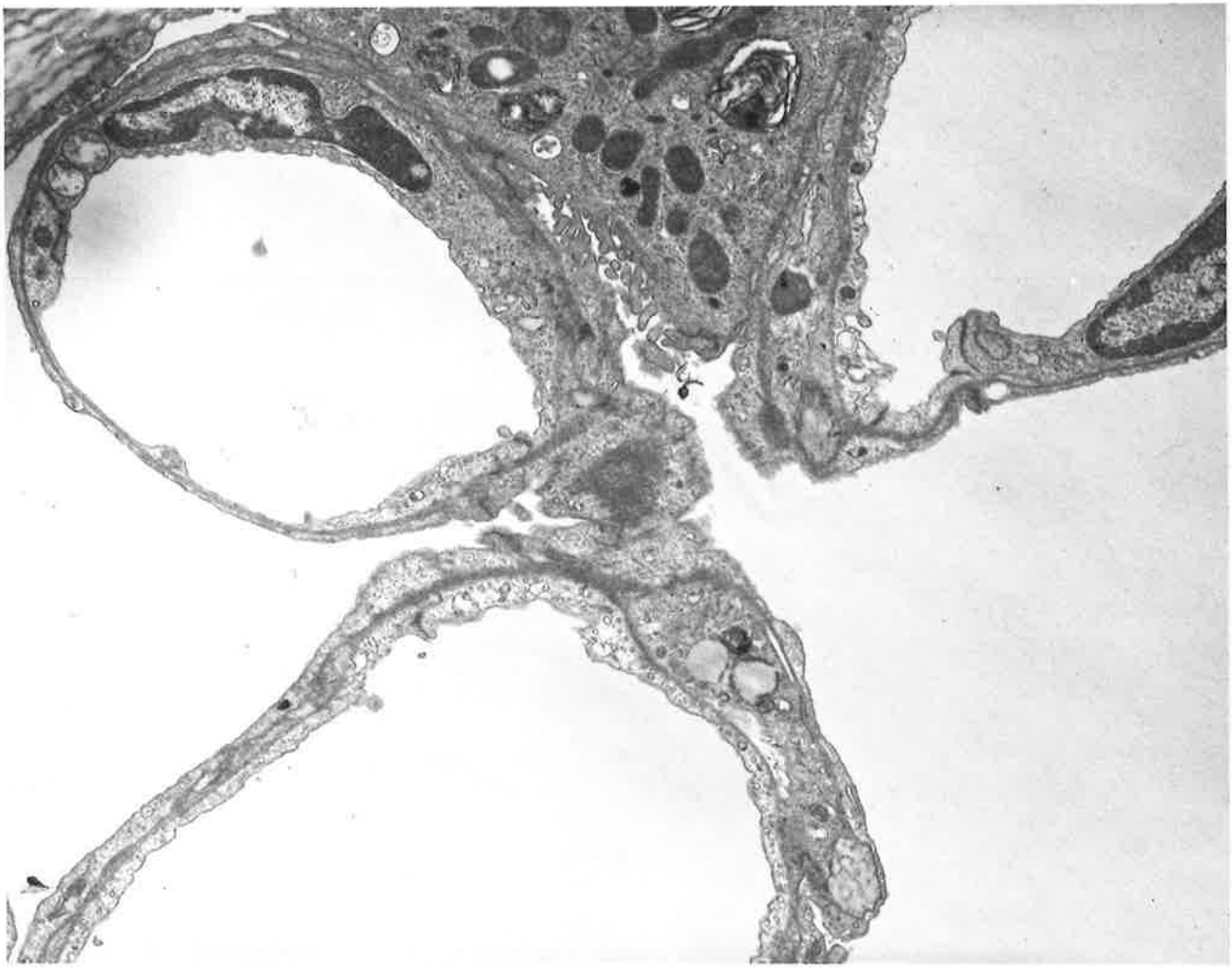

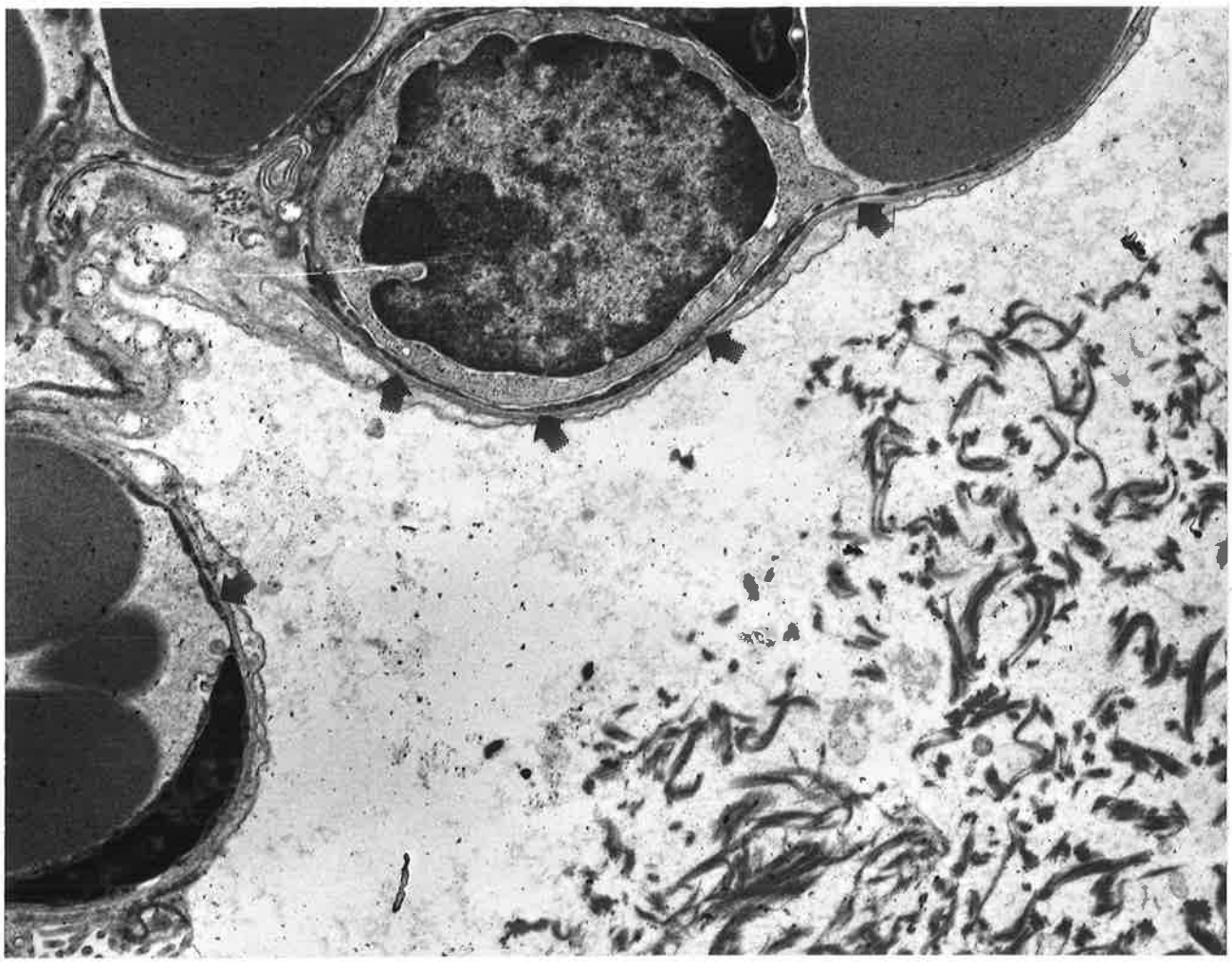

Figure 88. Toxin treated mouse. Lung. 24 hours post-inoculation. The capillary endothelial cytoplasm shows focally enhanced electron lucency and a few micropinocytotic vesicles are increased in size (arrows).
x 10,250.

Figure 89. Control mouse. Myocardium. Parallel bundles of myofibrils are shown with intercalated discs in a stepwise pattern. Rows of mitochondria, ~~lie~~ lying between the bundles, contain~~ing~~ed tightly packed cristae. The capillary basal lamina is closely applied to the surrounding parenchyma.
x 10,250.

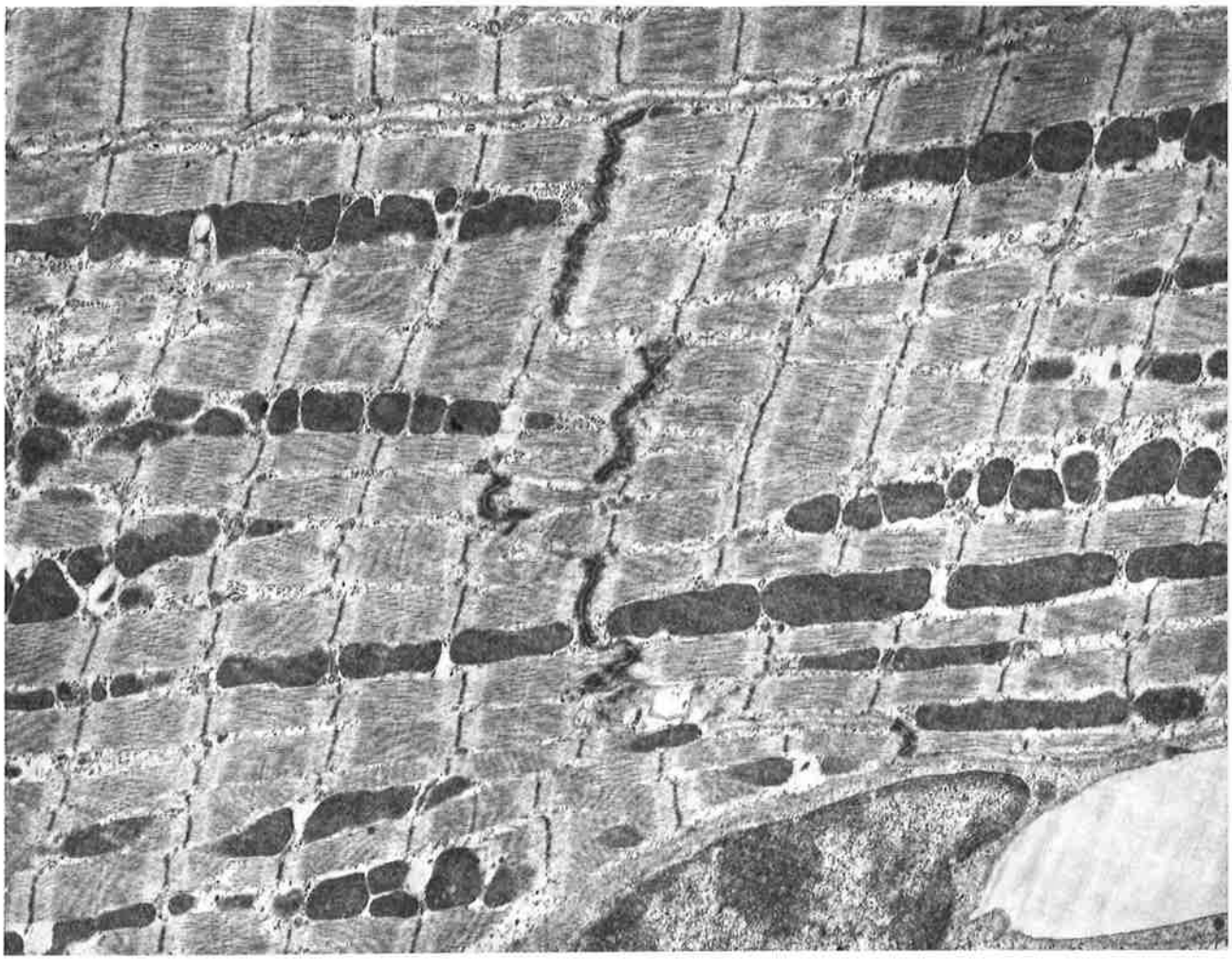

Figure 90. Toxin treated mouse. Myocardium. 4 hours post-inoculation. Extensive separation and degeneration of myofilaments, marked perivascular oedema and damaged capillary endothelium is shown.
x 10,250.

Figure 91. Toxin treated mouse. Myocardium. 24 hours post-inoculation. A less severely affected focus with disorganization of mitochondrial cristae (arrow); mitochondria in an adjacent area of cardiac muscle show the normal compact arrangement of cristae. Perivascular oedema is prominent.
x 6765.

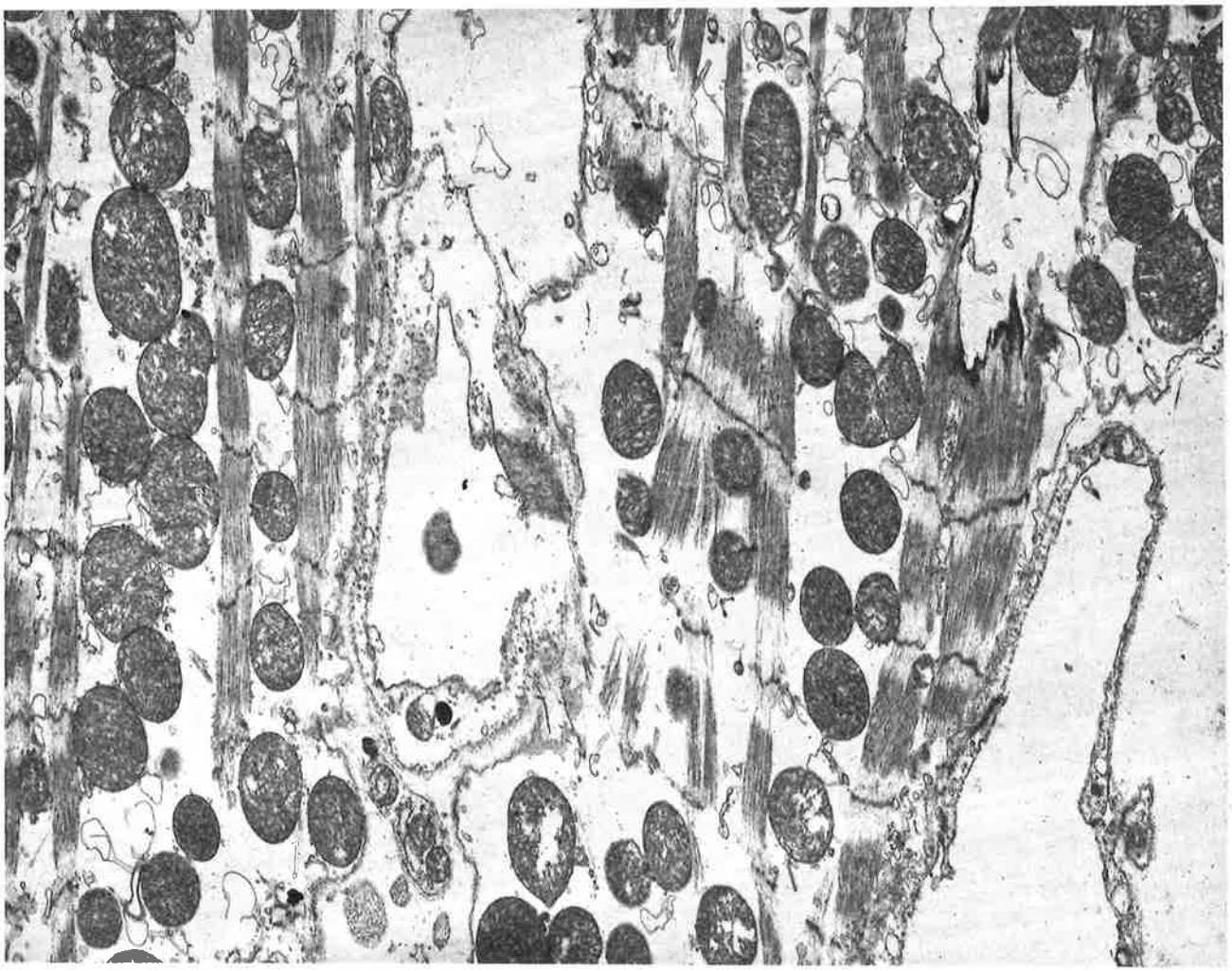

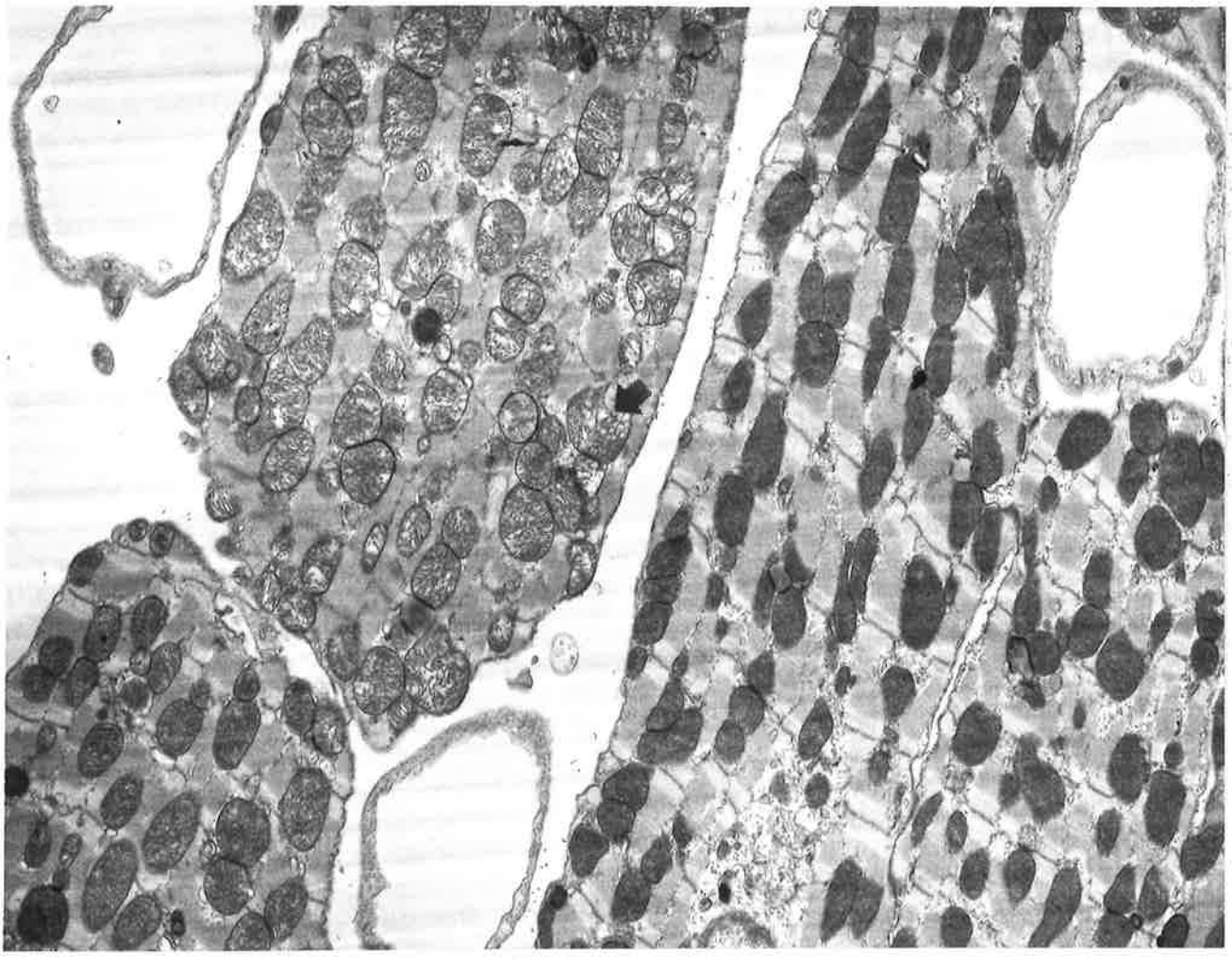

Figure 92. Toxin treated mouse. Myocardium. 4 hours post-inoculation. Marked swelling of the sarcoplasmic reticulum.
x 41,000.

Figure 93. Toxin treated mouse. Glomerulus. 4 hours post-inoculation. Capillary endothelial, epithelial and mesangial cells appear normal.
x 5330.

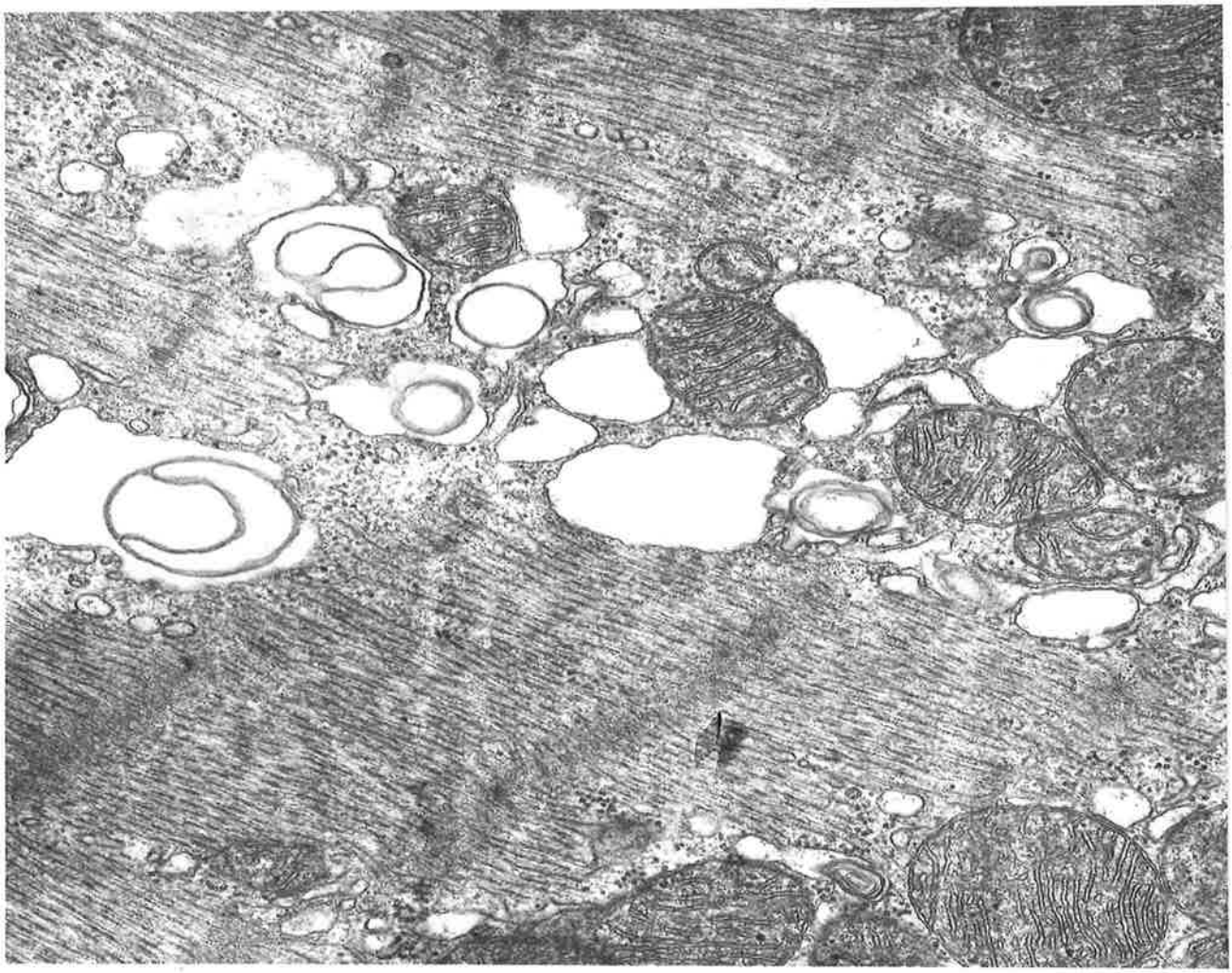

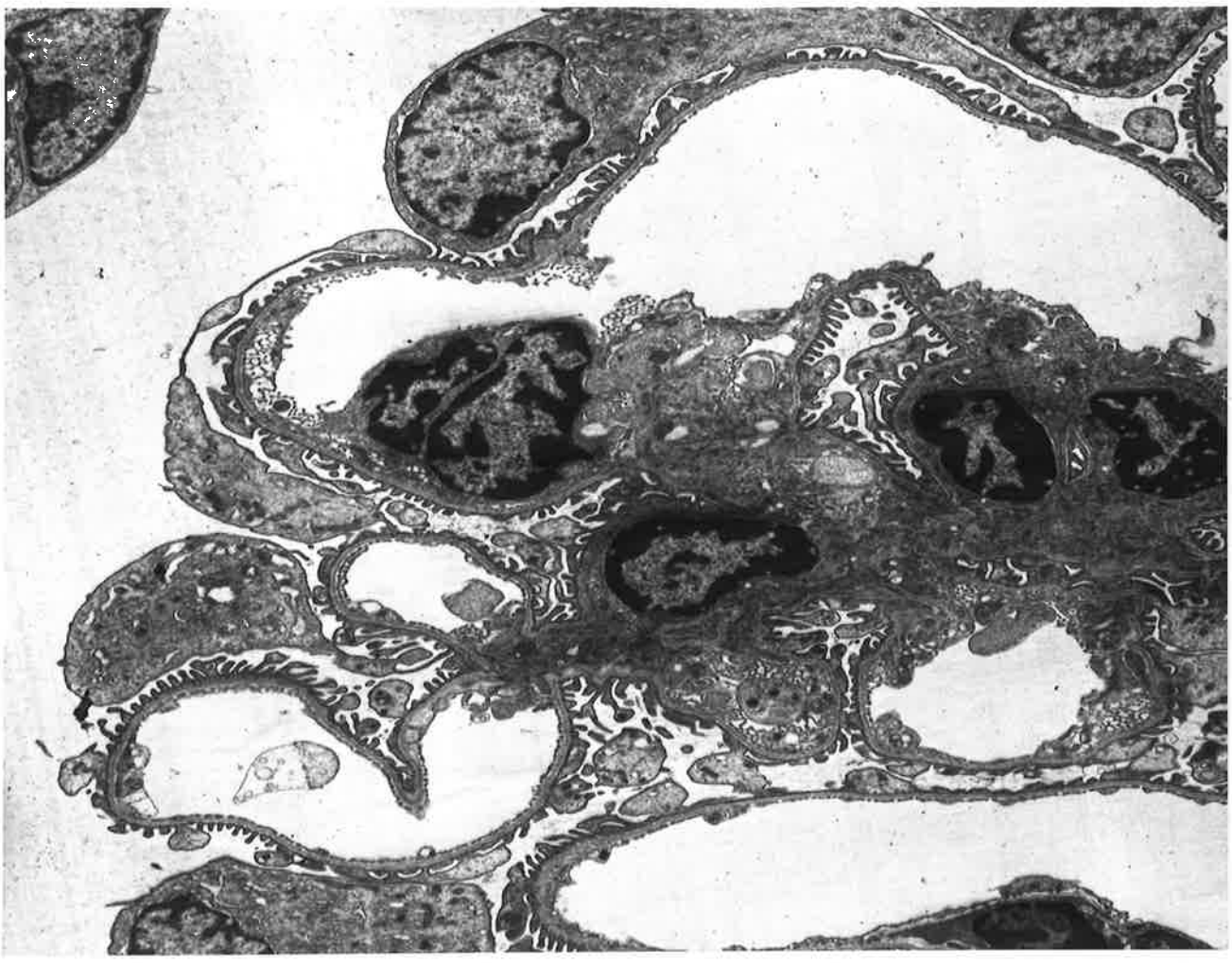

Figure 94. Toxin treated mouse. Proximal convoluted tubule. 4 hours post-inoculation. Enhanced electron lucency of the cytoplasm with some loss of organelle detail. Mitochondria, typically vertically disposed, appear well-preserved.
x 10,250.

Figure 95. Toxin treated mouse. Kidney. 4 hours post-inoculation. A capillary in the interstitium shows attenuation and a very electron dense cytoplasm (arrows). Degenerative changes in the brush border of the proximal tubule are evident.
x 6765.

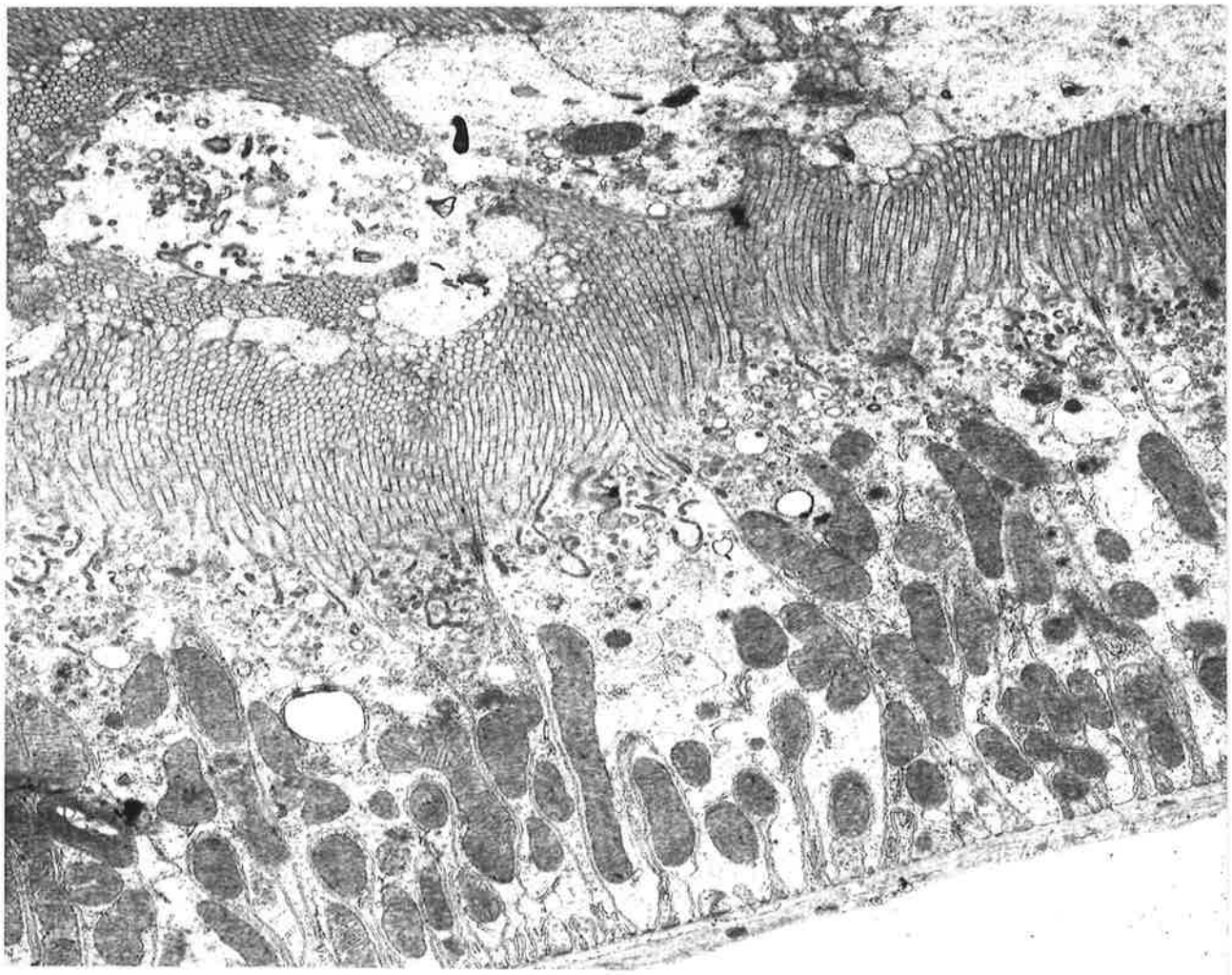

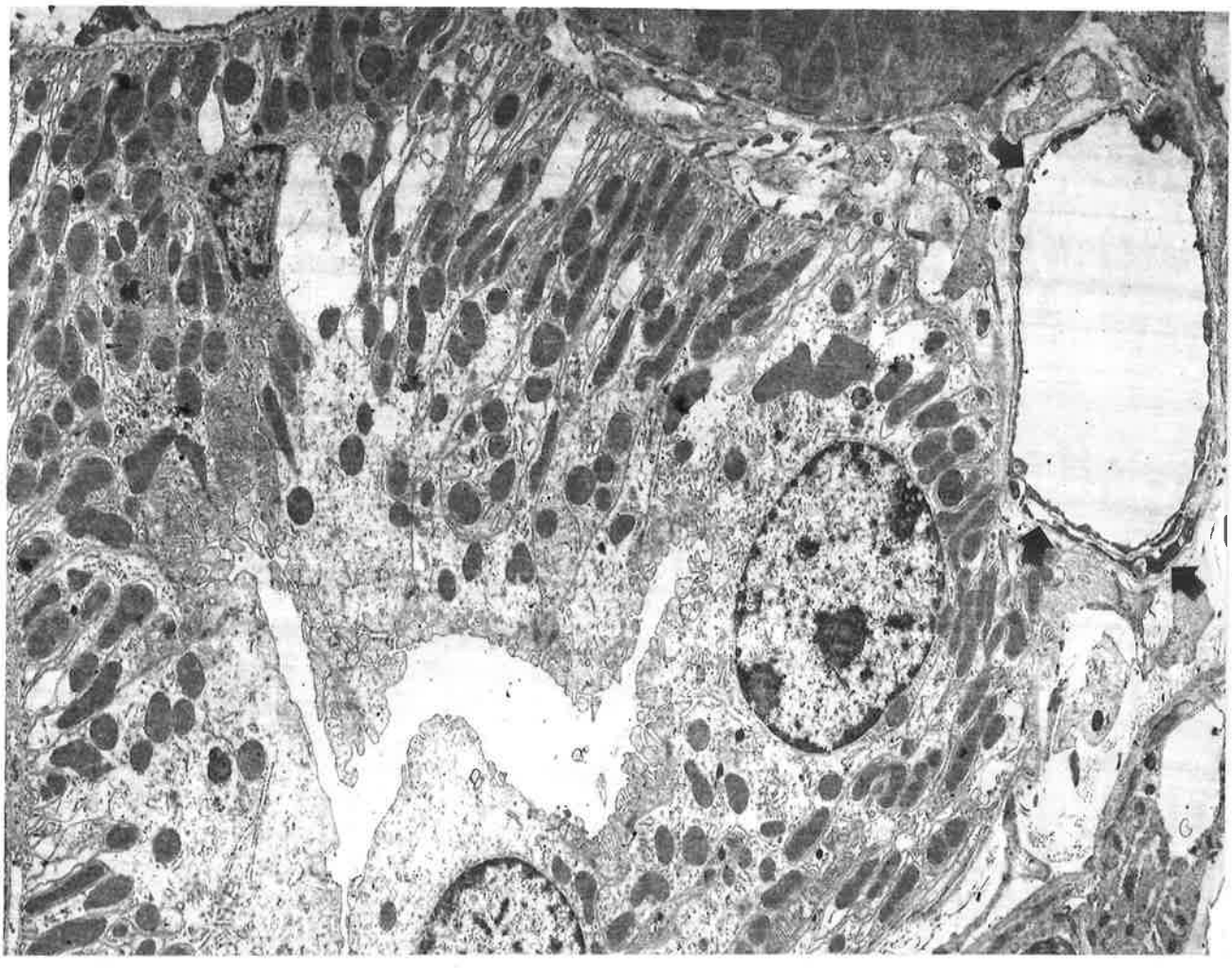

Figure 96. Control mouse. Lung. Most ferritin particles are confined within the vascular lumen but a few are present in cytoplasmic vesicles and the basal lamina and occasionally in the alveolar space.
x 67,650.

Figure 97. Toxin treated mouse. Lung. Modest increase in the number of ferritin particles in cytoplasmic vesicles in the capillary endothelium but few are present in the basal lamina and alveolar space.
x 53,300.

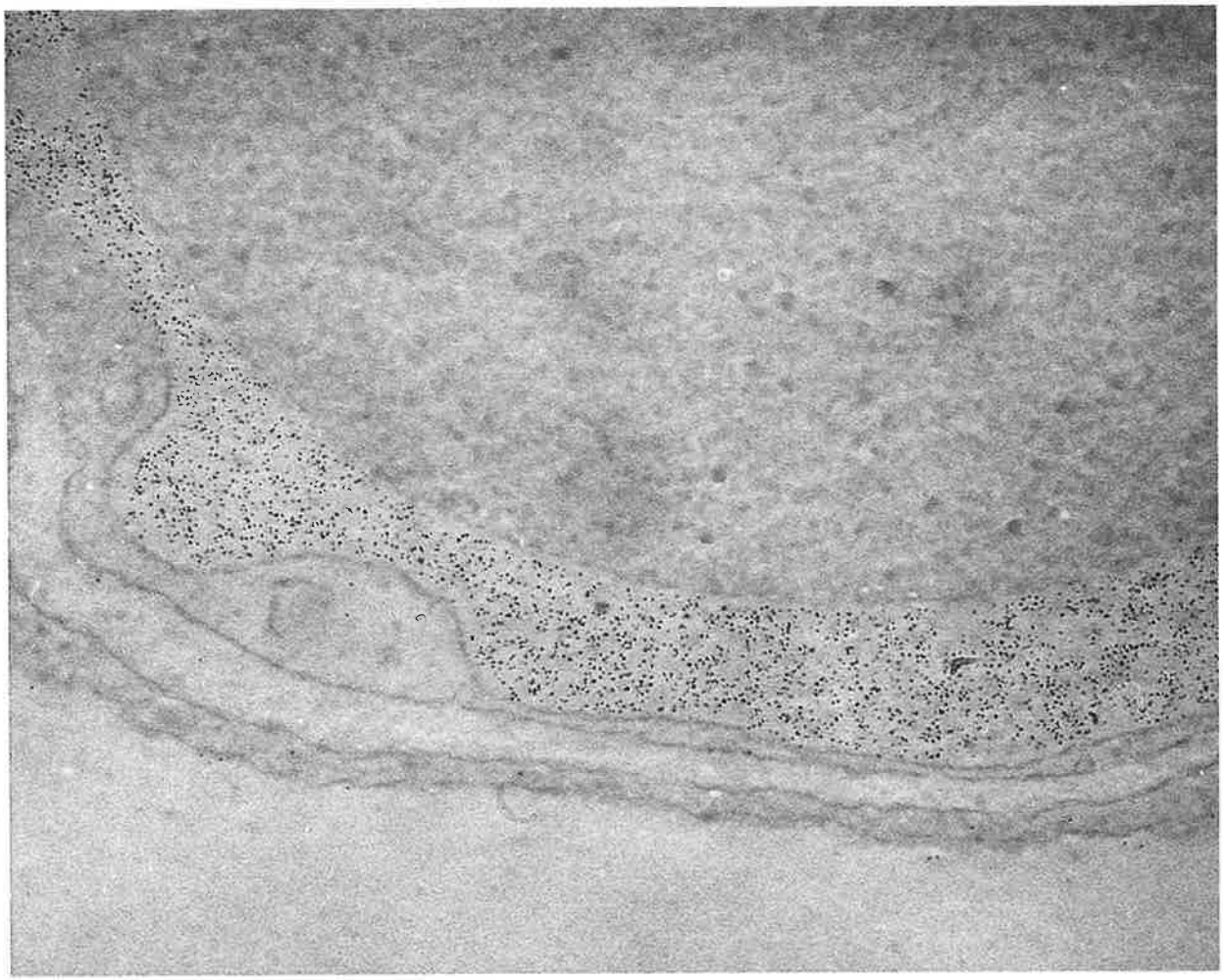

Figure 96.

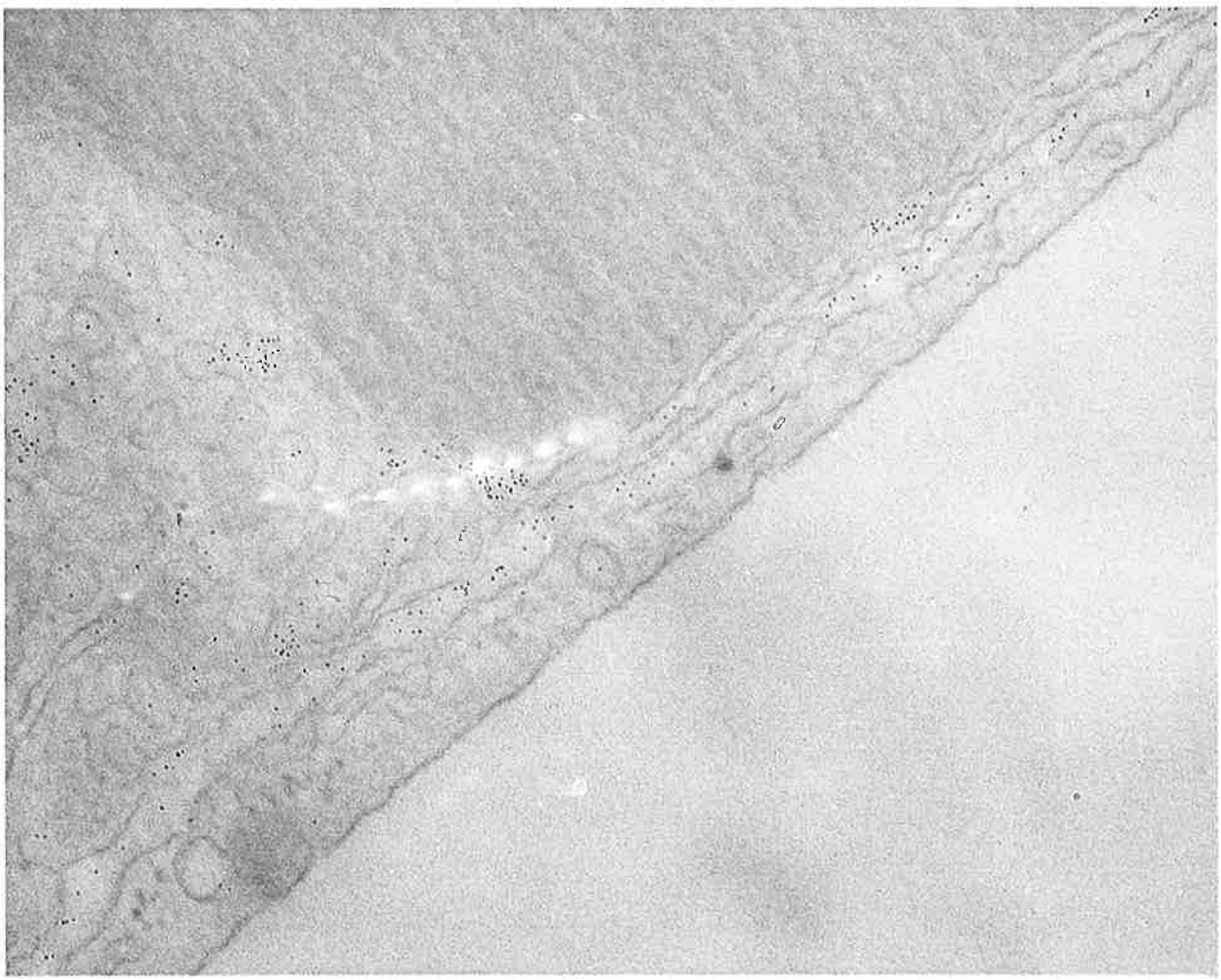

Figure 97.

Figure 98. Control mouse. Myocardium. Numerous ferritin tracer molecules in cytoplasmic vesicles of the endothelium and in the pericapillary connective tissue.
x 67,650.

Figure 99. Toxin treated mouse. Myocardium. Ferritin particles in endothelial cytoplasmic vesicles (arrows) and pericapillary tissue, extending a considerable distance beyond the blood vessel.
x 53,300.

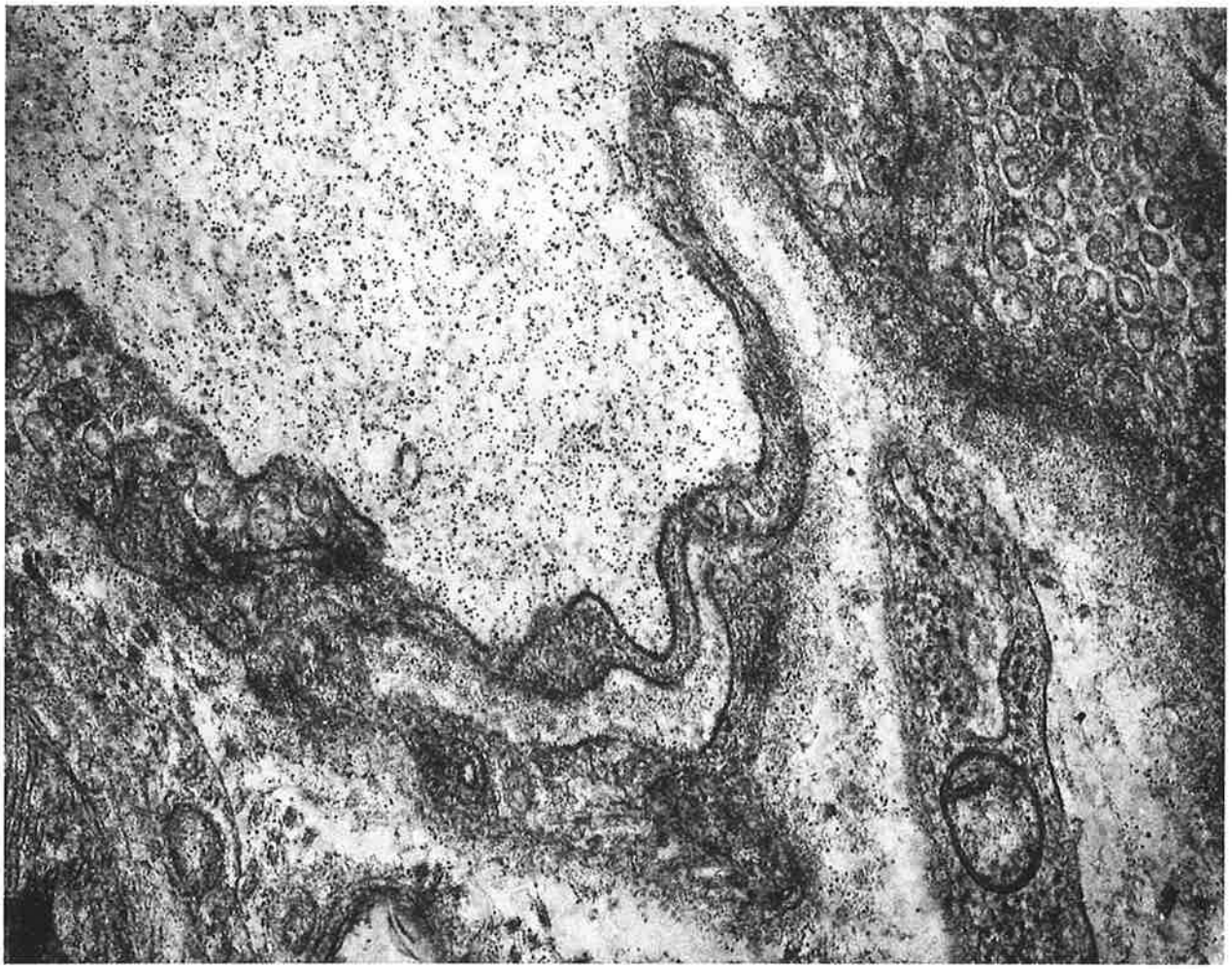

Figure 98.

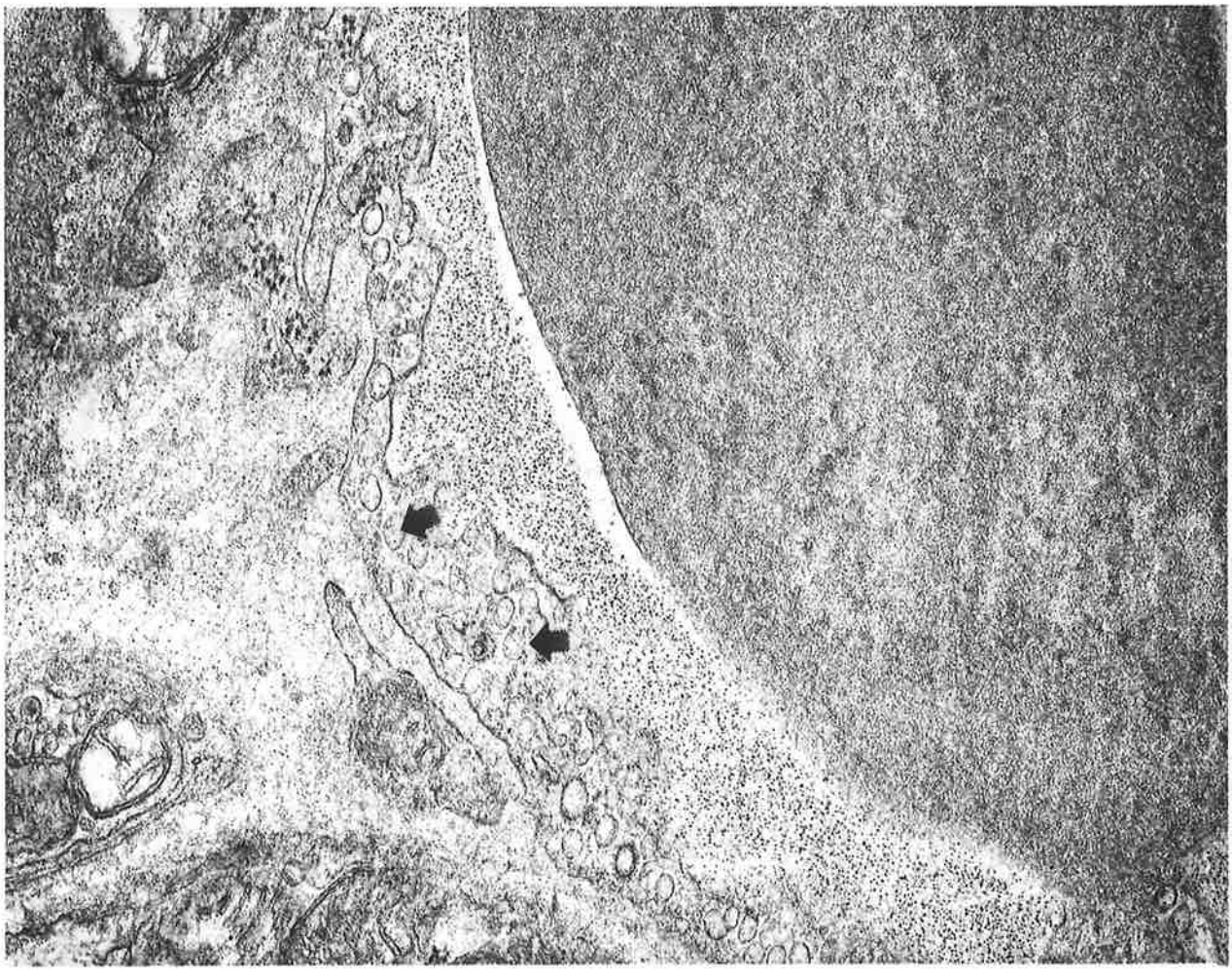

Figure 99.

Figure 100. Toxin treated mouse. Glomerulus. Ferritin particles are uniformly distributed in the basal lamina (arrow) and in the foot processes of podocytes. Only an occasional particle is seen in Bowman's space.
x 53,300.

Figure 101. Toxin treated mouse. Brain. Thorotrast particles in vesicles in the endothelial cytoplasm and basal lamina and a few in adjacent astrocytic end-feet.
x 53,300.

Figure 100.

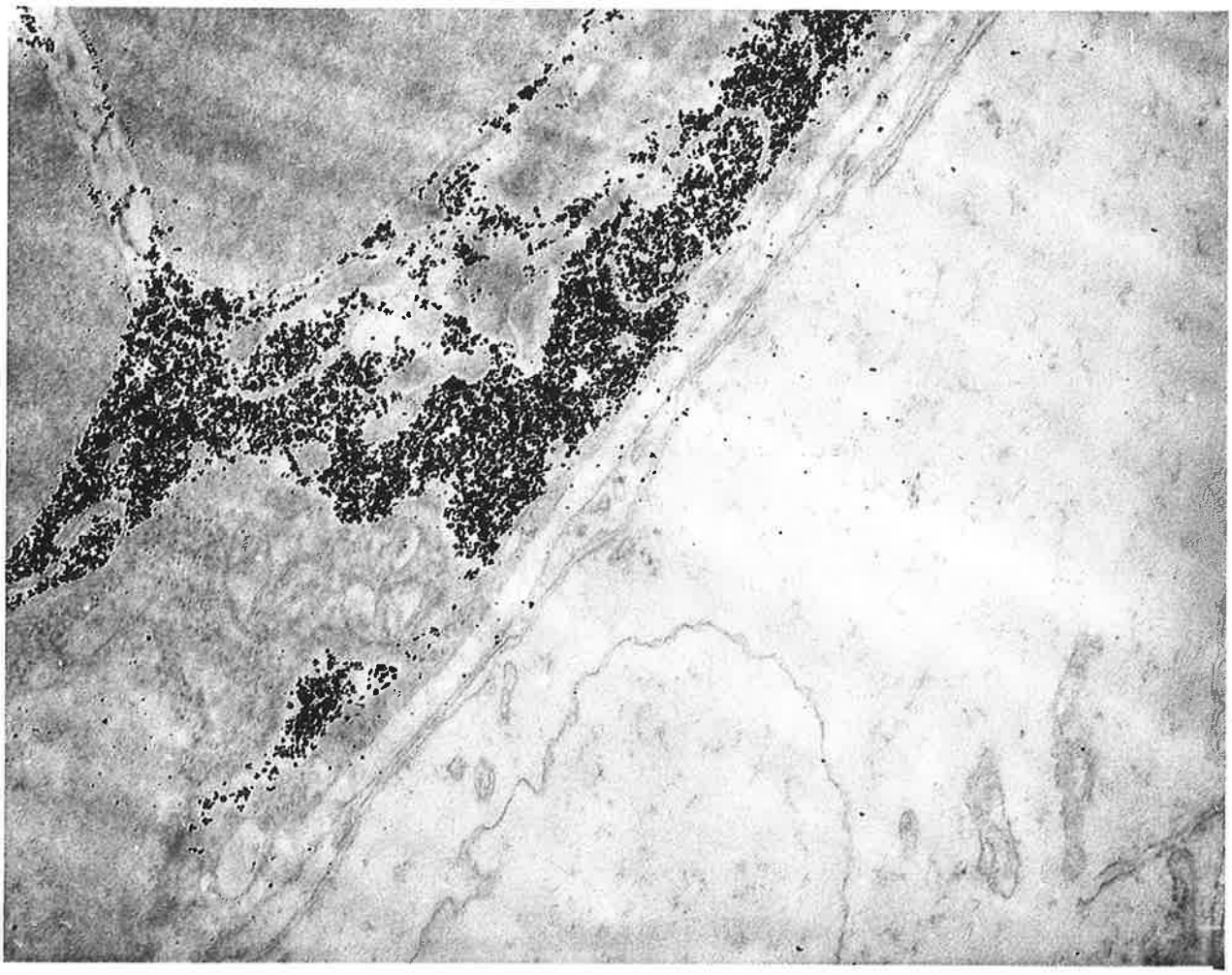

Figure 101.